UNIVERSITÉ FRANÇOIS – RABELAIS DE TOURS

ÉCOLE DOCTORALE EMSTU

E.A. 6293 GéoHydrosystèmes COntinentaux

THÈSE présentée par :

Aurore GAY

Soutenue le : **21 septembre 2015**

pour obtenir le grade de : **Docteur de l'université François – Rabelais de Tours**

Discipline/ Spécialité : **GEOSCIENCES – ENVIRONNEMENT**

Transfert de particules des versants aux masses d'eau sur le bassin Loire-Bretagne

THÈSE dirigée par :

DESMET Marc	Professeur, université François – Rabelais de Tours

THÈSE co-encadrée par :

CERDAN Olivier	Docteur, Bureau des Recherches Géologiques et Minières

RAPPORTEURS :

LAIGNEL Benoît	Professeur, Université de Rouen
OWENS Philip	Professeur, University of Northern British Columbia

---

JURY :

CERDAN Olivier	Docteur, Bureau des Recherches Géologiques et Minières
COLMAR Anne	Experte, Agence de l'Eau Loire Bretagne
DESMET Marc	Professeur, université François – Rabelais de Tours
GRIMALDI Catherine	Directrice de Recherches, INRA Rennes
LAIGNEL Benoît	Professeur, Université de Rouen
OWENS Philip	Professeur, University of Northern British Columbia
POIREL Alain	Expert, Electricité de France

Transfert de particules des versants aux masses d'eau sur le bassin Loire–Bretagne

Résumé

L'érosion des versants et le transfert des particules au sein des bassins versants constituent un facteur essentiel dans l'évolution des paysages en Europe de l'Ouest. Du fait des conséquences environnementales associées à l'érosion des sols et leur redistribution, de nombreuses études ont porté sur la quantification de ces processus. A l'échelle locale, l'instrumentation et l'utilisation de modèles à base-physique permettent de comprendre et représenter avec précision les transferts de sédiments. A plus large échelle, la tâche est rendue complexe du fait de la résolution et la qualité des données disponibles, ainsi que de la compréhension des intéractions entre les nombreux processus mis en jeu et leur intégration dans les modèles.

Au sein du bassin Loire Bretagne (155 000 km^2), la non-atteinte du bon état écologique des masses d'eau en 2015 est en partie due au colmatage des cours d'eau par les particules fines. A l'heure actuelle, l'identification des sources potentielles de ces particules se cantonne aux cartes d'érosion de versant. Toutefois, il n'existe pas de correspondance entre les quantifications et la distribution spatiale des taux d'érosion issues de ces cartes et les observations sur le terrain des dépôts de sédiments. Il est donc nécessaire d'identifier toutes les sources potentielles de particules et d'identifier et quantifier leur connectivité au sein de ce bassin.

Dans ce contexte, l'objectif de cette étude est de proposer une synthèse à large échelle du fonctionnement du bassin Loire-Bretagne en développant une approche basée sur le bilan sédimentaire et de quantifier chacun des différents compartiments, *i.e.* les sources, transferts et dépôts/exports à l'exutoire. Les défis scientifiques et techniques de cette étude reposent sur i) le développement de modèles appliqués à un large territoire très contrasté en utilisant des bases de données homogènes, ii) l'identification des processus et paramètres dominants dans le détachement et transfert des particules en zones de plaine et leur intégration dans les modèles, et iii) la production d'une évaluation quantitative et qualitative de ces transferts pour les décisionnaires.

Pour le bassin de la Loire, nos résultats indiquent que le stock de sédiments issus des nombreuses formes d'érosion, à savoir l'érosion diffuse, concentrée, mouvements de masse et érosion de berges, représente 1.6 * 10^7 $t.an^{-1}$ (contribution respective des sources à hauteur de 77.1%, 12.0%, 4.5% et 6.4%). Seulement $\sim$ 5% de ces particules détachées sont transportées jusqu'à l'exutoire et témoignent du fort taux de dépôt au sein du bassin versant. En parallèle, une valorisation de la base de données des éléments dissous permet de montrer l'importance des flux sédimentaires exportés sous forme dissoute ($\sim$90% des exports totaux).

L'analyse réalisée autour de 77 bassins versants au sein du site d'étude indique une forte variabilité spatiale dans la mise à disposition des particules et leur export. Cependant, aucune corrélation entre exports et caractéristiques des bassins versants (*e.g.*, pente, aire drainée, *etc.*) ne permet d'expliquer cette variabilité. Cette absence de corrélations attendues met en exergue les différences dans la nature des processus et paramètres mis en jeu dans le transfert particulaire qui existent entre les zones de montagnes et les zones de plaines, ainsi que le rôle de la distribution spatiale de ces processus et paramètres. La prise en compte du ruissellement par saturation et des éléments du paysage (tels que les haies) dans un indice de connectivité permet de fournir un nouvel aperçu de la redistribution des particules sur les versants.

La représentation des résultats de cette étude est proposée à différentes résolutions spatiales, du pixel à l'échelle du bassin versant, et permet ainsi de développer une approche qualitative du transfert de particules des zones d'érosion aux zones de dépôt au sein du bassin Loire-Bretagne. Ces comparaisons qualitatives permettent ainsi d'identifier les zones d'érosion à risque.

Mots clés

Bilan sédimentaire, Erosion de berges, Connectivité, Loire, Eléments dissous.

Particle transfers from hillslopes to water systems in the Loire and Brittany river basin

Abstract

Hillsolpe erosion and sediment transfer in river basins are the major drivers of landscape evolution in Western Europe. Due to the numerous environmental issues associated with soil erosion and redistribution, several studies have been carried out to quantify both processes. At fine spatial scale, monitoring and implementation of physically-based models provide a fine understanding and representation of the sediment transfers. At large spatial scale, the task is hampered by the resolution and quality of the available data, and the understanding and integration of the numerous processes interactions involved in sediment transfers.

In the Loire and Brittany river basin in France (155,000 km^2), the non-achievement of good status in 2015 of the water bodies is partly due to the clogging of streambeds by fine sediment. However, the existing identification of the sources of these particles is confined to the maps of hillslope erosion. Yet, the quantified rates and patterns of such erosion are not in adequacy with the in-field observations of sediment in-stream deposition. Therefore, there is a real need to identify all sources of sediment, and to understand and quantify the dynamics of the sediment connectivity within this area.

In this context, the aim of this study is to provide a large-scale view of the functioning of the Loire and Brittany river basin by developing a sediment budgeting approach and by quantifying each of the compartments of this budget, *i.e.* sources, transfers, and sinks/exports to outlet. The major scientific and technical challenges of this work include i) the development of modelling approaches applied over a large territory displaying various landscape characteristics and using homogeneous database, ii) the identification of the dominant processes and parameters of particle sources and redistribution within a lowland area and including them in the chosen models, and iii) the production of a quantitative and qualitative evaluation of particle redistribution that can be easily used by stakeholders.

Our results indicate that, on the Loire river basin, the sediment stock available from the miscellaneous forms of erosion, namely sheet and rill erosion, gully erosion, mass movement and bank erosion, represents $1.6 * 10^7$ $t.yr^{-1}$ (with contribution from sources to the stock of 77.1%, 12.0%, 4.5%, and 6.4% respectively). Only $\sim$ 5% of these detached particles finally reach the basin outlet indicating a substantial deposition on the way from source to outlet. In parallel, the use of the database of dissolved elements allows us to highlight the importance of the dissolved sediment fluxes ($\sim$90% of the total exports of the Loire river).

The use of 77 sub-catchments allows us to state that there exists a strong spatial

variability of the sediment supply and sediment exports within the study area. However, no correlation between sediment exports and catchment characteristics (*e.g.*, slope, basin area, *etc.*) may explain this variability. This absence of expected correlations emphasizes the differences in the nature of processes and parameters involved in sediment transfers between mountainous and lowland areas, and the role of the spatial distribution of these processes and parameters. The consideration of soil saturation and landscape features (such as hedgerows) in an index of connectivity permits to provide a new insight on hillslope soil redistribution.

Each result is presented at different spatial scales, from pixel-based information to catchment scale values, to provide a qualitative approach of sediment source-to-sink transfers within the Loire and Brittany river basin. This qualitative comparison allows for the identification of hotspots of sediment supply.

Key words

Sediment budget, Bank erosion, Connectivity, Loire river basin, Dissolved sediment yields.

Table des matières

Liste des figures

Liste des tableaux

Introduction générale

Les exports de sédiments depuis les zones de production vers les zones de stockage ou leur export à l'exutoire des bassins versants ont fait l'objet de nombreuses études depuis la deuxième moitié du 19^e siècle et sont aujourd'hui encore au coeur des recherches. En effet, le décapage de la couche superficielle du sol tend à appauvrir les sols et ainsi diminuer leur fertilité. D'autre part, le transfert des particules détachées vers les masses d'eau dégrade la qualité de l'eau *via* le colmatage des lits des rivières et l'apport de nutriments, pesticides et métaux lourds et est également responsable du remplissage des barrages et retenues d'eau. Ces diverses nuisances représentent ainsi un enjeu important pour la ressource en eau, son utilisation à des fins anthropiques ainsi que pour la biodiversité locale.

Contexte législatif

La Directive Cadre européenne sur l'Eau (DCE) adoptée en 2000 fixe un objectif communautaire pour la protection des eaux intérieures de surface, de transition, côtières et souterraines. Pour toutes ces masses d'eau, l'objectif est donc de prévenir et de réduire leur pollution, promouvoir leur utilisation durable, protéger leur environnement, améliorer l'état des écosystèmes aquatiques et atténuer les effets des inondations et des sécheresses. La DCE définit ainsi un cadre législatif pour la gestion et la protection des eaux par grand bassin hydrographique. Les mesures prévues dans le plan de gestion de chaque bassin hydrographique ont pour but, entre autres, d'améliorer l'état écologique et chimique des masses d'eau d'ici 2018.

Au niveau du territoire national français, la métropole est divisée en six districts hydrographiques auxquels correspondent six agences de l'eau. Parmi elle, l'Agence de l'Eau Loire Bretagne (AELB) gère un territoire d'environ 155 000 km^2, soit 28% du territoire métropolitain. En 2009, l'état des lieux pour ce territoire indiquait que "73% des cours d'eau présentent un risque de non atteinte de leurs objectifs environnementaux en 2021" (Comité de Bassin Loire-Bretagne, 2013 [60]). D'autre part, les deux enjeux majeurs identifiés dans l'état des lieux de 2004, et qui concernent d'une part, l'altération morphologique des cours d'eau et la présence des obstacles à l'écoulement et, d'autre part, les pollutions diffuses, restent encore aujourd'hui d'actualité. Le rapport du 3 mars 2015 publié par l'Agence Européenne pour l'Environnement [2] indique que 70 à 90 % des masses d'eau du bassin Loire Bretagne n'atteignent pas le degré de bon état écologique requis (Figure 1). Cette constatation s'explique, en partie, par l'envasement et le colmatage des cours d'eau (Etat des lieux établi par le Comité de Bassin Loire-Bretagne, 2013 [60]) sans que les sources des sédiments responsables ne soient clairement identifiées.

Pour mettre en place un programme de mesures et pallier ainsi ces problèmes, l'AELB s'est essentiellement basée sur les cartes d'aléa érosion de versants existantes

(Le Bissonnais *et al.*, 2002 [160]) afin d'identifier des "zones à risque". Ces cartes mettent en exergue les zones pour lesquelles le détachement de particules peut être le plus important. Cependant, il exite trois limites majeures à l'utilisation de ces cartes pour de telles applications. D'une part, seul le détachement des particules est considéré dans ce type de modèle. Leur transport jusqu'au cours d'eau n'est pas pris en compte ce qui ne permet pas de connaître la quantité de matière réellement exportée des versants vers les masses d'eau et susceptible de colmater le lit des rivières. D'autre part, si beaucoup de connaissances ont été acquises sur les processus mis en jeu dans le détachement et les exports de particules de versant, d'autres sources (érosion des berges, drainage agricole) restent à ce jour négligées dans les bilans sédimentaires. Enfin, le manque de quantification de ces sources de particules ainsi que leur transport au sein des cours d'eau, biaise ces analyses.

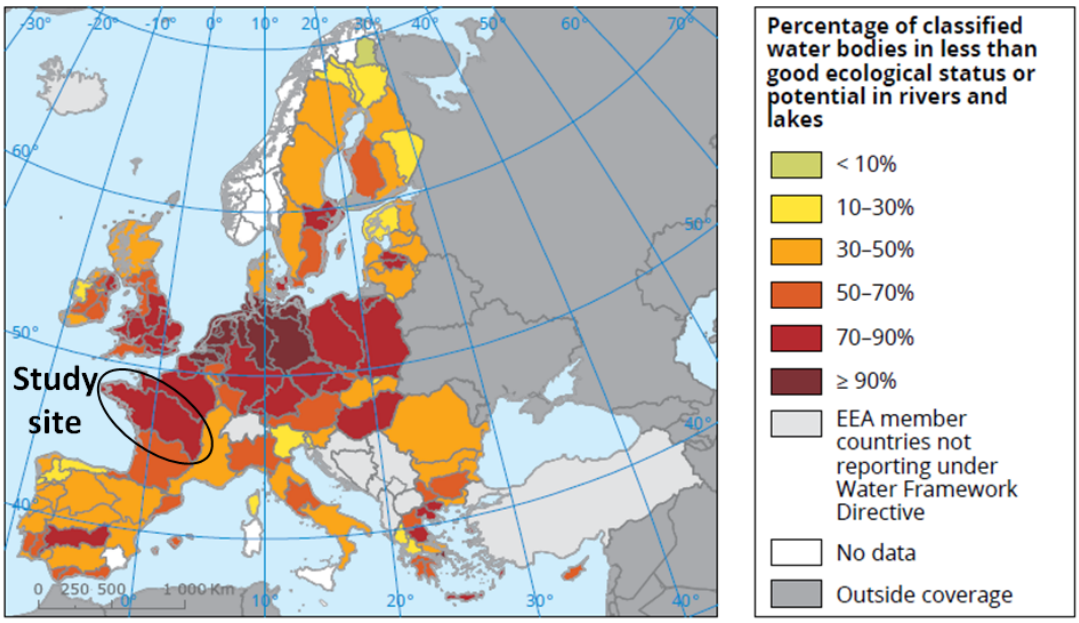

FIGURE 1 – Pourcentage des masses d'eau classées en deça d'un bon état écologique ou d'un bon potentiel écologique dans les rivières et les lacs pour les bassins hydrographiques définis par la Directive Cadre sur l'Eau (d'après l'Agence Européene pour l'Environnement [2]) – *Percentage of classified water bodies in less than good ecological status or potential in river and lakes in Water Framework Directive river basin districts and the study site, the Loire and Brittany river basin (from the European Environment Agency [2])*

Dans ce contexte, il est nécessaire de fournir à l'AELB, des données quantitatives et qualitatives sur l'intégralité des sources de particules ainsi que de leur transport à l'échelle du bassin Loire-Bretagne. Il s'agit donc de trouver une échelle de travail pertinente pour la modélisation au regard des données disponibles mais également au regard du découpage territorial utilisé par les décisionnaires.

Contexte scientifique

La compréhension fine des processus et des paramètres mis en jeu depuis la production jusqu'au dépôt des particules ainsi que leur quantification représente un défi majeur pour les scientifiques. En effet, ces processus sont complexes et s'expriment différement selon l'échelle de travail considérée ou diffèrent totalement d'une échelle à l'autre. Il existe donc plusieurs dynamiques d'évolution hydrogéomorphologiques des paysages dans le temps et dans l'espace en fonction des charactéristiques propres à chaque zone d'étude.

A l'échelle mondiale, les différentes publications issues des recherches font état d'un large panel de méthodologies visant à améliorer la quantification et la modélisation de ces différents processus. Des approches globales permettent de calculer la production locale de particules sur les versants (Wischmeier and Smith, 1978 [318]; Kirkby *et al.*, 2008 [144]; Cerdan *et al.*, 2010 [37]), les flux de matières à l'exutoire des grands bassins hydrographiques (Milliman and Meade, 1983 [192]; Milliman and Syvitsky, 1992 [193]; Ludwig and Probst, 1998 [174]), et de faire le lien entre production et export (Walling, 1983 [298]).

A l'échelle locale des petits bassins versants, la mise en place d'instrumentation permet de fournir une vision détaillée et quantifiée des différents processus liés à la production et au transfert de particules. Si l'utilisation de modèles distribués ou à base-physique permet de retranscrire la distribution spatiale et temporelle de chacun de ces processus et de fournir en sortie des grandeurs comparables aux mesures de terrain, le nombre de données requises représente un frein à leur utilisation à plus large échelle (Takken *et al.*, 1999 [268]).

L'un des apports clé de la fin du 19^e pour la compréhension du fonctionnement d'un bassin versant repose sur l'établissement de bilans sédimentaires (Dietrich *et al.*, 1982 [74]; Walling *et al.*, 2002 [300]). Ces bilans sont à l'heure actuelle toujours fortement employés car ils permettent de dresser un portrait global du bassin versant (Wilkinson *et al.*, 2013 [315]) ou d'une unité de bassin versant (Frings *et al.*, 2013 [92]), quelle que soit sa taille. Pour chaque compartiment du paysage, versant/rivière/exutoire, les entrées et sorties des particules sont considérées tout en tenant compte plus en détail des processus et paramètres en jeu au sein de chaque compartiment. De plus, les bilans sédimentaires permettent d'approcher les notions de changement d'échelle (Slaymaker, [261]) et ils constituent un outil de management facilement utilisable par les gestionnaires des bassins versants (Owens, 2005 [217]).

Récemment, l'essort du terme de "connectivité" a permis d'offrir un nouveau regard sur le transfert de sédiments via le développement de nouveaux concepts et outils pour mesurer et modéliser ces transferts et améliorer la compréhension du fonctionnement des bassins versants. Les résultats issus de ces recherches sont encourageants et indiquent que la prise en compte de la connectivité est primordiale dans l'évaluation des transferts de particules au sein de chaque compartiment du bilan sédimentaire (Delmas, 2011 [68]) mais également entre ces différents compartiments (Fryirs, 2013 [93]). Cependant, une grande majorité des études se focalise soit d'une part, sur des petits bassins

versants dont les résultats ne peuvent être extrapolés à l'échelle des grands bassins hydrographiques, soit d'autre part, sur les zones de montagne où les processus mis en jeu dans le transfert de particules diffèrent de ceux des zones de plaine. Ces études apportent donc une connaissance fine de ces divers aspects pour des zones particuliaires. Cependant, il existe peu d'étude intégratrice de ces processus sur de larges territoires avec des paysages contrastés.

Dans ce contexte, il est nécessaire d'améliorer la prise en compte des processus mis en jeu dans la connectivité sédimentaire des zones de plaine mais également, d'inclure cette connectivité dans l'établissement des bilans sédimentaires.

Problématiques, objectifs et structuration du mémoire

L'objectif de ce travail est de proposer une étude à large échelle du fonctionnement du bassin Loire-Bretagne en dressant un bilan sédimentaire global du bassin tout en tenant compte de la distribution spatiale des processus et paramètres en jeu dans les différents aspects de production, transfert et dépôt des particules. Les défis scientifiques et techniques sont d'une part, de proposer une modélisation homogène sur tout le site d'étude, qui tiennent compte de l'hétérogénéité des processus en jeu et des caractéristiques du bassin versant, et d'autre part, d'intégrer la notion de connectivité dans l'évaluation des transferts de particules, notamment dans les zones de plaine. De plus, la limite imposée par la disponibilité des bases de données, qui sont en constante évolution en terme d'homogénéité sur le territoire considéré, de qualité et de résolution spatiale, représente un défi récurrent dans la mise en place des différentes approches proposées dans cette étude. L'originalité de notre étude repose donc principalement sur l'échelle de travail adoptée qui, de par la taille du site d'étude, représente un challenge majeur. Enfin, il est également nécessaire de trouver un compromis dans la représentation des résultats pour que ceux-ci soient exploitables tant par la communauté scientifique que par les décisionnaires de l'Agence de l'Eau Loire Bretagne.

Ce manuscrit s'articule donc autour des trois grandes composantes du bilan sédimentaire, sources - transfert/dépôt - exports des sédiments, auxquelles correspondent trois grandes parties.

Le premier objectif de ce travail est de quantifier les **exports de sédiments à l'exutoire de bassins versants**. La collecte et la création de bases de données homogènes pour tout le site d'étude, et la mise en place de démarches de modélisation cohérentes avec les données disponibles sont réalisées. Les bases de données d'exports établies procurent un premier aperçu des transferts solides et d'éléments dissous au sein du site d'étude. Cette première partie se décline en trois chapitres:

Le chapitre 1 présente le site d'étude, le bassin Loire-Bretagne, sous les différents aspects topographiques, géologiques, climatiques, hydrologiques et d'occupation du sol. Nous dressons également un état des lieux des bases de données homogènes existantes pour ce site d'étude et auxquelles nous nous référons tout au long de ce travail.

Le chapitre 2 vise à quantifier les exports de sédiments à l'échelle de 111 sous-bassins versants sélectionnés. A l'issu de ce chapitre, 77 bassins versants présentant une moyenne annuelle stable de flux de sédiments sont conservés comme base de données pour toutes les analyses postérieures et dans l'établissement des bilans sédimentaires.

Le chapitre 3 propose une quantification des flux d'éléments dissous à l'exutoire de 90 bassins versants. Les flux d'éléments dissous et les flux solides sont comparés permettant de mettre en exergue l'importance de la charge dissoute dans les exports totaux des bassins versants.

Le second objectif de ce travail est de **quantifier la production de particules** *via* l'identification des sources potentielles de versants et de cours d'eau. La quantification de chaque source repose sur des aspects bibliographiques et la mise en place de modèles adéquats. Trois chapitres constituent cette seconde partie:

Dans *le chapitre 4*, les sources potentielles de particules sur les versants et leur quantification sont identifiées à partir de la littérature existante. Ce chapitre apporte également des propositions de modélisation de certains processus pour lesquels les données quantifiées à notre échelle de travail ne sont pas disponibles ou trop imprécises.

Dans *le chapitre 5*, l'érosion de berges à l'échelle du bassin Loire-Bretagne est quantifiée au moyen d'un modèle empirique simple. La contribution de cette source dans les bilans sédimentaires est ainsi évaluée et permet de compléter le compartiment "source" du bilan.

Enfin, le troisième objectif de ce travail est de **faire le lien entre sources de particules et dépôt ou exports à l'exutoire à l'échelle du paysage** en considérant les processus et paramètres mis en jeu dans la *connectivité* des versants. Cette dernière partie permet de modérer les apports de la production locale de particules des versants dans les bilans sédimentaires, et s'organise selon trois chapitres:

Le chapitre 6 propose une succinte revue bibliographique de la notion de connectivité et dresse le panel des définitions et des concepts proposés par la communauté scientifique. L'accent est mis sur les processus et paramètres mis en jeu dans la connectivité des zones de plaine.

Le chapitre 7 se focalise sur un processus de connectivité hydrologique de versant, le ruissellement par saturation. Ainsi, nous proposons un indice de connectivité, modifié à partir de nos connaissances sur la connectivité des zones de plaines et d'un indice topographique existant dans la litérature.

Le chapitre 8 intègre l'aspect structural de la connectivité de versant. Les haies, éléments structurant le paysage et caractéristiques majeures des zones agricoles de la Bretagne et du Massif Central, sont intégrées dans l'indice de connectivité modifié, et permettent ainsi de proposer *in fine* un bilan net des apports de versants aux cours d'eau.

Enfin, dans un chapitre de conclusion, nous reprenons les différents résultats de ces études afin de dresser un bilan sédimentaire global à l'échelle du bassin de la Loire. Les limites ainsi que les persectives de cette étude y sont exposées.

Première partie

Le bassin Loire-Bretagne et mise en place des bases de données d'exports solides et dissous

Chapitre 1

Présentation du bassin Loire-Bretagne et des bases de données

Ce manuscrit de thèse représente un ensemble cohérent et articulé autour de l'établissement du bilan sédimentaire du bassin Loire-Bretagne. Cependant, les thématiques abordées dans les différents chapitres sont très diverses. Aussi, tous les chapitres qui constituent ce manuscrit peuvent être lus indépendamment les uns des autres et sont composés d'une brève revue bibliographique, d'une présentation du site d'étude et des bases de données utilisées, adaptées en fonction du thème abordé dans l'étude.

Afin de proposer une vision globale préliminaire des caractéristiques du bassin Loire-Bretagne, le but de ce chapitre est de dresser un portrait général du site d'étude, ainsi que des données disponibles qui ont été utilisées dans ce travail. Dans un premier temps, les ressources informatiques utilisées (bases de données et logiciels) sont décrites. Dans un deuxième temps, les caractéristiques topographiques, géologiques, d'occupation du sol et climatiques sont présentées.

Sommaire

1.1 Ressources informatiques et bases de données

De nombreuses bases de données (BD) ont été mobilisées pour le travail présenté dans ce manuscrit. Pour un même paramètre, plusieurs BD sont parfois disponibles. Le choix d'une BD est basé sur: i) la résolution temporelle et/ou spatiale de la donnée, ii) la disponibilité de la BD, et iii) l'homogénéité de la donnée sur toute la zone d'étude. Les différentes BD retenues ainsi que leurs caractéristiques sont présentées dans le tableau 1.1. La description de chaque BD n'est pas exhaustive et ne sont cités que les paramètres qui ont été utilisés. Les limites propres à chaque base de données sont exposées par la suite dans le manuscrit en fonction de l'utilisation qui en est faite dans les études proposées.

La mise en forme et l'exploitation des données recueillies ont été réalisées grâce à des logiciels de SIG (sous ARCGIS 10.1 et interface python Arcpy) et de programmation (MATLAB 2012a et PYTHON 2.6.).

Tableau 1.1: Bases de données utilisées et leurs caractéristiques globales – *Database used in the study and their general characteristics*

Nom	Détails
HYDRO	Description : Banque Hydro fournit pour chaque station hydrométrique des valeurs de débit moyen journalier calculées à partir de hauteur d'eau et de courbes de tarage. Gestion : Service Central d'Hydrométéorologie et d'Appui à la Prévision des Inondations (SCHAPI) Référence : http://www.hydro.eaufrance.fr
OSUR2WEB	Description : Base de données issue des principaux réseaux de surveillance de la qualité des cours d'eau et des plans d'eau en Loire Bretagne. Elle fournit entre autres des valeurs de concentrations en matières en suspension, de concentration en éléments chimiques et des valeurs de conductivité. Gestion : Agence de l'eau l'Eau Loire-Bretagne (AELB)

Nom	Détails
	Référence : http://www.osur.eau-loire-bretagne.fr/exportosur/
BD Alti	Description : Modèle numérique de terrain (MNT) maillé (résolution de 50 * 50 m) établi à partir des scans de cartes au 1:25,000 1:50,000 et photographies aériennes au 1:20,000, 1:30,000 et 1:60,000. Gestion : Institut national de l'information géographique et forestière (IGN) Référence : http://professionnels.ign.fr/bdalti
Corine Land Cover	COoRdination de l'INformation sur l'Environnement Description : Carte d'occupation des sols sur une grille de 50 * 50m pour 38 états européens issue de la photo-interprétation d'images satellitales. Gestion : Agence européenne pour l'environnement. En France : Service de l'Observation et des Statistiques du Commissariat Général au Développement Durable (CGDD) du Ministère de l'écologie (MEDDE) Référence : http://www.statistiques.developpement-durable.gouv.fr/donnees-ligne/li/1825.html
RPG	Référentiel Parcellaire Graphique Description : Système d'information géographique permettant l'identification des parcelles agricoles (ou îlots parcellaires) pour chaque année civile. Cette donnée est issue des déclarations des exploitants agricoles de surfaces cultivées. Gestion : Agence de services et de paiement (ASP) Référence : https://www.data.gouv.fr/fr/datasets/registre-parcellaire-graphique-2010-contours-des-ilots-culturaux-et-leur-groupe-de-cultures-majorita/
RGA	Recencement Général Agricole Description : Système de questionnaires qui fournit pour chaque année civile et parcelle cultivée des informations relatives aux types de cultures, surface agricole utile, drainage agricole, etc. Gestion : Ministère de l'agriculture, de l'agroalimentaire et de la forêt Référence : http://www.agreste.agriculture.gouv.fr/enquetes/recensements-agricoles/
SOLAGRO	Description : Statistiques de linéaires de haies issues des données de l'Inventaire Forestier National (IFN) et infrastructures agroécologiques. Gestion : SOLAGRO Référence : Pointereau *et al.* 2007 [227]
BDTopo	Description : Description vectorielle 3D des éléments du territoire. Le champ "NATURE" de la base fournit des informations sur la végétation et notamment les haies. Gestion : Institut national de l'information géographique et forestière (IGN) Référence : http://professionnels.ign.fr/bdtopo
SAFRAN	Système d'Analyse Fournissant des Renseignements Atmosphériques à la Neige

Nom	Détails
	Description : système dŠanalyse à mésoéchelle de variables atmosphériques près de la surface. La donnée (cumul de pluie) au pas de temps journalier est fournie sous forme d'une grille (8 * 8 km) pour les 13 années de 1998 à 2010. Gestion : Météo France Accès aux données pour la recherche
ESDB v2.0	European Soil Database V2.0 Description : Base de données européenne sur les sols et sous-sols (échelle : 1:1 000 000). Gestion : Joint Research Centre (JRC) Référence : http://eusoils.jrc.ec.europa.eu/esdb_archive/ESDB/Index.htm
HWSD	Harmonized World Soil Database v1.2 Description : Base de données mondiale sur les sols et sous-sols (échelle : 1:1 000 000). Gestion : FAO/IIASA/ISRIC/ISS-CAS/JRC [85] Référence : http://webarchive.iiasa.ac.at/Research/LUC/External-World-soil-database/HTML/
BDCarthage	Base de Données sur la CARtographie Thématique des AGences de l'Eau et du Ministère de l'Environnement Description : Référentiel national des milieux aquatiques de surface (cours d'eau, plans d'eau). Gestion : Institut national de l'information géographique et forestière (IGN) Référence : http://www.sandre.eaufrance.fr/
SYRAH_CE USRA	Système Relationnel d'Audit de l'Hydromorphologie des Cours d'Eau Unités Spatiales de Recueil et d'Analyse Description : Outil d'évaluation des altérations physiques des cours d'eau. Gestion : Institut national de Recherches en Sciences et Technologies pour l'Environnement et l'Agriculture (IRSTEA) Référence : https://hydroeco.cemagref.fr/hydromorphologie/documents-a-telecharger
ROE	Référentiel d'Obstacle à l'Ecoulement Description : Base de données spatialisée des obstacles à l'écoulement. Gestion : Office National de l'Eau et des Milieux Aquatiques Référence : http://www.eaufrance.fr/observer-et-evaluer/pressions-sur-les-milieux/alterations-hydromorphologiques/
BDMvT	Base de données mouvements de terrain Description : Système de recueil, d'analyse et de restitution des informations sur les glissements de terrain, éboulements, effondrements, coulées de boue, érosion en France. Gestion : Bureau des Recherches Géologiques et Minières (BRGM) Référence : http://www.bdmvt.net/

1.2 Généralités sur le bassin Loire Bretagne

La France métropolitaine est découpée en six grands bassins hydrographiques auxquels correspondent six Agences de l'Eau (Figure 1.1). Le bassin Loire-Bretagne (*LBRB* par la suite) est l'un d'eux et s'étend sur $\sim$ 155 000 km^2 représentant ainsi 28 % du territoire métropolitain. Situé à la fois dans les terres et sur la zone côtière, il compte $\sim$ 2600km de côtes soit 40 % de la façade maritime métropolitaine. D'un point de vue administratif, il regroupe 36 départements, soit 10 régions, plus de 7300 communes et 12 millions d'habitants. D'un point de vue hydrographique, il est découpé en trois sous parties (Figure 1.2) : le bassin de la Loire et ses affluents ($\sim$ 117 800 km^2), les bassins côtiers bretons ($\sim$ 30 000 km^2) et côtiers vendéens ($\sim$ 117 800km^2). D'autres découpages hydrographiques sont évoqués par la suite. En effet, le découpage généralement utilisé pour la prise de décisions par les agences de l'eau est un découpage par "masses d'eau". Le *LBRB* en compte 2122 de taille variable, et pouvant correspondre à un simple plan d'eau et ses alentours (0.3 km^2), jusqu'à 1492.9 km^2 correspondant à la Conie et ses affluents (région de la Beauce).

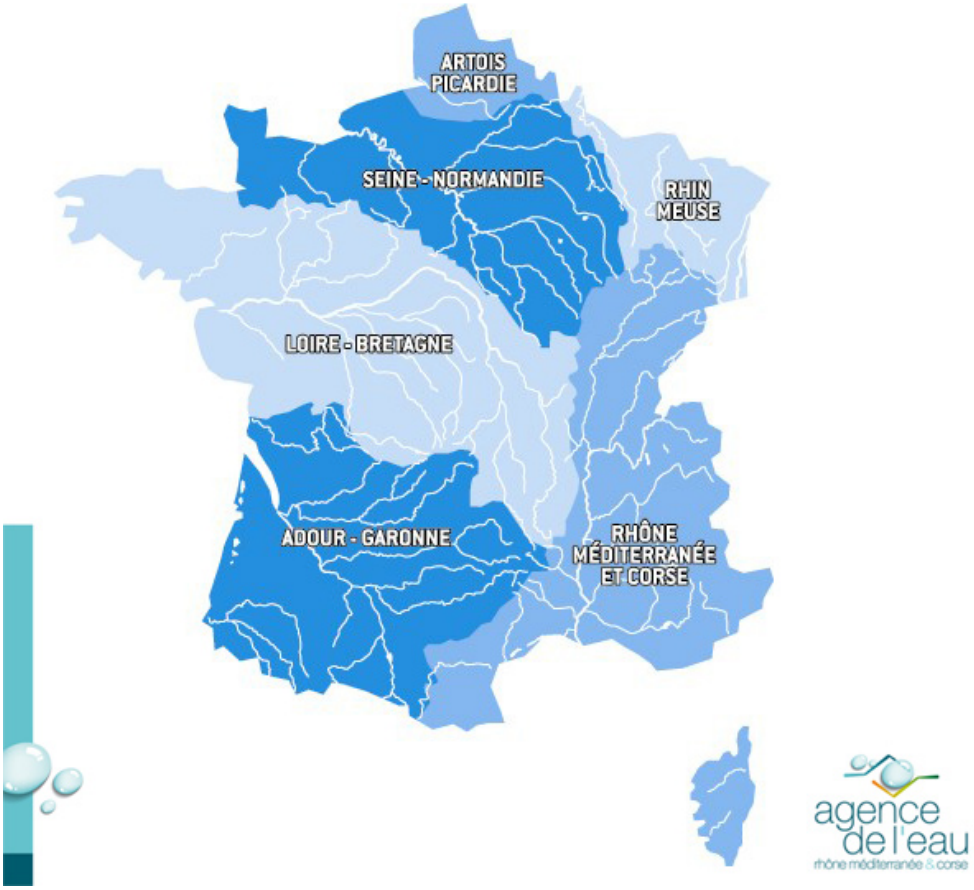

FIGURE 1.1 – Les six bassins hydrographiques de France métropolitaine – *The six hydrographic river basin of the French metropolitan territory*

1.3 Relief

Le relief du bassin de la Loire (Figure 1.2) est très contrasté. En amont, le Massif Central correspond à une zone de montagne avec un point culminant à 1847m et des pentes fortes allant jusqu'à 134.7 %. Plus en aval, le relief s'aplanit et laisse place à des zones de plaine. En Bretagne, le relief est également contrasté avec des zones de montagne au centre (altitude maximale = 385m, pentes maximales = 86.9 %) et des zones plus plates sur le pourtour côtier. La Vendée est un territoire peu contrasté en terme de topographie (altitude maximale = 278m, pente maximale = 52.2 %).

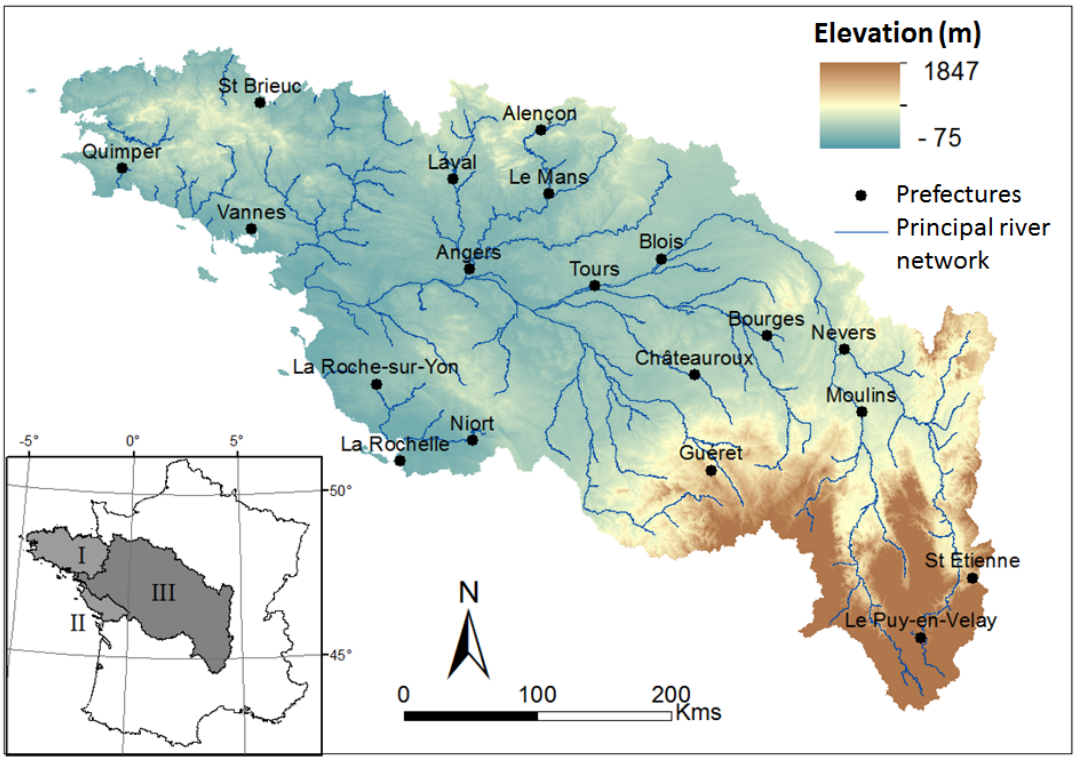

FIGURE 1.2 – Domaine de l'étude : le bassin Loire – Bretagne et altitudes issues du MNT (BDALTI ®). Les chiffres romains indiquent les trois régions hydrographiques : I la Bretagne, II la Vendée et III le bassin de la Loire – *Study site: The Loire and Brittany river basin and elevation from the DEM (BDALTI ®). Roman numerals correspond to the three hydrographic regions: I Brittany, II Vendée, and III the Loire river basin*

1.4 Hydrologie

La Loire, plus grand fleuve de France, s'étend sur 1013 km et compte plusieurs affluents notoires (longueur > 300 km) tels que le Cher, la Vienne, ou l'Allier. Son régime est de type pluvial avec des débits plus importants l'hiver et plus faibles l'été.

Son débit annuel moyen est de 911 $m^3.s^{-1}$ à Saint Nazaire. En Bretagne, de nombreux cours d'eau côtiers existent et le fleuve le plus important en terme de longueur et de débit dans cette zone est celui de la Vilaine (220 km, débit moyen annuel 76 $m^3.s^{-1}$ à Rieux). Au sein du *LBRB*, on compte environ 136 000 km de linéaire de cours d'eau (d'après la BD Carthage, Figure 1.3).

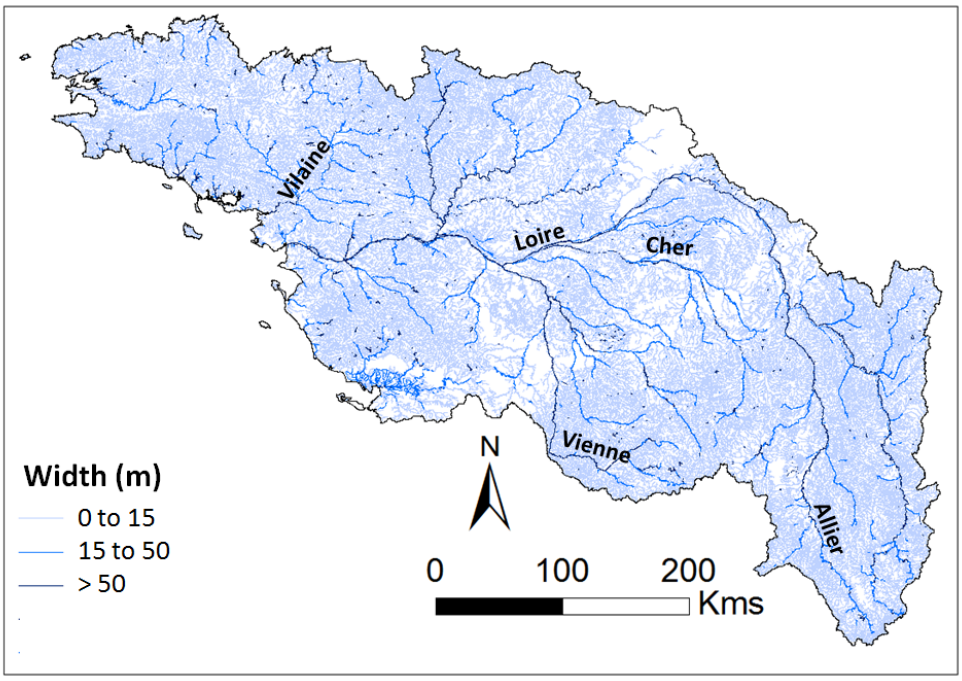

FIGURE 1.3 – Réseau hydrographique de surface sur le bassin LB (d'après la BD Carthage) – *Surface water network on the Loire and Brittany river basin, LBRB (BD Carthage)*

Ce réseau hydrographique est très dense sur les zones de fort ruissellement, principalement à l'ouest et à l'est du bassin où la densité de drainage atteint 3.17 $km.km^{-2}$ (Figure 1.4). Au centre du bassin, le réseau hydrographique est peu présent et correspond à des zones de forte infiltration, notamment en région de Beauce où la densité de drainage est la plus faible avec une moyenne de 0.04 $km.km^{-2}$.

Bien que considérée comme l'un des derniers fleuves sauvages d'Europe, plusieurs barrages (Grangent et Villerest sur la Loire, Figure 1.6, et Naussac sur l'Allier) ainsi que les prélèvements d'eau pour les usages industriels, agricoles, d'alimentation en eau potable ou de production d'électricité modifient le régime de son débit et la continuité sédimentaire. En effet, de nombreux obstacles à l'écoulement, référencés par le ROE, sont présents sur tout le bassin. Ces divers obstacles (barrages, digues, épis en rivière, grilles de pisciculture, obstacles induits par un pont, seuils en rivière) sont au nombre de 20688 (hors ouvrages entièrement détruits ou obsolètes, Figure 1.5), dont 3943 correspondent à des barrages au sens du ROE, i.e. "un barrage est un ouvrage qui barre plus que le lit mineur d'un cours d'eau permanent ou intermittent ou un talweg.

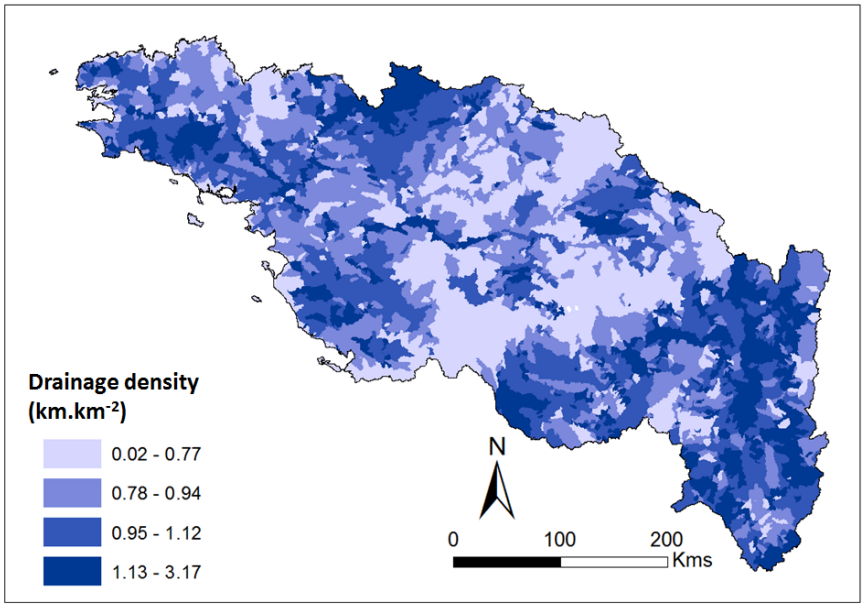

FIGURE 1.4 – Densité de drainage par masse d'eau – *Drainage density per watershed*

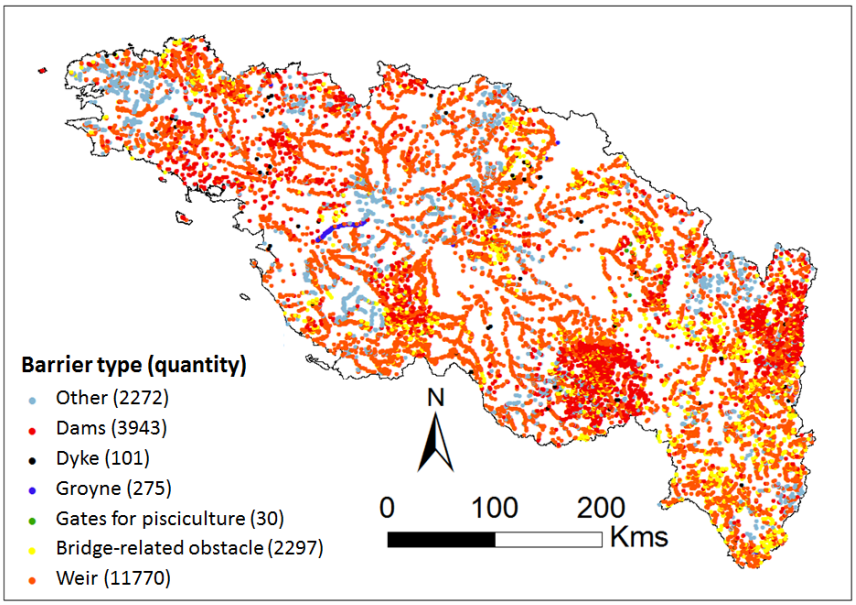

FIGURE 1.5 – Obstacles à l'écoulement sur le bassin Loire-Bretagne (hors obstacles détruits entièrement et obsolètes) d'après le référentiel des obstacles à l'écoulement (ROE) – *Barriers in rivers of the LBRB (except obsolete or entirely dismantled obstacles) from the référentiel des obstacles à l'écoulement (ROE)*

Un barrage peut être composé d'un élément fixe, d'un élément mobile ou des deux simultanément (composition mixte)". Ces obstacles sont ainsi susceptibles de modifier

le débit des cours d'eau, de bloquer le transfert des sédiments d'amont en aval mais également de modifier les processus d'érosion.

1.5 Géologie

La géologie du *LBRB* est très contrastée et regroupe trois grands ensembles (Figure 1.6). Le centre est constitué de roches sédimentaires appartenant à la partie sud du bassin parisien et la partie nord du bassin aquitain. De part et d'autre se trouvent des massifs cristallins : le Massif Central au sud-est et le Massif Armoricain à l'ouest.

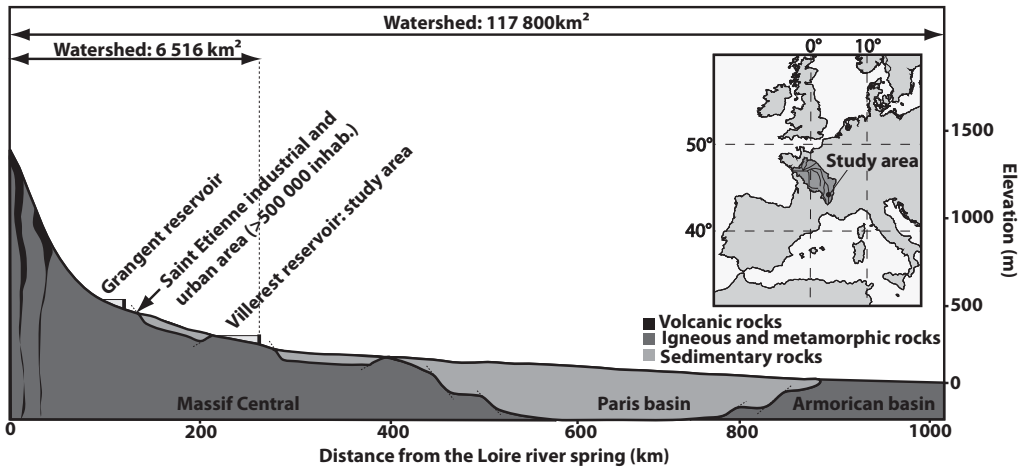

Location of the study area in the Loire river topographic and geologic profil (modified from Lino et al, 2000)

FIGURE 1.6 – Coupe géologique de la Loire (d'après Dhivert, 2014 [73]) – *Geologic profile of the Loire river (from Dhivert, 2014 [73])*

Le Bassin Parisien est un bassin sédimentaire approximativement semi-circulaire qui couvre la moitié nord de la France. Les formations géologiques, du Trias au Tertiaire, sont disposées en auréoles concentriques dont les plus récentes affleurent au centre et les plus anciennes en périphérie (Figure 1.7). Les grandes formations aquifères du bassin de la Loire sont situées dans la partie centrale du bassin. Sur les pourtours du bassin de Paris, des karstifications locales dans les formations carbonatées du jurassique peuvent exister. Le Massif Central est principalement composé de granites et un peu de formations volcaniques. La plaine de la Limagne située dans les vallées de l'Allier et de la Loire en amont de la confluence de ces deux fleuves, résulte du comblement par des formations détritiques d'un bassin d'effondrement. Le Massif Armoricain est caractérisé majoritairement par la présence de granites au nord et au sud et d'une alternance de schistes et grès au centre.

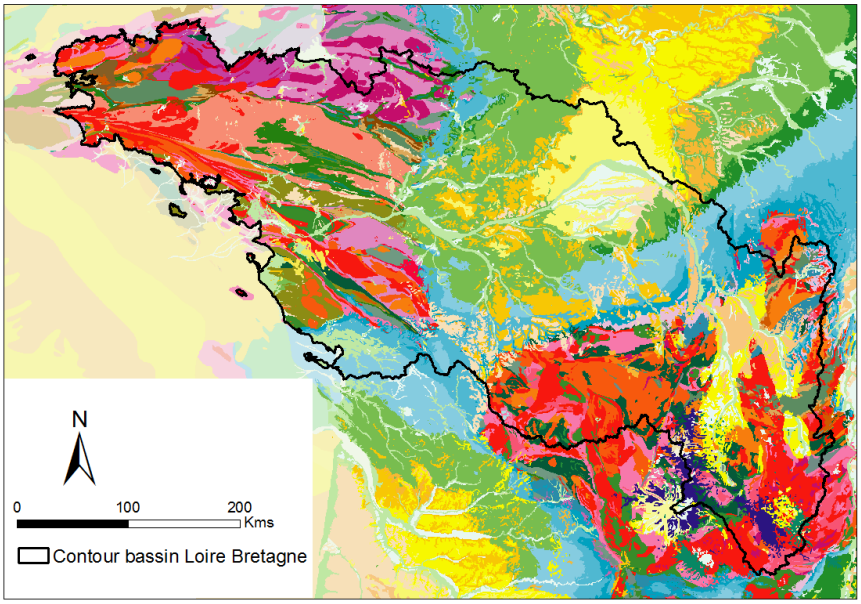

(a)

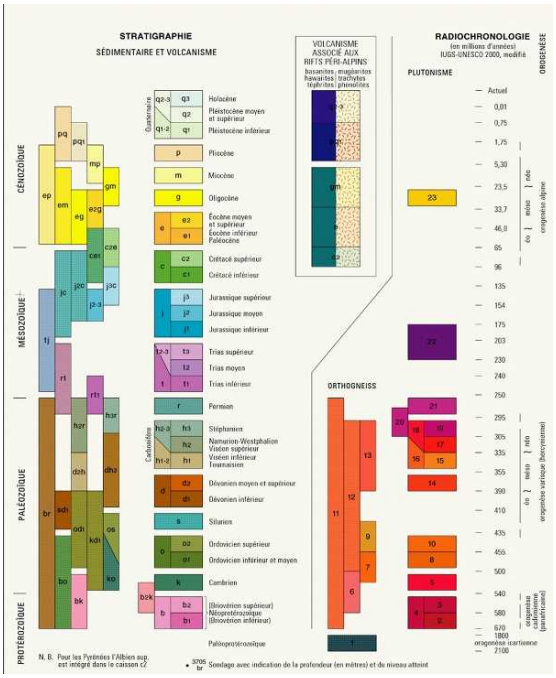

(b)

FIGURE 1.7 – (a) Géologie du bassin Loire Bretagne et (b) échelle des temps géologiques – *(a) Geology of the LBRB, and (b) Geologic time scale*

1.6 Occupation du sol

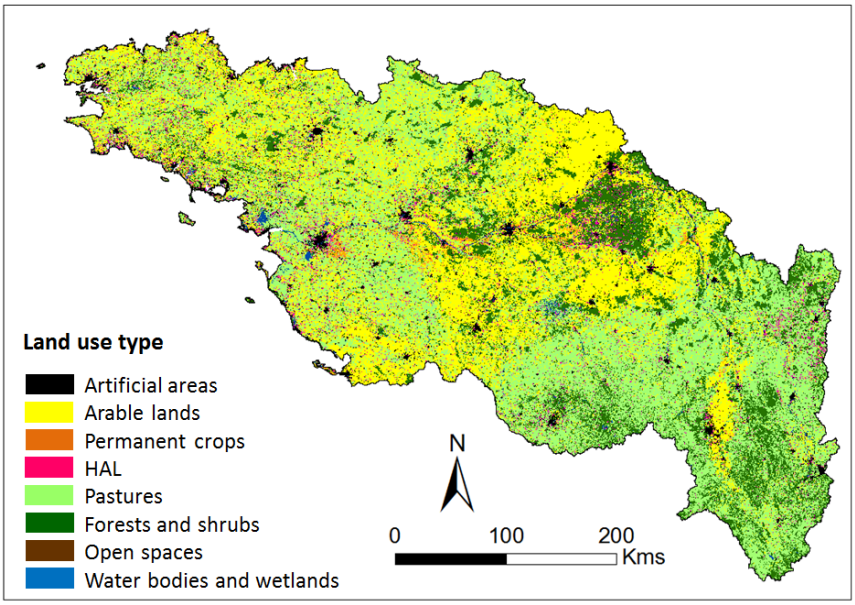

(a)

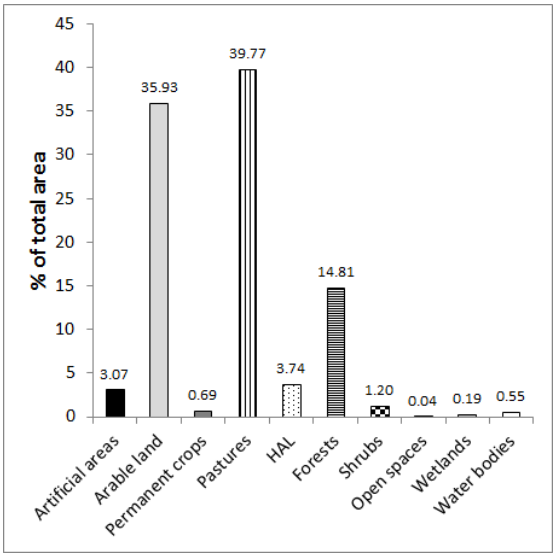

(b)

FIGURE 1.8 – Occupation du sol sur le territoire Loire Bretagne avec (a) Répartition géographique des types d'occupation du sol, et (b) Répartition statistique de l'occupation des classes. HAL = Heterogeneous Agricultural Lands (D'après Degan *et al., in prep* [67]) – *Land use type on the LBRB with (a) Geographic distribution of land use types, and (b) Statistical distribution of each land use type. HAL = Heterogeneous Agricultural Lands (from Degan et al., in prep [67])*

Trois données d'occupation du sol à des résolutions différentes sont disponibles sur le territoire Loire Bretagne. Elles ont été combinées par Degan *et al., in prep* [67] pour produire d'une part, une carte d'occupation du sol et d'autre part, une carte de taux de couvert végétal par saison, intégrant les rotations culturales sur trois ans (2008, 2009 et 2010). Les auteurs ont ainsi utilisé deux BD relatives au domaine agricole : le RPG (Référentiel Parcellaire Graphique) de 2008, 2009 et 2010, fournit une carte de polygones des îlots parcellaires ainsi que des informations précises sur le type de culture pratiqué au sein de chaque parcelle pour chaque année donnée, et le RGA 2010 (Recensement Général Agricole) permet d'apporter des informations sur les cultures saisonnières (*e.g.*, blé d'hiver, cultures de printemps). Enfin, la BD Corine Land Cover 2006 est utilisée pour compléter l'occupation du sol pour les zones où l'information est manquante (*e.g.*, forêts, zones urbaines). Cette BD est structurée en trois niveaux, du plus général (niveau 1), avec 5 catégories d'occupation du sol, au plus détaillé (niveau 3) avec 44 catégories et un niveau intermédiaire (niveau 2) à 15 catégories.

Le bassin Loire Bretagne est essentiellement dédié à l'agriculture (Figure 1.8(b)). En effet, les territoires agricoles constituent 80.13 % du bassin, dont 44.63 % sont dédiés aux cultures diverses (blé, orge, maïs, colza, *etc.*), 49.63 % aux prairies, 0.86 % aux cultures permanentes et 4.67 % aux cultures hétérogènes. Le reste du bassin est constitué de forêts (14.81 % du bassin) et de territoires artificialisés (3.07 % du bassin). D'un point de vue géographique (Figure 1.8(a)), la majorité des forêts se situe dans les zones montagneuses de l'amont du bassin de la Loire (Massif Central) ainsi qu'au niveau du Val de Loire (forêt d'Orléans et de Sologne). A l'inverse, les terres arables se situent sur les pourtours du bassin parisien et dans les plaines de la Limagne tandis que les prairies sont localisées sur les zones plus montagneuses en Bretagne et dans le Massif Central.

D'autre part, de fortes disparités dans les pratiques agricoles et environnementales existent sur le territoire. En effet, dans les années 1970, les politiques d'intensification de l'agriculture et du remembrement agricole ont conduit, d'une part, à l'arrachage massif des haies bocagères dans le but de regrouper les parcelles entre elles et, d'autre part, à l'implémentation de nombreux drains enterrés afin de cultiver de nouvelles surfaces. Aujourd'hui, certains drains ne sont plus actifs du fait de leur colmatage ou d'une utilisation différente des terres. Cependant, d'autres sont toujours entretenus. La Figure 1.9(a) présente la part de la superficie agricole utile (SAU) drainée pour chaque canton. Pour ce qui est des haies, de nouvelles politiques ont émergées depuis les années 1990, incitant à la remise en place du bocage. La Figure 1.9(b) présente la densité du linéaire de haies par SAU pour chaque commune.

D'après ces deux figures, deux ensembles peuvent être distingués. D'une part, au centre du bassin et dans la plaine de la Limagne, les zones agricoles dédiées aux céréales prédominent avec une forte part de SAU drainée et très peu de haies. D'autre part, en Bretagne et dans le Massif Central, le bocage est plus dense et la part de SAU drainée est très faible, ce qui est principalement dû au fait d'une occupation du sol à dominante pastorale et des fortes pentes qui permettent l'évacuation des eaux de pluie.

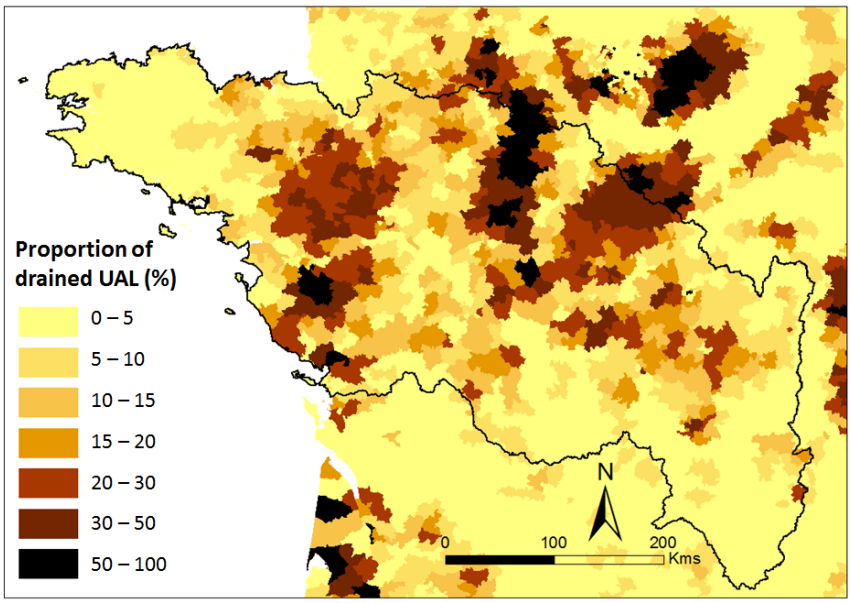

(a)

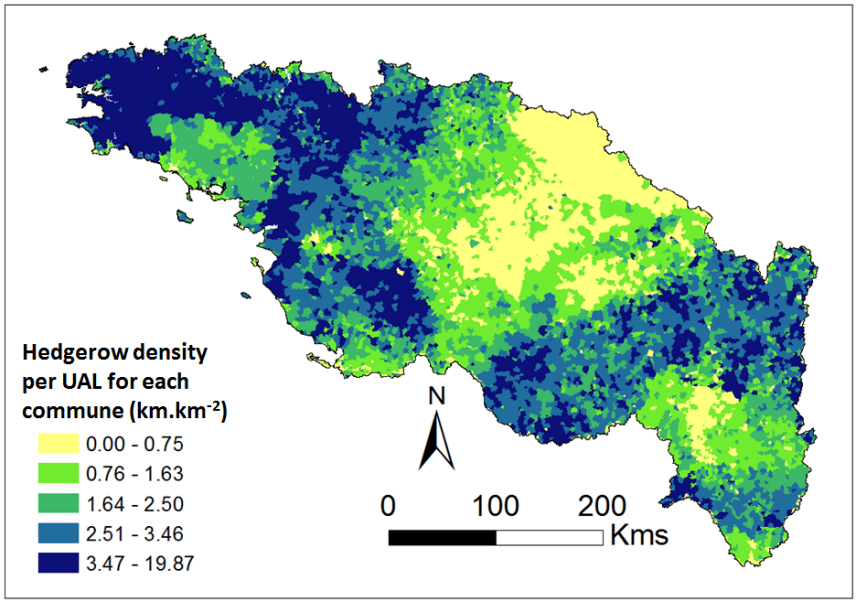

(b)

FIGURE 1.9 – (a) Part de la superficie agricole utile (SAU) drainée dans chaque canton (d'après les statistiques du RGA 2010) et (b) densité du linéaire de haies par SAU dans chaque commune (d'après les données SOLAGRO, Pointereau *et al.*, 2007 [227]) – *(a) Proportion of drained Usable Arable Land (UAL) in each canton (statistics of the RGA 2010) and (b) Density of hedgerows per UAL in each commune (SOLAGRO, Pointereau et al., 2007 [227])*

La Figure 1.9(b) souligne également les disparités existant au sein d'une même don-

née. En effet, les données du linéaire de haies sont issues de campagnes cartographiques s'étendant de 2000 à 2008. Ainsi, les communes de certains départements se dénotent comme dans le Morbihan pour lequel les valeurs de densité de haies sont nettement plus basses que celles affichées dans les communes de la région de la Bretagne.

1.7 Aspect climatique

Il existe de fortes disparités climatiques sur le $LBRB$. Les distributions de précipitations (Figure 1.10(a)) indiquent des précipitations abondantes sur les reliefs montagneux du Massif Central, du Morvan et du Massif Armoricain (cumul moyen annuel $>$ 1200 mm). Toutefois, la distribution des intensités de pluies (Figure 1.10(b)) est plus homogène. Les intensités de pluie les plus fortes se retrouvent dans le bassin amont de la Loire (Massif Central, intensité $>$ 12mm/jour de pluie) et correspondent aux événements cévenoles, tandis que les intensités de pluies les plus faibles se retrouvent dans le nord du $LBRB$, par exemple en région de Beauce et nord Bretagne (intensité $\sim$ 5 mm/jour de pluie).

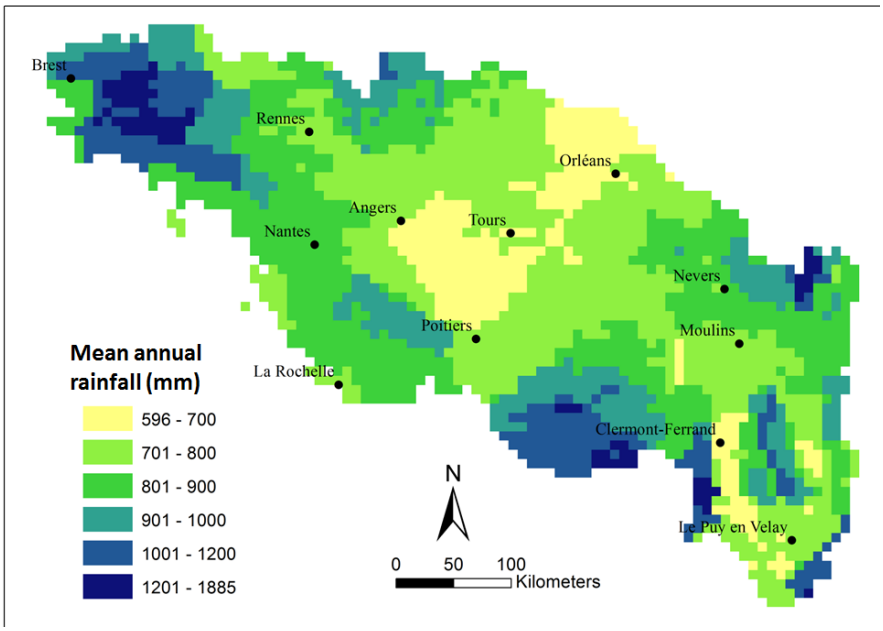

(a)

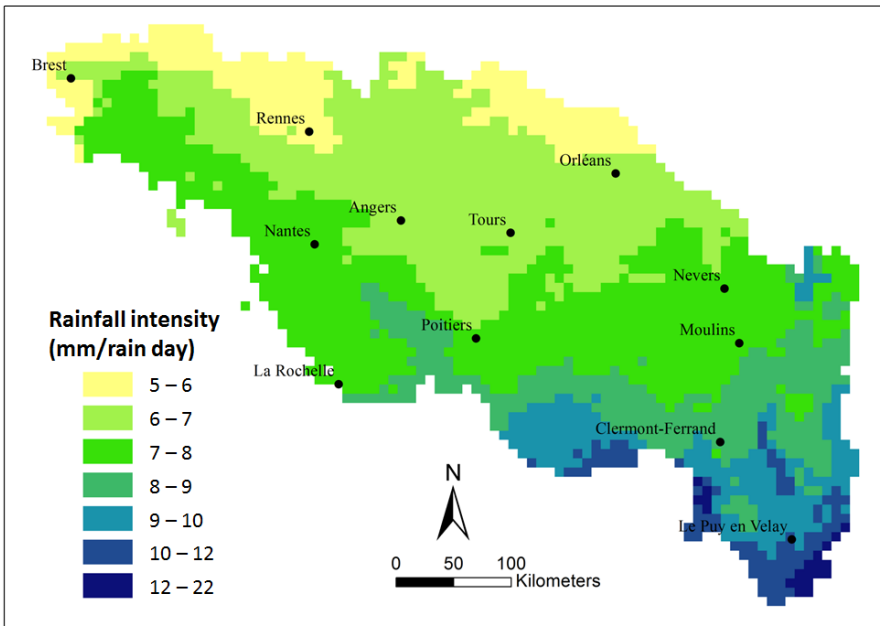

(b)

FIGURE 1.10 – Caractéristiques pluviométriques du bassin Loire Bretagne sur la période 1998 - 2010 (d'après la BD SAFRAN) avec (a) le cumul moyen annuel et (b) les intensités moyennes de pluie (en quantité de pluie par jour de pluie) – *Rainfall characteristics of the LBRB for the period from 1998 to 2010 (BD SAFRAN) with (a) The annual rainfall amount, and (b) The rainfall intensity (rainfall amount per rain day)*

Chapitre 2

Variabilité des flux de sédiments au sein du bassin de la Loire (France)

Après la collecte et la mise en forme des bases de données disponibles présentées dans le chapitre 1, l'objectif de ce chapitre est de calculer des flux sédimentaires à l'exutoire de 111 sous bassins versants sélectionnés dans le site d'étude en utilisant des données homogènes et une méthode de calcul unique afin de proposer une étude comparative inter-bassins des valeurs de flux particulaires.

Les valeurs de flux de matières en supsension calculées sont dans la moyenne basse des flux particulaires de la littérature à l'échelle mondiale. Cependant, les résultats obtenus indiquent une forte variabilité inter-bassins des exports mais également une variabilité annuelle intra-bassin. Cette variabilité interannuelle peut s'expliquer par les différences pluviométriques. Toutefois, à l'échelle du bassin Loire-Bretagne, de grandes tendances dans les valeurs de flux peuvent être observées avec des années à très faible ou très fort export de particules. L'utilisation de bassins versants emboîtés permet d'avoir un premier aperçu du transport solide dans les cours d'eau.

Ce chapitre constitue donc une première étape dans l'établissement des bilans sédimentaires, et également une première étape dans l'estimation du transport de matières au sein du territoire Loire-Bretagne. Les résultats de ce chapitre ont été publiés dans Journal of Hydrology (Gay A., Cerdan O., Delmas M., Desmet M., 2014. Variability of suspended sediment yields within the Loire river basin (France). J. Hydrol. 519, 1225-1237).

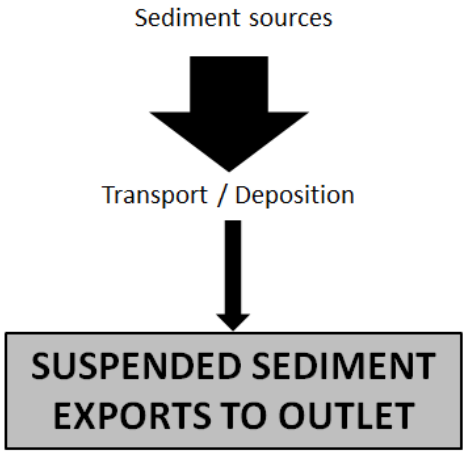

Variability of suspended sediment yields within the Loire river basin (*France*)

Sommaire

Abstract

Suspended sediment fluxes and their variability in time and space have received much attention over the past decades. Large databases compiling suspended sediment load (SL) data are often used to serve these purposes. Analyses of these databases have highlighted the following two major limitations: i) the role of lowland areas in sediment production and transfer has been minimised, and studies on small-scale catchments (with a drainage area of $\leq 10^2$ km^2) are practically non-existent in the literature; and ii) inhomogeneous data and calculation methods are used to estimate and compare the SL values.

In this context, the present study aims to complete the existing studies by providing a reliable comparison of SL values for various catchments within lowland river basins. Therefore, we focused on the Loire and Brittany river basins (*France*). 111 small to large catchments covering 78% of this area and representative of the basins landscape diversity were chosen. We first present a large database of area-specific suspended sediment yields (SY) calculated from the suspended sediment concentration and flow discharge data over 7 to 40 years of measurements at gauging stations. Two calculation methods are used, and the calculated loads are confined within a factor of 0.60 - 1.65 of the real values. Second, we analyse the temporal and spatial variability of the calculated SY values. Finally, using a nested catchment approach, we provide insight into sediment

transport from upstream to downstream gauging stations and into the role of small- and medium- scale catchments in sediment production and transfers.

The SL values at the outlet of the catchments range from $2.5*10^2$ to $8.6*10^5$ t.yr^{-1}, and the SY values range from 2.9 to 32.4 t.km^{-2}.yr^{-1}. A comparison with the limited values available in the literature for this region corroborates our estimations. Sediment exports from the Loire and Brittany river basins are very low compared with mountainous regions and European exports. However, a strong spatial variability within this territory exists. The expected results on the SY spatial pattern distribution and the correlation between SY values and basin sizes are not observed.

An analysis of the SY values at different time steps shows a strong effect of the seasonal availability of detached particles to be transported with a high concentration of suspended sediments during the winter and lower values during the summer and autumn. Annual variations are also observed, with export values varying by a factor 2 to 10 between years for one catchment and the amplitude of the annual variations varying between catchments. The influence of rainfall in the sediment exports is predominant, but investigations on physical characteristics of each catchment (*e.g.*, lithology, slope, land use) are required to better understand the production and transfer processes within a drainage basin. These annual variations imply that long-term data are required to provide mean SY values representative of the catchment functioning. From our calculations, 18 complete years of data are required to obtain a mean SY value with less than 10% of variation on average around the mean.

From our results on nested catchments over a long-time scale (40 years), it appears that most of the suspended sediment load entering the water system is transported downstream. Covariations of the annual-SY values are generally observed for two gauging stations located on the same river. The nested catchment approach is an interesting tool for the identification of active sediment sources within a large catchment and for the construction of detailed sediment budgets.

KEYWORDS : Sediment transfer ; Rainfall ; Nested catchment ; Time variability.

2.1 Introduction

Suspended sediment load (SL) values provide insight into drainage basin sediment production and transfers. The construction of detailed sediment budgets (Walling and Collins, 2008 [303]) and basin sediment management policies (Owens, 2005 [217]) rely on the mean values of the sediment load calculated at the catchment outlet. In this framework, it is essential to provide accurate average SL estimations and to understand the spatial and temporal variability of these values. To this aim, global and European SL databases (*e.g.*, Milliman and Meade, 1983 [192]; Milliman and Syvitsky, 1992 [193]; Vanmaercke *et al.*, 2011 [289]) have often been developed to aid in the comparison between basin sediment export capacity and to establish orders of priority for basin management.

The results from these investigations indicate that sediment fluxes are controlled

by the combination of hydroclimatic and geomorphologic factors (Jansen and Painter, 1974 [133]; Ludwig and Probst, 1998 [174]). Particular attention has been given to the scale dependence of suspended sediment exports, and it is common to attempt to establish a relationship between area-specific sediment yields (SY, t.km^{-2}.yr^{-1}) and drainage areas (A, km^2). A negative correlation (*e.g.*, Meybeck *et al.*, 2003 [189]; De Vente *et al.*, 2005 [64]) is expected between both variables due to a decrease in sediment production and an increase in sediment deposition on gentle slopes as the catchment area increases. However, this assumption is disputable because contradictory results have been reported (De Vente and Poesen, 2005 [63]; Vanmaercke *et al.*, 2011 [289]).

Further investigations on SL values have indicated the strong temporal variability of the sediment exports of the catchments that exists at different time scales. Sediment transport from local sources to the basin outlet strongly depends on the magnitude of the climatic events that set particles in motion and on the quantities of the detached particles that are momentarily stored on-land or in-channel and available for transport, *i.e.*, the sediment stock. At the event time scale, hysteresis patterns are used to characterise the provision and sources of this sediment stock and its exhaustion (Williams, 1989 [317]). At the season time scale, higher concentrations of suspended sediments are expected in summer due to extreme storm events (Walling and Webb, 1996 [301]). However, in primarily agricultural low land areas, higher concentrations of suspended sediments can be observed in winter compared with other seasons (Delmas *et al.*, 2011 [69]) and are due to changes in landscape (such as bare soils in winter) and variations in precipitation levels during the year. Finally, at the interannual time scale, discrepancies in the amount of sediment exports are observed between years (*e.g.*, Horowitz, 2003 [128]; Dang *et al.*, 2010 [54]). Based on a set of indicators, Meybeck *et al.* (2003) [189] have highlighted the temporal variability of sediment fluxes within a drainage basin and between catchments. In that study, the authors have proposed a typology of the sediment export capacity of the basins that reflects the sediment flux regime.

However, databases elaborated to draw these comparisons encounter two major limitations, primarily due to inhomogeneities of compiled data that concern the following: i) the differences in the calculation methodologies due to a different space/time scale resolution of the data (Walling and Webb, 1996 [301]) and ii) the spatial and size distribution of the catchments (Vanmaercke *et al.*, 2011 [289]).

Two primary calculation methodologies are commonly used to estimate the SL values, as follows: i) reservoir sedimentation rates (*e.g.*, De Vente *et al.*, 2005 [64]) and ii) in river measures of either the suspended sediment concentration C values or of the turbidity from which the C-values are calculated, and the fitting of empirical power laws that link C-values to flow discharges Q (*e.g.*, Webb *et al.*, 1997 [309]). The first method provides information on the volumes stored in reservoirs, such as dams. However, the difficulty in estimating these volumes leads to high associated uncertainties (Salas and Shin, 1999 [252]). The data from reservoirs are valuable long-term sediment transfer records (from 20 to 100 years) and offer insight into major changes in sediment exports at a decadal time step. However, a detailed understanding of interannual or seasonal

variability in sediment exports cannot rely on those rates. Conversely, the $C(Q)$ power laws provide this detailed information over very few decades. However, the accuracy and resolution of the $C(Q)$ power laws strongly depend on the frequency of the measured $C-Q$ data at the gauging station (Horowitz, 2003 [128]). For small catchments, the use of a turbidimeter provides accurate hourly to daily measurements over a few years and allows for the characterisation of sediment exports for each event but does not provide long-term average SL values. Conversely, medium or large catchments are less frequently monitored, and daily to monthly measurements of the in-river suspended sediment concentration are the most frequent time steps available for these data. Thus, power laws have received much attention in the past decade, and many authors have proposed different equations to reduce the associated uncertainties, to consider infrequent $C-Q$ data (Phillips *et al.*, 1999 [221]; Asselman, 2000 [8]; Delmas *et al.*, 2011 [69]) and to correct the underestimation generally observed when using classic power laws (Cheviron *et al.*, 2014 [40]). Still comparing the loads derived from different equations appears to present a bold challenge.

Until now, SL values have been estimated for different sizes of river basins. However, SL estimations for small catchments with an area of $A \leq 10^2$ km^2 remain scarce (Vanmaercke *et al.*, 2011 [289]). The authors have also indicated the unequal spatial distribution of the available data. Certain areas concentrate the research efforts (Walling and Webb, 1996 [301]). For example, the Yellow River in Asia and its tributaries for which the estimated sediment exports can be as high as 53,500 t.km^{-2}.yr^{-1} (in Walling and Webb, 1996 [301]) have been the subject of numerous publications, whereas plain river basins are less documented. Similarly, at a medium catchment scale in Europe, the Mediterranean area has concentrated much of the research efforts along with mountainous catchments (Coynel *et al.*, 2004 [50]; Piégay *et al.*, 2004 [224]; Mano *et al.*, 2009 [178]; Navratil *et al.*, 2011 [205]) or coastal rivers (Estèves and Ludwig, 2003 [82]). All of these studies display sediment export values at least twice as high compared with those obtained from the limited studies on small lowland catchments (*e.g.*, Sogon *et al.*, 1999 [262]; Lefrançois *et al.*, 2007 [164]; Oeurng *et al.*, 2010 [215]).

Inter-catchment SY variability has been investigated at different time and space scales; however, the internal variability of large river basins and the role of small-scale catchments in sediment production and transfers has been less discussed. Recent investigations using nested catchment approaches (Duvert *et al.*, 2011 [80]; Armijos *et al.*, 2012 [7]) have provided new insight into SL variability and into erosion/deposition patterns within drainage basins of Central and Latin America. However, these studies are limited in space and time for the $C-Q$ time series, thus affording a limited overview of the internal fluxes of the entire basin.

Analysis of the available SL values across the French territory confirms the lack of data in the lowland areas and for small size catchments. Numerous estimations exist for large rivers, for example, the Rhône river (*e.g.*, Pont *et al.*, 2002 [231]), the Seine river (*e.g.*, Roy *et al.*, 1999 [249]), the Garonne river (*e.g.*, Schäfer *et al.*, 2002 [254]), and the Loire river (*e.g.*, Ludwig and Probst [174]; Delmas *et al.* 2012 [70]). The latter is the largest of all of the rivers in France and is considered to be "one of the last

wild rivers of Europe" but has undergone several alterations due to human activities, such as sediment extraction and dam and dyke construction (Garcin *et al.*, 2006 [101]), which may influence sediment transport and volumes. However, studies on sediments in the Loire river have primarily focused on nutrients and dissolved loads in the upper area of the basin (Grosbois *et al.*, 2000 [114]) or on sediment dynamics in secondary channels of the river (*e.g.*, Rodrigues *et al.*, 2006 [247]). To our knowledge, no study has been performed with the goal of understanding the temporal and spatial variability of sediment transport within the Loire river basin.

In this context, the objectives of the present study are the following: i) to develop and discuss a homogeneous (in data and calculation methodologies) database of SY values over a decadal time scale (from 7 to 40 years) for small- to large-sized catchments in the Loire and Brittany river basins, ii) to highlight the temporal and spatial variability of sediment fluxes within this area, and iii) to understand the role of small and medium size catchments in sediment production, transport, and contribution to the overall Loire river basin budget.

2.2 Material and Methods

2.2.1 Study site

The French metropolitan territory is divided into six river basin districts, and for each district, a river basin agency is in charge of the water resources. The Loire Brittany river basin (named $LBRB$ hereafter) is one of the districts and represents 28% of the territory ($\sim$ 155,000 km ^{2}).

From a geological viewpoint, the centre of the $LBRB$ lies on the sedimentary formations of the Parisian basin and the Aquitaine basin. This area is primarily dominated by floodplains and croplands. The eastern and western parts of the study area lie on old granitic formations. To the east, the Massif Central includes a mountainous area with steep forested slopes (maximum = 134.7%), the highest point of the study site (1849 m), and the Limagne basin. In contrast, the Armorican basin in the western part of the $LBRB$ is also a mountainous area (maximum altitude = 385 m) but displays gentler slopes (maximum = 86.9%) and is dominated by croplands.

From an administrative and hydrological viewpoint, the $LBRB$ is divided into three primary areas for which sediment exports to the sea have been recently estimated (Delmas *et al.*, 2012 [70]). The Loire river basin drains an area of approximately 117,800 km^2 from its source to the Atlantic Ocean, and the sediment delivery to the ocean is approximately 0.86 Mt.yr^{-1}. The Brittany region is approximately 30,000 km^2. Suspended sediment exports from the Breton rivers have been estimated at 0.24 Mt.yr^{-1}. The remaining area is the Vendée and is composed of small watersheds in the Atlantic coastal area.

The selection of 111 catchments results from a compromise between the available data and the requirement to be representative of the diverse characteristics of the Loire

river basin. The selected catchments are distributed throughout the *LBRB* (Figure 2.1) in a variety of climatic, geologic, and geomorphologic contexts representing the intrinsic landscape diversity and accounting for approximately 78% of this territory, with a total surface of 122,960 km^2. The *Loire* river and its three principal tributaries (with a river length $>$ 300 km), the *Allier* river, the *Cher* river, and the *Vienne* river are the largest drained areas among the *LBRB*.

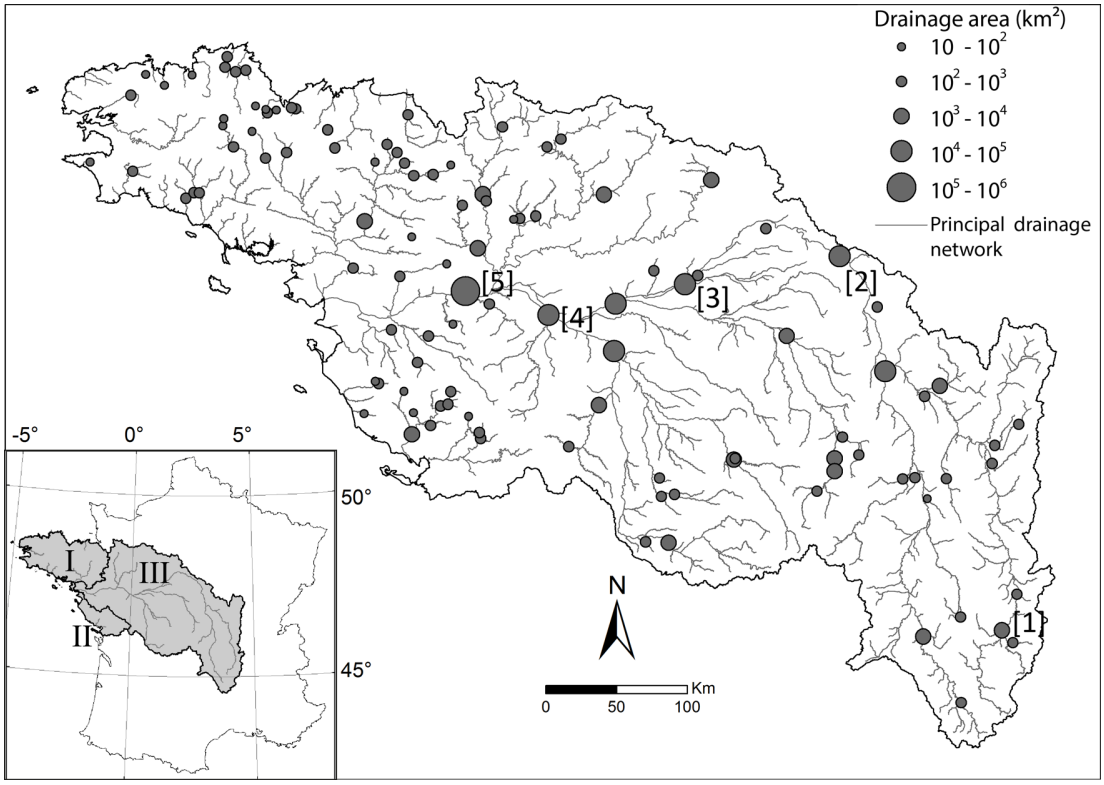

FIGURE 2.1 – Localisation of the 111 catchment outlets and their drainage area. Arabic numerals under the square brackets indicate the five stations located on the Loire river from upstream [1] to downstream [5]. Roman numerals indicate the three administrative regions: I Brittany, II Vendée, and III the Loire river basin

The mean altitude of the catchments vary from 36 m for the *Ognon*, a catchment close to the Loire estuary, to 1,127 m for the *Allier* basin's head (Figure 2.2). The mean annual rainfall values range from 672 mm for the *Loir* river basin's head, a tributary of the mid-Loire river, to 1,233 mm on the *Odet* Breton catchment. The drainage basin areas range from 13 km^2 for the Breton catchment *Lestolet* to 110,250 km^2 for the *Loire* river basin close to its estuary. Overall, the catchments are located in a lowland temperate area and are not subjected to flashfloods. During the study period, no significant land use changes occurred because major changes transpired at the beginning or at the end of this period. Parcel consolidation modified the landscape in the early 1970s, and for a limited number of years, new agricultural practices emerged.

These recent changes do not affect the results for the study period.

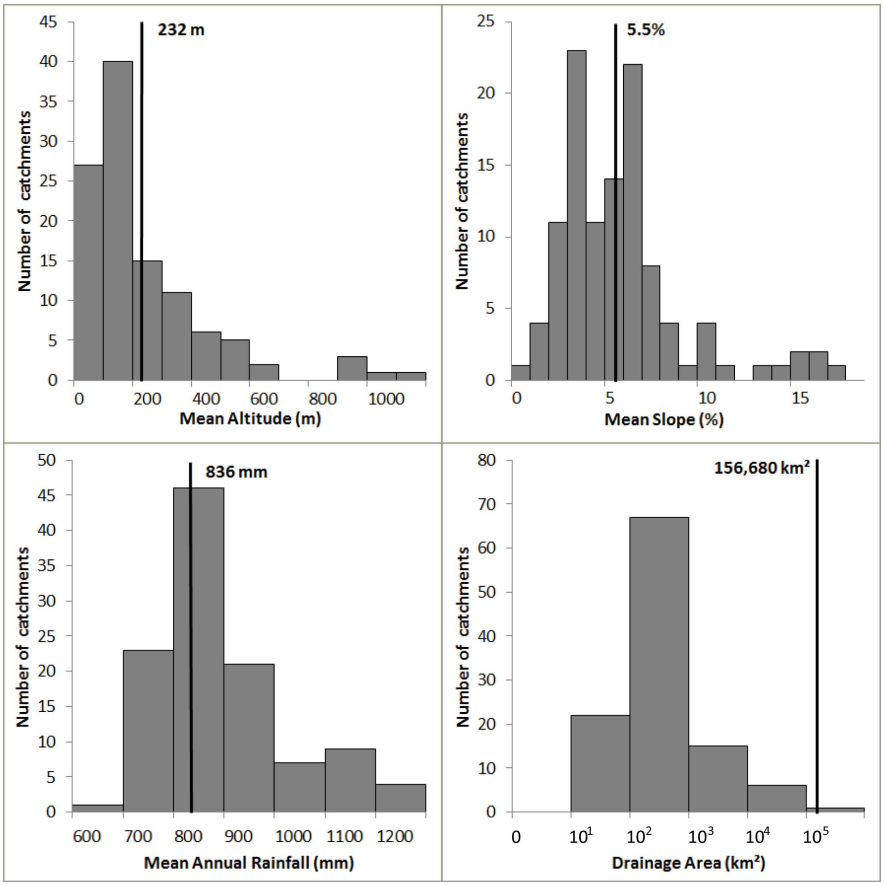

FIGURE 2.2 – General characteristics of the 111 selected catchments. The bold lines and numbers represent the values calculated for the entire Loire Brittany river basin

2.2.2 Data collection and calculation methods

The 111 selected catchments were mapped using the *Watershed* tool in the Spatial Analyst program (ArcGIS10) and the use of a digital elevation model at a 50m resolution (BD Alti ® IGN). The water flow discharge data (Q) are collected from the national database HYDRO FRANCE and correspond to the daily mean values calculated from continuous stage records. The Loire Brittany River Agency database OSURWEB provides instantaneous suspended sediment concentration values (C) that correspond to once-in-a-month sampling from a water quality sampling program referring to the ISO norm 5667-1 (AFNOR norms T90-511, T90-512, T90-513). The samples are collected at the water surface and in the middle of the river (from bridges), and are then filtered using a 0.45 μm filter in the laboratories that are labeled with an ISO norm to ensure the repeatability of the measurements. Then, the Q and C data are associated in space and time according to the methodology presented by Delmas *et al.*, (2012) [70].

For the prediction of suspended sediment loads, we used the relationships based on

the classic $C(Q)$ power law linking suspended sediment concentration (C) and water flow discharge (Q) but including a correction term to overcome the underestimation generally observed in classic rating curves (Cheviron *et al.*, 2014 [40]). We chose two methods proposed by Delmas *et al.*, (2011) [69]. These methods were specifically developed to overcome the lack of data especially on suspended sediment concentration and were tested on high frequency data from the USGS database. We briefly present both methods below. Each relationship was adjusted on existing $C - Q$ couples using the PEST software (Doherty, 2004 [76]) and was then extrapolated to the entire flow discharge time series.

The Storage method (Equation 2.1) integrates a storage-dynamic correcting factor $a_5\delta S$, in which a_5 is a parameter obtained through optimisation and δS accounts for the daily variation of the sediment stock.

$$C = aQ^b + a_5\delta S \tag{2.1}$$

The IRCA (*Improved Rating Curve Approach*) (Equation 2.2) is based on the subdivision of the Q datasets in the following three samples: rising, falling, and base flow discharge data. The average suspended sediment concentrations associated with the base flow Q data are extrapolated to the entire base flow Q population. IRCA manages rising and falling discharge data according to Equation2.2.

$$\begin{cases} \text{For rising discharges: } C_R = a_R Q_R^{b_R} + a_{5R}\delta S \\ \text{For falling discharges: } C_F = a_F Q_F^{b_F} + a_{5F}\delta S \end{cases} \tag{2.2}$$

where C_R and C_F correspond to the sediment concentration to be estimated for the rising and falling discharges, Q_R and Q_F, respectively, the instantaneous discharge (the mean daily value from continuous stage records) for the rising and falling discharge, a_R, b_R, a_{5R} and a_F, b_F, a_{5F}, respectively, which are fitted parameters in rising and falling equations obtained through optimisation. The δS value accounts for the daily variations in the sediment stock (as in Equation 2.1).

The statistical representativity of our data was tested for each catchment: the Wilcoxon test was applied to the three sample types at each station to verify that the Q data (in rising, falling, and base flow discharge) for which the C values were available were representative of the corresponding Q population at this station (rising, falling, and base flow discharge populations). If the data were representative, then the IRCA was favoured. If the data were not representative, then the following two samples were considered for the Wilcoxon test: Q data within base-flow conditions and outside base-flow conditions (regardless of the rising and falling discharge). If the Q data were representative of the Q population, then the Storage method was then applied. The IRCA was applied to 83 stations, whereas the Storage method was applied to 28 stations.

The mean SL values are calculated from the entire flow discharge time-series. The mean specific sediment yields (SY) are calculated as the mean sediment load divided

by the basin area.

2.2.3 Uncertainties on sediment load estimations

The recent study by Cheviron *et al.* (2014) [40] has provided information on the performance of the IRCA when combining the effects of bias on the C and Q data and the infrequent C data. One of the major outcomes of that previous study is that IRCA is capable of managing infrequent C data. Compared with a simple $C = aQ^b$ rating curve, IRCA is more sensitive to the number of available C measurements than to the sampling frequency. For example, with more than 200 $C - Q$ couples at each site, the error on the calculated values with IRCA is in the [-20%,+20%] interval. In the present study, 38 of the 111 catchments presented more than 200 $C - Q$ couples ($\sim$ 16 years of monthly sampling). For the 73 remaining stations, the minimum number of $C - Q$ couples corresponding to a minimum of $\sim$ 7 years of monthly sampling is 84. In this case, the error corresponds to a maximum of 30%.

When estimating suspended sediment fluxes at very fine time scale (*e.g.*, daily or yearly) or space scale(*e.g.*, transect), other uncertainties due to the lateral and vertical gradient in suspended sediment concentration (Horowitz *et al.*, 1990 [129]), to the daily flow variations (Moatar *et al.*, 2006 [198]) or the scale dependency of uncertainties (Walling and Webb, 1981 [304]) have to be taken into account.

In the present study where mean sediment fluxes are estimated over a decadal time scale, we assumed our case to be the worst-case scenario, *i.e.*, with a systematic error for the Q values in the [-5%,+5%] interval, a random error on C within the [-30%,+30%] interval and a C sampling frequency every 30 days on average. In this case, the authors showed that IRCA provides estimations of mean sediment fluxes values in the 0.60 - 1.65 range.

2.2.4 Analysis of the temporal and spatial variability of the SY values

First, the data are analysed on a seasonal basis, and we investigate the variability of the C and Q data at this time scale. Then, the data are analysed on a yearly basis (calendar years). For certain catchments, the complete flow discharge time-series data are not available at this time-step. Thus, years for which data are missing were not considered in this analysis. Only the *Isac* catchment presents a lack of complete annual flow discharge time-series and is excluded from the dataset for the temporal variability analysis. For the 110 remaining catchments, we investigate the interannual and the inter- and intra-catchment variability using the annual-SY values. We also use one of the metrics proposed by Meybeck *et al.* (2003) [189] to quantify this variability and to characterise each catchment according to its flux duration, *i.e.*, the percentage of sediment transported within a given period. We calculate the Ts_{50}% value, which is the time required to transport 50% of the total annual suspended load. Finally, on a hydrological yearly basis, the SY data are compared with the specific annual rainfall amount available for the years between 1998 and 2010.

The effect of the annual SY variability on the mean SY values is investigated. Using the 39 catchments for which more than 30 complete years of data are available, the moving averages of the SY values are calculated for each catchment and various time steps from 2 to 42 years of data and are compared with the mean values obtained for the entire time period. For each time step and catchment, the coefficient of variation of the moving average to the mean value is calculated as the ratio of the standard deviation to the mean.

2.3 Results and discussion

2.3.1 SY values at the outlet of the 111 catchments

A large specific sediment yield database is developed in this study using homogeneous data and calculation methods. Table 2.1 provides the mean SY values calculated from the entire flow discharge time-series, drained areas, number of complete years of the Q time-series available, and the river names for the 111 catchments. The data are presented arbitrarily in alphabetical order. For the 13 rivers characterised by at least two gauging stations, the catchments are ranked in increasing order of drained areas and differentiated by a number in the square brackets. The database displays a wide range of SY values. The estimated sediment loads range from 2.5 x 10^2 t.yr^{-1} to 8.6 x 10^5 t.yr^{-1}, with a mean value of 3.2 x 10^4 t.yr^{-1} (std = 1.2 x 10^5). The SY values range from 2.9 t.km^{-2}.yr^{-1} to 32.4 t.km^{-2}.yr^{-1}, with a mean value of 11.7 t.km^{-2}.yr^{-1} (std= 5.1).

Figure 2.3 provides the size distribution of the mean SY values. 95% of the catchments have a SY value between 3 and 20 t.km^{-2}.yr^{-1}. The remaining 5% correspond to 6 catchments distributed as follows: two Breton catchments, the *Isac* and the *Ille*, with SY values under 3 t.km^{-2}.yr^{-1}, and four catchments, the Vendeen basin the *Grand Lay [2]*, and three catchments located in the Loire river basin (the *Moine*, the *Furan* and the *Beuvron*), with values above 20 t.km^{-2}.yr^{-1}. All of these catchments are small- to medium-sized ($A < 600$ km^2).

By comparison, the values found in the literature for analogous catchments in the Brittany region are similar to those found in this study. Lefrançois *et al.* (2007) [164] and Vongvixay *et al.* (2010) [295] reported sediment exports from 12 to 36 t.km^{-2}.yr^{-1} for three Breton catchments with $A < 5$ km^2.

Tableau 2.1 Drainage area, mean specific sediment yields (SY), basin number attributed, and station code (from HYDRO FRANCE) of the 111 selected watersheds. The number of complete years of Q time-series available are presented in brackets next to the mean SY values. Rivers for which several stations are available are presented in increasing order of drained areas and are differentiated by the numbers under square brackets

River name	Basin code	Area (km^2)	SY ($t.km^2.yr^{-1}$)	Station number	River name	Basin number	Area (km^2)	SY ($t.km^2.yr^{-1}$)	Station code
Acolin	1	389	9.68 (17)	K1833010	Leff [1]	57	42	17.11 (12)	J1803010
Allier [1]	2	519	4.71 (18)	K2090810	Leff [2]	58	341	9.02 (35)	J1813010
Allier [2]	3	2260	5.50 (35)	K2330810	Lestolet	59	13	19.27 (9)	J5205210
Allier [3]	4	14347	12.22 (28)	K3650810	Lié	60	299	13.03 (29)	J8133010
Andelot	5	209	13.51 (37)	K3153010	Loing	61	122	19.79 (39)	N3024010
Arconce	6	591	14.91 (38)	K1173210	Loir	62	1157	4.94 (30)	M1041610
Aron	7	1466	19.65 (31)	K1773010	Loire [1]	63	3249	8.98 (40)	K0550010
Aumance	8	927	11.92 (28)	K5383010	Loire [2]	64	35575	10.40 (12)	K4180020
Autise	9	244	13.52 (28)	N5101710	Loire [3]	65	40487	9.30 (11)	K4800010
Auzance	10	59	9.24 (3)	N2013010	Loire [4]	66	80999	9.07 (22)	L8000020
Besbre	11	453	8.24 (12)	K1533020	Loire [5]	67	110241	7.83 (12)	M5300010
Beuvron	12	38	32.44 (33)	M6014010	Mandouve	68	29	12.47 (17)	J1524010
Blavet [1]	13	88	3.95 (11)	J5212120	Marillet	69	50	9.07 (3)	N3304120
Blavet [2]	14	566	6.28 (6)	J5402120	Mayenne [1]	70	827	15.76 (15)	M3060910
Bouble	15	561	18.32 (29)	K3373010	Mayenne [2]	71	2901	14.42 (35)	M3340910
Bourbince [1]	16	339	18.75 (28)	K1363010	Merdereau	72	118	16.24 (23)	M0114910
Bourbince [2]	17	819	17.67 (42)	K1383010	Mère	73	59	16.89 (10)	N7114010
Brame	18	232	13.18 (9)	L5323010	Moine	74	366	21.48 (15)	M7213020
Brenne	19	261	10.43 (35)	K4873110	Nohain	75	476	5.01 (41)	K4094010
Cher [1]	20	1669	3.48 (8)	K5210910	Odet	76	203	15.37 (39)	J4211910
Cher [2]	21	1836	5.85 (5)	K5220910	Nil	77	319	11.88 (13)	K5363210
Cher [3]	22	4520	8.26 (32)	K5490910	Ognon	78	146	8.44 (16)	M8205020
Cher [4]	23	13678	12.27 (22)	K6720910	Oudon [1]	79	133	6.62 (19)	M3711810
Chère	24	60	5.11 (15)	J7803020	Oudon [2]	80	1417	11.12 (20)	M3861810
Chevré	25	151	12.70 (21)	J7083110	Ouette	81	119	8.72 (22)	M3514010
Clain	26	2853	6.02 (35)	L2501610	Oust [1]	82	28	13.22 (33)	J8002310
Cosson	27	749	4.12 (4)	K4793010	Oust [2]	83	253	12.91 (9)	J8022320
Couesnon	28	856	16.03 (38)	J0201510	Petite Boulogne	84	89	13.13 (12)	N1014010
Creuse	29	1233	7.41 (41)	L4220710	Petite Creuse	85	853	15.85 (40)	L4411710
Dhuy	30	211	6.14 (16)	K4383110	Petite Maine	86	192	11.70 (7)	M7433110
Dore	31	105	7.27 (21)	K2821910	Queffleuth	87	95	11.81 (21)	J2614020
Dunières	32	217	3.16 (24)	K0454010	Rance	88	143	14.04 (26)	J0611610
Ellé	33	575	11.45 (37)	J4742010	Rosette	89	113	6.26 (32)	J1114010
Elorn	34	201	15.57 (41)	J3413020	Sarthe	90	906	14.90 (29)	M0050620
Erdre [1]	35	99	13.17 (40)	M6323010	Scorff	91	299	13.59 (38)	J5102210
Erdre [2]	36	465	7.40 (41)	M6333020	Semme	92	174	14.03 (9)	L5134010
Evron	37	139	9.93 (25)	J1324010	Smagne	93	185	11.92 (36)	N3222010
Flume	38	92	10.12 (21)	J7214010	Tardes	94	859	5.73 (34)	K5183010
Furan	39	175	29.09 (31)	K0614010	Taude	95	46	10.46 (24)	M0674010
Gorre	40	180	16.42 (19)	L0914020	Trieux	96	414	12.55 (19)	J1721720
Gouessant	41	244	7.18 (28)	J1313010	Urne	97	44	15.42 (13)	J1405310
Gouët	42	136	10.41 (29)	J1513010	Vaige	98	238	12.79 (21)	M0653110
Goyen	43	89	5.19 (41)	J4014010	Vègre	99	400	11.66 (27)	M0583020
Grand Lay [1]	44	130	25.25 (38)	N3001610	Vendée	100	156	12.67 (9)	N7101810
Grand Lay [2]	45	405	9.03 (8)	N3031610	Vie	101	122	14.67 (11)	N1001510
Guindy	46	122	14.42 (26)	J2034010	Vienne [1]	102	3387	14.07 (31)	L0700610
Horn	47	50	12.82 (40)	J3014310	Vienne [2]	103	19817	11.41 (32)	L7000610
Huisne	48	1911	11.51 (24)	M0421510	Vilaine [1]	104	57	11.17 (22)	J7000610
Ille	49	103	2.94 (20)	J7103010	Vilaine [2]	105	147	9.43 (39)	J7010610
Illet	50	111	7.12 (19)	J7114010	Vilaine [3]	106	567	8.21 (22)	J7060620
Isac	51	548	2.91 (0)	J9202510	Vilaine [4]	107	4146	11.86 (28)	J7700610
Jaudy	52	165	13.36 (26)	J2023010	Vincou	108	286	11.91 (41)	L5223020
Jolan	53	64	15.3 (17)	K3074010	Vonne	109	304	7.51 (38)	L2253010
Laïta	54	852	11.36 (37)	J4902011	Yar	110	58	13.28 (28)	J2314910
Lay	55	1723	10.29 (2)	N3511610	Yon	111	41	17.33 (18)	N3403010
Layon	56	919	12.69 (38)	M5222010					

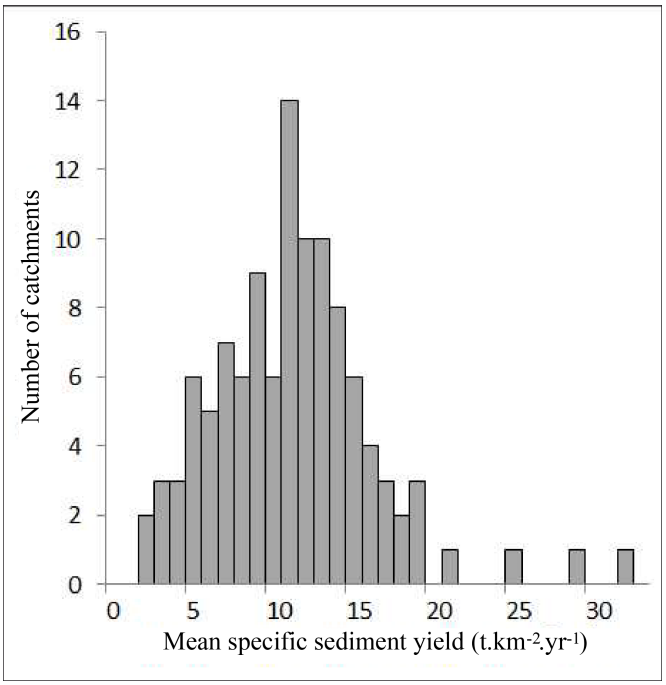

FIGURE 2.3 – The size distribution of the mean specific sediment yield calculated for the 111 watersheds

The Loire river values found in the literature range from 4 t.km^{-2}.yr^{-1} (Jansen and Painter, 1974 [133]), *i.e.*, 2 times less than our prediction, to 27 t.km^{-2}.yr^{-1} (Ludwig and Probst, 1998 [174]), which is 3.5 times greater than our findings. For example, Meybeck *et al.*, (2003) [189] found a value of 13.87 t.km^{-2}.yr^{-1}, whereas Négrel and Grosbois (1999) [209] estimated the SY value for the Loire river at the gauging station of Orléans to be 9.5 t.km^{-2}.yr^{-1} during May 1995 and March 1996. This station is located between the *Loire [2]* and *Loire [3]* stations in this study and agrees quite well with our estimations at those stations (10.40 and 9.30 t.km^{-2}.yr^{-1}, respectively). To our knowledge, no other estimations of specific sediment yields using data from gauging stations exist for catchments within our study area.

However, compared with other small and medium size French catchments up to 10^3 km^2 (Mano *et al.*, 2009 [178]; Oeurng *et al.*, 2010 [215]), the catchments presented in this study display lower values of sediment exports. This finding is not surprising given that low SY values are generally observed in lowland areas compared with the value calculated for Mediterranean and mountainous regions (Delmas *et al.*, 2009 [71]; Vanmaercke *et al.*, 2011 [289]). In contrast, the Loire river exports less sediment than do other large French rivers, for which the values range from 16 t.km^{-2}.yr^{-1} for the Rhine river (Ludwig and Probst, 1998 [174]) up to 111 t.km^{-2}.yr^{-1} for the Rhône river (Delmas *et al.*, 2012 [70]). Concerning the contribution from the Loire and Brittany basins to the global sediment exports from earth to sea, the SY value of this area is below the mean values calculated for Europe's contribution, which is between 30 - 35 t.km^{-2}.yr^{-1} (Collins, 1986 [44] and Holeman, 1968 [125]) and 88 t.km^{-2}.yr^{-1} (Ludwig

and Probst, 1998 [174]).

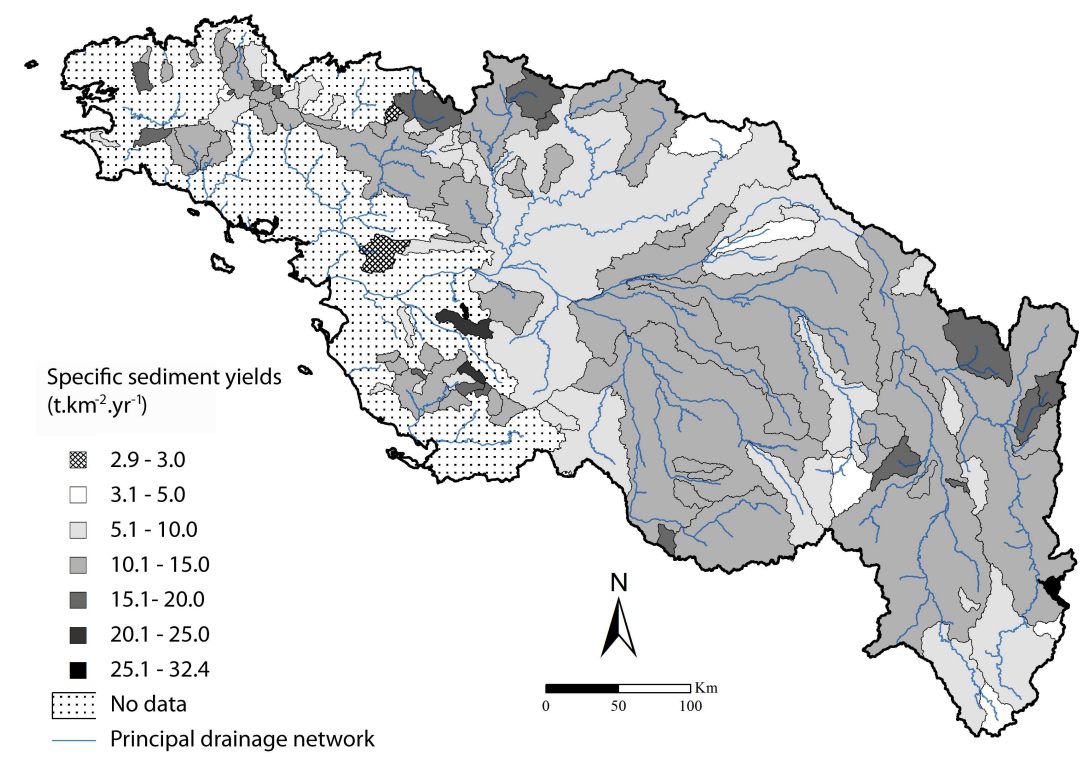

FIGURE 2.4 – The mean specific sediment yield estimated for the 111 catchments in the Loire Brittany river basin. Catchments that are nested in other catchments are presented on top

Compared with nearby rivers, the contribution of the sediment exports to the sea by the Loire river appears low. Nonetheless, there is still an internal diversity of the *SY* values that can be observed. Figure 2.4 displays the spatial distribution of the *SY* values and the shape of the basins. The values are grouped into seven classes. Boundaries were chosen to highlight extreme values of the range of the calculated *SY* values, but no spatial distribution of the values was found. Higher values are generally expected in upstream portions of basins in which the slopes are steeper, thus causing the erosion and transport to be more significant compared with that in lowland areas. However, the *SY* values appear to be homogeneously distributed over the Loire river basin, displaying none of the spatial patterns that are generally observed (*e.g.*, Delmas *et al.*, 2009 [71]; Vanmaercke *et al.*, 2011 [289]). Two catchments located in the southeastern part of the upstream Loire basin and the direct tributaries to this river illustrate the discrepancies found over the entire river basin. For approximately the same drainage area ($\sim$ 200 km^2), the two catchments located in the Massif Central, the *Furan* and the *Dunières*, display opposite extreme *SY* values of the range, 29.09 and 3.16 t.km^{-2}.yr^{-1}, respectively. Conversely, the Vonne, a subcatchment of the Loire river, and the *Loire[5]*

at its estuary display similar SY values (7.51 and 7.83 t.km^{-2}.yr^{-1}, respectively), whereas their drainage areas are opposite (300 and 10^5 km^2, respectively).

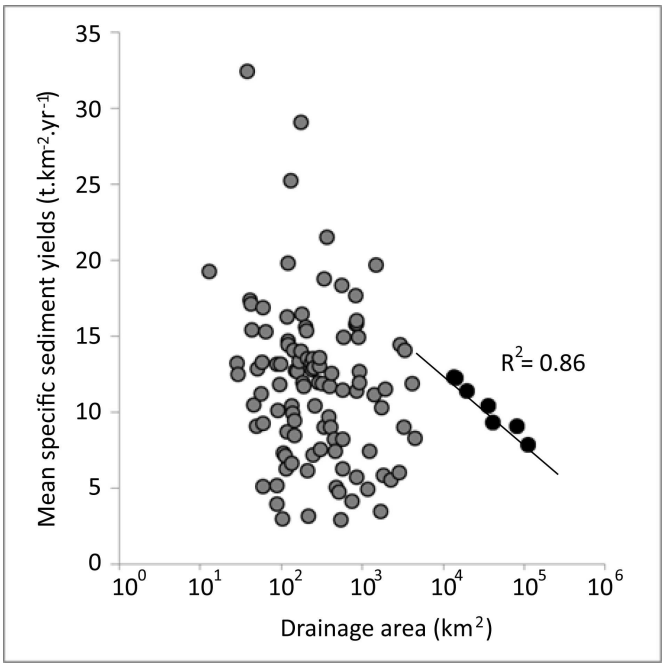

FIGURE 2.5 – Relationship between the 111 mean specific sediment yields at a basin outlet and their drainage area. The drainage area axis is presented as log transformed for a better representation of the data. The black dots (and the associated regression line) represent gauging stations at the confluence between the three principal Loire tributaries and this river (the *Allier[3]*, the *Cher[4]* and the *Vienne[2]*) and to four gauging stations on the Loire river (*Loire [2-5]*)

No correlation appears between drainage areas A and SY values (Figure 2.5) considering the 111 catchments. For a given A value, the SY values may vary by a factor of 2 to 10. This result is contradictory to the conventional findings that indicate clear relationships of the type $SY = f(A)$ (*e.g.*, de Vente *et al.*, 2005 [64]). However, this result confirms the recent findings from Vanmaercke *et al.* (2011) [289], who found no correlation between the variables when considering diverse catchments together. However, we note that for a group of catchments with $A \geq 10^4$ km^2, a negative correlation exists (with R^2=0.86). Those catchments correspond to the three principal Loire tributaries at their confluence with this river (the *Cher [4]*, the *Allier [3]*, and the *Vienne [2]*) and to the four downstream gauging stations on the Loire river (*Loire [2 - 5]*). The most likely explanation for this finding is that there is a threshold phenomenon and that for catchments larger than 10^4 km^2, the common negative trend observed between basin size and sediment yield due to more deposition in large basin applies.

2.3.2 Temporal and spatial variability of sediment exports

2.3.2.1 Seasonal variability of the suspended sediment concentration

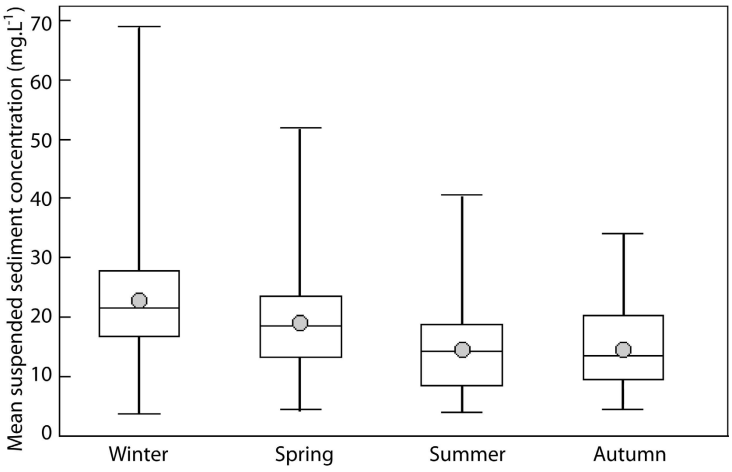

(a)

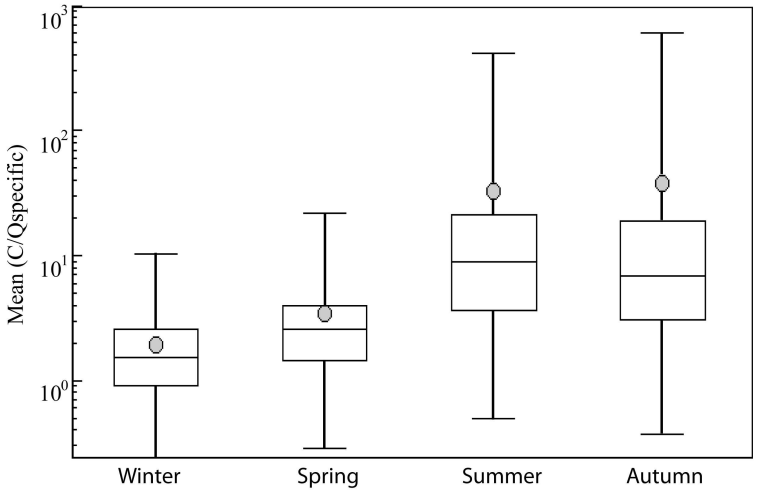

(b)

FIGURE 2.6 – Boxplots showing the seasonal variability of the suspended sediment concentration. The grey circles represent the mean values

Variations in the suspended sediment concentration (C) are shown in Figure 2.6(a). The winter season displays the highest C values (C median = 21.5 mg.L^{-1}), whereas autumn's median C value is the lowest (C median = 13.3 mg.L^{-1}) but has a mean C value similar to that for the summer season ($\sim$ 14.7 mg.L^{-1}). Conversely, the median value of the ratios between C and the area-specific discharge $Qspecific$ (Figure 2.6(b))

is higher during the summer (8.9) than it is during all of the other seasons, and the lowest value is found in the winter season (1.5). However, the mean values of the $C/Qspecific$ ratio reveal that the highest ratio is found in the autumn season (37.6 vs 32.8 for summer). The Kruskal-Wallis test is applied to the four seasonal subdivisions of the C and $C/Qspecific$ values. The results indicate that all four populations in both cases are significantly different.

The C values are more homogeneous in autumn than in summer, whereas the opposite is observed for the ratio $C/Qspecific$. These contrasts can be explained by a progressive exhaustion of the sediment stock until the autumn season while precipitations slowly increase between summer and autumn followed by a renewal and a remobilisation of the sediment stock and more significant rain events during the winter. In addition, the evolution of the vegetation cover throughout the year generates a different hydrologic and sedimentary response to the rainfall events. Winter bare soils or winter crops combined with higher precipitation amounts lead to more erosion (Ronfort *et al.*, 2011 [248]) and sediment transport than in other periods. Our results on the Loire river basin corroborate those of Delmas *et al.* (2011) [69] on French rivers. Those authors observed the same trends in the seasonal C values and the $C/Qspecific$ values and include snow melt runoff and evapotranspiration as explaining factors for the temporal variability of those data.

2.3.2.2 Interannual variability in SY

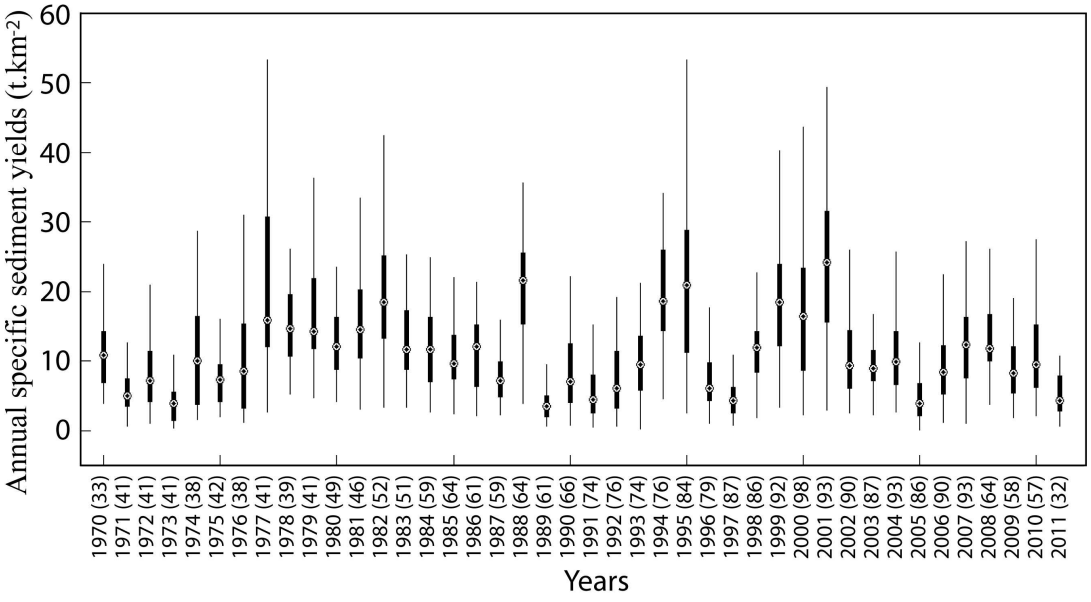

FIGURE 2.7 – Boxplots showing variations of calculated specific sediment yields for each year. The number of stations for which data are available for the specified year is in brackets

The annual variability in the SY values has been investigated for 42 years from 1970 to 2011 and for the 110 catchments altogether. The results are presented in Figure 2.7. Note that the number of basins for which data are available progressively increase between 1970 and 2010 and reflect the increasing demand for data on water systems due to the evolution of water policy.

Concerning the annual-SY values, the maximum median value is observed in 2001 with 24.37 t.km^{-2} exported, whereas in 1989, the median value is of 3.48 t.km^{-2}. However, considering catchments individually, we note that they do not display the highest or lowest values of their own range for those specific years. For example, 17 of the 61 catchments for which annual-SY data are available in 1989 present the lowest SY value of their own range in this year. This result indicates that the trend in variations observed for the annual-SY values at the $LBRB$ scale does not apply to individual catchments. A potential explanation for these findings is that specific variations of the annual-SY values are linked to internal variations in the precipitation amounts.

Figure 2.8 presents the relationship between the annual specific rainfall amount and the annual specific sediment yield for all of the catchments. A weak but significant correlation (R^2=0.39, $p - value \leq 0.0001$) is found between both variables. The scattering around the trend line is large.

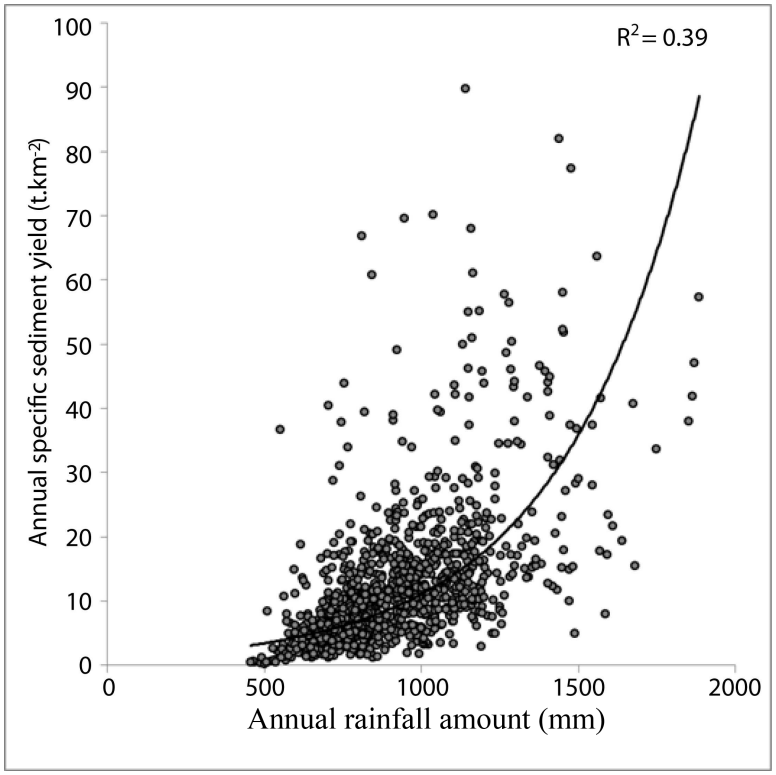

FIGURE 2.8 – Specific rainfall amount and the SY value calculated for each hydrological year and catchment. The total number of data points is 991 ($R^2 = 0.9$, $p - value \leq 0.0001$)

From these results, three conclusions may be drawn. First, the annual SY values are heterogeneous, and the total load exported by the 110 catchments by year varies. Therefore, to investigate sediment fluxes and provide a reliable and stable mean SY value, it is very important to consider this annual variability. We estimate (Figure 2.9) that 18 years (with a complete Q time-series) are required to obtain a mean SY value with less than 10% variation on average and 30 years for less than 5% variation.

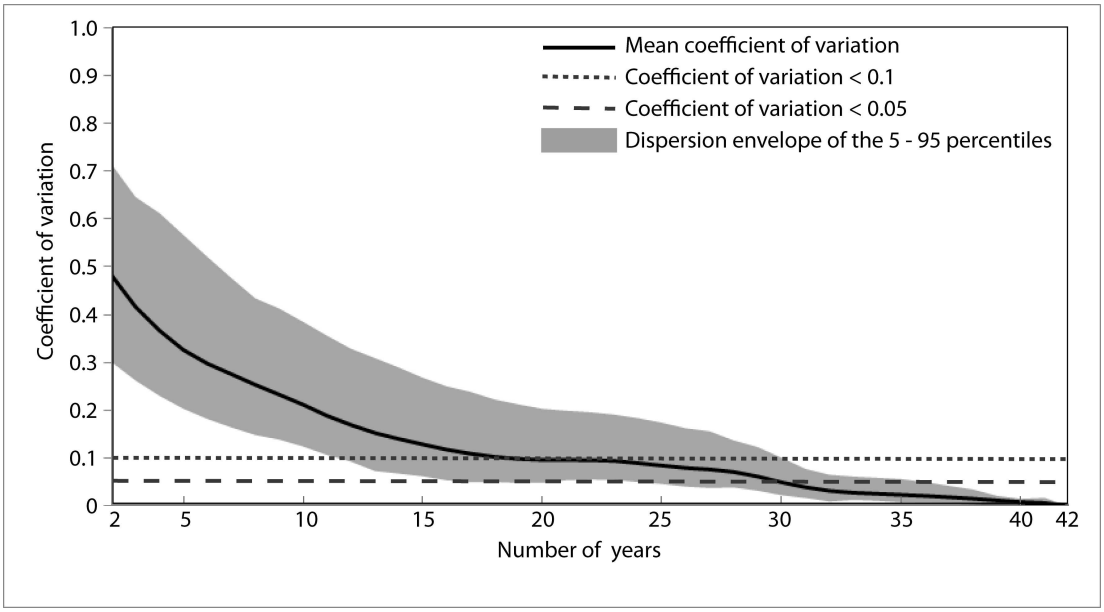

FIGURE 2.9 – Variation and dispersion of coefficients of variation between the moving average and the mean SY values for an increasing number of years in the moving average calculation. The bold line represents the mean coefficient of variation for all 39 catchments. The dispersion envelope corresponds to the 90%-confidence interval (5th and 95th percentiles)

Second, the interannual variability in the SY values may be explained by the annual differences in the precipitation amounts, and Figure 2.8 presents the positive relationship between both variables. Indeed, rainfall strongly influences flow discharge. In the $LBRB$, strong rainfall events occur as expected during the winter but may also occur during the summer. The combination of changes in land use and land cover throughout the year (Cerdan *et al.*, 2010 [37]) and crop rotation over the year with rainfall events may produce an opposite sediment response at the catchment outlet according to the time of the year when soils are bare or inversely protected by crops. Strong interannual variability in erosion rates in connection with annual rainfall variations have also been reported in the literature (Evrard *et al.* ,2010 [84]) and confirm the predominant role of rainfall event intensity and of crop type and spatial distribution (Cerdan *et al.*, 2010 [37]; Ronfort *et al.*, 2011 [248]) in erosion and sediment fluxes. To better consider the annual rainfall variation in sediment load estimations, one possible perspective would be to construct rating curves for wet and dry years independently.

While variables such as lithology or topography may explain the differences in mean sediment production and transfers, the observed temporal variability may also reflect the exhaustion of the sediment stock or its remobilisation from in-stream deposits. Sediments momentarily stored within river systems can represent as much as 80% of the total sediment load present in the channel (*e.g.*, Collins *et al.*, 2005 [43], Navratil *et al.*, 2010 [206]), and their remobilisation depends on the flow discharge and, thus, on climatic conditions.

Finally, our results indicate a certain trend in the variations of the annual-SY values within the $LBRB$ with years having low or high sediment production rates. Thus, even if the Loire river basin is heterogeneous in its physical properties and in the annual-SY at our resolution scale, it may be perceived as a homogeneous whole compared with other large entities in national or international perspectives.

2.3.2.3 Inter- and intra-catchment variability

The annual variability in the SY values for each catchment is presented in Figure 2.10. Certain catchments display low interannual variability, whereas this variability is very high for other catchments. For example, on the *Moine* river, the SY values range from 1.02 t.km^{-2} in 1995 to 97.08 t.km^{-2} ten years later in 2005, representing a factor of $\sim$100 between both years. This catchment is not an isolated case because other catchments display high ratios between their maximum and minimum values of SY. Such differences in amplitude between years have been reported, for example, for the Têt catchment (Serrat *et al.*, 2001 [256]), which is located in the French Pyrenees and is characterised by a Mediterranean climate with short violent storm events. Surprisingly, our catchments displaying strong interannual SY variability are not located in the mountainous areas of the study site in which strong rain events are observed but are instead located in the lower parts of the Loire basin and in the Vendeen coastal area.

Indicators of flux duration (Meybeck *et al.*, 2003 [189]) are used to quantify the variability of sediment fluxes. Here, we compare the percentage of time required to export 50% of the sediment load ($Ts_{50}\%$) annually for each basin (Figure 2.11). Similar to the annual SY values, the catchments display strong intra- and inter-catchments discrepancies in the $Ts_{50}\%$ values. For example, between 1 and 130 days may be required for one catchment to export half of its solid flux (example taken from the *Andelot* catchment located in the *Allier* river basin).

However, considering the 110 catchments together, the interannual variability in the $Ts_{50}\%$ values is less pronounced than for the SY values. Moreover, the pattern of variations observed from Figure 2.7, with minimum and maximum median values in 1989 and 2001, respectively, do not apply to the annual values of this indicator. Given that the rainfall amount and especially extreme events exert a certain level of control on the volumes of sediments transported to the outlet, we hypothesised that it also had an influence on the time of transport (the less time required to transport half of the sediment load, the more sediment yield at the outlet). However, no relationship was found between annual values of SY and of $Ts_{50}\%$. This result indicates that quantities

of sediment transported to the outlet depend not only on rainfall amount or on its intensity but also on the time of year when strong rainfall events occur, as explained in section 2.3.2.1, and on the antecedent flow condition and availability of the sediment stock. Moreover, no relationship is found between the basin area and the mean time required to export half of the solid flux ($Ts_{50\%}$), except for the seven catchments with $A \geq 10^4$ km^2. For these basins, a weak correlation is found between A and $Ts_{50\%}$ ($R^2 = 0.42$).

Based on the $Ts_{50}\%$ values, Meybeck *et al.* (2003) [189] proposed a classification of the catchment's solid flux duration in six classes, from a very long to an extremely short duration. According to this classification, a medium duration of solid flux (3.4 to 8% of the time, representing 12 to 29 days per year) concerns 61% of our catchments, whereas 39% are classified as short- or long-term duration fluxes. Only two catchments present very long time flux duration values, and one, the *Beuvron*, is characterised by a very short flux duration value ($Ts_{50}\%$ between 1.4 and 0.4). We found that the Loire river is in the long-term flux duration class (8 to 16.5% of the time), whereas Meybeck *et al.* (2003) [189] found that this river should be classified in the medium class. This difference can be attributed to the length of the studied period because the previous authors used only one year (1999) to calculate the $Ts_{50\%}$ value, whereas 12 years were considered in this study. Hence, this result emphasises the requirement for long-term sediment flux records to draw conclusions on the global functioning of the river.

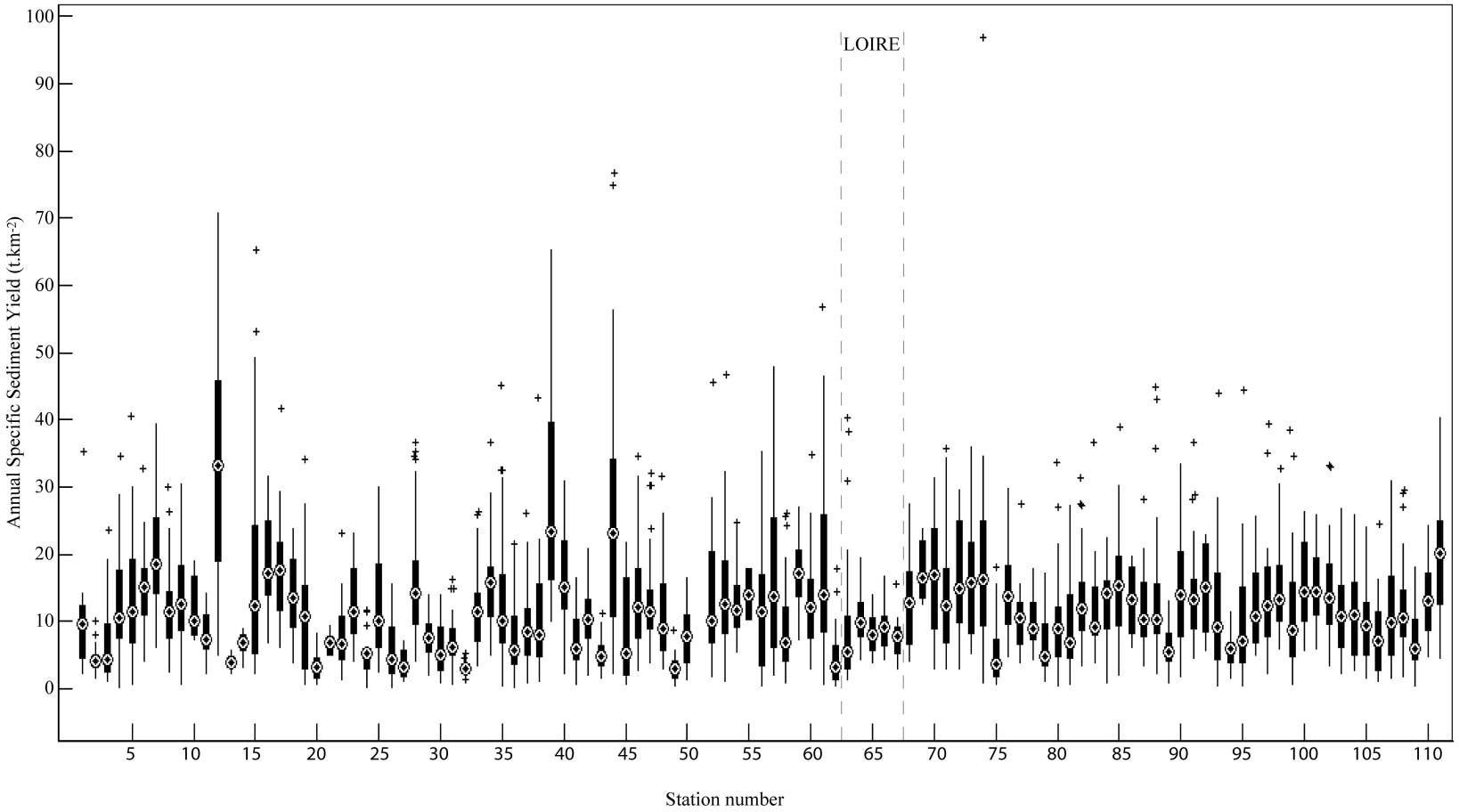

FIGURE 2.10 – Boxplots showing the variability of the calculated annual SY values for each station. For more details on the station and code number, refer to Table 2.1

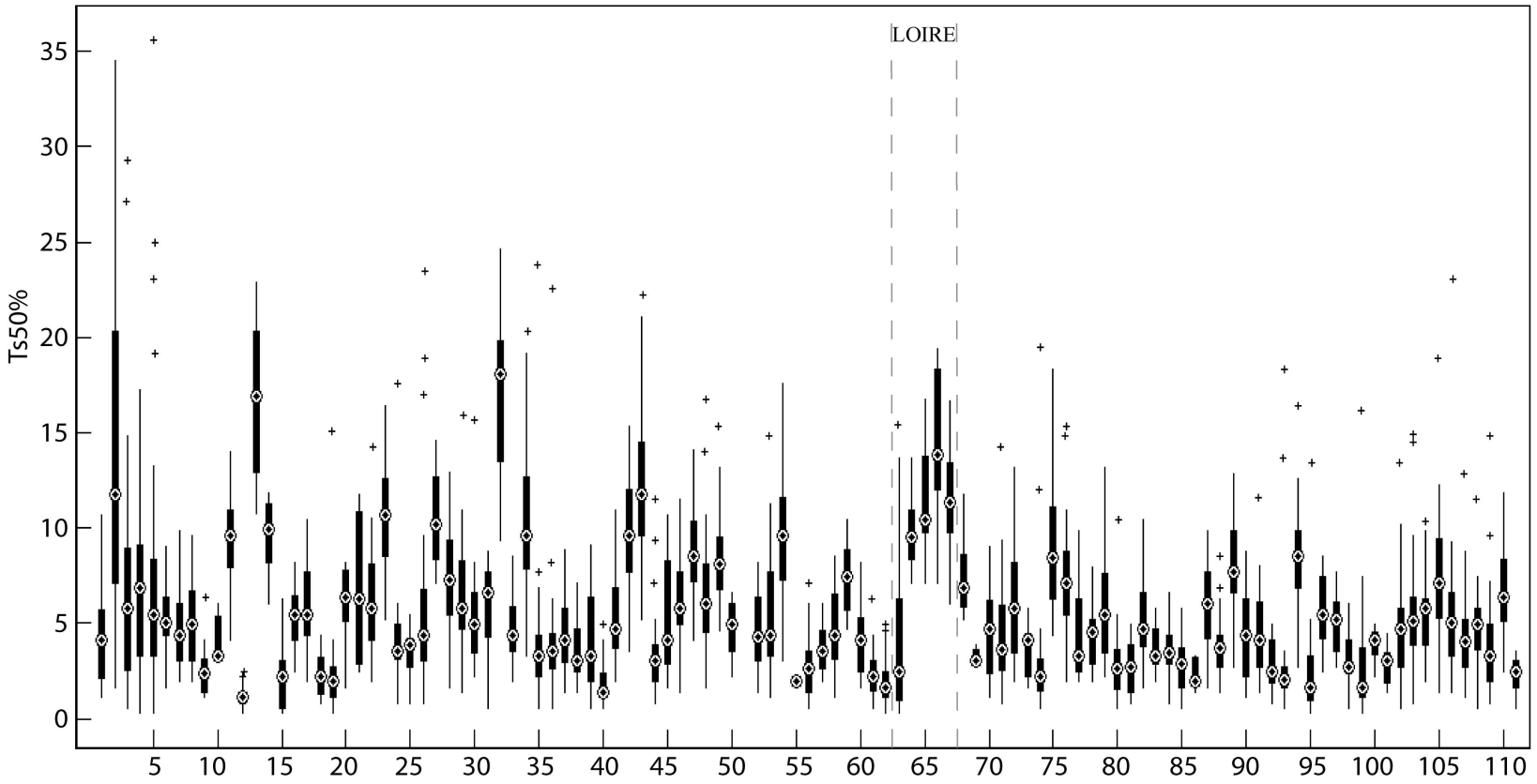

FIGURE 2.11 – Boxplots showing the variability of the time required to annually export half of the sediment load ($Ts_{50\%}$) for each station

2.3.3 Contributions from nested catchments

Among the 111 selected catchments, 27 are nested in at least one other catchment and present long-time values of the annual SY (a period longer than 18 years). These catchments are considered in this study to further analyse the dynamics of sediment fluxes and provide insight into sediment transport from upstream to downstream areas. Catchments are grouped by pairs: a nested and a nesting catchment (Figure 2.12(b)). Because certain catchments are nested in more than one catchment, in this study, we consider a catchment and the smallest one in which it is included. Therefore, in one case, a catchment may be an including one, whereas in another case, it is considered as included in another catchment.

First, for each of the 27 couples of the stations, we calculate the percentages of the drained area and sediment load coming from the upstream station to the downstream station. The results of these investigations are presented in Figure 2.12(a), and each dot represents a couple of catchments. A linear correlation exists between the total suspended sediment load at one station and the load coming from the upstream station, according to the percentage of the drainage area contribution ($R^2 = 0.9$). This regression line roughly follows the 1:1 line, which indicates an equal contribution in area and sediment load between both stations.

In a second phase, we consider 6 rivers that are characterised by two or more gauging stations and long-time load records. From these couples, we investigate the annual linearity of sediment transfers from the upstream to the downstream station. The example obtained from the *Erdre* river shows that the interannual variations of the SY values at two gauging stations on this river (Figure 2.13) display similar trends. Both the annual-SY values at the upstream and downstream stations vary in the same manner, except for the year 1985 to 1986, in which a decrease in the SY value is observed at the upstream station but the SY value increases downstream. However, the proportions in the increase or decrease of the SY values between two years and between the two stations are not conserved. An increase in the SY values between 1978 and 1979 for the upstream station is approximately 208%, whereas this value is only of 109% at the downstream station. Similar results are observed for the 5 other rivers for which several gauging stations are available.

From these findings, three conclusions may be drawn. First, the fact that a strong correlation exists between the contribution in the sediment load and the area from the upstream to the downstream station and that the trend line follows the 1:1 line (Figure 2.12(a)) indicate that there is no in-stream deposition on the way between the stations. This result suggests that there is no scale effect in sediment transport. However, certain couples do not exactly follow the trend line, and for these couples, the nested catchment approach allows the identification of active sediment sources and transfers within a drainage area. For dots located above the 1:1 line, high sediment production and transfers are expected to occur in the nested catchment. This configuration enhances the hypotheses that basin heads are very active in sediment production and transfer, whereas most of the sediments are deposited in the plain. Conversely, for dots located

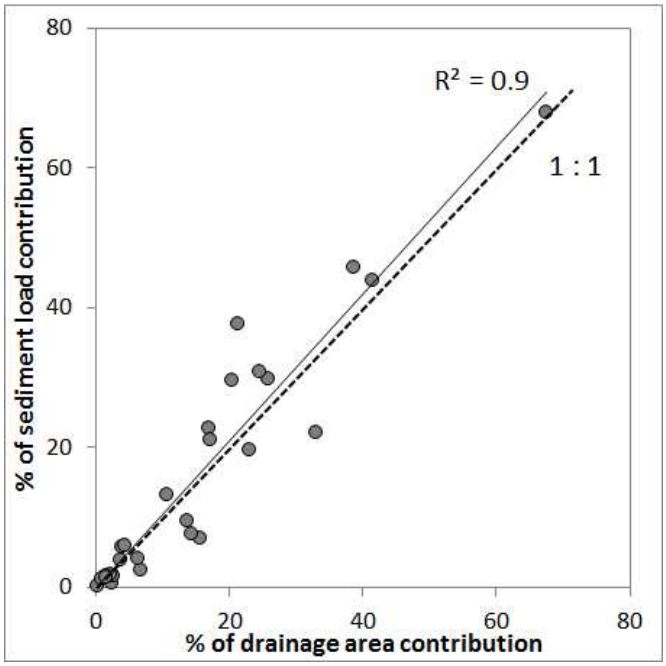

(a)

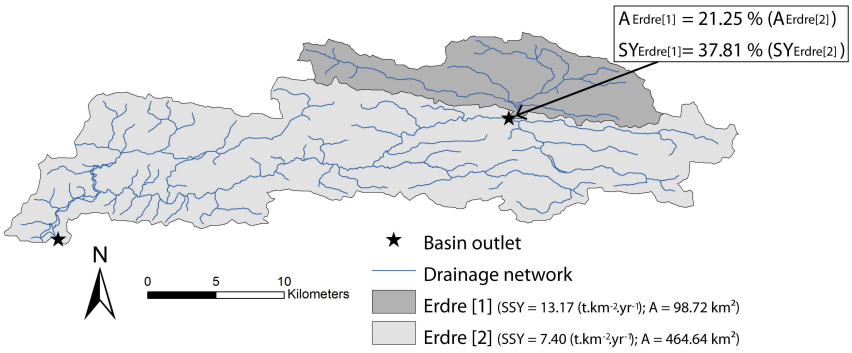

(b)

FIGURE 2.12 – Contribution of a nested to nesting catchment with a) percentage of area and sediment load contribution of 27 nested catchments to the first including catchment and b) example from the *Erdre* river of a couple of catchments

under the regression line, more active sources and transfer paths are expected in the downstream part of the catchment compared with the nested one.

Second, it is interesting to note that a linearity in the SY values exists between the two stations, although the amplitude of variation between years is not proportional. These variations may be attributed to processes in place along the river network and between both outlets, such as in-stream deposition and remobilisation.

Moreover, in previous sections, we have underlined that no clear relationships could be found between SY values and different variables when all of the catchments of

the *LBRB* are considered together. However, considering the subunits, such as nested and nesting catchments within this entire territory, a linearity can be found between the processes from one catchment to another. Therefore, investigations into sediment transport should be based on smaller hydrological units rather than the entire *LBRB*.

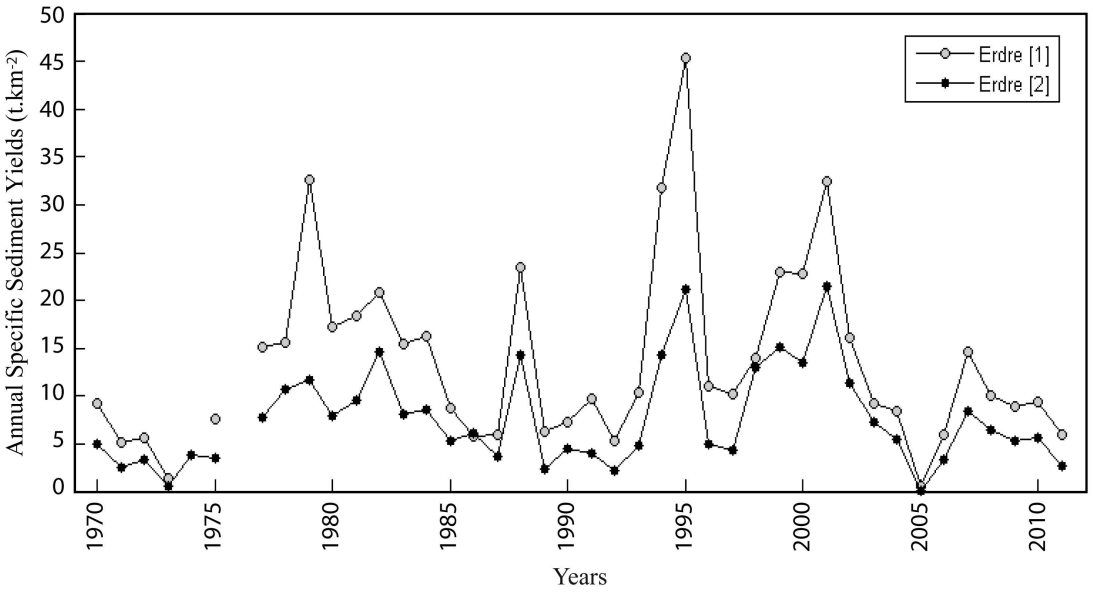

FIGURE 2.13 – Annual specific sediment yields calculated for the *Erdre* river at two gauging stations. Between two consecutive points, lines are traced to represent the general trend

Finally, the nested catchment approach appears to be a useful tool for the construction of a detailed sediment budget for a catchment. For example, on the Loire river basin, the three main Loire tributaries (*Allier*, *Cher*, *Vienne*) together contribute to 66.1% of the total suspended sediment load at the Loire estuary while accounting for 40.6% of its surface. The small and medium catchments included in the Loire river basin represent 12.7% of the total surface but account for 19.0% of the total suspended sediment load. To complete those sediment budgets, in-stream deposition rates should be estimated to better provide information on the contribution of upstream catchments to the final outlet.

2.4 Conclusion

So far, very few studies have focused on sediment exports within lowland areas and over a long-time scale. To bridge this gap and complete the existing studies, we use homogeneous suspended sediment concentration data and calculation methods to develop a large specific sediment yield database over a lowland territory: the Loire and Brittany river basins (*France*). We provide 111 values of specific sediment yields for a

set of catchments with various landscape and climatic characteristics. **Our SY values range from 2.91 to 32.44 t.km^{-2}.yr^{-1}, and these estimations lie within a factor of 0.60-1.65 of the real values.** The use of this homogeneous database allowed comparisons to be made among the SY values across spatial and temporal scales.

No spatial pattern distribution and no correlation between the SY value and the drainage area are observed. These findings suggest that sediment export is a complex process that cannot be evaluated with a single variable, such as the basin size. However, our results clearly indicate that rainfall events exert control in the annual sediment exports. At the interannual time scale and the inter-catchment space scale, strong discrepancies in sediment exports are found, and **the annual rainfall amount explains $\sim$ 40% of the annual specific sediment yields over the entire Loire Brittany river basin.** At the seasonal time scale, differences in sediment availability exist because higher suspended sediment concentrations are found during the winter season than in other seasons. Along with the rainfall events, variations of land use and thus of land cover through the year may also take part as controlling factor in annual sediment exports and explain discrepancies in the interannual SY variability.

When calculating mean sediment exports, it is crucial to have long-term data to be representative of the catchment functioning. Data over very few years may lead to the under- or overestimation of the mean SY value. **From our calculation, 18 years of complete annual data are required to provide a reliable mean SY value, which is with a maximum average variation of 10%.**

Finally, we provide a conceptual insight into in-stream sediment transport. We use a nested catchment approach to evaluate the sediment contribution coming from upstream catchments to downstream stations. From our calculations, **90% of the total suspended sediment load at a catchment outlet may be explained by the total amount of sediments and drainage area coming from upstream nested catchments.** Further investigations into the 6 rivers for which several gauging stations exist show that similar trends in interannual sediment export exist and that a linearity in processes exist from one catchment outlet to the other. This approach is promising for the construction of detailed sediment budgets and for the identification of active sediment sources and transfer zones at the subcatchment scale.

2.5 Epilogue: Further analysis on the driving factors of SSY

In sediment exports investigations, it is common to seek a relation between sediment yields and basin characteristics, such as topography, climate, geology, and landuse (*e.g.*, Jansen and Painter, 1974 [133]; Ludwig and Probst, 1998 [174]). Statistical analyses (*e.g.*, Raux *et al.*, 2011 [235]) are carried out to identify the controlling factor(s) of sediment exports. The compilation of these parameters in indices (Delmas *et al.*, 2009 [71]) then allows for the prediction of sediment yields in unmonitored catchments.

The SDR (Walling, 1983 [298]) is an index commonly used to infer the sediment transport capacity of the catchment. It is calculated as the ratio between sediment yield and gross erosion and thus considers the result of different processes of soil redistribution within the catchment. Usually, SDR values are comprised between 0 and 1, such that when the SDR is high (close to 1), all eroded particles are transported to the outlet of the catchment, while in case of a SDR close to 0, detached particles are deposited within the catchment. In the literature, most SDR values equal 0.1, indicating that 10% of detached particles finally reach the catchmtn outlet, the remaining 90% being deposited on the way.

Tableau 2.2: Description of the chosen variables

Variable	Data sources
Topography	
Mean and maximum slope (%)	DEM at 50m resolution from BDAlti ® IGN
Mean and maximum altitude (m)	
Percentage of deposit areas (slope <2%)	Delmas *et al.*, 2009 [71]
Morphology	
Catchment area (km^2)	
Compacity index (Gravelius)	
Hydrology	
Drainage density (DD, $km.km^{-2}$)	
Mean and median $IDPR$ (-)	Mardhel and Gravier, 2006 [180]
Flow discharge ($L.s^{-1}$)	
Land use	
Percent of Arable lands	CLC 2006 + RPG 2010 (*)
Percent of urban areas	CLC 2006 + RPG 2010 (*)
Climate	
Annual rainfall (mm)	SAFRAN, Météo France, Degan *et al., in prep* [67]
Sediment supply	
Soil erosion ($t.km^{-2}.yr{-}1$	Cerdan *et al.* 2010 [37])

In this framework, a statistical analysis and calculation of the SDR is realised using the 77 catchments for which more than 18 years of data are available. Fourteen commonly used variables (Table 2.2) are selected. A simple analysis (correlation matrix) between SSY and these catchment variables is carried out.

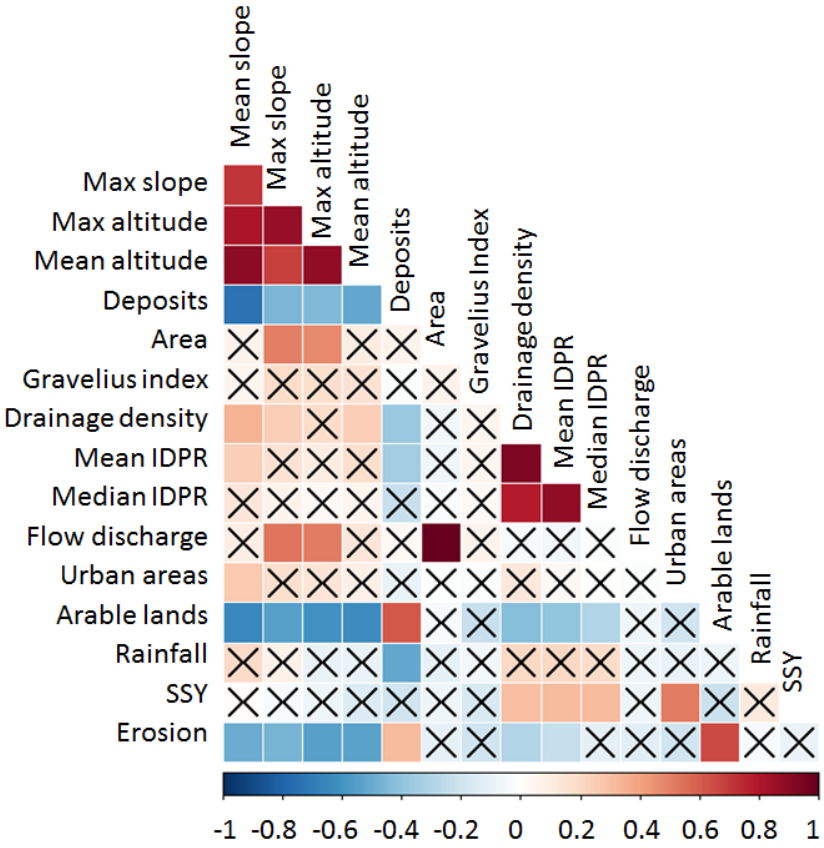

FIGURE 2.14 – Correlation matrix (pearson correlation): coefficients close to 1 (dark red) or 1 (dark blue) show respectively, a strong positive or negative correlation between variables. Crosses indicate non-significant values at a significance level $\alpha = 0.05$.

Unsurprisingly, there exist a strong correlation of the topographic variables (slope, altitude, deposits) between them. Hillslope erosion is positively correlated with the percentage of arable lands and negatively correlated with the slope and altitude.

No clear correlation is found between the SSY and the variables for the 77 catchments (Figure 2.14). Indeed, expected correlation with flow discharge, mean or maximum elevation (Raux *et al.*, 2011 [235]; Delmas *et al.*, 2012 [70]), or hillslope erosion (Gao and Puckett, 2011 [99]) are not observed. A weak but significant correlation is found with hydrological parameters such as drainage density, mean and median $IDPR$ (correlation of 0.31 for all three variables with SSY). Both variables have already proven to be good indicators of sediment transfer within the European area (Delmas *et al.*, 2009 [71]; Delmas, 2011 [68]) and should be considered in further analysis on sediment

transport. The positive correlation observed between SSY and the percentage of urban areas can be attributed to the impervious properties of such areas and thus of the transfer of water and particles without deposition. However, the absence of correlation between the percentage of urban area and $IDPR$ (which is considered as a surrogate of landscape runoff) and SSY does not allow to conclude on the impact of urban areas on final sediment exports.

The effect of rainfall has already been investigated previously in this study. The absence of a significant correlation in the present analysis is attributed to the strong interannual variability of rainfall but also to the number of years available for the calculation of the mean annual rainfall (13 years from 1998 to 2010) which do not match the period over which the SSY are calculated.

The absence of correlation between SSY and catchment characteristics indicates that soil redistribution may be driven by more than one parameter. We believe that an extensive analysis using other factors, statistical tests and indices may provide interesting results to explain the variability of sediment yields. However, the purpose of this study is not to investigate further on the relationships that may exist between sediment yields and catchment characteristics but to focus on the spatial production and redistribution of particles through more distributed approaches. For information, we provide a table of the characteristics of the 111 catchments in the Appendix A.

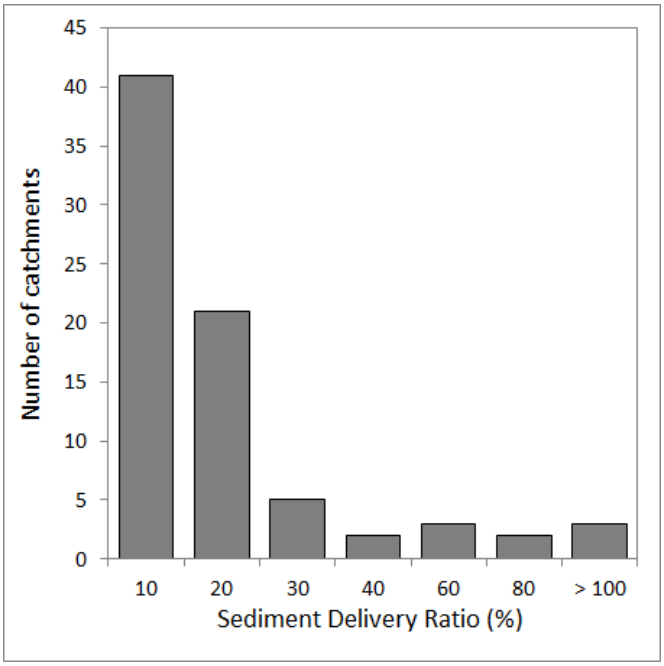

FIGURE 2.15 – Effectif of the values of the Sediment Delivery Ratio for the 77 catchments

The values of SDR are comprised between 2% and 122% (Figure 2.15). While most of the catchments display low SDR values, consistent with literature data, eight catchments have higher SDR values than 60%, three of them exceeding 100%. These

high values, indicating higher exports than particle sources provide, clearly highlight the lack of consideration of all sources of sediment and the need to identify and quantify these sources. The expected inverse relationship between SDR and catchment area resulting from the increase in deposition with increasing drainage area (Milliman and Meade, 1983 [192]; Millilman and Syvitski, 1992 [193] is not observed (not shown on the graph), and thus does not allow us to infer sediment yields in areas where data are not available.

Chapitre 3

Variabilité des flux d'éléments dissous sur le bassin Loire-Bretagne

Suite aux calculs de flux particulaires établis au Chapitre 2, une valorisation de la base de données d'éléments dissous permet de calculer des flux d'éléments dissous à l'exutoire de 90 sous bassins versants sélectionnés dans le site d'étude en utilisant des données identiques et une méthode de calcul unique. Cette étude menée en parallèle permet d'apporter de nouveaux éléments de compréhension sur le fonctionnement du bassin Loire-Bretagne mais également de montrer l'importance des flux sédimentaires exportés sous forme dissoute.

Les résultats indiquent une forte variabilité spatiale et temporelle des flux d'éléments dissous. D'une part, la variabilité spatiale est attribuable aux caractéristiques pluviométriques et lithologiques de chaque bassin, mais surtout à l'occupation du sol (et notamment aux pratiques agricoles) qui joue un rôle prépondérent dans la charge en éléments dissous à l'exutoire. D'autre part, les variations interannuelles des pluies jouent également un rôle dans les exports annuels à l'échelle des bassins versants. Les grandes tendances de flux annuels à l'échelle Loire-Bretagne, observées pour le transport solide, se retrouvent pour les flux d'élément dissous.

De manière générale, le flux moyen d'éléments dissous sur le bassin Loire-Bretagne calculés à partir des 90 bassins versants est nettement plus important que le flux moyen particulaire pour ce même territoire. Une comparaison stricte par bassin versant entre les exports sous forme dissoute et particulaire est proposée pour 52 bassins versants et indique une prépondérance de charge dissoute dans les exports totaux des bassins.

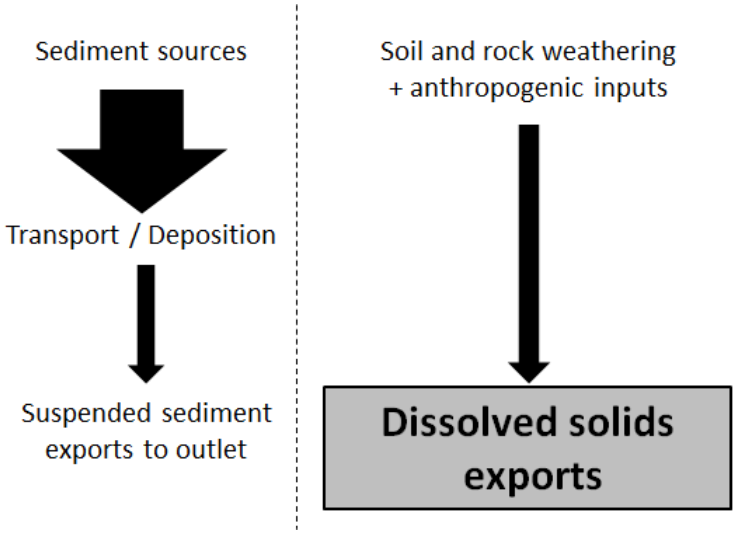

Sommaire

3.1 Introduction

Chemical and mechanical erosion are key processes of landscape evolution and represent major environmental issues. Indeed, consequences of such erosion are numerous and include mud flows, decrease in soil fertility, and water quality and habitat degradation. While mechanical erosion supplies the solid load to water systems, rock and soil weathering supply the dissolved load (Négrel *et al.* 2007 [210]).

Weathering processes strongly depend on geological and topographical conditions at each site (Gaillardet *et al.*, 1999 [97]). Indeed, weathering rates vary according to lithology, and, compared to granites for example, weatering rates of carbonate rocks are 20 times (Meybeck, 1986 [186]). Landuse type and especially land management has also become an important factor of control of the chemical composition of waters (Grosbois *et al.*, 2001 [115]). According to these authors, anthropogenic inputs may influence up to 40 % the chemical composition of the water with a large preponderance of inputs from agricultural lands over those of urban areas. In general, the proportion of inputs from arable lands, industries, and domestic pollution has become significant in the last decades in the composition of surface and underground waters (Roy *et al.*, 1999 [249]; Grosbois *et al.*, 2000 [114]; Meybeck *et al.*, 2004 [188]; Négrel *et al.*, 2007 [210]) and cannot be neglected in dissolved load budgets.

Large database compiling dissolved solid fluxes from worldwide rivers (*e.g.*, Gaillardet *et al.*, 1999 [97]; Meybeck, 2003 [187]; Viers *et al.*, 2009 [292]; Meybeck and Moatar, 2012 [190]) have helped to better understand the spatial and temporal variability of the dissolved element fluxes. Indeed, if at the world-scale, the dissolved loads exported from lands to the oceans have been estimated at 3.6 to 6.8 $*10^9$ $t.yr^{-1}$ by Meybeck and

Ragu in 1997 [191], some rivers contribute more to these exports than others. It is the case, for example, of the *Amazon* and the *Changjiang* rivers, which together, represent 21% of the global exports (Gaillardet *et al.*, 1999 [97]).

In general, world-scale studies give suspended sediment exports as the highest contributor to total catchment exports (*e.g.*, Milliman and Meade, 1983 [192]; Singh *et al.*, 2008 [259]), especially in flashy environments. However, recent findings from Cerdan *et al.* (2012) [36] highlighted the preponderance of dissolved elements fluxes over solid fluxes and the need to take both loads into account in the calculation of sediment yields of medium to long-term response catchments. The authors concluded that, in comparison to the suspended sediment yields (SSY), the dissolved solid yields (DSL) are much more important, and may be up to 10 times greater than SSY (example from the *Seine* river) and thus represent up to 91% of the total exports of the basin. Their results also confirm the existence of a strong spatial variability in dissolved and solid exports with both exports being higher for some rivers than for others.

In France, several studies have been carried out to quantify the fluxes of dissolved elements. However, there exist a gap in the spatial resolution of studied catchments combined with differences in targeted dissolved elements. On the one hand, several studies have investigated the total dissolved and solid exports of large river basins such as the *Seine* river (Roy *et al.*, 1999 [249]), the *Loire* river (Grosbois *et al.*, 2001 [115] for dissolved loads, Delmas *et al.*, 2012 [70] for suspended solid loads), and the *Garonne* river (Semhi *et al.*, 2000 [255] for dissolved loads, Schäfer *et al.*, 2002 [254] for suspended solid loads), and Cerdan *et al.*, 2012 [36] provide an overview of both exports for all of those large rivers. On the other hand, at the small to medium catchment scale ($< 10^3 \text{km}^2$), studies generally focus on exports of a particular element (*e.g.*, copper, Monbet, 2004 [199]; phosphorus, Dupas *et al.*, 2015 [79]) rather than on the total dissolved exports of the catchment.

Such gap cannot help to understand the internal spatial variability of dissolved exports that may exist within large river basins and to draw the link between the dissolved exports and the basin characteristics such as the lithology or the land use practices. Moreover, most of these studies give either mean values of dissolved exports or values for very short time periods (1 to 3 years) but the temporal variability of dissolved loads at the decadal time scale is not investigated.

In this context, the objective of this study is to provide an insight into the spatial and temporal variability of dissolved loads for one large river basin, the Loire and Brittany river basin. To this aim, we calculate and discuss dissolved load fluxes for a large variety of catchments within this area, using identical data and calculation methods to allow for inter-comparison. After a brief state of the art on the origins of dissolved elements, the calculation methods and associated uncertainties, we present the material and methods chosen for the purpose of this study (Section 3.2). Then, the results are presented in Section 3.3 and are discussed in the light of data taken from the literature and compared to suspended sediment fluxes calculated for the same area.

3.1.1 Origins and characterisation of dissolved elements

The chemical composition of surface waters is controlled by eight ions, known as major dissolved ions (*e.g.*, Gaillardet *et al.*, 1999 [97], Moatar and Meybeck, 2007 [196], Négrel *et al.*, 2007 [210]), the cations – Calcium (Ca^{2+}), Magnesium (Mg^{2+}), Sodium (Na^{+}) et Potassium (K^{+}) – and the anions – Chloride (Cl^{-}), Sulphate (SO_4^{2-}), Nitrate (NO_3^{-}) and Bicarbonate (HCO_3^{-}) – and silicate (SiO_2) when available. The total dissolved solids (TDS) is composed primarily by these eight elements and sometimes by trace elements (Viers *et al.*, 2009 [292]) and constitute an indication of the level of water mineralization. The origin of these TDS is twofold.

Tableau 3.1: Solubility of rocks and minerals and *, sum of released cations in μeq.L^{-1} (from Stallard, 1988, Meybeck, 1986, Meybeck, 1987 in Picouet, 1999 [222])

	Minerals (from Stallard, 1988)		**Rocks** (from Meybeck, 1986)		
Solubility	Name	Released elements	Name	$\sum^{+}$	Primarily released elements
Highly soluble	Halite	Na_+, Cl^-	Evaporites	20000	Na_+, Cl^-, Ca_{2+}, SO_4^{2-}
	Gypsum	Ca^{2+}, SO_4^{2-}			
Soluble/ medium weathering rate	Pyrite	cations, SO_4^{2-}	Pyriteous schists	5000	Na_+, Cl^-, SO_4^{2-}, HCO_3^-
	Calcite	Ca_{2+}, HCO_3^-	Calcareous rocks, limestone and marble	4000	Ca_{2+}, HCO_3^-
	Dolomite	Ca_{2+}, Mg^{2+}, HCO_3^-	Dolomie	4000	Ca_{2+}, Mg^{2+}, HCO_3^-
			Calcareous marls, flysch	3000	Ca_{2+}, Mg^{2+}, HCO_3^-
Low weathering rate	Amphibole	Ca^{2+}, SiO_2, HCO_3^-	Serpentinite	1500	Mg^{2+}, SiO_2, HCO_3^-
	Olivine	Mg^{2+}, SiO_2, HCO_3^-	Amphibolite	1500	Ca^{2+}, SiO_2, HCO_3^-
	Anorthite	Ca^{2+}, SiO_2, HCO_3^-	Basalt	600	Ca^{2+}, Mg^{2+}, SiO_2, HCO_3^-
	Albite	Na^{+}, SiO_2, HCO_3^-	Rhyolite	400	Ca^{2+}, Na^{+}, SiO_2, HCO_3^-
	Orthose	K^{+}, SiO_2, HCO_3^-	Trachyandesite	400	Ca^{2+}, Na^{2+}, Mg^{2+}, HCO_3^-, SiO_2
	Micas	Mg^{2+}, K^{+}, SiO_2, HCO_3^-	Schists	500	Ca^{2+}, Na^{2+}, Mg^{2+}, HCO_3^-, SiO_2
			Micaschists	400	Ca^{2+}, Na^{2+}, Mg^{2+}, HCO_3^-, SiO_2
Very low weathering rate	Montmorillonite	Na^{+}, SiO_2, HCO_3^-	Calcoalcalin granites, Calcoalcalin gneiss	300	Ca^{2+}, HCO_3^-, SiO_2
	Kaolinite	Na^{+}, SiO_2, HCO_3^-	Alcalin granites, Alcalin gneiss	150	Na^{+}, HCO_3^-, SiO_2
	Quarz	SiO_2			
			Pure clay	300	cations, SiO_2, HCO_3^-
			Quartzose sandstones	150	cations, SiO_2, HCO_3^-

On the one hand, the dissolved elements may be of natural origin, *e.g.*, from the chemical weathering of soils and rocks, the rainfall inputs, the exchanges between biological compartments or the soil-desorption exchanges. The two latter types of inputs are generally considered constant over the years and are not included in the input-output tables at the catchment scale. However, the dissolved elements from the weathering of rocks predominate in the dissolved solid loads. Thus, it is necessary to identify the various controlling factors (Gaillardet *et al.*, 1999 [97]). Indeed, depending on the nature of the underlying rock formations, weathering results in the formation of all the elements listed above or part of them (see Table 3.1). In addition, atmospheric

inputs via rainfall should be taken into account as they introduce in the system, particles and salts from marine evaporation (Davy *et al.*, 1997 [58]).

On the other hand, the elements can come from anthropogenic inputs and its is essential to take them into account in the ionic balance, especially in the case of highly anthropised areas (Grosbois *et al.*, 2001 [115]). Urban, agricultural and industrial emissions influence the content of major elements (Roy *et al.*, 1999 [249]). Nitrates are the most "publicized" elements in the framework of pollution reduction policies *via* the Nitrate Directive. But other elements may come from anthropogenic sources, such as Calcium, Magnesium and Sulfate. Rejections from Wastewater Treatment Plants ($WWTP$) also supply surplus of Phosphorus, Nitrates, Ammonium and Chloride. The contribution of anthropogenic inputs to the total dissolved exports vary from 9 to 40% (Grosbois *et al.*, 2001 [115] and Roy *et al.*, 1999 [249], respectively).

3.1.2 Sampling strategies and approximations

The concentration of dissolved solids can be calculated directly or indirectly from field data. The choice of a particular method depends on the sampling frequency strategies which vary according to the needs of the study, as well as to the allocated budget.

At the small catchment ($< 10^2$ km^2) and short-time scales ($\sim$ 3 years), studies rely on high-frequency data (*e.g.*, hourly to daily values of TDS concentration, conductivity and flow discharge Q values). In this case, time-series of these three components are "easily" constructed and no approximation is necessary.

In contrast, at larger scales, in France for example, the concentration of the major elements are derived from measurement programs supported by the water agencies. Samples are taken in the river and analysed in the laboratories. During these different steps, strict protocols (AFNOR-norm number NF EN 27888 for conductivity and NF T90-111 for TDS) are applied to ensure the repeatability of measurements and the representativeness and comparability of measurements. In this case, the sampling frequency generally corresponds to monthly or sometimes bimonthly measurements (Moatar *et al.*, 2009 [195]). Indirect methods are used to construct the daily time-series of TDS and conductivity where data are missing.

The electrical conductivity γ, is a measure of the ion activity of the water and thus of its capacity to conduct electrical current. A linear relationship between the conductivity and TDS exists (Rodier *et al.* 2009 [246]) such that, when the TDS level increases, the conductivity increases. It is possible to use the conductivity as a proxy for the TDS concentration by adding an adjustement factor in the relation between the water mineralization, accounting for the entire chemical dataset, and the conductivity (Table 3.2).

In general, the number of conductivity measures is higher than that of TDS. When both data are available for the same dates and hours, it is possible to construct a linear relationship between the two parameters, which takes the form $TDS = b * \gamma$ (Cerdan

Tableau 3.2 Water mineralization from conductivity at 20°C. (*): to be multiplied by 1.116 for conductivity at 25°C (from Rodier *et al.* 2009 [246])

Conductivity (μS.cm^{-1})	Mineralization (mg.L^{-1})
$\gamma < 50$	1.365079 γ (*)
$50 < \gamma < 166$	0.947658 γ (*)
$166 < \gamma < 333$	0.769574 γ (*)
$333 < \gamma < 833$	0.715920 γ (*)
$833 < \gamma < 10000$	0.758544 γ (*)
$\gamma > 10000$	0.850432 γ (*)

et al., 2012 [36]). Due to a dilution effect (Picouet, 1999 [222]), the concentration in TDS (and thus the value of the conductivity) is lower during high flows than during low flows. Thus, an inverse relation is generally expected between the flow discharge Q and the electrical conductivity. The construction of daily TDS time series consists of a double regression between TDS and conductivity on the one hand and conductivity and Q on the other hand (Petelet-Giraud and Négrel, 2011 [220]).

3.1.3 Methods for dissolved loads calculation

Fluxes of a precise dissolved element can be calculated by adding the inputs from its different sources. However, this method requires the knowledge of all responsible sources and the precise quantification of the inputs. Thus, the common method used to calculate fluxes for one or several elements (*e.g.*, TDS) is based on several equations established for suspended sediment or dissolved solid fluxes.

At the annual or decadal time scale, dissolved solid fluxes are calculated from instantaneous fluxes. The latter are calculated by the integration on the cross-section of the product of the flow velocity and concentration at any point on the cross-section (Raymond, 2011 [236]). Thus, the solid and dissolved fluxes combine flow discharge and concentration values as in Equation 3.1 (Moquet, 2011 [200]).

$$F_x = C_x * Q \tag{3.1}$$

with F_x the flux of the element x (either solid of dissolved), C_x the concentration of the element x, and Q the flow discharge.

Starting from this basis, different equations have been developed. Moatar *et al.* (2009) [195] propose a series of nine equations for fluxes calculation from discrete concentration samplings. In most cases, infrequent concentration data (once-in-a-month data) are used for these calculations and Phillips *et al.* in 1999 [221] proposed a series of 22 equations to be used in this case. From their results and further applications, two approaches have been particularly recommended for the calculation of dissolved solid

fluxes (see Equations 3.2 and 3.3).

$$F = K \left(\frac{\sum C_i \, Q_i}{n} \right) \tag{3.2}$$

$$F = K \left(\frac{\sum C_i \, Q_i}{\sum Q_i} \right) \bar{Q} \tag{3.3}$$

with F the annual flux of the element, K a unit conversion factor, C_i the concentration of the element at time i, Q_i the flow discharge at time i, n the number of samples, and $\bar{Q}$ the mean annual flow discharge.

If the method 3.2 is widely used for the calculation of dissolved solid fluxes (Monbet, 2004 [199]; Li *et al.*, 2007 [169]; Négrel *et al.*, 2007 [210]; Worrall *et al.*, 2009 [319] and 2012 [320]), the method 3.3 is clearly recommended for this purpose (Moatar and Meybeck, 2007 [196]; Stutter *et al.*, 2008 [266]; Wen *et al.*, 2008 [311]; Jiann et Wen, 2009 [136]; Moatar *et al.*, 2009 [195]) as the associated uncertainties and bias are the smallest (Walling and Webb, 1985 [305]; Littlewood *et al.*, 1998 [171]; Raymond, 2011 [236]; Moatar *et al.*, 2012 [197]).

This method 3.3, called *DWC* (for *Discharge Weighted mean Concentration method*) has been used by the OSPAR Convention (Convention for the Protection of the Marine Environment of the North-East Atlantic) in the calculation of dissolved fluxes when infrequent concentration are the only available data. However, when high-frequency data are available, the method 3.2 is preferred as it is assumed that the variations of the concentration during the sampling are negligible. Thus, numerous data are needed if one wants to use this method.

3.1.4 Uncertainties on dissolved fluxes

Uncertainties associated to dissolved solid fluxes calculations are of several kinds. First, they concern errors on input data, and second, the bias and imprecision of values induced by the model itself.

Uncertainties associated to the input data are strongly related to in-field sampling methods and laboratory processing of the samples. Concerning flow discharge data, Cheviron *et al.* (2014) [40] proposed a systematic bias in the order of ± 20% for mean daily values (from the HYDRO FRANCE database). As for the concentration data, there is no systematic pre-determined bias as it is strongly related to the sampling conditions, the storage of the samples, and the delays between sampling and analysis. But the most likely error rate lies between 5 and 10% (Petelet-Giraud, 2014 *personnal communication*).

The combination of infrequent concentration data and daily flow discharge data to estimate daily TDS concentrations, generates errors on fluxes calculation. Even if Rode and Suhr (2007) [245] affirm that “the concentrations of most dissolved substances

in river water will vary over a limited range and the use of infrequent samples may introduce only relatively limited errors into load assessments", it is necessary to provide the reader with an evaluation of the reliability of load calculations and of the values of the given average fluxes (Picouet *et al.*, 2002 [223]; Quilbé *et al.*, 2006 [234]; Moatar *et al.*, 2009 [195]). Two parameters allow for the evaluation of such uncertainties, the bias and the imprecision, that are determined by comparing "real" indicators, based on the daily monitoring, and "simulated" indicators, from degraded information at various time steps. The bias is calculated according to Equation 3.4 and measures the difference between the median of the simulated indicators and the real value (Moatar *et al.*, 2006 [198]).

$$e_i = 100 * \left(\frac{F_i - F_{ref}}{F_{ref}} \right) \tag{3.4}$$

with e_i the bias, F_i the flux at year i and F_{ref} the annual reference flux. The imprecision (Δe) characterizes the degree of dispersion and is defined as the difference between the 90^{th} and 10^{th} percentiles of the relative errors (Equation 3.5, Delmas *et al.*, 2012 [70]).

$$\Delta e = (e_i^{90} - e_i^{10}) \tag{3.5}$$

Finally, the Root Mean Square Error ($RMSE$) combines the median bias (e_{50}) and imprecision as in Equation 3.6 and allows for the comparison of uncertainties calculated for each dataset (Moatar *et al.*, 2009 [195]).

$$RMSE = \sqrt{e_{50}^2 + \Delta e^2} \tag{3.6}$$

Two other metrics can also be used to study the variability of dissolved fluxes. The hydrological variability is characterized by the $W_{2\%}$ indicator, *i.e.* the cumulative flow volume discharged during the upper 2% of the highest daily flow. The geochemical variability can be assessed using the truncated b_{50sup} exponent quantifying the concentration versus discharge relationship for the upper half of flow values. $W_{2\%}$ can be calculated from continuous flow measurements, and the b_{50sup} indicator can be calculated from infrequent sampling. This makes it possible to predict *a priori* the level of uncertainty at any station (Moatar *et al.*, 2012 [197]), by combining both indicators to calculate the $M_{2\%}$, the quantity of riverine material discharged in 2% of time as in Equation 3.7. This flux variability indicator is correlated with the uncertainty levels (biases and imprecisions) and thus allows for the approximation of these levels.

$$M_{2\%} = W_{2\%} + 27.5 * b_{50sup} \tag{3.7}$$

Finally, the b_{50sup} indicator allows for the description of the concentration-river flow variations at higher flows. Six classes are defined by Meybeck and Moatar (2012) [190]:

- b_{50sup} < -0.6 : *very diluting process*; a very rare category, in which river fluxes tend to be constant;
- -0.6 < b_{50sup} < -0.2 : *diluting*; most TDS, some phosphate and ammonia downstream of urban sewage inputs;

- -0.2 < b_{50sup} < 0.2: *stable*; some TDS as in karstic regions, and nutrient seasonal variations, as for nitrate.
- 0.2 < b_{50sup} < 0.8: *weakly concentrating*; total P (Phosphorus) and TNK (total Kjeldahl nitrogen), and SPM (Suspended Particulate Matter) in low-relief river basins;
- 0.8 < b_{50sup} < 1.4: *concentrating material*; SPM in medium erosive basins;
- b_{50sup} > 1.4: *very concentrating*; SPM in highly erosive basins.

3.2 Material and methods

In this study, the calculation of dissolved solid loads (DSL) for the $LBRB$ from infrequent concentration measurements results from different steps that are necessary to select the stations and associated catchments. These steps are presented in Figure 3.1 and detailed here after.

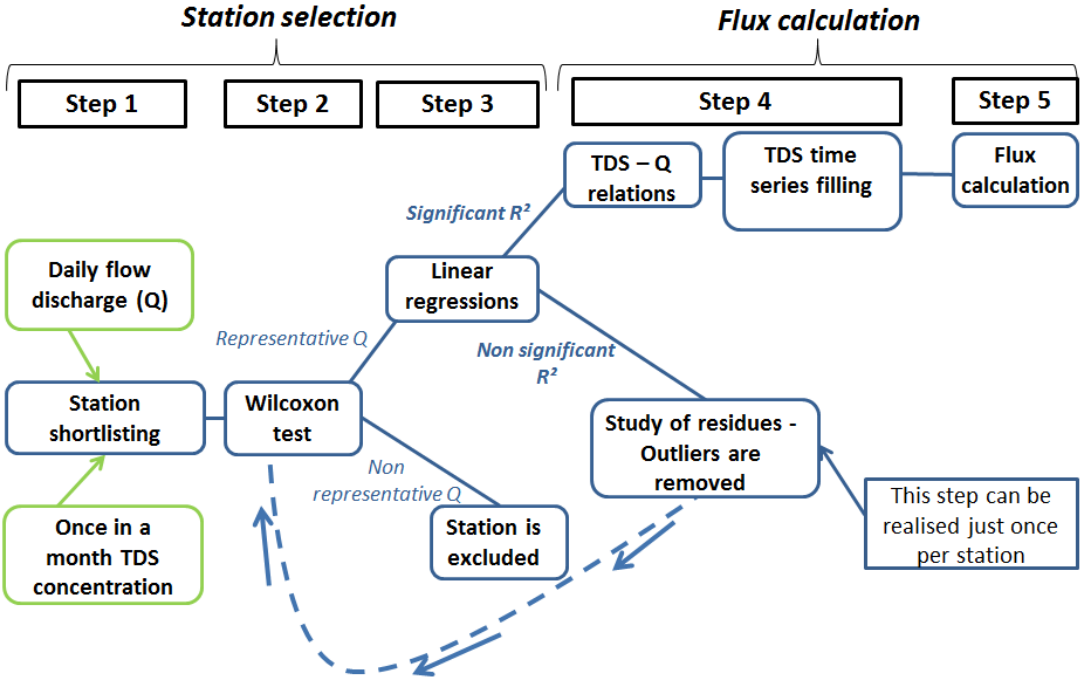

FIGURE 3.1 – Steps of the selection of the stations and of the calculation of TDS fluxes

Step 1 : Database and station selection: Daily flow discharge data are available from the national database BANQUE HYDRO. Only data after 1970 were used in this study to ensure the homogeneity of data acquisition and calculation (rating curves). The complete chemical datasets (Ca^{2+}, Mg^{2+}, Na^{+}, K^{+}, Cl^{-}, SO_4^{2-}, NO_3^{-}, HCO_3^{-}) are taken from the OSURWEB database and correspond to once-in-a-month sampling from a water quality sampling program referring to the ISO norm 5667-1 (AFNOR norms NF EN 27888 for conductivity and NF T90-111 for TDS). Only stations with a

minimum of 72 monthly conductivity measures (six years of data) were used for fluxes calculation. Then, the Q and water quality (TDS and conductivity) data are associated in space and time according to the methodology presented by Delmas *et al.* (2012) [70].

Step 2 : Data representativity The Wilcoxon test was performed to test the statistical representativity, at each station, of the Q data for which the TDS and conductivity values are available (in rising, falling, and base flow discharge), in the corresponding complete Q population at this station (rising, falling, and base flow discharge populations respectively).

Step 3 : Quality of regressions and study of residues To fill missing data in TDS time series, we applied a dual regression between (i) the conductivity and the TDS values, and (ii) conductivity and flow discharge values. For both regressions, the coefficient of determination R^2 is calculated and the quality of the linear regression is investigated using the Fisher Snedecor test.

In case of a poor quality of the regression, a study of the residues is realised. First, the normality of residuals is tested. Then, if one of the samples is characterized as atypical by one of the three chosen criteria – the standardized residuals, the studentized residuals and the levers – the sample is removed from the dataset. This step can be realised just once for each station. When samples have been removed, the new dataset is submitted to Wilcoxon test as described in Step 2

Step 4: TDS time-series filling The filling of the TDS time-series is a two-stage process for each station (Petelet-Giraud and Négrel, 2011 [220]). First, a linear relation is established from a log-log plot between the TDS concentration and the conductivity (γ). This relation takes the form $TDS = a_2 + b_2 * \gamma$. Then, a second linear relation is adjusted on log-log plots between the conductivity γ and the flow discharge Q of the form $\gamma = 10^{a_1} * Q^{b_1}$. Finally, the TDS concentration is estimated for each daily Q-value as in Equation 3.8.

$$TDS = a_2 + (b_2 * 10^{a_1} * Q^{b_1}) \tag{3.8}$$

Step 5: Dissolved load fluxes calculation and uncertainties For the calculation of fluxes, the method 3.3 was chosen ($F = K \left(\frac{\sum C_i \, Q_i}{\sum Q_i} \right) \bar{Q}$, see page 63 for full details).

For each catchment, the indicators $M_{2\%}$, $W_{2\%}$ and b_{50sup} are calculated. For the 19 catchments with more than 50 TDS data, the $RMSE$ was calculated to investigate the effects of sub-sampling.

3.3 Results and discussion

3.3.1 Concentration of TDS and relation adjustment

TDS yields have been calculated for 90 catchments in various areas and distributed all over the Loire and Brittany river basin. For five of the catchments, outliers have

been removed and for the others, the complete dataset of conductivity and TDS is used.

Mean concentration of TDS per catchment range from ~ 50 to ~ 800 mg.L^{-1} which is in the range of the concentration of large river basin (Gaillardet *et al.*, 1999 [97]). Figure 3.2 presents the regressions obtained between TDS and conductivity values (Figure 3.2(a)) and conductivity and flow discharge (Figure 3.2(b)) for the *Oeil [1]* catchment. Both regressions present good relationship between variables with R^2 of 0.92 (TDS - conductivity) and 0.52 (conductivity - Q). This example represents an average case of the regressions obtained between the three variables.

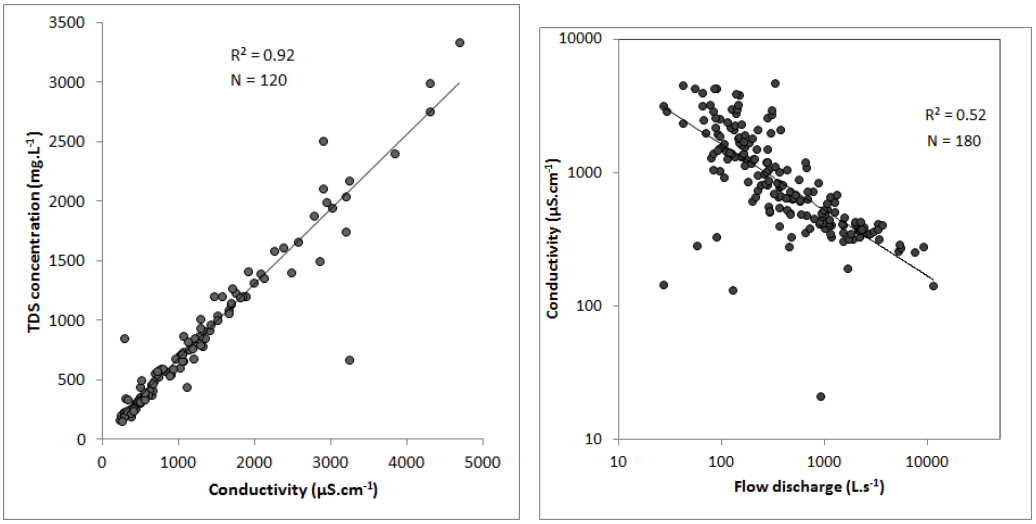

(a) (b)

FIGURE 3.2 – Example of relations between (a) the TDS concentration and the conductivity, and (b) the conductivity and the flow discharge, from the catchment the *Oeil [1]*

Concentrations of TDS vary throughout the year (Figure 3.3). Indeed, the mean value of TDS concentration is higher during summer (380.82 mg.L^{-1}) than in other seasons while the spring season displays the lowest mean and median values (237.94 and 183.15 mg.L^{-1} respectively). The Kruskal-Wallis test indicates that all four populations are significantly different. This result is consistent with trends observed at the world-wide scale. Indeed, concentrations are generally higher during summer and autumn seasons due to low flow discharge while higher discharge values in winter and spring lead to a phenomenon of dilution and thus lower concentrations of dissolved elements (Mortatti and Probst, 2003 [202]; Stutter *et al.*, 2008 [266]). Moreover, concentration in each element vary differently from each others throughout the year. According to the results from Grosbois *et al.* (2000) [114] on the Loire river basin, three geochemical behaviours exist according to flow discharge variations. While concentrations in nitrates tend to increase with increasing flow discharge due to important hillslope runoff, concentration in other elements such as Na^+, Mg^{2+}, K^+, SO_4^{2-}, and Cl^- increase during low flows. Finally, for elements such as Ca^{2+} and HCO_3^-, their concentration increase up to

an intermediate flow of 300 m^3 and then decrease for higher flows. Further research are thus needed to better understand the weight of each element in the TDS concentration for each season.

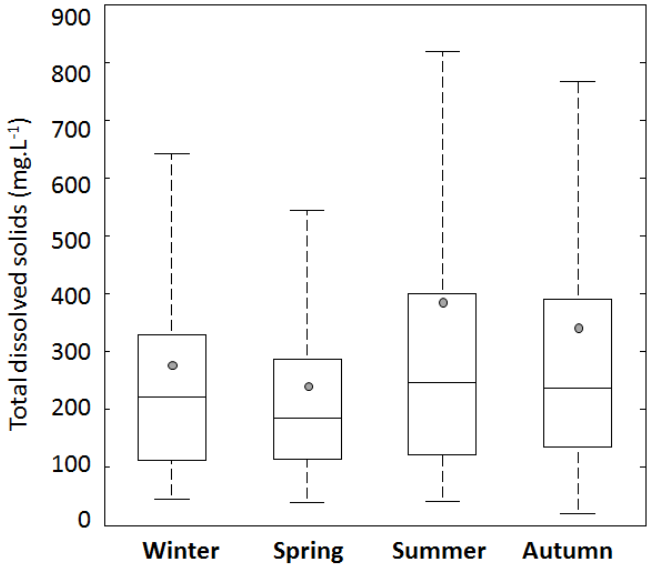

FIGURE 3.3 – Boxplots showing the seasonal variability of the Total Dissolved Loads for the entire $LBRB$

3.3.2 Database of dissolved yields for the 90 catchments

Mean DSL values range from 3.98 * 10^2 to 7.13 * 10^6 t.yr^{-1} (mean = 3.19 * 10^5 t.yr^{-1}, std = 1.12 * 10^6). Specific dissolved solid yields (DSY) values for each catchment are presented in Table 3.3 and range from 13.71 to 199.90 t.km^{-2}.yr^{-1} (mean = 62.56 t.km^{-2}.yr^{-1}, std = 34.07). This range is similar to the range of values calculated for large French rivers (Cerdan *et al.*, 2012 [36]). DSL calculated for the Loire at Orléans by Grosbois *et al.* (2000) [114] for the year 1995-1996 are of 13 * 10^5 tons. In this study, we calculated fluxes in the same order of magnitude with an export estimated at 19 * 10^5 tons for the same time period. On a world-wide perspective, the specific dissolved yields calculated for the $LBRB$ are higher than the mean world average of 35 t.km^{-2}.yr^{-1} (Jha *et al.*, 1988 [135]).

As expected, no relationship between drained area and DSL is found confirming the results from Cerdan *et al.* (2012) [36] and highlighting the importance of the spatial variability of the weathering processes within the drained areas. Indeed, it is commonly acknowledged that chemical erosion rates are more sensitive to lithological, topographical and anthropogenic factors (Gaillardet *et al.*, 1999 [97]; Granet *et al.*, 2007 [112]; Viers *et al.*, 2009 [292]) than to scale-dependency. The effect of these other factors is investigated hereafter.

Figure 3.4 presents the spatial distribution of the 90 watersheds selected and the

calculated *DSY* values. There exist an internal diversity of the *DSY* values that are evenly distributed throughout the *LBRB* such that no real pattern can be distinguished. It is not surprising to note that the highest *DSY* is found for the *Furan* river, a catchment that is also characterised by one of the highest values of specific sediment yield in the *LBRB* (Gay *et al.*, 2014 [104]). These high exports of dissolved and solid elements in the *Furan* catchment are explained by the presence of numerous mines and industries. In contrast, the upstream parts of the *Allier* and *Loire* rivers display low yields. Low *DSY* can also be found in the upstream areas of the *Vienne* and the *Creuse* rivers. The lithology in this area is primarily gneisses and granites with low weathering rates and with lands largely dedicated to pastures with low erosion rates.

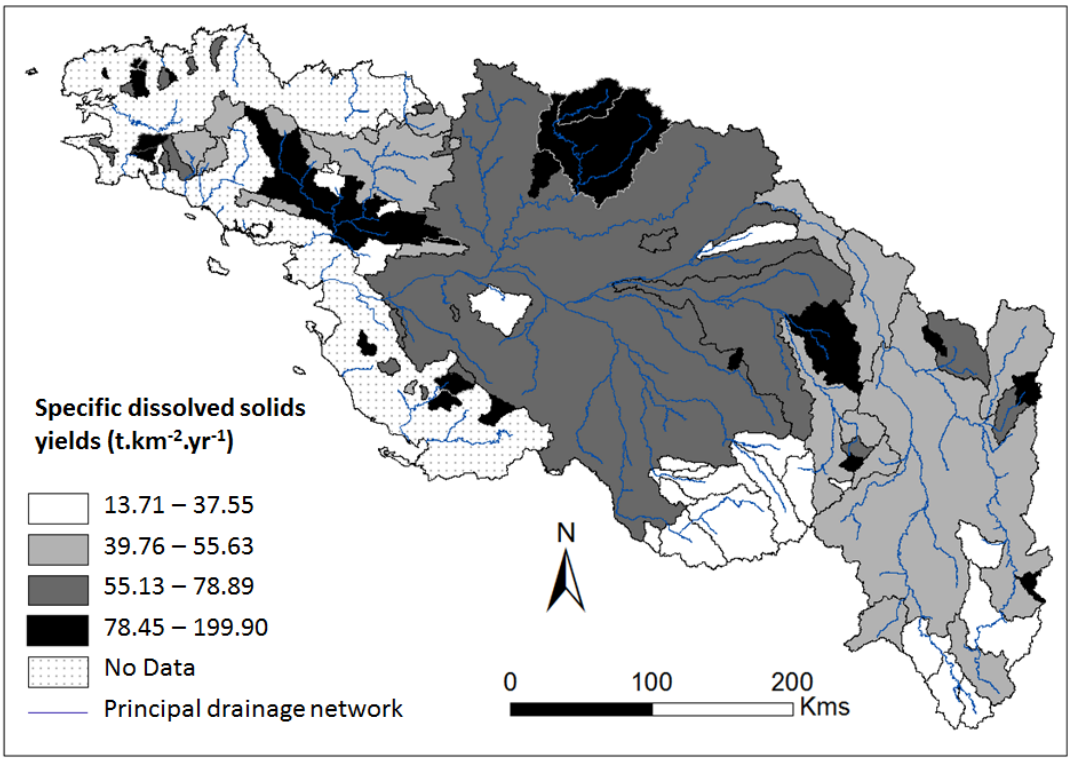

FIGURE 3.4 – Map of the 90 selected catchments and their specific dissolved solid yield which are classified according to quartiles classes

Tableau 3.3 Drainage area, mean specific dissolved yields (DSY), basin number attributed, and station code (from HYDRO FRANCE) of the 90 selected catchments. The number of complete years of Q time-series available are presented in brackets next to the mean dissolved yield values. Rivers for which several stations are available are presented in increasing order of drained areas and are differentiated by the numbers under square brackets

Name	Bassin number	Drained area (km^2)	DSY ($t.km^{-2}.yr^{-1}$)	Station code	Name	Bassin number	Drained area (km^2)	DSY ($t.km^{-2}.yr^{-1}$)	Station code
Aber-Benoit	1	27	104.81 (33)	J3213020	Jarlot	46	44	105.72 (31)	J2603010
Aff [1]	2	29	13.71 (34)	J8602410	Laïta	47	852	78.16 (38)	J4902011
Aff [2]	3	346	32.09 (34)	J8632410	Layon	48	919	33.70 (8)	M5222010
Allagnon	4	981	40.47 (20)	K2593010	Lié	49	299	52.95 (30)	J8133010
Allier [1]	5	519	26.34 (15)	K2090810	Lignon	50	662	26.68 (24)	K0773210
Allier [2]	6	1345	25.47 (23)	K2240810	Loch	51	183	53.81 (41)	J6213010
Allier [3]	7	2260	25.56 (23)	K2330810	Loire [1]	52	1322	40.57 (27)	K0260010
Aron (Gd Fougeray)	8	113	29.44 (23)	J7824010	Loire [2]	53	3249	34.03 (42)	K0550010
Aron (Verneuil)	9	1466	59.94 (33)	K1773010	Loire [3]	54	32607	49.37 (41)	K4000010
Arroux	10	2263	44.66 (38)	K1341810	Loire [4]	55	65575	53.07 (15)	K4180020
Arz	11	161	49.59 (34)	J8813010	Loire [5]	56	36984	51.34 (40)	K4350010
Aumance	12	927	42.05 (12)	K5383010	Loire [6]	57	115234	61.83 (18)	M8000010
Autise	13	244	92.87 (37)	N5101710	Loysance	58	82	66.40 (42)	J0144010
Beuvron	14	38	63.60 (37)	M6014010	Marillet	59	50	43.49 (27)	N3304120
Blavet [1]	15	19	61.77 (31)	J5202110	Mignonne	60	67	77.04 (36)	J3514010
Blavet [2]	16	566	49.65 (8)	J5402120	Moros	61	21	66.19 (42)	J4514010
Boron	17	77	31.04 (13)	K5054010	Odet [1]	62	203	84.88 (42)	J4211910
Bouble	18	561	43.50 (36)	K3373010	Odet [2]	63	328	105.28 (14)	J4231910
Bourbince [1]	19	339	151.77 (31)	K1363010	Ñil [1]	64	124	114.97 (15)	K5343210
Bourbince [2]	20	819	69.34 (40)	K1383010	Ñil [2]	65	319	73.56 (11)	K5363210
Brame	21	232	22.24 (10)	L5323010	Ognon	66	146	69.39 (42)	M8205020
Brenne	22	261	58.66 (35)	K4873110	Petite Creuse	67	853	26.87 (42)	L4411710
Canne	23	182	80.20 (16)	K1764020	Pont-l'Abbé	68	32	69.72 (28)	J4124420
Cher	24	4520	44.32 (13)	K5490910	Queffleuth	69	95	64.97 (23)	J2614020
Cosson	25	749	19.97 (16)	K4793010	Ringoire	70	95	92.92 (11)	K7207510
Couesnon	26	496	50.16 (42)	J0121510	Sarthe [1]	71	906	113.02 (12)	M0050620
Creuse	27	1233	26.56 (42)	L4220710	Sarthe [2]	72	5246	106.29 (12)	M0500610
Doulaye	28	37	57.46 (28)	N3308210	Scorff	73	299	51.10 (42)	J5102210
Ellé	29	575	51.80 (42)	J4742010	Semme	74	174	23.66 (10)	L5134010
Elorn	30	201	99.80 (42)	J3413020	Smagne	75	185	104.19 (42)	N3222010
Erdre [1]	31	99	78.95 (42)	M6323010	Stêr Goz	76	72	66.46 (42)	J4614010
Erdre [2]	32	465	40.37 (42)	M6333020	Tardes	77	859	26.67 (10)	K5183010
Falleron	33	121	80.60 (17)	N0113020	Valière	78	31	86.97 (23)	J7324010
Flume	34	92	39.14 (23)	J7214010	Vègre	79	400	109.46 (12)	M0583020
Furan	35	175	199.90 (39)	K0614010	Vie	80	122	61.94 (17)	N1001510
Gartempe	36	1400	22.09 (10)	L5301810	Vienne [1]	81	2293	31.76 (42)	L0400610
Gorre	37	180	28.99 (22)	L0914020	Vienne [2]	82	3387	29.27 (34)	L0700610
Goyen	38	89	77.04 (42)	J4014010	Vilaine [1]	83	57	48.01 (23)	J7000610
Grand Lay [1]	39	130	69.21 (17)	N3001610	Vilaine [2]	84	147	69.07 (23)	J7010610
Grand Lay [2]	40	405	153.32 (11)	N3031610	Vilaine [3]	85	4146	49.01 (12)	J7700610
Guillec	41	45	110.90 (41)	J3024010	Vilaine [4]	86	10129	114.81 (1)	J9300610
Guindy	42	122	78.73 (28)	J2034010	Vincou	87	286	20.63 (10)	L5223020
Horn	43	38	108.22 (21)	J3014330	Yar	88	58	66.65 (31)	J2314910
Ille	44	103	37.49 (22)	J7103010	Yèvre	89	1973	102.13 (4)	K5712310
Isac	45	548	20.52 (11)	J9202510	Yvel	90	300	37.73 (34)	J8363110

In Brittany, the range of DSY values is wide and varies from 13.71 for the *Aff[1]* to 114.81 t.km^{-2}.yr^{-1}) for the *Vilaine[4]*, the largest and longest river in this region which drains a catchment of $\sim 10^4$ km^2. Concerning the latter, in the upstream parts, dissolved yields are in the same order as mean values obtain for the entire $LBRB$ while downstream, the DSY is double. We hypothesize that the massive input of TDS originate from the *Oust* river, a right bank tributary of the *Vilaine* river. The *Oust* is known to drain intensive agricultural lands, mostly dedicated to livestock breeding, and in-stream high concentrations in nitrates and phosphorus are often measured. In general, concentration in nitrates are high in Brittany and have thus a strong influence on the DSY calculated. Indeed, the recent study from Dupas *et al.*, 2015 [78] indicates that nitrates from agricultural sources in Breton rivers are amongst the highest values in the French territory. These values range from 0.83 t.km^{-2}.yr^{-1} for catchments in the eastern part of the Brittany region to 8.13 t.km^{-2}.yr^{-1} at the centre and to the West of Brittany (Dupas *et al.*, 2013 [77]).

It is thus important to note that site-specific discrepancies between catchments, and especially land management practices, can lead to a high variability of dissolved loads and the preponderance of one element (*e.g., Nitrates*) over the others in the final loads estimations.

3.3.3 Indicators of flux duration and uncertainties

The range of values of $W_{2\%}$ (8.88% for the *Jarlot* river to 31.49% for the *Vilaine [4]* river) is similar to the range of values calculated by Meybeck *et al.* (2003) [189] for rivers in different parts of the world. High values of $W_{2\%}$ indicate flashier flood response of the catchment than in the case of low values.

The b_{50sup} indicator varies from -0.42 to 0.06. Most values are negative or close to zero and thus correspond to the "*diluting*" and "*stable*" classes defined by Meybeck and Moatar (2012) [190] and presented in Section 3.1.1(page 60). Except for one catchment (the *Loysance* in Brittany), the $M_{2\%}$ indicator are all positive and comprised between 3.0% and 29.0%. From the abacus of imprecision of Moatar *et al.* (2009) [195], with the range of $M_{2\%}$ such as the one obtained here, the maximal interval between two TDS samplings should be of 5 to 20 days in order to keep the bias lower than 1% and the imprecision in the range of $\pm$ 20%.

The study of uncertainties carried out on 19 catchments, for which more than 50 TDS, conductivity and Q data are available for the same dates, reveals that the percent of relative error ($Er\%$) between specific dissolved yields and estimated yields from degraded data are comprised between 2.4 and 20.1% (mean = 7.0%). The values of calculated $RMSE$ vary from 6.7 to 59.2 t.km^{-2}.yr^{-1} (mean = 20.0 t.km^{-2}.yr^{-1}). Both values have been calculated using random samplings of 25 TDS-data and thus indicate a very small relative error when using degraded datasets.

3.3.4 Spatial and temporal variability of the dissolved solids loads

Figure 3.5 presents the annual variability of DSY and SSY for comparison. Though there exist a strong inter-annual variability, the observed trends give evidence of a certain homogeneity of DSY among the $LBRB$. These trends can be attributed to the variations in rainfall amount and intensity between years which affect the flow discharge. Strong similarities in DSY and SSY trends are observed. Indeed, in 1989 values of the dissolved solid (median = 29.56 t.km^{-2}) and sediment yields (median = 3.48 t.km^{-2}) are the lowest while highest values are observed in 2000 (median = 91.50 t.km^{-2}) for DSY and 2001 for SSY (median = 24.37 t.km^{-2}). Both years display two of the highest DSY export values which is not the case for SSY, and we hypothesised that the time gap of one year between peaks of DSL and SSY is due to the differences in transport. If dissolved elements are carried directly from sources to oceans, the sediment is likely to be deposited on the way and periodically resuspended. Yet, further research is needed to clearly identify the existence of such pattern.

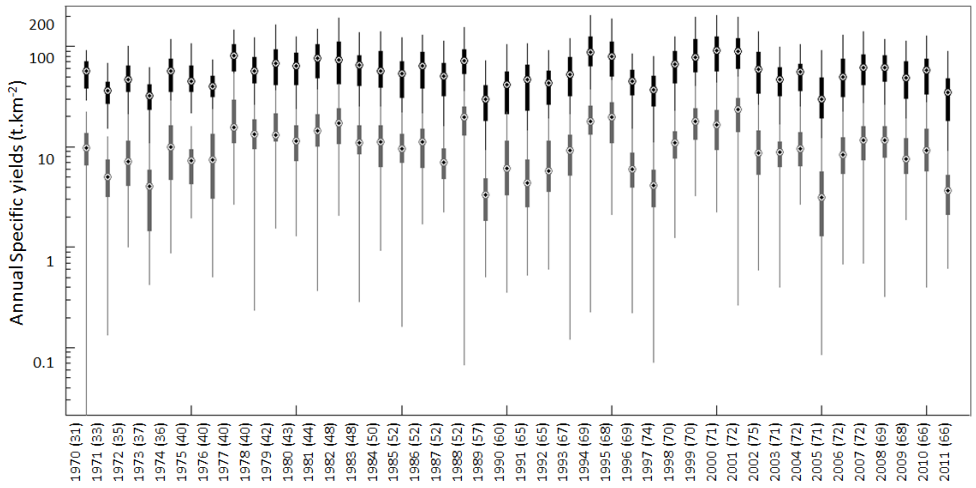

FIGURE 3.5 – Boxplots showing the annual variability of the annual specific dissolved solid yields (DSY, black boxplots) and specific suspended sediment yields (SSY, grey boxplots) values. The number of stations for which DSY data are available for the specified year is displayed under brackets

Similarly, Figure 3.6 displays the internal variability of DSY for each of the catchments and inter-catchment DSY variability. From this figure, it is clear that there exist an internal variability for each catchment. Two catchments stand out of the others. The first one, number 35, corresponds to the *Furan* catchment. The other one, number 40, corresponds to the *Grand Lay [2]* catchment. The latter exports every year 153.32 t.km^{-2} (median value) but the interannual variability is among the highest with a factor 10 between the minimal and maximal values. There exist also strong differences between catchments which is investigated from the point of view of lithology and land use in the next section.

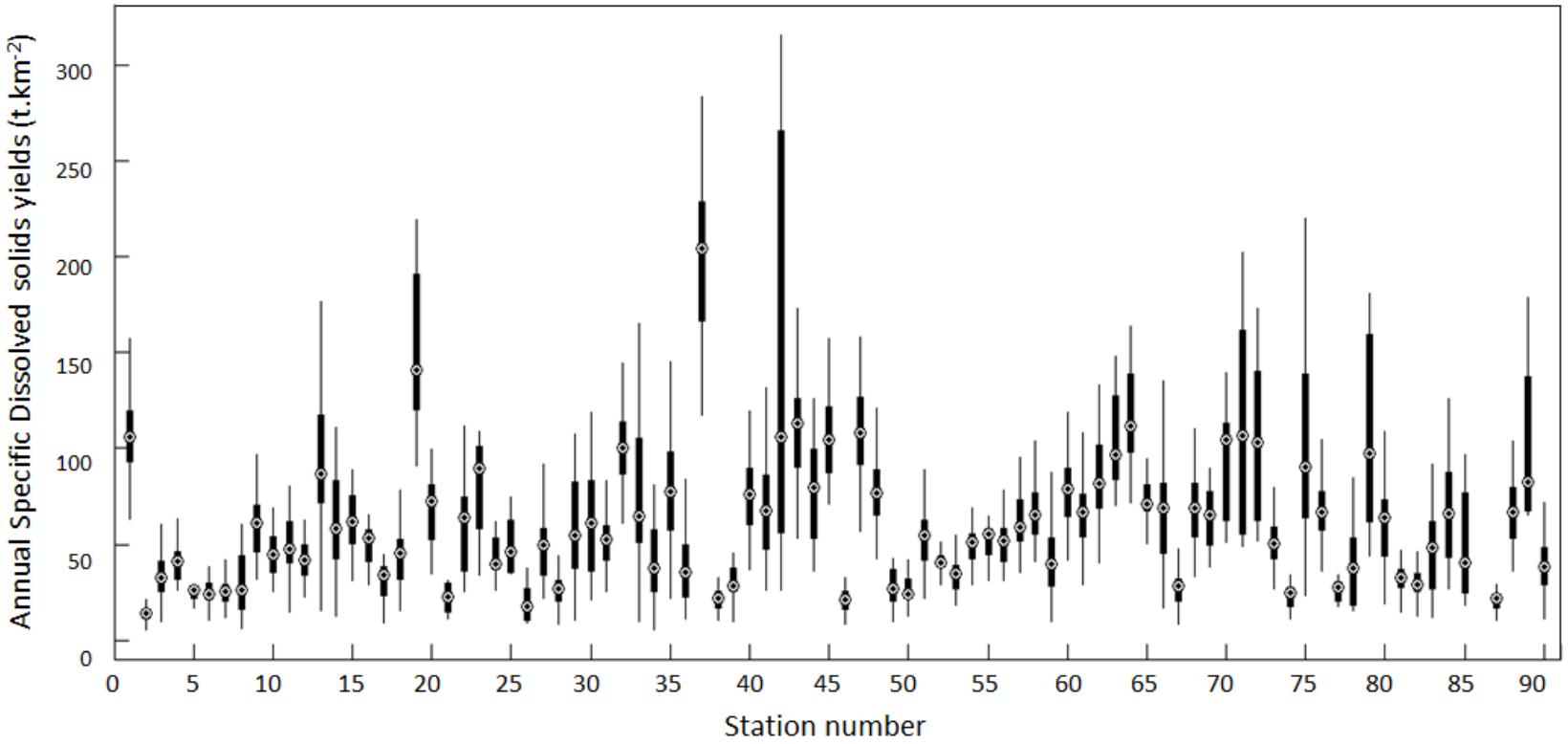

FIGURE 3.6 – Boxplots showing the variability of the calculated annual dissolved yields values for each station. For more details on the station and code number, refer to Table 3.3

3.3.5 Influence of lithology and landuse

As described in the Section 3.3.2, lithology and landuse, especially the agricultural land management, influences the DSL. Figure 3.7(a) presents the variations of DSY according to the monolithological catchments (*i.e.*, one lithology type covering at least 60% of the catchment). As expected, DSY are the highest on calcareous rocks and the lowest on gneisses with a factor 2.5 between median DSY values. According to Picouet (1999) [222] (see also Table 3.1, page 60), weathering rates of gneisses are up to 26 times lower than that of calcareous rocks. The difference in values of the multiplying factor for the different lithology between weathering rates and TDS fluxes may be attributed to the fact that most catchment are not purely monolithological. Moreover, other sources may influence the chemical composition of waters.

The effect of landuse type (dominant landuse if represented on more than 50% of the catchment) is investigated in Figure 3.7(b). Once again, results are as expected, *i.e.*, higher DSY are found in catchments were arable land is the dominant landuse type (median = 77.04 $t.km^{-2}.yr^{-1}$) while in catchment dominated by pastures the DSY are lower (median = 48.01 $t.km^{-2}.yr^{-1}$). The very few number of forested catchments does not allow to conclude on the effect of such landuse type on DSY.

The combined effect of lithology and landuse is also investigated in Figure 3.7(c). While little variation is observed between median of DSY for catchments dominated by pastures and arable lands on schists, strong discrepancies exist between both landuse types on granites. Indeed, the median DSY values of pasture catchments on granites is of 42.05 $t.km^{-2}.yr^{-1}$ while this value is of 77.04 $t.km^{-2}.yr^{-1}$ for arable lands on granites and almost reach the median value observed for cropped catchments on calcareous rocks (97.52 $t.km^{-2}.yr^{-1}$). This result highlights the importance of landuse type over lithology in certain contexts.

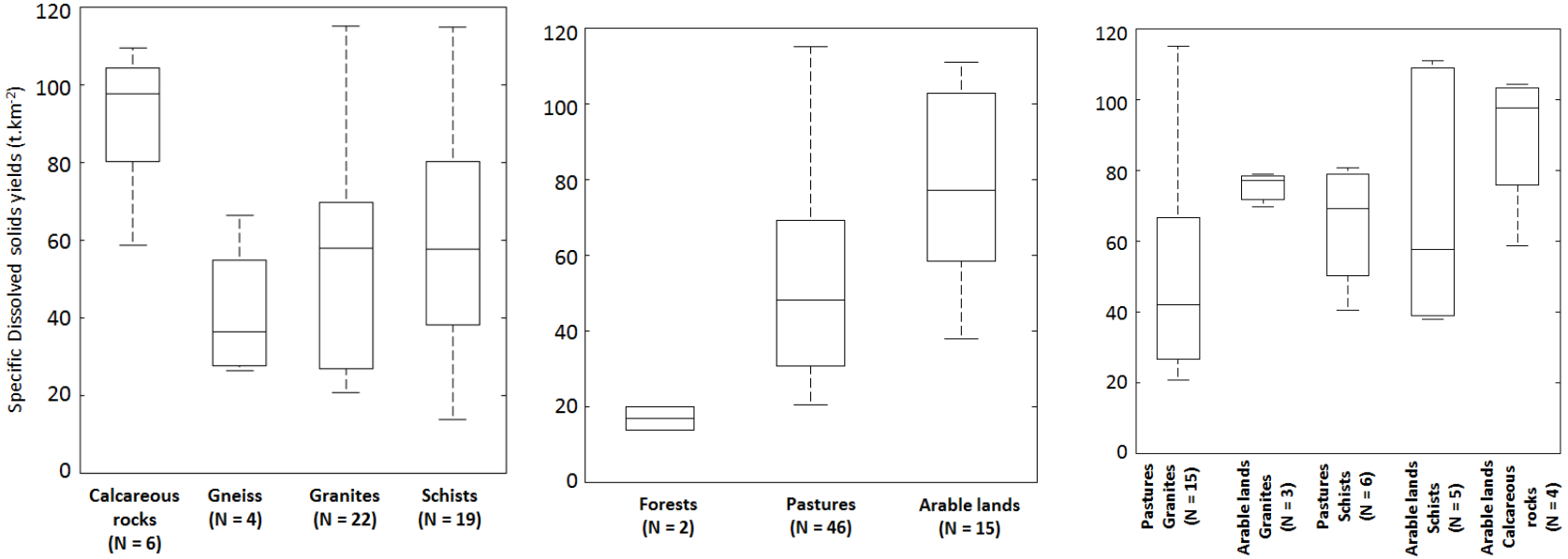

(a) (b) (c)

FIGURE 3.7 – Variations of specific dissolved yields according to (a) lithology, (b) landuse type, and (c) landuse and lithology. The number of catchments N is indicated under brackets

However, the effect of all combination types on DSL cannot be investigated as some combinations are poorly represented (Figure 3.8). It is the case for calcareous rocks lithology where the landuse type is arable land in 60% of cases while pastures and forests are minority land use types (23% and 13% of calcareous rocks respectively). Forests are evenly distributed on all nine lithologies. Pastures and arable lands are equally represented only on the shists of Brittany and helped to draw the comparison between both combination on the Figure 3.7(c).

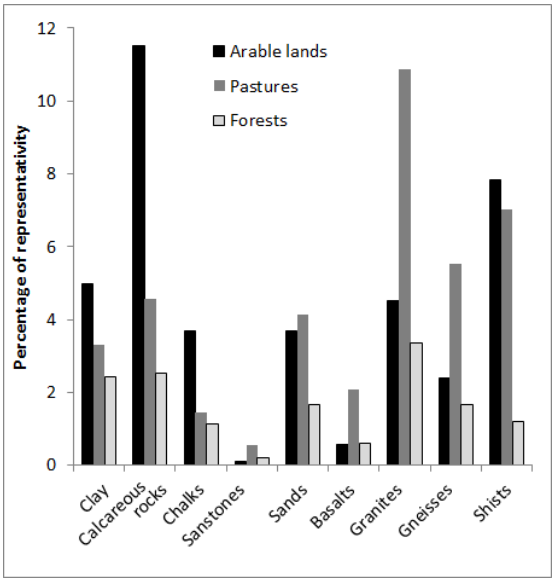

FIGURE 3.8 – Representativity of the combination of the different lithologies and four land use types on the $LBRB$. Minor landuse type are not represented

3.3.6 Contribution of dissolved and solid loads to total exports

For 52 catchments, DSY calculated in the present study and suspended sediment yields, SSY (Chapitre 2), are available and the contribution from both phases to total exports is analysed. Results of these investigations are presented in Table 3.4. The superiority of solute transport over particulate transport has been highlighted in similar environment (temperate areas with low relief, Probst, 1986 [232]). In the present study, it is clear that the dissolved fluxes are predominant in the total exports with a contribution of at least 62.78% of the exports and up to 94.44%. This result confirms those of other studies (*e.g.*, Grosbois *et al.*, 2001 [115]; Cerdan *et al.*, 2012 [36]).

Figure 3.9 presents the spatial distribution of the contribution of the DSL to the overall exports for each of the 52 catchments. For 58% of the catchments this contribution is relatively high, comprised between 80 and 90% of the total exports. But regional discrepancies are observed. Indeed, weakest contributions are found in the upper parts of the *Vienne* and the *Creuse* rivers. As underlined previously, these catchments display low values of TDS and their SSY are similar to mean values of the $LBRB$ sediment exports. The most likely explanation is that the lithology of these

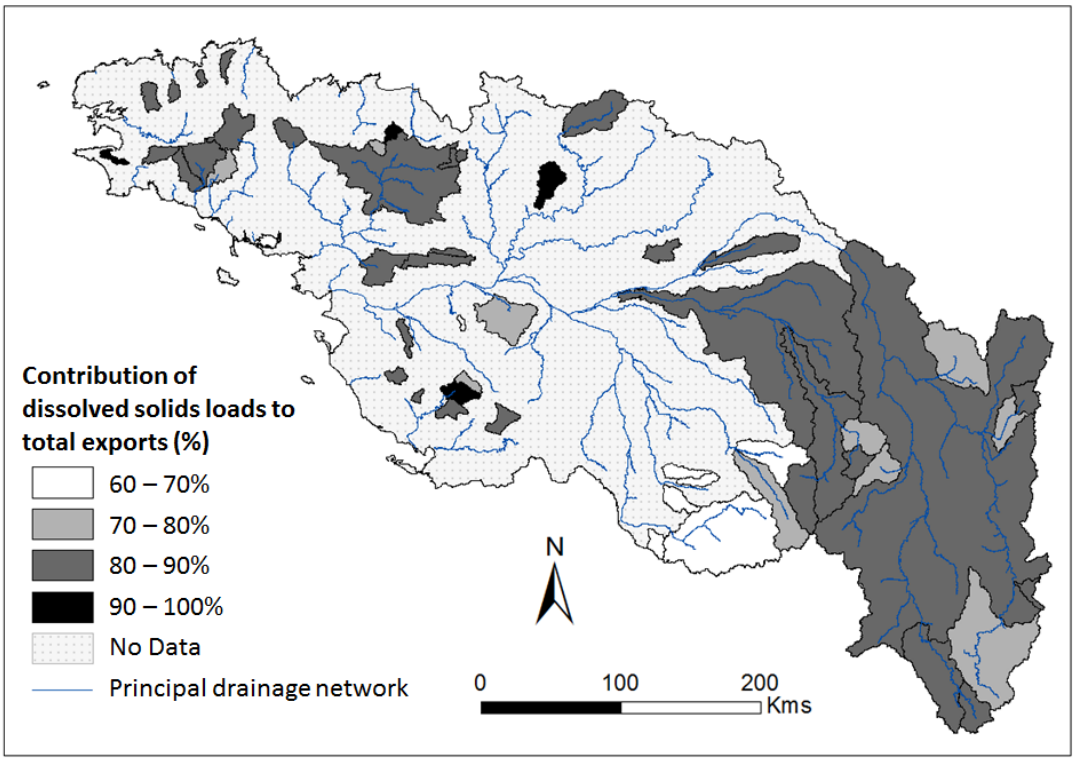

FIGURE 3.9 – Map of the 52 catchments and the contribution from the dissolved solid loads to the total exports of each catchment.

catchments is primarily granitic and gneissic and the land use type is forests and pastures and endure little anthropogenic changes resulting in low weathering and mean erosion rates.

Different studies (*e.g.*, Gaillardet *et al.*, 1999 [97]; Roy *et al.*, 1999 [97]) have highlighted the control of chemical denudation by physical denudation through positive correlation between both variables. However, from Figure 3.10(a), it is clear that, for the 52 studied catchments, no correlation exists between DSY and SSY and this result corroborates findings from Cerdan *et al.* (2012) [36]. The authors explained such absence of correlation by the fact that the calculation of DSY includes the weathering of silicates, carbonates or evaporites, and contribution from anthropogenic sources while studies from Gaillardet *et al.* (1999) [97] and Roy *et al.* (1999) [97] only consider silicate weathering fluxes. Still, other explanations for such finding may be given. These explanations are primarily related to the strong interannual variations of SSY and DSY and thus to the spatial and temporal variations of rainfall throughout the study site. Indeed, Gay *et al.* (2014) [104] indicate that for SSY, 18 years of data are needed to give a mean SSY value with less than 10% of variation. While dissolved elements are not subjected to deposition and resuspension processes, it is still important to have an important number of data in order to catch the inter-annual climatic variability presented in Figure 3.5 and thus give mean stable values of DSY. Therefore, the

comparison of exports of different catchments should consider loads established from similar number of data and coinciding time periods of these data for the compared catchments.

When looking in details, year by year, to the relation between SSY and DSY for each of the 52 catchments (Figure 3.10(b)), the correlation between both variables is improved. At the catchment scale, the coefficient of correlation between annual values of DSY and SSY range from 0.46 to 0.99 with a mean value of 0.90 for the 52 catchments. At the annual time scale, the correlations obtained for annual DSY and SSY vary considerably. While a very weak inverse correlation is observed between both variables in 1978, stronger correlation may be found for other years. However, these correlations are often driven by the extreme values of SSY and DSY of the *Furan* catchment. For example, the coefficient of correlation falls from 0.59 to 0.44 for the year 2005 and from 0.51 to 0.12 for the year 1996 when the *Furan* is set aside.

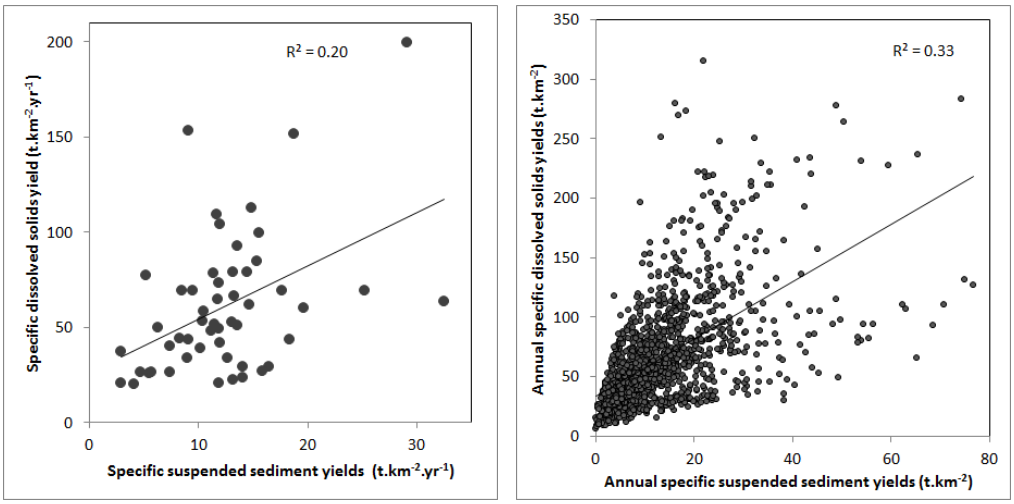

(a) (b)

FIGURE 3.10 – Relations between DSY and SSY concidering (a) mean values, and (b) annual values

These relations established at various spatial and temporal scales confirm the internal spatial variability within the $LBRB$ for both SSY and DSY but also for annual rainfall that drive sediment and dissolved fluxes. While precipitations might be homogeneous on the entire territory (in 2005) and thus offer little variations in both fluxes, more contrasted rainfall events can lead to strong discrepancies in solid and dissolved exports of the catchments over the $LBRB$.

Tableau 3.4 Dissolved solids yields, suspended sediment yields, total yields and contribution (%) from each phase to total exports for the 52 catchments

Station code	Name	Drained area (km^2)	Specific solid load ($t.km^{-2}.an^{-1}$)	Specific dissolved load ($t.km^{-2}.an^{-1}$)	Total flux ($t.km^{-2}.yr^{-1}$)	Contribution from solids (%)	Contribution from dissolved elements (%)
J2034010	Guindy	121.82	14.42	78.72	93.14	15.49	84.51
J2314910	Yar	58.50	13.28	66.65	79.93	16.61	83.39
J2614020	Queffleuth	95.29	11.81	64.97	76.78	15.38	84.62
J3413020	Elorn	200.66	15.57	99.79	115.36	13.50	86.50
J4014010	Goyen	88.87	5.19	77.04	82.23	6.31	93.69
J4211910	Odet [1]	202.72	15.37	84.87	100.24	15.34	84.66
J4742010	Ellé	574.59	11.45	51.80	63.25	18.10	81.90
J4902011	Laïta	851.71	11.36	78.16	89.52	12.69	87.31
J5102210	Scorff	299.48	13.59	51.10	64.69	21.01	78.99
J5402120	Blavet [3]	565.77	6.28	49.65	55.93	11.23	88.77
J7000610	Vilaine [1]	56.82	11.17	48.01	59.18	18.88	81.12
J7010610	Vilaine [2]	146.79	9.43	69.07	78.50	12.01	87.99
J7103010	Ille	102.60	2.94	37.49	40.43	7.27	92.73
J7214010	Flume	91.69	10.12	39.14	49.26	20.55	79.45
J7700610	Vilaine [3]	4146.39	11.86	49.01	60.87	19.49	80.51
J8133010	Lié	298.65	13.03	52.95	65.98	19.75	80.25
J9202510	Isac	548.32	2.91	20.51	23.42	12.41	87.59
K0550010	Loire [2]	3249.13	8.98	34.03	43.01	20.88	79.12
K0614010	Furan	174.53	29.09	199.90	228.99	12.70	87.30
K1363010	Bourbince [1]	338.77	18.75	151.77	170.52	11.00	89.00
K1383010	Bourbince [2]	818.93	17.67	69.34	87.01	20.31	79.69
K1773010	Aron (Verneuil)	1465.53	19.65	59.94	79.59	24.69	75.31
K2090810	Allier [1]	518.69	4.71	26.34	31.05	15.17	84.83
K2330810	Allier [3]	2260.13	5.50	25.56	31.06	17.71	82.29
K3373010	Bouble	560.77	18.32	43.50	61.82	29.63	70.37
K4180020	Loire [4]	35575.42	10.40	53.07	63.47	16.38	83.62
K4793010	Cosson	749.27	4.12	19.97	24.09	17.11	82.89
K4873110	Brenne	261.16	10.43	58.66	69.09	15.09	84.91
K5183010	Tardes	859.17	5.73	26.67	32.40	17.68	82.32
K5363210	Ñil [2]	319.20	11.88	73.56	85.44	13.91	86.09
K5383010	Aumance	927.18	11.92	42.05	53.97	22.09	77.91
K5490910	Cher [1]	4520.05	8.26	44.32	52.58	15.71	84.29
L0700610	Vienne [2]	3387.16	14.07	29.27	43.34	32.46	67.54
L0914020	Gorre	180.03	16.42	28.99	45.41	36.16	63.84
L4220710	Creuse	1233.23	7.41	26.56	33.97	21.81	78.19
L4411710	Petite Creuse	853.13	15.85	26.87	42.72	37.11	62.89
L5134010	Semme	174.38	14.03	23.66	37.69	37.22	62.78
L5223020	Vincou	285.55	11.91	20.63	32.54	36.60	63.40
L5323010	Brame	232.24	13.18	22.24	35.42	37.21	62.79
M0050620	Sarthe [1]	906.05	14.90	113.02	127.92	11.65	88.35
M0583020	Vègre	400.01	11.66	109.46	121.12	9.63	90.37
M5222010	Layon	918.76	12.69	33.70	46.39	27.35	72.65
M6014010	Beuvron	38.26	32.44	63.60	96.04	33.78	66.22
M6323010	Erdre [1]	98.72	13.17	78.95	92.12	14.30	85.70
M6333020	Erdre [2]	464.64	7.40	40.37	47.77	15.50	84.50
M8205020	Ognon	146.33	8.44	69.39	77.83	10.85	89.15
N1001510	Vie	121.67	14.67	61.94	76.61	19.15	80.85
N3001610	Grand Lay [1]	129.53	25.25	69.21	94.46	26.73	73.27
N3031610	Grand Lay [2]	404.77	9.03	153.32	162.35	5.56	94.44
N3222010	Smagne	184.87	11.92	104.18	116.10	10.27	89.73
N3304120	Marillet	49.78	9.07	43.49	52.56	17.25	82.75
N5101710	Autise	244.16	13.52	92.87	106.39	12.71	87.29

3.4 Conclusion and perspectives

In this chapter, we investigate the internal variability of dissolved solid fluxes of a large river basin, the Loire and Brittany river basin. To this aim, we have developed a large database of dissolved solid yields using homogeneous data and calculation methods. Ninety catchments are selected and **mean dissolved solid yields for these catchments range from 13.7 to 199.9 t.km^{-2}.yr^{-1}**. The use of identical database for the calculation of all DSY allowed us to compare the inter- and intra-catchment exports variability and define factors of control in dissolved fluxes.

Results confirms that **the lithology and the landuse type are two of the controlling factors of the discrepancies between dissolved solids yields**. Indeed, exports are 2.5 times higher for catchments with a calcareous lithology than in granitic or gneissic catchments, which is consistent with the factor ~ 20 that exists between weathering rates of calcareous and granitic rocks (Meybeck, 1986 [186]). Exports are found to be higher for catchments dominated by arable lands than that of those dominated by pastures. While the $LBRB$ displays highly contrasted areas with clearly identified lithologies and land use types, no spatial pattern distribution in dissolved yields of the 90 catchments is distinguished, because catchments are large and generally lie on several contrasted lithological formations associate with several landuse types, resulting in the mixing of multiple influences.

At the annual time scale, **dissolved fluxes display a strong variability at the catchment scale, in accordance with rainfall variability**. However, homogeneous trends between years at the $LBRB$ scale are observed and corroborates the trends of suspended sediment fluxes. At the seasonal time scale, expected trends in concentrations of TDS are observed, with highest values in summer related to lower flow discharge during this season.

Comparison with suspended sediment yields values was possible for 52 catchments. **The exports of dissolved solids are much higher than that of suspended sediment, contributing by 62.78 to 94.44% to the total exports,** confirming results from other studies. Moreover, there exist a relation between both yields, indicating that the physical and weathering rates are correlated. However, this relation is only valid if the inter-annual variability of fluxes is taken into account and thus if long-term data are available to give stable mean values of both fluxes.

As an interesting perspective, the study of ratios (Ca/Na, K/Na, Mg/Na, Cl/Na, SO_4/Na, HCO_3/Na) should allow for the tracing of the catchment lithologic signature and of the anthropogenic inputs (Gaillardet *et al.*, 1999 [97]; Négrel *et al.*, 1993 [208]). Another perspective to this work concerns the study of uncertainties. Indeed, in this study, we considered the uncertainties on input parameters and bias and imprecision of methods independently. The propagation of uncertainties should also be investigated for a full understanding of the limits of the study.

Deuxième partie

Quantifications des sources de particules

Chapitre 4

Erosion des versants : synthèse des processus sources et quantifications

Les différentes formes d'érosion de versant ont fait l'objet d'études depuis de nombreuses années permettant ainsi d'apporter, d'une part une meilleure compréhension des processus mis en jeu à différentes échelles spatiale et temporelle, et d'autre part, une quantification de la contribution des sources de particules de versants dans les bilans sédimentaires.

L'objectif de ce chapitre est donc d'identifier, à partir de la littérature existante, les différentes types d'érosion contribuant de manière significative au compartiment source dans les bilans sédimentaires à notre échelle de travail. Six formes d'érosion de versants sont indiquées et des quantifications sont apportées pour trois d'entre elles (érosion diffuse, concentrée et mouvement de masse) à partir de données issues de la littérature ou de modèle établis dans cette étude.

Différentes pistes de réflexions sur la provenance de particules issues de la zone de subsurface (drains agricoles) sont également proposées.

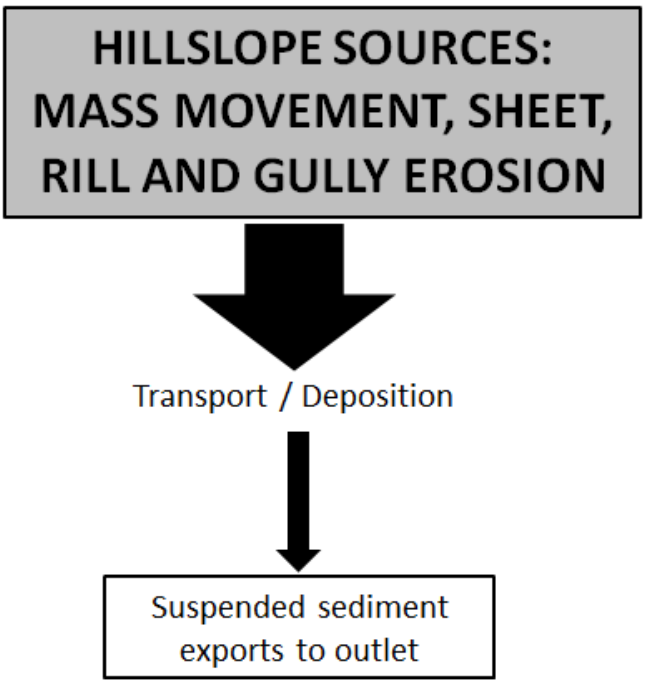

Sommaire

4.1 Introduction

"Soil erosion" covers a wide range of processes that participate in the landscape evolution. Several types of erosion can be distinguished. For example, the chemical erosion refers to the degradation of rocks and soils by processes of dissolution while the particulate erosion concerns mechanical processes. The latter is characterised by three different stages, i) particle detachment, ii) transport, and iii) deposition. These stages are ensured by erosive agents (Morgan, 2005 [201]), such as water, wind and biological factors. Due to its numerous in-site and off-site consequences, soil erosion constitutes major environmental, agronomic and economic issues. Indeed, soil erosion causes soil losses and thus a decrease in soil fertility. Detached particles can then be transported to the nearest water course where they are likely to be deposited, and thus to participate in river clogging, reservoir siltation and to the degradation of the quality of waters.

In the Western European agricultural context, aeolian erosion is negligible. In this area, particle detachment and transport are primarily controlled by the hydraulic forces. Anthropic activities and biota also participate as a source of particles. Considering different spatial scales, the processes involved in soil erosion differ. At the plot scale ($\sim$1m^2), splash erosion, *i.e.* the detachment of particles due to the impact of raindrops, or the activity of the microfauna (*e.g.*, ants, Cerdà and Doerr, 2010 [35]) are amongst the dominant processes involved in soil erosion. However, at the hillslope ($\geq$ 10m^2) to the catchment scale, their influence is lessen and other processes take over, such as sheet and rill erosion, gully erosion and agricultural practices. Nonetheless, whatever the considered scale, erosion is a threshold phenomenon that appears when the conditions of detachment and transport are met.

Numerous studies have been carried out to qualify, quantify and model the different forms of hillslope erosion. In this chapter, we briefly present those sediment sources and existing or generated quantified data that are used in the rest of the manuscript. For information purpose only, we also present different particle sources that have not been

included in our researches due to their minor importance regarding other processes or due to a lack of data.

4.2 Mechanical sources

4.2.1 Sheet and rill erosion and gully erosion

Sheet erosion, also known as diffuse erosion, is barely visible in the landscape. Nevertheless, it induces a progressive scouring of the topsoil layer and its contribution to the sediment budget cannot be neglected. This form of erosion is found on gentle slopes and where the rainfall intensity is low to moderate. Rills appear as the flow concentrate in linear features due to either steeper slopes or the existence of linear elements in the landscape, such as furrows or field borders. However, rills can easily be erased through ploughing and do not constitute a permanent element of the landscape.

To quantify this process, numerous models have been built and run at different pixel sizes. For this study, we chose to use the European map of soil erosion rates from Cerdan *et al.* (2010) [37]. The model combines data on soil type, slope, and land use characteristics and has been calibrated and validated using a large database of erosion plots for all over Europe. It finally provides quantitative rates of erosion at the one hectare resolution.

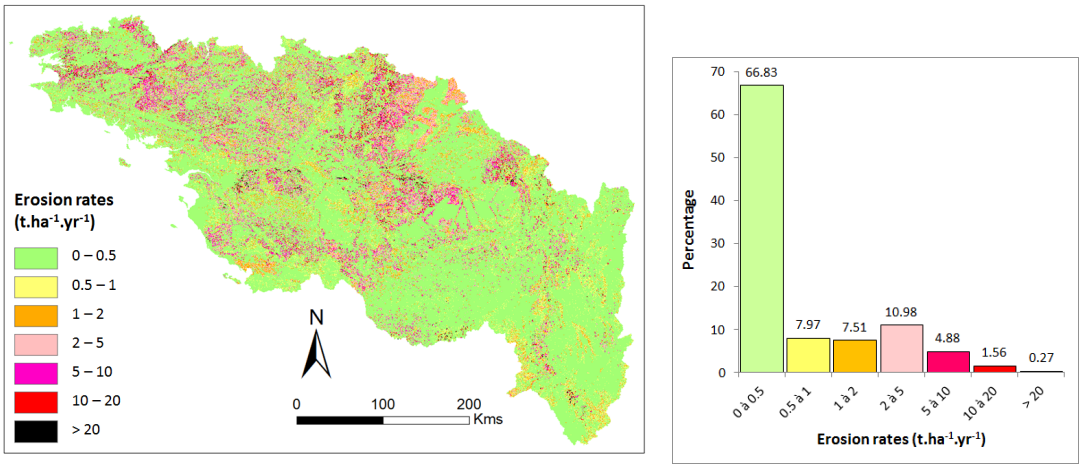

(a) (b)

FIGURE 4.1 – Quantified rates of sheet and rill erosion on the *LBRB* according to Cerdan *et al.*, 2010 [37]): (a) map with seven classes, and (b) percentage of representativity of each class

Over the *LBRB* (Figure 4.1(a)), the mean erosion rate is of 1.23 t.ha^{-1}.yr^{-1} (std = 2.89). Most of the study area displays low erosion rates, with 66.83% of the territory with an erosion rate lower than 0.5 t.ha^{-1}.yr^{-1}. However, 17.69% of the territory

presents an erosion rate higher than 2 t.ha^{-1}.yr^{-1}. These area prone to erosion are located in the western half of the $LBRB$ and in the Limagne plain (Massif Central).

Other models have been developed to quantify sheet and rill erosion. However, considering the purpose of this study, *i.e.* to provide quantitative rates of hillslope erosion with homogeneous pixel size, these models have disadvantages which prevented us from using them. For example, the PESERA model (Kirkby *et al.*, 2008 [144]) displays a coarser pixel size as the model is run over a grid of 1km*1km, while the MESALES model (Le Bissonnais *et al.*, 2002 [160]) specially adapted to the $LBRB$ (Degan *et al.*, *in prep* [67]) only provides qualitative classes of erosion hazard but no quantification is given.

4.2.2 Gully erosion

Contrary to diffuse erosion, gullies are linear elements easily identifiable in the landscape. They result from the concentration of water flows that provoke an incision in soils (Morgan, 2005 [201]). Most of the time, such features are said irreversible, *i.e.*, they cannot be suppressed by tillage practices. According to the context of their appearance, the contribution of gullies to the overall sediment supply varies from 10% to 94% (Poesen *et al.* (2003) [226]). In lowland areas, gullies are less frequent than in hilly areas due to gentler slopes. Hence, little research has been carried out to estimate their spatial distribution at the national and $LBRB$ scale.

Nonetheless, it is possible to predict the development of gullies using an equation of sediment transport (De Vente *et al.*, 2008 [65], Equation 4.1). This equation takes four parameters, the discharge q that can be estimated from the contributing area, the local slope S, the soil erodibility k and an empirical parameter b that needs to be calibrated.

$$T = q.k.S^b \tag{4.1}$$

Delmas (2011) [68] have proposed to use the *Indice de Drainage et Persistence des Réseaux* ($IDPR$, Mardhel *et al.*, 2004 [179]) as a weighing factor for the discharge parameter. The $IDPR$ compares the theoretical river network deduced from elevation to the real network. Low $IDPR$ values indicate that infiltration of surface waters dominates while high values reflect important runoff due to low permeability of underlying soils and rocks (soil saturation). For the introduction of this parameter in Equation 4.1, the same protocol as the one proposed by Delmas (2011) [68] has been applied to produce a map of quantified rates of gully erosion on the $LBRB$ (Figure 4.2). The mean rate for this entire territory is of 0.05 t.ha^{-1}.yr^{-1} (std = 0.07). Unsurprisingly, the model gives higher gully concentration in the Massif Central and Massif Armoricain where slopes are steeper than anywhere else in the basin. At the centre of the $LBRB$, gullies may develop locally on its gentle slopes in areas where the overland flow is generated through soil saturation, a processes that is reflected by the $IDPR$.

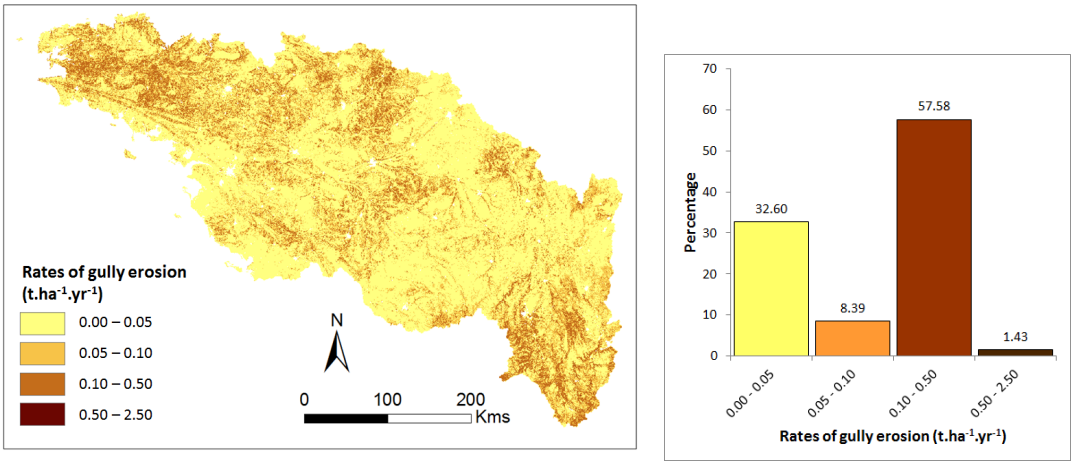

(a) (b)

FIGURE 4.2 – Gully erosion on the *LBRB* according to Delmas, 2011 [68]): (a) map with four classes, and (b) percentage of representativity of each class

4.2.3 Gravity induced erosion: mass movements

Mass movements cover a large panel of sediment erosion processes that result from a gravity induced disequilibrium. These ground instabilities are triggered through the combined effects of intrinsic parameters such as the lithology, the topography, the soil moisture content, and the land use type, and external factors such as the seismicity and the climate (Campy *et al.*, 2003 [32]).

For the Western European area, a map of the sensitivity to mass movements has been produced for large river basins (Delmas *et al.*, 2009 [71]). This map results from the definition of thresholds for the sensitivity of the landscape to mass movements considering the combination of the lithology and the slope percentage. The resulting binary map indicates the presence or the absence of mass movement hazard.

To provide a quantitative rate of the sediment supply available from mass movement activities, a new approach is developed by Poisvert (2013) [228]. The methodology is described in Figure 4.3. First, in order to obtain the most detailed map of the lithology for the study area, different data with different spatial resolution are combined depending on data availability. When possible, the data with the finest resolution and as much information as possible is chosen. Four different data were considered (from lowest to highest resolution/information given): the map of the soil parent material at 1:1,000,000 from the SGBDE (European Commission, 2004 [45]), the surficial formations from the map of the regolith at 1:1,000,000 from Lacquement *et al.* (2009) [150] and which considers allochtonous and autochtonous formations, and finally, hillslope formations from the geological map at 1:50,000. From the obtained map of lithology, classes of sensitivity named *SMMC* (for "Sensitivity to Mass Movement Class") are then attributed to each area depending on priority rules defined in consultation with local experts. Information on lithology, slope classes and mountainous areas (as defined by

Nordregio (2004) [212]) are then combined to obtain several classes of mass movement hazard within the $LBRB$.

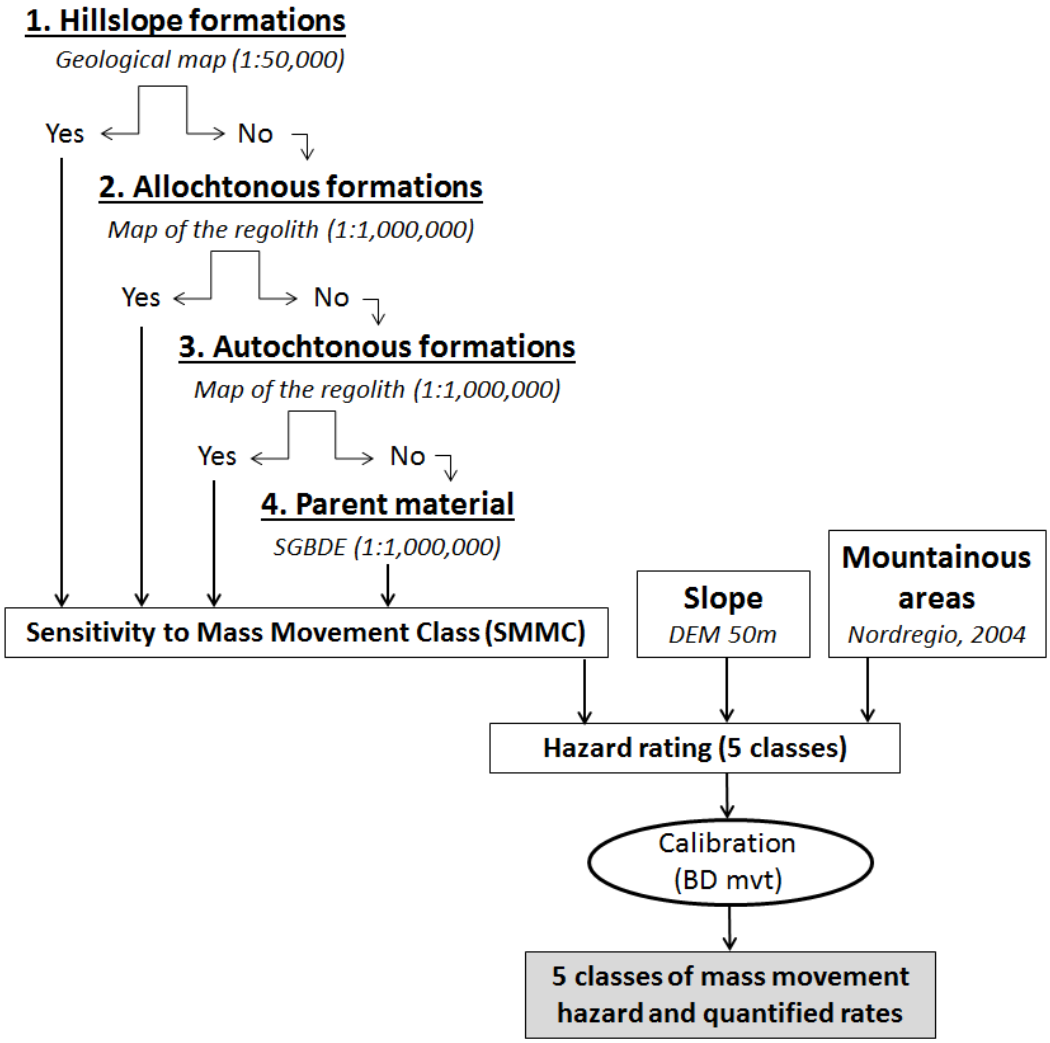

FIGURE 4.3 – Methodology for the mass movement hazard rating and quantification

Second, the quantification of removed particles (in $t.ha^{-1}.yr^{-1}$) is realised by combining the map of the hazard classes and data on landslides and mudflows from the BDMvT (BRGM). On the study area, 1035 events (192 mudflows and 843 landslides), for which quantitative rates of volumes displaced are recorded or can easily be calculated, have been selected. For each hazard class, the median value of the corresponding volumes is calculated, divided by the number of years of observation with regular surveys of mass movement (40 years) and the area of the corresponding hazard class, and multiplied by the number of events recorded in this class. Finally, a distributional analysis is conducted to group hazard classes in five quantified classes (Figure 4.4(a)).

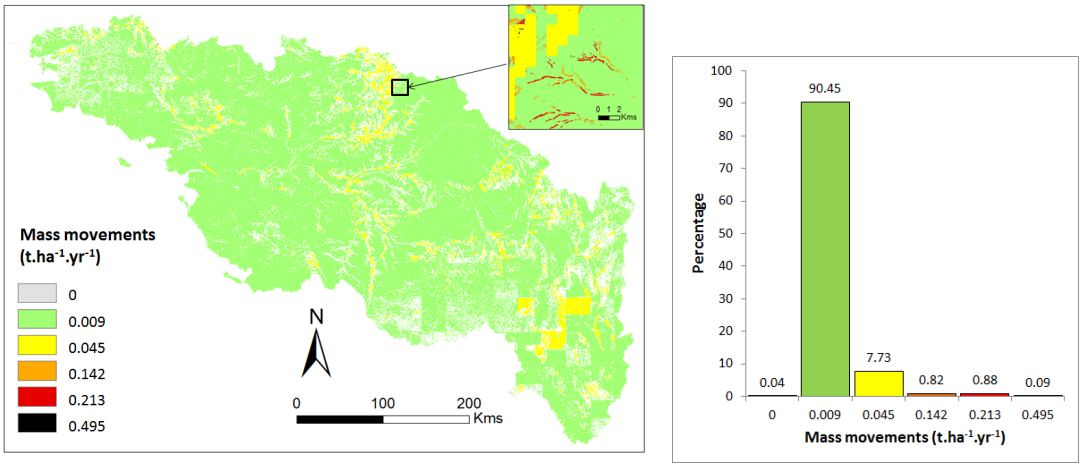

(a) (b)

FIGURE 4.4 – Mass movement hazard (t.ha^{-1}.an^{-1} in the *LBRB* (from Poisvert, 2013 [228]): (a) map with five classes, and (b) percentage of representativity of each class

On the *LBRB*, the mean rate of particles detached and transported via mass movement processes represents 0.01 t.ha^{-1}.an^{-1} which is 100 times less than the mean erosion rate. However, their spatial distribution differ with higher values of mass movement activities in the surroundings of the Parisian basin and in the upper part of the Loire bassin, while in Brittany, mass movements are very low.

The precise estimation of the location of mass movements is clearly limited by the resolution of the available data (hybrid map of the lithology) and especially by the availability of the geological map over the entire study area. However, the constant evolution and updating of database in the future may help to provide a finer evaluation of the mass movement activity on the *LBRB*.

4.3 Anthropic activities and biota

The mechanization and intensification of agriculture throughout the 19^{th} century have clearly modified the landscapes and agricultural practices, leading to other forms of erosion and thus new contribution to sediment sources. Though in the context of this study, the contribution of these sources to the overall sediment budget might be negligible compared to other sources previously described, they cannot be ignored and are thus presented in this section. Moreover, animal activities are also responsible for variations in particle availability.

4.3.1 Subsurface erosion: the implementation of buried drain tiles

Because its effects are hardly visible in the landscape, subsurface erosion processes *via* drain tiles have received much less attention than surface processes. However, dif-

ferent studies have highlighted, through direct sediment sampling at drain tile outlets in the river (*e.g.*, Penven *et al.*, 2000 [219]; Deasy *et al.*, 2009 [66]) or through fingerprinting techniques (*e.g.*, Russell *et al.*, 2001 [250]), the importance of the contribution of the subsurface area to the sediment budget of a watershed. This contribution ranges from 15% (Kiesel *et al.*, 2010 [140]) to 55% (Russell *et al.*, 2001 [250]) and thus represents a non-negligible source of sediment. However, drain tiles are generally considered as vectors for particles but not as a direct source. Nonetheless, it is hypothesised that soils around the tile are impoverished in fine particles through leaching processes. But, experiments need to be realised to confirm this hypothesis and provide quantitative rates of such process.

In the 1970s, the different policies on land consolidation and the transformation of extensive into intensive agriculture has led to a massive implementation of buried pipes in order to drain lands that were originally improper for cultivation. At the farm scale, maps of the drain network are easily available. However, at the *LBRB* scale, the only available data consist of statistics of the percentage of drained plots (with non-clogged drains) at the canton scale. At the national scale (Figure 4.5(a)), 46.5% of the lands implemented with drained tiles are located in *LBRB*. In all, 21.1% of the French cantons with more than 50% of drained areas are located in the *LBRB*. In this basin (Figure 4.5(b)), it is clear that drained area concentrate in the middle and the downstream parts of the Loire river. Still, these statistics do not provide a detailed view of the spatial distribution of the drain tiles. Furthermore, these data rely on farmers declaration for the "Rescencement Général Agricole" (RGA) and statistics only consider the town of headquarters of the farm while farmers may own lands over several cantons.

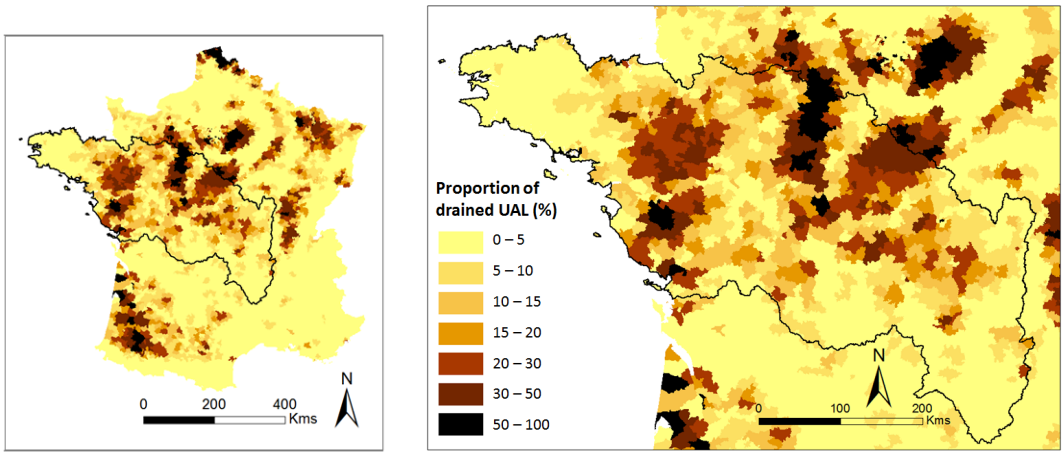

(a) (b)

FIGURE 4.5 – Proportion of the usable agricultural land (UAL) implemented with drain tiles in each canton (from the statistics of the RGA2010) in (a) the French territory and (b) the *LBRB*

Thus, in order to obtain a spatial data of the location of buried pipes, a map of

probability of the drained areas is realised (Figure 4.6). The estimation of the potential presence of drain tiles results from the combination of four factors:

- **Soil hydromorphy** (SGBDE): hydromorph soils regularly reach saturation. To identify hydromorph soils, we use the variable "Water Regime" from the SGBDE. Soils with a water regime higher or equal to 2 (maximal value = 4) are considered as hydromorph;
- **Presence of clay** (SGBDE): the presence of a clayey parent material and thus of an impermeable layer may induce soil saturation;
- **Topography** (DEM): a threshold of slope $< 5\%$ is defined. Under this value, lands are likely to be artificially drained;
- **Land use** (CLC 2006 + RPG 2010, Degan *et al., in prep* [67]): only arable lands are likely to be implemented with drain tiles.

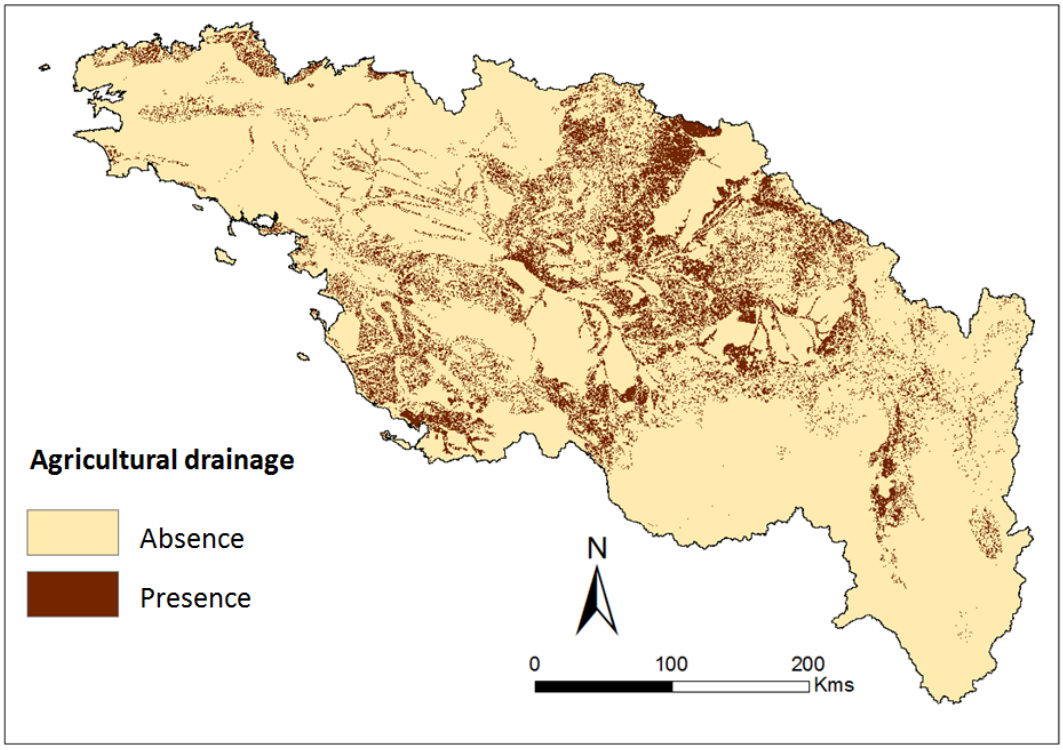

FIGURE 4.6 – Map of the probability of presence of drain tiles

The SGBDE provides information on soils considering: i) Soil Typological Units (STU) for which data on soil properties are available, an ii) Soil Mapping Units (SMU) that gather several STU and the proportion of each STU in one SMU is known. Thus, the map of drained areas resulting from the combination of the different factors indicates the percentage of drainage in each SMU. A threshold has been established by agreement with experts: for each arable land pixels presenting a slope gentler than 5% and being in a SMU with more than 15% of hydromorphic soils (STU), the pixel is considered as

"potentially drained". Under the threshold of 15% of hydromorphic soils in a STU, the drainage system is considered to be absent in that pixel.

About 15% of the *LBRB* present a probability of being artificially drained with a high concentration of this probability in the sedimentary Parisian basin and in the Limagne plain. The spatial distribution of potentially drained areas presents similarities with the statistics from the RGA (Figure 4.5). However, no correlation between both data is found due to the differences in the resolution of the considered data and limits associated to the farmers declaration in the RGA.

4.3.2 Tillage erosion

The integration of man-induced erosion through anthropic activities in erosion modelling and quantification is relatively recent. The first studies on this topic have emerged in the 1990s. Agricultural practices, such as tillage, have been identified as a factor of increase in particle availability and transfers and a new term has emerge to qualify this form of erosion, known as tillage erosion.

First, Van Oost *et al.*, 2005 [286] indicate that the mechanisation and intensification of agriculture in temperate areas during the last five decades have led to the multiplication by a factor two to three of particle transfers. Indeed, the tillage direction strongly modifies the direction of water flux (Souchère *et al.*, 1998 [263]) and solid fluxes (Takken *et al.*, 2001 [269]; Van Oost *et al.*, 2003 [287]) and contribute in the increase of sediment transfers from lands to rivers.

Second, Govers *et al.* (1996) [111] state that tillage practices also play a role in particle detachment and thus their availability and cannot be only considered as vector of soil redistribution. Indeed, the contribution of tillage erosion at the plot scale may represent up to 80% of the total net erosion (Chartin *et al.*, 2013 [39]; Lacoste *et al.*, 2014 [149]). However, most of the studies carried out to quantify tillage erosion rely on plot-scale data. At the watershed scale, recent progress in erosion modelling have allowed for the integration of tillage erosion processes in models (*e.g.*, LandSOIL model, Ciampalini *et al.*, 2012 [41]). Still, detailed knowledge of the land use type and tillage direction for each area is required and thus represents a limits to an accurate modelling of tillage erosion for large river basins.

4.3.3 Particle availability from biota activities

The presence of cattle lead to particle detachment in two ways. Trimble (1995) [278] indicates that in upper areas of hillslopes, cattle trampling induces soil compaction and thus an increase in runoff and erosion. In riparian areas, its effects include a decrease in the riparian vegetation and an increase in bank instabilities that lead to mass failure from the banks and thus to a large contribution in sediment to the river system.

4.4 Conclusion: contribution of hillslope erosion to sediment budget

In this chapter, we briefly present the different hillslope sources that play a significant part in sediment budgets at large spatial scale. For the Loire and Brittany river basin, quantified rates are given for each source according to literature data and models (sheet and rill erosion and gully erosion) or from the computation of a simple model developed for the purpose of this study (mass movements).

In the *LBRB*, **the dominant source of particles is sheet and rill erosion with 1.23 t.ha^{-1}.yr^{-1} of particles being detached on average. Gully erosion and mass movement represent a lesser contribution to the sediment budget with a supply of respectively 0.05 t.ha^{-1}.yr^{-1} and 0.01 t.ha^{-1}.yr^{-1}.** The proportion of the mean contribution of each sources to the overall sediment budget is in accordance with literature data as diffuse erosion generally represents $\sim$ 85% of the hillslope sediment supply (*e.g.*, Walling, 1999 [299]).

The model developed in this study for the quantification of detached particles through mass movements present interesting perspectives for applications at the national scale and integration of finer data as work on acquisition progresses. Further investigations on the contribution of field drain tiles to subsurface erosion are needed to provide quantitative rates of this source to the sediment budget.

Chapitre 5

Erosion de berges : modélisation sur le bassin Loire Bretagne

L'érosion de berges a longtemps été négligée dans les sources des bilans sédimentaires. Cependant, depuis la fin des années 1990, de plus en plus d'études se focalisent sur la quantification de ce phénomène et la qualification des divers processus en jeu. Une étude menée en parallèle[1] *a permis de mettre en exergue l'importance d'un de ces processus sur un petit cours d'eau de plaine, via une importante campagne de terrain et collecte et exploitation de données. A l'échelle du bassin Loire Bretagne, l'application d'une telle méthodologie n'est pas réalisable et le peu de données de terrain existantes ne permettent pas d'estimer l'érosion de berges pour tous les cours d'eau du site d'étude. Aussi, le recours à un modèle simple d'érosion de berges est nécessaire pour éviter la surparamétrisation et être en adéquation avec les données disponibles.*

L'objectif de ce chapitre est donc de proposer une adaptation d'un modèle de retrait de berges par érosion fluviale pour améliorer la prise en compte de différents paramètres dans les estimations d'érosion de berges. L'application de ce modèle sur les cours d'eau du site d'étude apporte ainsi une première quantification chiffrée des valeurs de retrait de berges et d'identifier les différences de distribution spatiale d'érosion de berges existants à l'échelle du bassin Loire Bretagne. D'autre part, cette étude permet de compléter le compartiment "source" des bilans sédimentaires à l'échelle des 77 bassins versants pour lesquels des flux de sédiments ont été calculés.

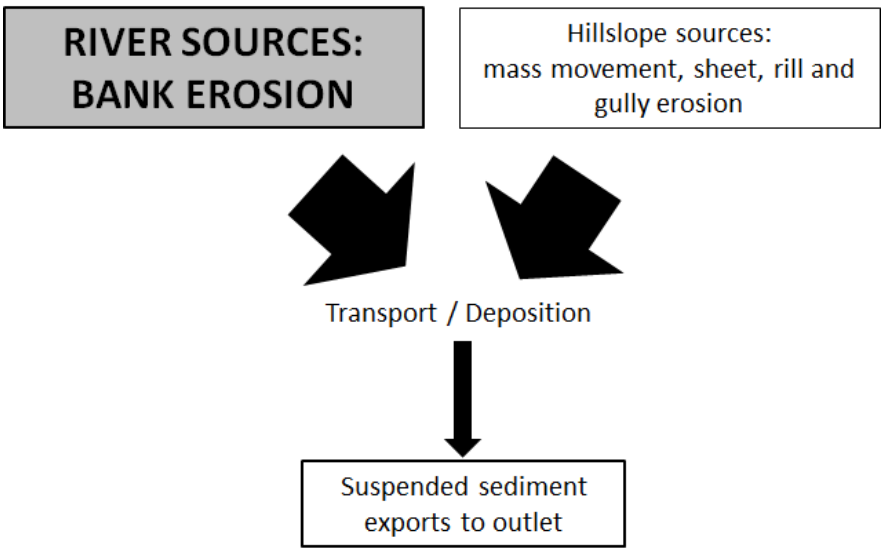

1. Landemaine V., Gay A., Cerdan O., Salvador-Blanes S., and Rodrigues S. 2015. Morphological evolution of a rural headwater stream after channelisation. Geomorphology, 230, 125-137. Annexe D

Sommaire

5.1 Introduction

River bank erosion plays an important role in channel morphology and catchment sediment dynamics. Though bank erosion is a natural process and is necessary for the functioning of river ecosystems (Florsheim *et al.*, 2008 [87]), such process is also responsible for the losses of neighbouring agricultural lands, excess of sediment supply to rivers and downstream sedimentation problems (Walling, 1999 [299]). Because the sediment is introduced directly into the channel system and can directly be transported downstream (Owens, 2005 [217]), it is thus crucial for river and basin sediment management to quantify this sediment input. While it may be possible to define hot spots for hillslope soil erosion according to land characteristics (*e.g.*, steep areas, extreme climatic events), the spatial distribution of bank erosion appears as complex. Hooke (1980) [127] has provided a basis for the understanding of the observed magnitude or bank erosion and has linked erosion rates to catchment area and inherent properties of the banks. Still, general rules to infer bank erosion from site location are less evident than for hillslope erosion and specificities of each site needs to be considered.

Recent studies have helped to better understand processes and factors involved in riverbank erosion. Three different processes have been identified (Lawler, 1995 [157]) and there exist a spatial zoning in the dominance of each process over the others throughout the catchment (Abernethy and Rutherfurd, 1998 [1]). In upper reaches, bank weathering and weakening (subaerial preparation processes) is the dominant process. In mid-basin reaches, bank erosion is primarily controlled by hydraulic forces (fluvial entrainment) while in downstream reaches, bank slumping (mass failure) prevails. These natural processes of bank erosion can be compared to man-induced bank erosion that have been highlighted by different authors (*e.g.*, Surian and Rinalid, 2003 [267]) and results from the control exerted on the streams by anthropic activities.

Different factors control bank erosion or protection. Together with the flow discharge

magnitude (Harvey, 2001 [121]), the most important factor is probably the role played by the riparian vegetation. If numerous authors have demonstrated the protective role of the riparian vegetation (Bartley *et al.*, 2008 [13], Zaimes *et al.*, 2008 [323]) and the increase in bank stability due to the root networks (Simon and Collinson (2002) [258]; Polvi *et al.*, 2014 [229]), Simon and Collinson (2002) [258] also indicate that riparian vegetation can have a detrimental effect on bank stability through weight surcharge and depending on antecedent conditions. Bank stability is also dependant on bank texture and on whether the material is cohesive or not (Thorne, 1982 [276]). Lick *et al.* (2001) [170] confirmed the importance of bulk density and particle size in bank erosion rates and Couper *et al.* (2003) [48] found that high silt-clay content increase bank resistance to fluvial erosion while it increases its susceptibility to subaerial erosion.

The growing interest in river bank erosion has led to the use of a large panel of methods to assess bank erosion rates. At small spatial scale and time-scale (maximum of 2 to 3 years), river bank erosion volumes can be assessed using field data from erosion pins (*e.g.*, Bull, 1997 [28]), fingerprinting (*e.g.*, Russell *et al.*, 2001 [250]; Foucher *et al.*, *submitted* [91]), LIDAR data (*e.g.*, Rhoades *et al.*, 2009 [243], Grove *et al.*, 2013 [116]), aerial photographies (Thoma *et al.*, 2005 [274]; Day *et al.*, 2013 [59]), historical documents (Landemaine *et al.*, 2015 [151]), the combination of these different tools (Bartley *et al.*, 2008 [13]; Kessler *et al.*, 2013 [139]), or can be achieved through numerical modelling (Darby *et al.*, 2002 [57]).

However, at larger spatial scales ($>10^3$ km^2), the contribution of river bank erosion to sediment budgets has long been the most uncertain source term (Hughes and Prosser, 2003 [131]) because of the difficulty to correctly assess bank retreat due to a lack of data and to the number of processes involved in bank retreat. Concerning fluvial bank erosion, the only quantitative rules to assess stream bank retreat are simple empirical equations first developed for meander migration rate modelling, and based on mean annual flood discharge (Rutherfurd, 2000 [251]) or bankfull discharge (Walker and Rutherfurd, 1999 [297]). Further development of these equations have allowed for the integration of bank characteristics. In 2001, Prosser *et al.* [233] introduced the rate of riparian vegetation as a weighing factor to account for bank stability. Later, Bartley *et al.* (2004) [12] also added the floodplain width, to account for the constraint of the substratum on the bed and banks of the river in order to decrease bank retreat rates in rocky gorges. These equations have been integrated in the sediment budget model SED-Net and applied over large areas primarily in lowland Australian river basins and coastal areas. Such equations seem very promising as a first approach of bank retreat due to the low number of required data, their flexibility to take into account different parameters and the potentially large spatial extent for the model application.

In European lowland catchments, bank retreat has been estimated to be less than 2 cm.yr^{-1} (Laubel *et al.*, 2003 [156]; Veihe *et al.*, 2011 [290]) to more than 20 cm.yr^{-1} (Bull, 1997 [28]; Evans *et al.*, 2006 [83]) and up to 250 cm.yr^{-1} (Hooke, 1980 [127]). The associated contribution from banks to fine-grained sediment budget vary from 2% in an Irish catchment (Evans *et al.*, 2006 [83]) to 80.4% in a German catchment (Kiesel *et al.*, 2013 [141]) and up to 94% in a Danish catchment (Kronvrang *et al.*, 2013 [148]).

Such erosion rates and contribution from the banks to the sediment supply to the river and to the sediment budget highlight the importance to take this source into account and thus to provide reliable rates of bank erosion coupled with a comparative approach of the erosion of streambanks.

In the lowland area of the Loire river basin (*France*), the non-achievement of good status of the water bodies (European Environment Agency, 2015 [2]) is partly due to river clogging by fine sediment. Therefore, the task for water agencies is to understand and assess the sources of such sediment. If numerous models allow for the quantification of hillslope erosion rates (*e.g.*, Kirkby *et al.*, 2008 [144]; Cerdan *et al.*, 2010 [37]), little work has been done to quantify sediment inputs from river bank erosion. Still, from the very few studies on the topic, it is clear that this process cannot be ignored in the sediment budget of this large river basin. For example, Latapie *et al.*, 2014 [154] focused on the sediment dynamics and changes in channel morphology in the Middle Loire. Their results indicate a significant narrowing of the channel width and stream bed incision. Upper parts of the *Allier* and *Loire* rivers are also very active channels (Gautier *et al.*, 2000 [103]). More specifically, important lateral mobility in the upper *Allier* river has been observed. However, these qualitative works focus on large fluvial systems and do not provide quantitative rates of observed processes. Moreover, the contribution from small river systems to the sediment budget is clearly neglected.

In this context, the objective of this study is to calculate bank retreat values and bank erosion volumes due to fluvial entrainement in small to medium size rivers within a large lowland area, the Loire and Brittany river basin. The database used in this study and the methodology are described in Section 5.2. Results of bank retreat rates and volumes are presented and discussed in section 5.3 and values are compared with literature data. First, the presented results include coarse and fine particles. Then, only fine particles are considered to provide an estimation of the contribution of bank erosion to fine-grained sediment budgets for different catchments within the study area.

5.2 Materiel and methods

5.2.1 Study area

The French metropolitan territory is divided into six hydrographic river basin districts. The Loire Brittany river basin (named *LBRB* hereafter, Figure 5.1) is one of the districts and represents 28% of the metropolitan territory ($\sim$ 155,000 km ^{2}). Wasson *et al.* (2002) [307] proposed a division of the French territory into smaller entities that present homogeneous geological, topographical and climatic characteristics. These entities are named “Hydro-écorégions” (*HER*) and a 2-level nomenclature is available. In the present study, we use only the partition of the territory according to level 1 to which correspond 22 *HER* at the national scale. The *LBRB* comprises 10 *HER* that are presented Figure 5.1.

To the east, the *Massif Central nord and sud* and the *Cévennes* are characterized

by old granitic formations, extreme climatic events, steep slopes (maximum = 134.7%, mean = 10.5%) and lands dedicated to forests and pastures with an important network of hedgerows. At the centre of the Massif Central, the *Dépressions sédimentaires* corresponds to the cropped plains of the Limagne and Forez. At the centre of the *LBRB*, the sedimentary Parisian basin is divided into three *HER*. The *Tables calcaires* is an agricultural lowland area with very gentle slopes, the *Côtes calcaires* displays steeper slopes but remains primarily an agricultural area, and finally, the *Dépôts argilo-sableux* is a forested lowland area with impermeable underlying geological formations. To the west, the *Massif Armoricain* is composed of old granitic formations and arable lands characterized by a dense network of hedgerows, and benefits from an oceanic climate.

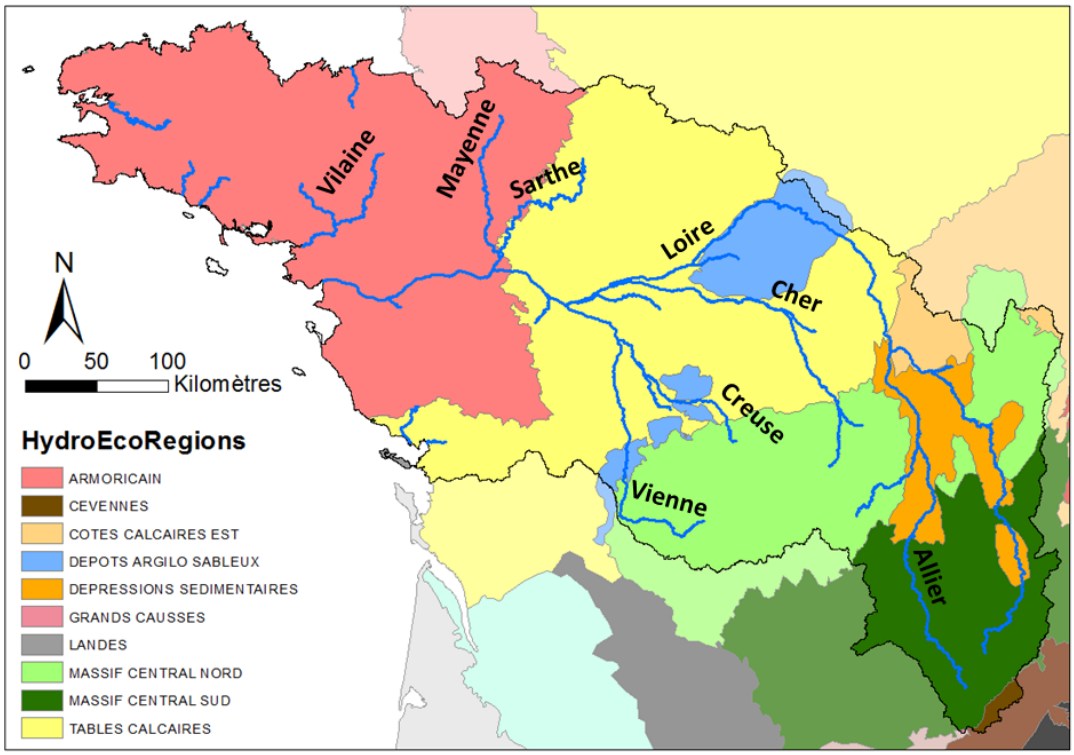

FIGURE 5.1 – Location of the Hydro-écoregions within the *LBRB*

Two *HER* are poorly represented in the *LBRB*: the *Landes*, which is only represented in then *LBRB* by the Island "Ile de Ré", where no river is present, and the *Grands Causses* for which the representation in the *LBRB* is of 9km^2 and only 3km of streams are located in this area. Therefore, the *Grands Causses* streams are associated with the closest *HER*, the *Massif Central sud*, for the remaining of this study.

5.2.2 Database

5.2.2.1 The stream network : the $SYRAH_{CE}$ database

The French $SYRAH_{CE}$ database 2006 is managed by *IRSTEA* and was implemented following requests on the knowledge of the water quality of water bodies by the Water Framework Directive. The purpose of this database is to provide decision makers with a tool to evaluate the physical degradation of streams and thus to assess the risk of non-achievement of good environmental status of watercourses.

The $SYRAH_{CE}$ is a GIS vector layer covering the French river network and provides information on hydraulic parameters and variables for each hydrographic section. The division of the stream network is realised on the basis of the *HER* and of homogeneous geomorphologic characteristics of the sections (Valette *et al.*, 2008 [281]). Those characteristics depend on (by order of importance): the width of the alluvial plain, the slope and the shape of the valley bottom, the hydrology, and the nature of the substratum. The confluence with a tributary leads to a new hydrographic section only if: i) the Strahler rank of the tributary is at most $n-1$ the one of the main stream and up to $n-2$ for streams with Strahler rank ≥ 5, and ii) the flow discharge of the tributary is high enough to provoque a hydrologic discontinuity.

Only the streams of a Strahler rank greater than 3 in the entire hydrographic network are considered in $SYRAH_{CE}$ database, and Strahler ranks are recalulated for each hydrographic section. In the $LBRB$, 70278 km of the stream network is provided by this database which corresponds to $\sim 52\%$ of the entire river network in this area. The representation of each stream order is as follows (P, the percent of the total stream length): P 1st order = 59.69%, P 2nd order = 17.95%, P 3rd order = 11.10 %, P 4th order = 6.63%, P 5th order = 2.95%, P 6th order = 0.89%, P 7th order = 0.79%. For each section, different parameters are available and two of them are considered in this study: the specific flood discharge and the width of the floodplain.

The $USRA$ (Unités Spatiales de Recueil et d'Analyse) database is a GIS vector layer which is complementary to the $SYRAH_{CE}$ database and provides further information on streambank properties. Each $SYRAH$ section is divided in several $USRA$ sections of identical length, that is proportional to the $SYRAH$ section Strahler rank, and are homogeneous in their geomorphologic properties. From the $USRA$ database, we extracted information on the percentage of riparian vegetation (corresponding to trees within 30m around the section) and calculated the mean percentage of this vegetation for each of the $SYRAH$ sections.

5.2.2.2 The stream network : the Carthage database and pretreatments

The BDCarthage ® IGN is a GIS vector layer which provides an exhaustive mapping of the stream network for the $LBRB$ and a more partial information for the rest of the French territory. The network is divided in elementary hydrographic sections displaying similar properties (state, nature, width, flow direction, navigability).

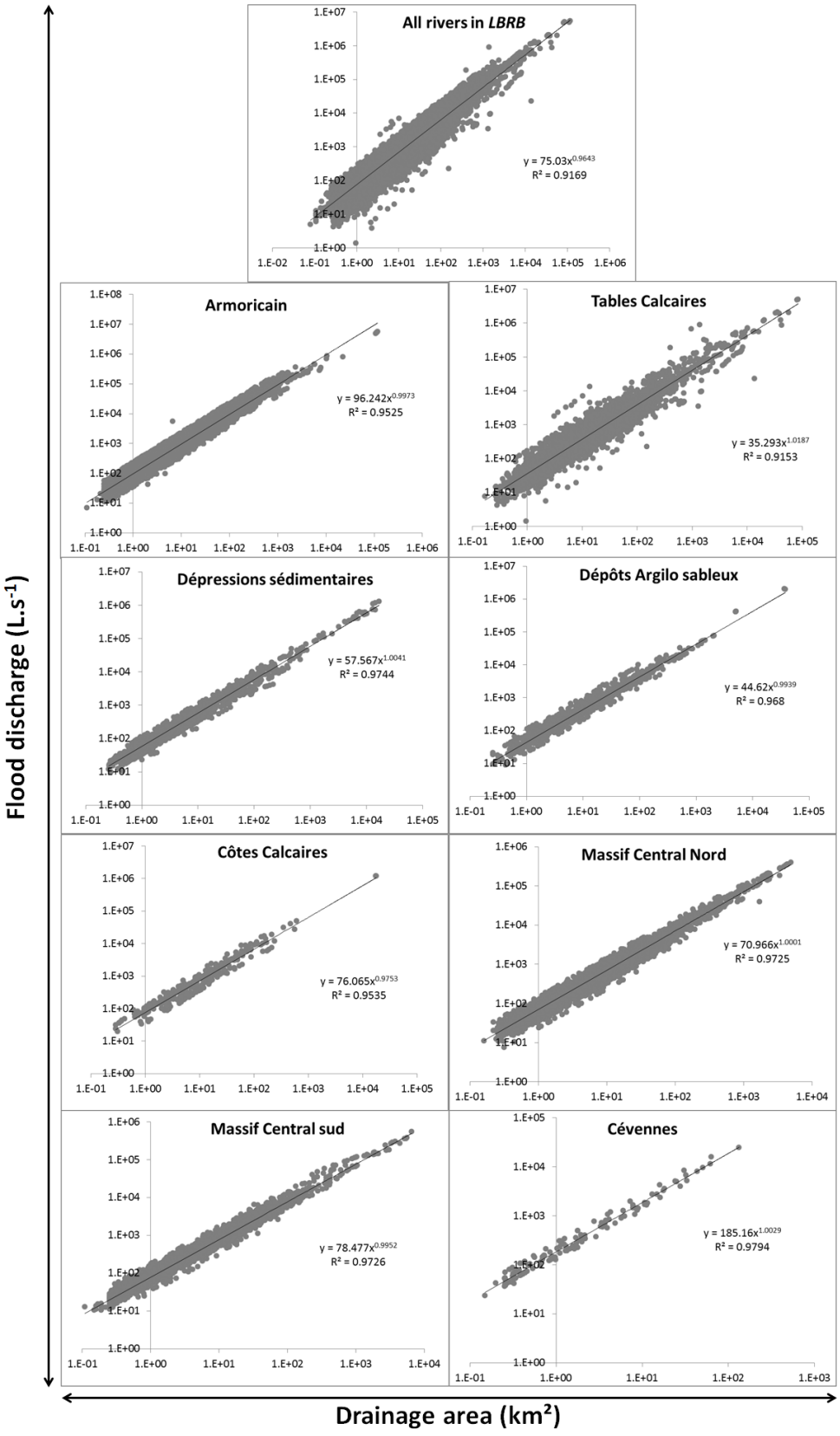

FIGURE 5.2 – Relations between flood discharge and drainage area for all streams and for each Hydro-écorégion

The presence of a tributary automatically delimits a new hydrographic section. For each section, the drained area is calculated. However, no information on flood discharge, percentage of riparian vegetation or floodplain width is available for the sections. We extracted Carthage sections where no information from $SYRAH_{CE}$ was available.

We estimated flood discharge for the Carthage network, based on the relation between the bankfull discharge Q_{bf}, the drainage area A and the streambed slope S (Williams, 1978 [316]) which takes the form of Equation 5.1 and where α, a, and b are empirical parameters that need to be calibrated.

$$Q_{bf} = \alpha \, A^a * S^b \tag{5.1}$$

The $SYRAH_{CE}$ database was used to calibrate the empirical parameters, and the relation 5.1 is adjusted eight times according to each *HER* (Figure 5.2). In our case, the drained area explains at least 91% of the relation and 97% at most. Therefore, the slope was not taken into account.

5.2.2.3 Erodibility, particle size and mass density

In order to get information on the bank texture, we used the Harmonized World Soil Database (*HWSD*, FAO/IIASA/ISRIC/ISS-CAS/JRC 2009 [85]) which is a 30 arc-second raster. For each soil map unit, the *HWSD* gives soil properties information for the topsoil layer (0 to 30 cm) and for the subsoil layer (30 to 100cm). In this study, we consider only the subsoil layer and assumed that below 100cm, the soil properties are similar to the ones of the subsoil layer. The stream network and the *HWSD* subsoil map are superimposed to obtain for each newly created section, the texture class, the percentage of sand and the percentage of fine particles (silt and clay), and the density of the material composing the soils, and thus the banks.

5.2.2.4 Bank height

The national database HYDRO FRANCE gather information on hydrological variables at different gauging stations on the French territory. On the *LBRB*, measures of maximal water height at 802 gauging stations, distributed all over this territory, are available. We assumed this water height to be equivalent to the bank height at bankfull discharge. Gauging stations and $SYRAH_{CE}$ hydrographic sections are geographically linked together to obtain for each water height value the corresponding Strahler rank order. For the purposes of this study, we assumed that the distribution of the effectif of water heights in each stream order class (Table 5.1) is the same as the distribution of the population for each class.

Water heights are grouped according to Strahler ranks (Table 5.1, Figure 5.3) and the expected positive trend between both variables, such that water height of Strahler rank n is higher than water height of Strahler rank *n-1*, is observed. This is consistent with hydraulic geometry theory – the higher the stream order, the higher the banks

– and previous findings (Lymburner, 2006 [176]). The Shapiro-Wilk test indicate a non-normal distribution. Therefore, we use median values, instead of mean values, and extrapolate the median values to each hydrographic section according to its stream order.

For stream sections from the BDCarthage, we affected a median height of 1.415m, which corresponds to the median height of streams of a Strahler order of 1 in the $SYRAH_{CE}$ database.

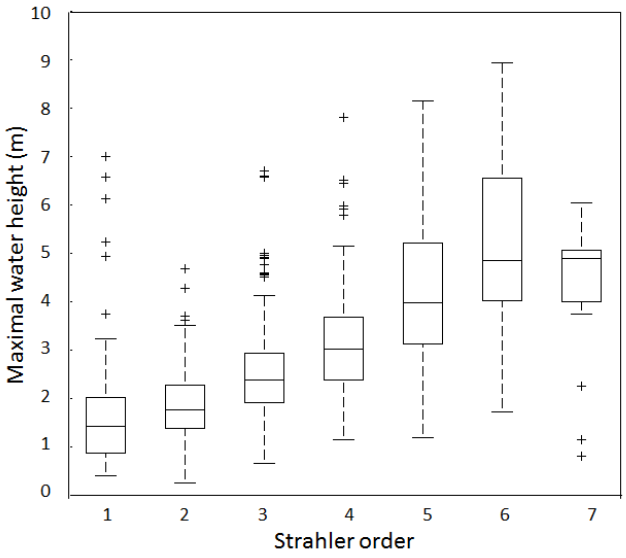

FIGURE 5.3 – Relationship between maximal water height and Strahler order

Tableau 5.1 Mean, median water height for each Strahler order

Strahler order	Effectif (% of the total population)	Mean value (m)	Median value (m)
1	86 (10.7)	1.712	1.415
2	187 (23.3)	1.858	1.750
3	262 (32.7)	2.513	2.380
4	167 (20.8)	3.133	3.020
5	68 (8.5)	4.195	3.975
6	15 (1.9)	5.287	4.850
7	17 (2.1)	4.293	4.890

5.2.3 Bank retreat assessment

5.2.3.1 Model of bank retreat through fluvial entrainment

Streams with higher Strahler order than 3 as defined in $SYRAH_{CE}$ are not taken into account in fluvial bank retreat assessment. Indeed, for such streams, bank erosion

processes are completely different due to the sandy texture of the bed and the banks of these streams (primarily the *Loire*, *Allier*, and *Cher* rivers) which are dominated by mass failures and changes in bar morphology and location (Rodrigues *et al.*, 2006 [247]). Furthermore, the stream network with a higher Strahler order than 3 accounts for only 5.72 % of the entire stream network and thus represents a minor part of this network. Therefore, the equations described in this section are applied only on streams of Strahler order from 1 to 3 (as defined in the $SYRAH_{CE}$ database).

Based on equations found in the literature (Prosser *et al.*, 2001 [233], Bartley *et al.*, 2004 [12]) and available data for the study area, we develop a new equation of bank retreat (Equation 5.2). This equation gives a strong weight to the flood discharge parameter which has been recognised as the driving factor of fluvial bank erosion (Harvey, 2001 [121]; Bizzi and Lerner, 2013 [16]). Additional factors account for local variations of the stream channel and surroundings characteristics.

$$BR = a \ * \ k \ * \ (1 - R_{Vegetation})(1 - e^{bF_x}) \ Q_{Bf}^{c} \tag{5.2}$$

with BR the bank retreat (m.yr^{-1}), a, b and c empirical parameters, k a factor of erodibility, $R_{Vegetation}$ the rate of riparian vegetation, F_x the width of the floodplain and Q_{Bf}^{c} the bankfull discharge.

The values of the empirical parameter a, b and c are defined according to literature data: a is set to 0.008 (Prosser *et al.*, 2001 [233]), b to -0.008 (Bartley *et al.*, 2004 [12]), and c to 0.6 (Prosser 2001 [233], and Hughes and Prosser, 2003 [131]).

The bankfull discharge is not an available data in the river network database. In general, the bankfull discharge is comparable to the $Q2$ (one in 2-years flood, Wilkerson 2008 [314]) which is considered to be the morphogenic flow (most significant in hydromorphology). On the *LBRB*, in 95% of all cases, the flood discharge $Q_{0.99}$ (the statistic flow not exceeded in 99% of the time on the flow duration curve) is comprised between 0.5 and 1.5 of the $Q2$ (Valette and Cunillera, 2010 [282]). Therefore, we calculated minimum and maximum bank retreat values as in Equation 5.3.

$$\begin{cases} \text{Minimal bank retreat: } BR_{min} = 0.008 * k * (1 - R_{Vegetation})(1 - e^{-0.008F_x}) \ 0.66 \ Q_{0.99}^{0.6} \\ \text{Maximal bank retreat: } BR_{max} = 0.008 * k * \underbrace{(1 - R_{Vegetation})}_{\text{Vegetation factor}} \underbrace{(1 - e^{-0.008F_x})}_{\text{Floodplain factor}} \ 2 \ Q_{0.99}^{0.6} \end{cases} \tag{5.3}$$

The factor of erodibility k is defined according to the soil texture classes. In the *HWSD*, 13 classes of texture are proposed according to the classification of the *FAO*. The classes are grouped into four categories and a value of erodibility is proposed for each category (Table 5.2).

The rate of the banks with riparian vegetation range from 0 (no riparian vegetation) to 1 (important riparian vegetation). Though the vegetation plays a role in the limitation of erosion, its presence does not lead to a complete absence of erosion (Rutherfurd, 2000 [251]). In order to avoid zeros in Equation 5.2, we resample the values of the rate

Tableau 5.2 Erodibility values according to texture values of the subsoil layer in the Loire and Brittany river basin taken from the Harmonized Soil World Database (FAO/IIASA/ISRIC/ISS-CAS/JRC 2009 [85])

Texture value	Texture type	Erodibility factor (k)
3	Clay	0.5
5 and 7	Clay loam and silt loam	0.75
9 and 10	Loam and sandyclay loam	1
11, 12 and 13	Sandy loam, loamy sand and sand	2

of vegetation such that the vegetation factor $(1 - R_{Vegetation})$ cannot take null values (Figure 5.4). This resampling allows for a maximal bank erosion of up to $\sim 36\%$ in the case of a dense riparian vegetation, and up to 100% if no riparian vegetation exists.

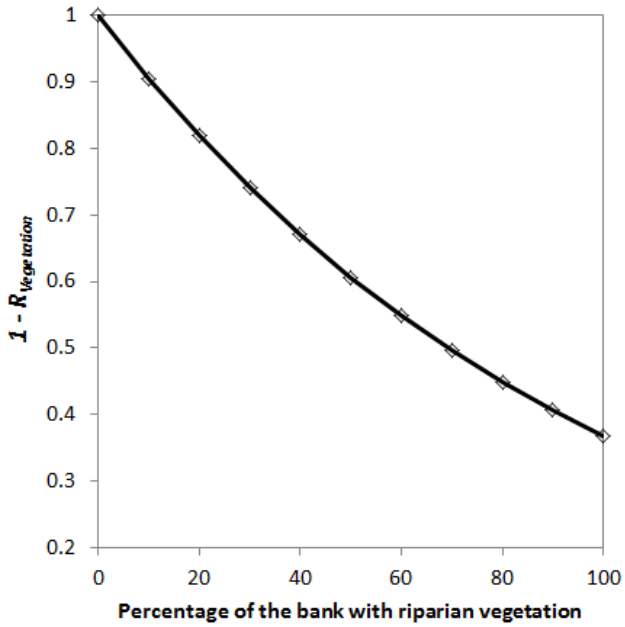

FIGURE 5.4 – Values of the factor $1 - R_{Vegetation}$ according to the percentage of riparian vegetation

The floodplain width parameter express the constraint of the substratum on the bed and banks of the river (Bartley *et al.*, 2008 [13]). Indeed, in case of a hard substratum, the bank erosion is limited. The floodplain width is included in Equation 5.3 such that rivers with a floodplain width close of zero (*e.g.*, rocky gorges) would not undergo bank erosion.

For the Carthage stream sections a simpler equation (Equation 5.4) is used to assess bank retreat. It is based on the SedNet equation (previously described) of bank retreat and to equations used for sediment transport (De Vente *et al.*, 2008 [65]) through the

addition of the factor of erodibility k.

$$\begin{cases} \text{Carthage minimal bank retreat: } BR_{min} = 0.008 * k * \ 0.66 \ Q_{0.99}^{0.6} \\ \text{Carthage maximal bank retreat: } BR_{max} = 0.008 * k * \ 2 \ Q_{0.99}^{0.6} \end{cases} \tag{5.4}$$

5.2.4 Sensitivity analysis

A simple sensitivity analysis is realised to determine the sensitivity of the model to the variation of the different input parameters and determine which has the greatest influence on the model outputs. This analysis is based on the calculation of the S sensitive parameter (Nearing *et al.*, 1990 [207], Equation 5.5).

$$S = \frac{(O_2 - O_1)/O_{\bar{1,2}}}{(I_2 - I_1)/I_{\bar{1,2}}} \tag{5.5}$$

where I_1 and I_2 are the least and greatest values of the input used, respectively, and $I_{\bar{1,2}}$ is their average value. O_1 and O_2 are the output for the two input values, and $O_{\bar{1,2}}$ is the average value of the two outputs.

The sensitivity analysis is conducted for different areas within the $LBRB$. In each area, the range of input values over which S is tested corresponds to the extremes in the natural conditions, *i.e.*, the minimal and maximal values of each input parameter (vegetation factor, floodplain factor, and flood discharge) in the area. First, the sensitivity analysis is realised for the entire $LBRB$ and for each *HER*. However, as the k factor is a discrete variable that takes only four values, it is not included in the sensitivity analysis. Therefore, in a second step, the sensitivity analysis is realised for each erodibility value (k factor). Finally, *HER* and erodibility classes are combined and the sensitivity analysis is conducted over these sub-areas. The ranges of inputs over which S is tested for each area are reported in Tables 5.3 and 5.4.

The sensitivity analysis is conducted 10^5 times for each parameter and each considered area and the mean value of the S is calculated. In addition, to evaluate the impact of subsampling on the sensitivity parameter values, we randomly choose from 2 to the total number of streams in the $LBRB$ (29,645 sections), the sensitivity of each parameter is evaluated 10^5 times using minimal and maximal values of the so-called parameter in the entire $LBRB$. The random analysis is also performed 10^5 times for each of the number of samples to choose.

Tableau 5.3: Number of streams and range of test for the different parameters considered for the different areas (see text)

		Number of streams	Range of test for the three parameters		
			Vegetation	Floodplain	Flood discharge
	LBRB	29645	0.37 - 1.00	0.29 - 1.00	0.001 - 98.043
HER	Massif Central sud	3590	0.37 - 1.00	0.29 - 1.00	0.010 - 49.552
	Massif Central nord	5291	0.37 - 1.00	0.32 - 1.00	0.007 - 52.388
	Cévennes	168	0.37 - 1.00	0.38 - 1.00	0.023 - 15.998
	Dépressions sédimentaires	1539	0.37 - 1.00	0.34 - 1.00	0.010 - 24.805
	Tables calcaires	5537	0.37 - 1.00	0.32 - 1.00	0.001 - 42.433
	Côtes calcaires	437	0.37 - 1.00	0.44 - 1.00	0.019 - 31.267
	Dépôts argilo-sableaux	1164	0.37 - 1.00	0.36 -1.00	0.009 - 53.527
	Massif Armoricain	11918	0.37 - 1.00	0.33 - 1.00	0.010 - 98.040
Erodibility	0.5	2456	0.37 - 1.00	0.35 -1.00	0.004 - 46.925
	0.75	4373	0.37 - 1.00	0.34 - 1.00	0.005 - 42.433
	1	15260	0.37 - 1.00	0.29 - 1.00	0.004 - 98.043
	2	7391	0.37 - 1.00	0.29 - 1.00	0.001 - 63.039

Tableau 5.4: Number of streams and range of test for the different parameters considered for the different *HER* and erodibility values

HER		Erodibility factor			
		0.5	0.75	1	2
Massif Central sud	Number of streams	208	113	927	2298
	Vegetation - range of test	0.37 - 1.00	0.37 - 0.99	0.37 - 1.00	0.37 - 1.00
	Floodplain - range of test	0.38 - 1.00	0.40 - 1.00	0.29 - 1.00	0.29 - 1.00
	Flood discharge - range of test	0.013 - 12.768	0.019 - 35.155	0.013 - 14.641	0.010 - 49.552
Massif Central nord	Number of streams	258	717	2861	1421
	Vegetation - range of test	0.37 - 1.00	0.37 - 1.00	0.37 - 1.00	0.37 - 1.00
	Floodplain - range of test	0.42 - 1.00	0.40 - 1.00	0.32 - 1.00	0.34 - 1.00
	Flood discharge - range of test	0.007 - 15.761	0.011 - 21.080	0.011 - 52.388	0.011 - 52.388
Cévennes	Number of streams	NoData	NoData	24	144
	Vegetation - range of test	NoData	NoData	0.37 - 1.00	0.37 - 1.00
	Floodplain - range of test	NoData	NoData	0.41 - 0.99	0.38 - 1.00
	Flood discharge - range of test	NoData	NoData	0.041 - 8.026	0.024 - 15.998
Dépressions sédimentaires	Number of streams	199	900	253	187
	Vegetation - range of test	0.40 - 1.00	0.37 - 1.00	0.39 - 1.00	0.37 - 0.98
	Floodplain - range of test	0.35 - 1.00	0.34 - 1.00	0.34 - 1.00	0.38 - 1.00
	Flood discharge - range of test	0.030 - 16.947	0.028 - 16.947	0.010 - 24.806	0.015 - 16.947
Tables calcaires	Number of streams	1492	1676	1514	848
	Vegetation - range of test	0.37 - 1.00	0.37 - 1.00	0.37 - 1.00	0.37 - 0.99
	Floodplain - range of test	0.42 - 1.00	0.35 - 1.00	0.33 - 1.00	0.37 - 1.00
	Flood discharge - range of test	0.004 - 39.273	0.005 - 42.433	0.004 - 42.433	0.001 - 39.273
Côtes calcaires	Number of streams	156	88	154	39
	Vegetation - range of test	0.37 - 0.98	0.37 - 0.93	0.37 - 0.98	0.50 - 0.93
	Floodplain - range of test	0.44 - 1.00	0.45 - 1.00	0.45 - 1.00	0.52 - 1.00
	Flood discharge - range of test	0.024 - 31.267	0.034 - 27.464	0.019 - 27.464	0.045 - 31.267
Dépôts argilo-sableaux	Number of streams	41	286	151	685
	Vegetation - range of test	0.37 - 1.00	0.37 - 1.00	0.37 - 0.99	0.37 - 0.98
	Floodplain - range of test	0.60 - 1.00	0.38 - 1.00	0.36 - 1.00	0.39 - 1.00
	Flood discharge - range of test	0.026 - 9.910	0.016 - 10.683	0.009 - 13.677	0.009 - 53.527
Massif Armoricain	Number of streams	102	593	9375	1769
	Vegetation - range of test	0.42 - 1.00	0.37 - 1.00	0.37 - 1.00	0.37 - 1.00
	Floodplain - range of test	0.52 - 1.00	0.38 - 1.00	0.33 - 1.00	0.40 - 1.00
	Flood discharge - range of test	0.014 - 46.925	0.014 - 38.994	0.007 - 98.043	0.015 - 63.039

5.2.5 Volume and mass of bank erosion

Assuming that the loss of river bank takes a uniform parallelepiped form over the entire section (*e.g.*, Kessler *et al.*, 2013 [139]), we calculate the volume of eroded particles for each section as the product of the bank retreat (see Section 5.2.3), the bank height and the section length. Moreover, to get a mass of detached particles from the banks, the erosion rate is calculated as the product of the volume eroded in each section and the density of the soil particles (Bull 1997 [28], Laubel *et al.*, 2003 [156], Equation 5.6).

$$BE = BR * \ B_{Height} * \ B_{Length} \ * \rho \tag{5.6}$$

with BE the bank erosion (kg.yr^{-1}), BR the mean bank retreat (m.yr^{-1}), B_{Height} the median bank height of the section (m), B_{Length} the length of the section (m), and ρ the bulk density (kg.m^{-3}). Finally, the bank erosion was multiplied by the percentage of sand to get the contribution from coarse and fine particles. As Equation 5.3 is applied twice in order to get a minimal and a maximal value of the bank retreat, Equation 5.6 was also applied twice to obtain a minimal and a maximal value of bank erosion.

5.3 Results and discussion

The distinction of results of bank retreat rates obtained from the two different database allows for a finer analysis of the outputs of the two equations which display different degrees of complexity. Therefore, we first present the results obtained using the $SYRAH_{CE}$ database. The rates of bank retreat, volumes of bank erosion, and their spatial distribution are analysed. The results from the sensitivity analysis are presented and we provide an estimation of the contribution from fluvial bank retreat to the sediment budget of 77 catchments. Second, we present the results obtained using the Carthage database and integrate the contribution of these small streams to the sediment budgets previously described.

5.3.1 Bank retreat rates and volumes for the $SYRAH_{CE}$ sections

5.3.1.1 Bank retreat rates

In this study, we applied a large scale model of bank retreat on the Loire and Brittany river basin. Two values of flood discharge are used in order to give a minimal and maximal value of bank retreat for each stream. Minimal bank retreat values range from 3.8 * 10^{-3} to 12.02 cm.yr^{-1} with a mean value of 0.42 cm.yr^{-1} (median = 0.20 cm.yr^{-1}, std = 0.51). Maximal bank retreat values range from 1.15 * 10^{-2} to 36.43 cm.yr^{-1} with a mean value of 1.29 cm.yr^{-1} (median = 0.61 cm.yr^{-1}, std = 1.54). Ranges of maximal and minimal bank retreat values for each Strahler stream order are displayed in Figure 5.5. As expected, bank retreat values increase with increasing stream order. Such trend is related to i) an increase in flood discharge with drainage

area and thus with strahler order, and ii) in some slope contrasted areas (*Massif Central nord and sud* and the *Massif Armoricain*) to an increase in floodplain width as upper streams leave mountainous lands to enter large lowland areas.

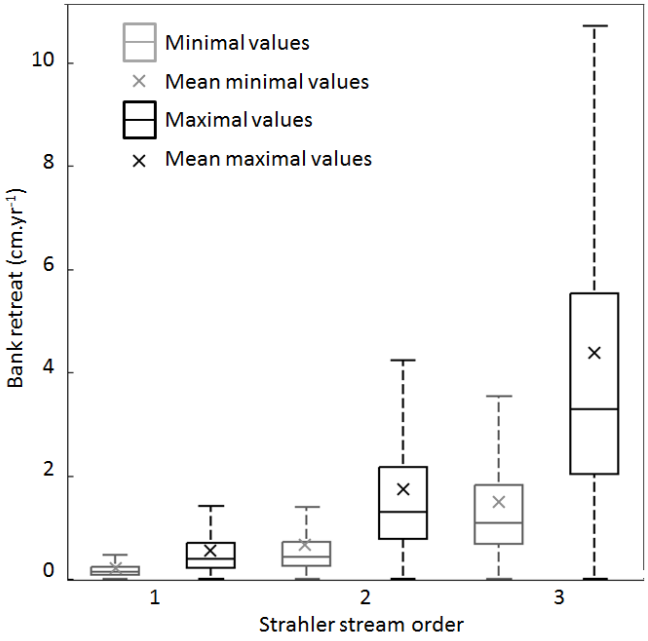

FIGURE 5.5 – Boxplots of the minimal and maximal bank retreat values calculated from Equation 5.3 per strahler order streams

Values of bank retreat calculated in this study are in the range of values taken from literature data that use equations based on stream flood discharge and bank characteristics. All of these studies (De Rose *et al.*, 2002 [62]; Hughes and Prosser, 2003 [131]; Hughes *et al.*, 2003 [132]) deal with large Australian catchments ($> 10^3$ km^2) and our mean value of bank retreat is in the same order of magnitude as the values proposed by these authors. The widest range of bank retreat values is for the Murray-Darling basin (Hughes and Prosser, 2003 [131]) where it rises from 0.1 cm.yr^{-1} to 30 cm.yr^{-1}, and up to 1m for the main stream of the catchment. The lower values found in the present study are attributed to i) the very low flood discharge of some streams within the *LBRB*, and ii) to the addition of the erodibility factor which can divide by 1.3 to 2 the initial values of bank retreat.

However, in European areas, the comparison with literature data is rather delicate for several reasons. Firstly, no application of such equation have been found to provide a strict comparison of bank retreat values. Secondly, values provided by the literature corresponds to field data (*e.g.*, erosion pins) that cover all forms of erosion and thus sum the bank retreat rates induced by different processes and site specificities that may induce strong variations in the dominance of erosion process (Henshaw *et al.*, 2013 [124]). Finally, the choice of site location for the conduction of field campaign is based on the likelihood of high magnitude of erosion. Therefore, literature data from studies on European streams are not representative of the range of bank erosion rates,

do not allow for a strict comparison and may lead to overestimations of bank erosion if values are extrapolated.

Furthermore, there is a growing awareness of the impact of human activities on the landscape and of accelerated bank erosion in areas affected by human disturbances. Consequently, human disturbed rivers being increasingly studied and the distinction between bank erosion due to "natural processes" and man-influenced processes is no more possible. Both changes on hillslopes (Shields *et al.*, 2010 [257]; Wasson *et al.*, 2010 [308]) and in streams (Surian and Rinaldi [267]) affect the stream regime and thus the bank erosion. Moreover, the spatial distribution of the human interventions in the landscape have an impact on the bank erosion patterns (Vanacker *et al.*, 2005 [288]). Recently, the growing interest for the impact of channelization on stream morphology (*e.g.*, Nakamura *et al.*, 1997 [204]; Sipos *et al.*, 2007 [260]; Ciszewki *et al.*, 2014 [42]; Landemaine *et al.*, 2015 [151]) has highlighted the strong disequilibrium in channel morphology and water regime induced by channel works. This disequilibrium may persist over several years after the works and still participate in increases of bank erosion. As a result, high sediment deposition rates are observed in these streams (Landwehr *et al.*, 2003 [152]; Kroes and Hupp, 2010 [147]). Therefore, there is a real need to take this human impact into account in the bank retreat assessment.

This lack of consideration of human disturbances in the calculation of bank retreat represents a limitation to the present study. Yet, even if these channelisation works have been carried out in tens of thousands of kilometres streams in France (Malavoi and Adam 2007 [177]), the precise location and nature of the works undergone in streams of the *LBRB* remain unknown. Further researches are needed to i) detect channelized streams (Brookes *et al.*, 1983 [27]) and ii) integrate such parameter in the model development. The lack of consideration of man intervention in the present model may lead to underestimation in anthropised areas, and particularly in the Parisian basin where intensification of agriculture in the 1970s has led to severe land transformations.

5.3.1.2 Spatial distribution

There exist a spatial zoning of the values of bank retreat and the class boundaries in Figure 5.6 were chosen to highlight the highest values. From a geological view point, highest values concentrate in the Massif Central and Armorican basin. The latter represents 34% of the *LBRB* area, and 40.67% of the streams is affected by a maximal bank retreat greater than 1.0 cm.yr^{-1}. This area concentrates 44.16% of the entire river network of the *LBRB* affected by such bank retreat values. These high rates can particularly be found at the south east of the Armorican region where flood discharge values are among the highest of the range of values in the *LBRB*. Most of the river network in this area corresponds to coastal rivers – where the sediment might be directly evacuated to the sea – or to small tributaries to the *Loire* river. In the Parisian basin, the bank retreat rates are low, except in the surroundings of the Loire valley and of two of its main tributaries, the *Cher* and the *Indre* rivers where large floodplains and sandy soils lead to a high bank erodibility and thus high bank retreat estimations.

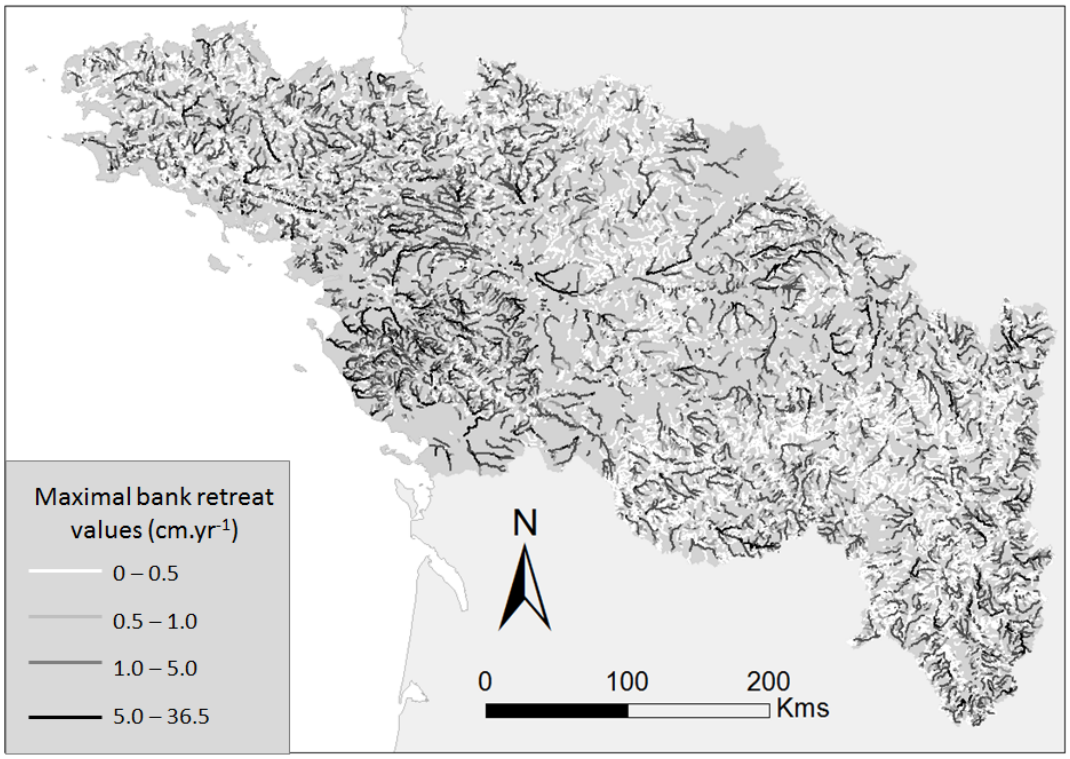

FIGURE 5.6 – Spatial distribution of maximal bank retreat

From the *HER* view point, Table 5.5 gives the mean and median values of the vegetation factor, the floodplain factor, the flood discharge and the maximal bank retreat for each region. Figure 5.7 provides the percentage of erodibility classes in each *HER*. Highest values of bank retreat are found for the *Cévennes* (1.66 cm.yr^{-1}) closely followed by the *Massif Armoricain* and the *Dépots argilo-sableux* (1.54 cm.yr^{-1}). In the *Cévennes* and *Dépot argilo-sableux HER*, the high rates of bank retreat are primarily explained by the sandy texture of the soils which leads to a high erodibility of the banks. In the *Massif Armorican*, 80% of the area displays an erodibility value of 1. Therefore, the other three parameters play an important role in the bank retreat values calculated for this region.

The lowest mean and median values of bank retreat are found for the *Dépressions sédimentaires HER*, where mean values of the vegetation factor, the floodplain factor and the flood discharge correspond to the mean of the range of values observed for all *HER* together. The *Massif Central nord* also displays low mean and median values of bank retreat which are similarly explained by the average values of all parameters. Higher bank retreat values are found for the southern part of the Massif Central, while mean values of the floodplain and vegetation factors and of flood discharge values are lower. In this area, bank retreat rates are driven by the erodibility factor as 64% of the *HER* area corresponds to the sandy textural class ($k = 2$).

Tableau 5.5: Mean, median (weighted by the stream length) and standard deviation of the parameters vegetation, floodplain, and flood discharge, and for the bank retreat rate for each *HER*. Highest mean and median values are highlighted in bold characters, and lowest values in italic characters

		Massif Central sud	Massif Central nord	Cévennes	Dépressions sédimentaires	Tables calcaires	Côtes calcaires	Dépôts argilo-sableux	Massif Armoricain
Vegetation factor	mean	0.59	0.62	0.64	0.68	0.66	**0.74**	*0.56*	0.66
	median	0.55	0.61	0.60	0.68	0.66	**0.76**	*0.54*	0.66
	std	0.17	0.15	0.17	0.14	0.15	0.13	0.14	0.14
Floodplain width factor	mean	*0.62*	0.70	0.68	0.75	**0.87**	0.85	**0.87**	0.86
	median	*0.58*	0.70	0.68	0.75	0.92	0.90	**0.93**	0.91
	std	0.18	0.16	0.17	0.20	0.15	0.14	0.18	0.14
Flood discharge ($m^3.s^{-1}$)	mean	2.08	2.22	*1.95*	2.13	3.24	**3.62**	2.49	3.28
	median	0.45	0.43	*0.40*	0.51	0.63	**1.00**	0.45	0.67
	std	2.80	3.45	2.47	3.03	4.34	3.99	5.48	4.83
Maximal bank retreat ($cm.yr^{-1}$)	mean	1.13	0.91	**1.66**	*0.89*	1.25	1.47	1.54	1.54
	median	0.52	0.45	**0.78**	*0.44*	0.54	0.77	0.68	0.74
	std	1.20	1.07	1.61	1.23	1.37	1.65	1.96	1.73

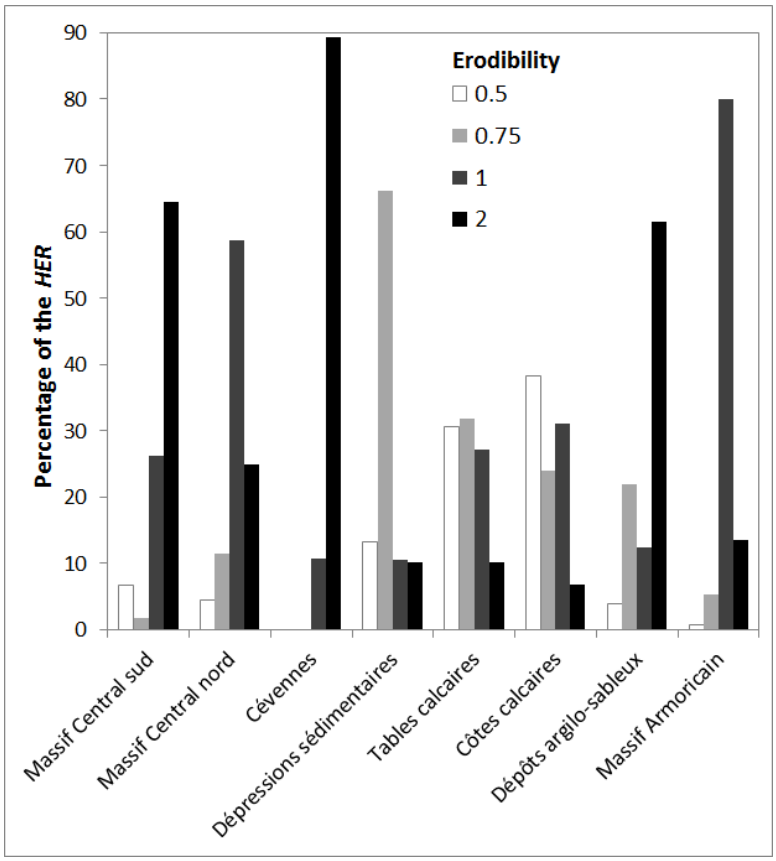

FIGURE 5.7 – Percentage of each class of erodibility in each *HER*

Of course, mean and median values do not reflect the spatial distribution of the different parameters and thus the local variations of bank retreat values that result from particular combinations of these four parameters. There exists a weak but significant correlation between the vegetation and floodplain factors for the *Massif Central sud*, *Massif Central nord*, and *Massif Armoricain* ($R^2 = 0.30$, $R^2 = 0.21$, and $R^2 = 0.36$, respectively), such that as floodplain widens, less riparian vegetation exists. All three *HER* correspond to the less "managed" areas of the *LBRB*. The landscapes are also highly contrasted, with pastures and forests on steep slopes in upper areas and agricultural lands with less vegetation in the valley system. Conversely, no relation between both parameters is found for the other five *HER*, which illustrates the complexity of the landscape in these areas: the large floodplains of the *Dépôts argilo-sableux* are associated with high riparian vegetation density due to the presence of a vast forest, but no negative correlation between both parameters is found. In other *HER*, and especially in the *Tables calcaires*, floodplains are generally wide (highest floodplain factor value and least standard deviation value) but the riparian vegetation presents complex spatial distribution. Moreover, this *HER* is characterised by equal representation of all four erodibility classes.

This absence of spatial organisation of the landscape parameters, especially in anthropised areas (here, the Parisian basin) clearly indicates that global assumptions

concerning bank retreat trends cannot be formulated. In this respect, bank erosion cannot be inferred from catchment global characteristics, and bank characteristics cannot be extrapolated to areas where data are missing.

5.3.1.3 Sensitivity of the model to input parameter variations

The sensitivity analysis was conducted over the entire *LBRB* river network and for different areas within the whole basin. Results of the values of the sensitivity parameter are reported in Table 5.6.

In this study, the choice of input parameters is clearly based on our current understanding and knowledge of bank erosion processes and prioritization of involved parameters, applied to the currently available data for the study site. In this respect, the sensitivity analysis first allows us to verify whether our assumption concerning the predominant role of flood discharge in bank retreat over the other parameters is reflected in the mathematical model used in this study. At the *LBRB* spatial scale, the flood discharge appears as the most influential parameter ($S = 0.98$), followed by the vegetation parameter ($S = 0.90$) and finally the floodplain width ($S = 0.87$). A strong correlation exists between bank retreat rates and flood discharge ($R^2 = 0.78$, Figure 5.8). A weaker, but also significant, correlation is found between bank retreat rates and drainage area ($R^2 = 0.66$, not shown on the graph) because of the correlation that exists between flood discharge and drainage area.

Tableau 5.6: Number of streams and S values for the different parameters according to areas

			S value for the three parameters		
		Effectif	Vegetation	Floodplain	Flood discharge
	LBRB	29645	0.90	0.87	***0.98***
HER	Massif Central sud	3590	0.90	0.87	***0.94***
	Massif Central nord	5291	0.90	0.89	***0.96***
	Cévennes	168	0.91	***0.92***	0.87
	Dépressions sédimentaires	1539	0.89	0.89	***0.94***
	Tables calcaires	5537	0.90	0.88	***0.97***
	Côtes calcaires	437	0.91	***0.95***	0.91
	Dépôts argilo-sableaux	1164	0.91	0.91	***0.94***
	Massif Armoricain	11918	0.91	0.89	***0.97***
Erodibility	0.5	2456	0.90	0.91	***0.97***
	0.75	4373	0.91	0.90	***0.97***
	1	15260	0.92	0.89	***0.99***
	2	7391	0.89	0.87	***0.98***

Second, the sensitivity analysis allows us to detect variations in the importance of the parameters according to the different *HER*. At this spatial scale, the flood discharge remains the most influential parameter, except for the *Cévennes* and *Côtes calcaires*, for which the floodplain width displays the highest S values. However, in these regions, the number of streams considered is very low and influences the results of the sensitivity analysis (see further in the text for analysis of the effect of subsampling). In 6 out of 8 *HER*, the riparian vegetation is the second most influential parameter in the bank retreat assessment while for the *Dépressions sédimentaires* and *Dépôts argilo-sableux*, the floodplain width and the riparian vegetation have the same influence.

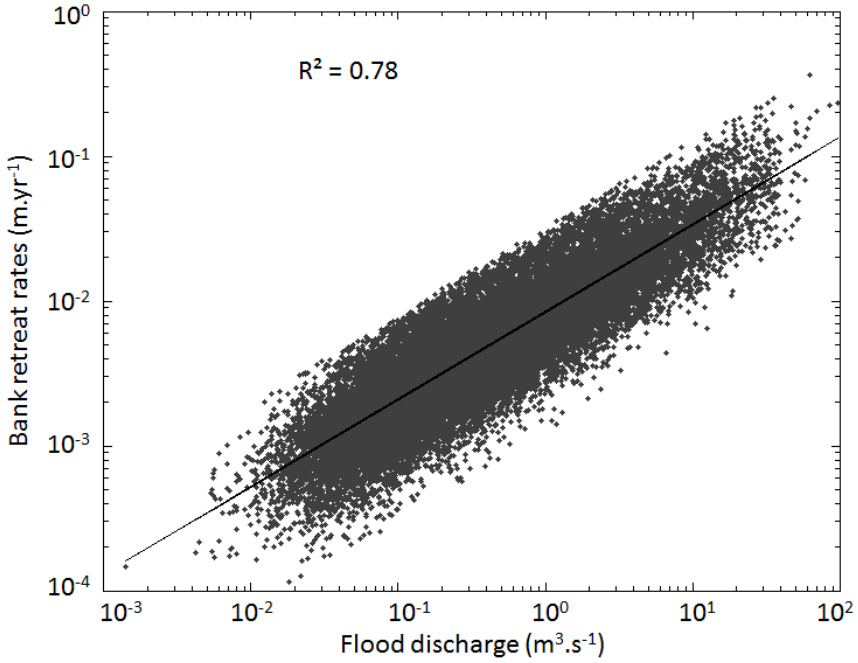

FIGURE 5.8 – Relation between bank retreat rates and flood discharge in the *LBRB*

Finally, according to textural classes, the flood discharge and vegetation are the two most important parameters, except in clayey soils where the floodplain parameter affects model outputs the most. However, the sensitivity parameter is affected by the chosen range of values tested, which corresponds to natural conditions. In case of low erodibility, the minimal floodplain value is higher than in other erodibility classes and thus restrain the range of values.

Yet, these results should be taken with precautions and should be considered in association with the number of streams considered for each area. Indeed, their exist a minimal number of streams under which the flood discharge is clearly not the dominant parameter (Figure 5.9). Our results on the effect of subsampling on the sensitivity parameter values indicate that under $\sim$ 200 samples (stream sections), the vegetation and floodplain factors affect the model outputs more than the flood discharge, with a predominance of the vegetation from three samples considered. From $\sim$ 200 to $\sim$ 400, the floodplain factor becomes the least important parameter while the flood discharge

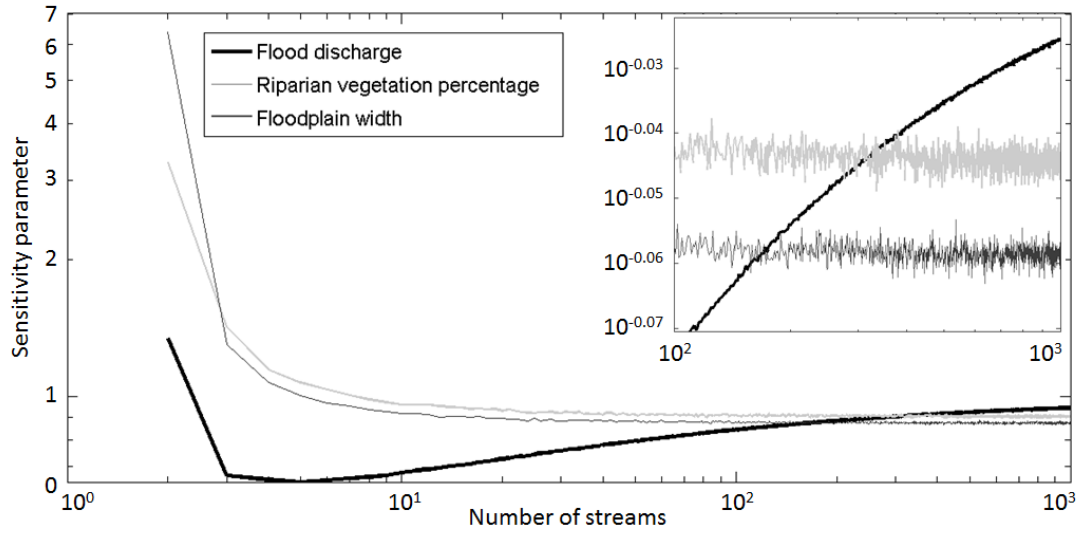

FIGURE 5.9 – Values of the sensitivity parameter S for the flood discharge, the riparian vegetation and the floodplain width according to the number of streams considered in the analysis of the sensitivity. A zoom on values for 100 to 1000 considered streams is provided. X and Y axis are presented on log-scale for a better representation

is the second dominant parameter. For more than 400 samples, the flood discharge clearly becomes the driving factor of the calculated bank retreat while vegetation is the second most important parameter and finally the floodplain factor. From 10^3 random samples, the trends in S values get stable (not shown on the graph).

However, the random strategy used in this study does not take into account the frequency distribution of each parameter within each considered area (see probability density functions in Appendix C). Further researches are thus needed to better take into account this variability in the sensitivity analysis (*e.g.*, use of Monte Carlo simulations). Still, this result suggests that i) the bank retreat rates provided in this study should not be considered at finer spatial scale than the *HER*, and ii) further researches are needed to calibrate the c exponent attributed to the flood discharge.

In the light of these results, Table 5.7 presents the sensitivity parameter values considering both *HER* and erodibility classes (Table 5.7). S values for areas displaying a number of stream sections less than 400 are given for information purpose only. In all areas with more than 400 stream sections, the flood discharge is the most important parameter. In general, the vegetation is the second most important parameter, except in areas where the range of test of the floodplain is smaller (larger minimal floodplain width). This is the case for areas displaying high erodibility values ($k = 2$) in the *Dépressions sédimentaires*, the *Tables calcaires*, the *Dépôts argilo-sableux*, and the *Massif Armoricain HER*.

Tableau 5.7: Number of streams and values of S for the different parameters considered for the different *HER* and erodibility values. Highest S values are highlighted in bold and italic. Areas displaying more than 400 stream sections are coloured in blue

HER		Erodibility factor			
		0.5	0.75	1	2
Massif Central sud	Number	208	113	927	2298
	Vegetation	0.9	0.91	0.91	0.91
	Floodplain	***0.92***	***0.92***	0.9	0.88
	Flood discharge	0.88	0.85	***0.92***	***0.96***
Massif Central nord	Number	258	717	2861	1421
	Vegetation	0.91	0.91	0.91	0.91
	Floodplain	***0.94***	***0.93***	0.9	0.9
	Flood discharge	0.9	0.93	***0.96***	***0.95***
Cévennes	Number	NoData	NoData	24	144
	Vegetation	NoData	NoData	0.93	0.91
	Floodplain	NoData	NoData	***0.96***	***0.92***
	Flood discharge	NoData	NoData	0.73	0.86
Dépressions sédimentaires	Number	199	900	253	187
	Vegetation	***0.93***	0.90	***0.91***	0.89
	Floodplain	0.91	0.91	0.90	***0.91***
	Flood discharge	0.88	***0.94***	0.90	0.88
Tables calcaires	Number	1492	1676	1514	848
	Vegetation	0.91	0.92	0.91	0.90
	Floodplain	0.94	0.91	0.89	0.91
	Flood discharge	***0.96***	***0.96***	***0.96***	***0.95***
Côtes calcaires	Number	156	88	154	39
	Vegetation	0.92	0.94	0.93	***1.07***
	Floodplain	***0.97***	***0.98***	***0.97***	1.02
	Flood discharge	0.88	0.85	0.88	0.80
Dépôts argilo-sableaux	Number	41	286	151	685
	Vegetation	0.94	0.93	***0.93***	0.91
	Floodplain	***1.12***	***0.94***	0.92	0.92
	Flood discharge	0.79	0.89	0.87	***0.94***
Massif Armoricain	Number	102	593	9375	1769
	Vegetation	0.94	0.92	0.91	0.91
	Floodplain	***1.03***	0.92	0.90	0.93
	Flood discharge	0.86	***0.93***	***0.98***	***0.96***

5.3.1.4 Volumes of bank erosion and contribution to sediment budget

The volumes of bank erosion vary from 5.4 * 10^{-5} to 4.5 * 10^{-1} $m^3.m^{-1}.yr^{-1}$ for minimal values of bank retreat and from 1.6 * 10^{-4} to 1.4 $m^3.m^{-1}.yr^{-1}$ for maximal values of bank retreat. In all, between 7.32 * 10^5 and 2.22 * 10^6 $t.yr^{-1}$ are eroded from the banks on the entire *LBRB* corresponding to an erosion rate of 12.05 to 36.56 $t.km^{-1}.yr^{-1}$ in this area. In the Loire river basin, the sediment supply to rivers represents between 5.33 * 10^5 and 1.61 * 10^6 $t.yr^{-1}$ from which 43% corresponds to fine particles. The patterns of erosion volumes are more or less similar to those of

bank retreat previously described, with higher volumes eroded in the south east of the Armorican basin than in other regions.

The contribution of fine particles from the banks is at least of 3.31 * 10^5 t.yr^{-1} and at most 1.00 * 10^6 t.yr^{-1}. Overall, the supply in fine sediment is greater than that of coarse particles (sand rate < 50 %) and is particularly more important in the Limagne plain and in the upstream part of the *Sarthe* river with $\sim$ 75 % of eroded material corresponding to fine particles. To the contrary, in granitic areas with upper sandy soils, *e.g.* in the *Massif Central sud*, the rate of the contribution of coarse particles largely exceeds that of fine particles (coarse particles >65% of eroded material). Similar trends are observed in the Sologne region (between the *Loire* and the *Cher* rivers).

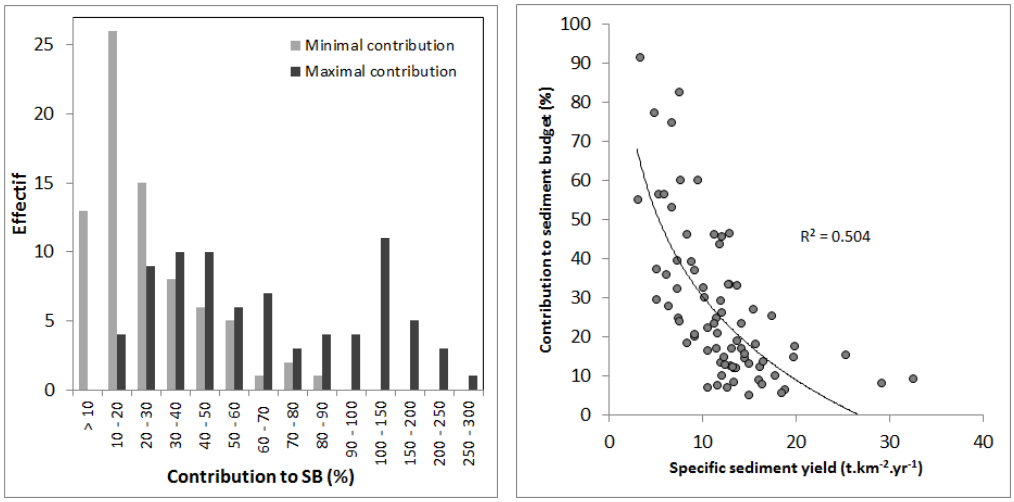

(a) (b)

FIGURE 5.10 – For the 77 catchments : (a) Minimal and maximal contribution of bank erosion to overall sediment budget, and (b) Relationship between contribution to sediment budget and specific sediment yields

The minimal and maximal bank erosion rates are compared to suspended sediment yields (SSY) calculated within the $LBRB$ (Gay *et al.*, 2014 [104]). As the authors state that 18 years of data are needed to obtain a mean stable value of sediment flux at the catchment outlet, we considered in this study only the corresponding 77 catchments. The range of contribution of bank erosion induced by fluvial erosion to catchment sediment budget is wide (Figure 5.10(a)) and is comprised between 4.68 and 83.83% for the minimal values and 14.19 and 254.04 % for the maximal values. Though some of the maximal contribution values are higher than the catchment sediment budget itself, in-stream and overbank deposition on the way to the catchment outlet are not taken into account. These catchments are thus particularly interesting for further research on sediment deposition as a minimal quantification of the these deposited sediment is then available. Similar excess of sediment supply by bank erosion have been reported by De Rose *et al.* (2002) [62] and Trimble, 1997 [277] for example. The latter found that channel contribution accounted for $\sim$ 140 % of the sediment yield but taking into account the sediment deposition, this contribution was about two-third of the SSY.

The proportion of contribution to sediment budget strongly varies through time and may be divided by up to four times from the event to annual time scale (Bull, 1997 [28]) and varies from year to year (Kronvang *et al.*, 2013 [148]) depending on rainfall events and flow discharge magnitude. Over longer time steps (*e.g.*, decade), the use of flood discharge (*e.g.*, the one in two year flood discharge) as a basis for bank retreat assessment allows for the consideration of inter-annual variability of riverbank erosion rates and contribution to sediment budget. Results from the application of bank retreat equations (mostly in Oceania or in coastal catchments) reveal that the contribution from bank erosion to sediment budget is in general medium to low with values ranging from 2% (Bartley *et al.*, 2004 [12]; De Rose and Basher, 2011 [61]) to at most 21% (Nelson and Booth, 2002 [211]; McKergow *et al.*, 2005 [182]) but can also represent a major source in the sediment supply to rivers (87 % of the sediment supply, De Rose *et al.*, 2002 [62]). This range of values clearly matches our contribution values as for 54 out of 77 catchments, the minimal contribution does not exceed 30% without taking sediment deposition into account.

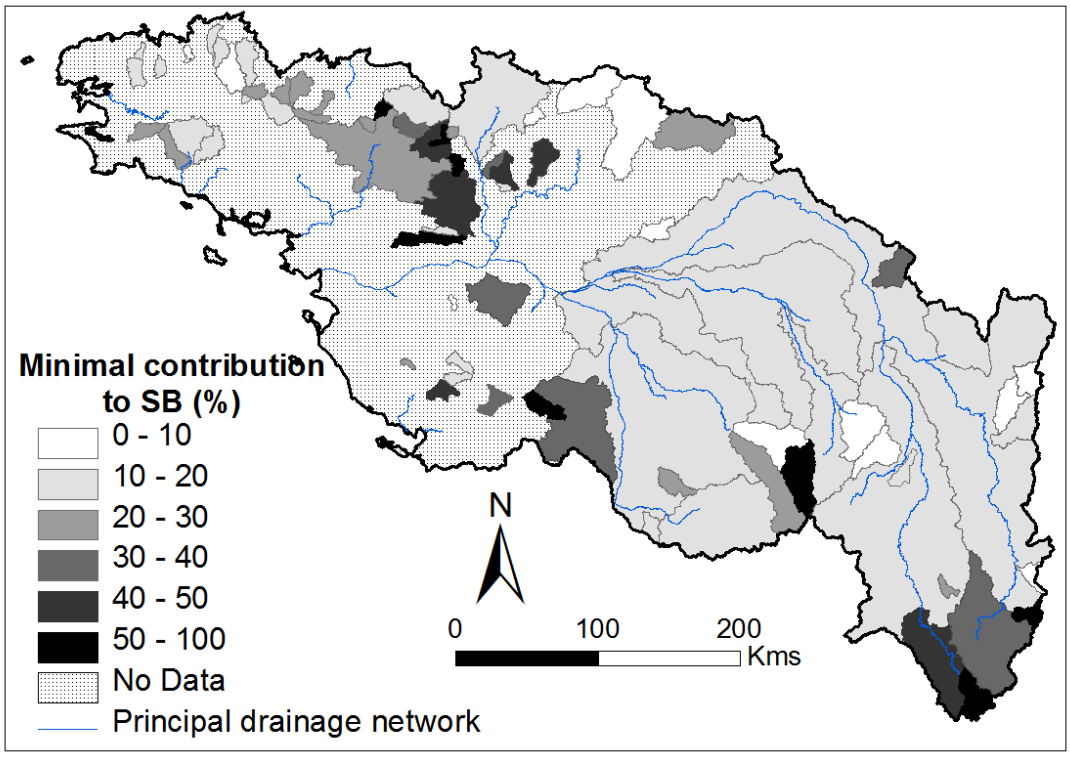

FIGURE 5.11 – The minimal contribution of bank erosion to overall sediment budget for the 77 catchments. Catchments that are nested in other catchments are presented on top.

The spatial distribution of the percentages of contribution from riverbank erosion (Figure 5.11) indicates important contribution in the upstream parts of the *Massif*

Central sud where suspended sediment yields are low and at the frontier between the *Massif Armoricain* and *Tables calcaires*, where SSY are also among the lowest values calculated for the $LBRB$. Large catchments at the centre of the $LBRB$ display low contribution from fluvial erosion of small and medium streams.

There exists an inverse relation between suspended sediment yields and the contribution from bank erosion such that the highest the sediment yield, the weakest the contribution from the banks. From this correlation, two conclusions may be drawn. First, De Rose and Basher (2011) [61] reported very low contribution from river bank in catchment characterised by high suspended sediment yield, and concluded that the major source of suspended sediment came from other processes (primarily mass movement). Therefore, a complete sediment budget from hillslope and river supply and deposition is needed to better understand the contribution from the banks. Second, as there is no relation between suspended sediment yield and the drained area (see Gay *et al.*, 2014 [104]), the percentage of contribution from the banks cannot be inferred from the flood discharge magnitude at the outlet of the catchment which is strongly related to the drainage area.

5.3.2 Total bank erosion in the $LBRB$

Bank erosion is assessed on the Carthage stream sections using a simple equation of bank retreat. We briefly describe the obtained values and patterns of bank erosion and then we provide a final map of the contribution from the banks to sediment budget for catchments in the $LBRB$.

5.3.2.1 Bank retreat rates and volumes from the BDCarthage

A simpler equation based on flood discharge and stream bank erodibility is applied to the Carthage stream sections to provide estimations of bank retreat. The calculated rates range from 3.0 * 10^{-4} to 7.18 cm.yr^{-1} with a mean value of 9.05 * 10^{-2} cm.yr^{-1} (median = 3.41 10^{-2} cm.yr^{-1}, std = 0.46) for the minimal value of flood discharge to 1.0 * 10^{-3} to 21.77 cm.yr^{-1} with a mean mean value of 0.27 cm.yr^{-1} (median = 0.10 cm.yr^{-1}, std = 1.39) for the maximal value of flood discharge. Even though the equation takes less parameters with a range [0,1] (floodplain and vegetation factors), the bank retreat values are below the values from $SYRAH_{CE}$ database. Such results are due to the smaller drainage area of the Carthage sections and thus smaller $Q_{0.99}$ values.

From the *HER* view point, similar trends as the one described for the results on the $SYRAH_{CE}$ database are observed (Table 5.8). Higher mean values are found for the *Cévennes* and lowest mean values for the *Dépressions sédimentaires*. However, median values are higher for the *Massif Central sud* and lowest values for the *Tables calcaires*. These discrepancies result from the lack of consideration of the riparian vegetation and the floodplain width in the simpler bank retreat equation. Indeed, as previously described, the *Massif Central sud* is characterised by narrow floodplains and important

riparian vegetation which limit the erosion in the full bank retreat model. To the contrary, the large floodplains of the *Tables calcaires* and average vegetation on the banks tend to favour erosion in this region.

These results clearly highlight the limits of the simpler equation for the comparison with results from the full equation at the *HER* scale resolution. Still, at the *LBRB* spatial scale, the results from the sensitivity analysis (Section 5.3.1.3, page 115) on the importance of the flood discharge parameter in the calculation of bank retreat rates allows us to consider the results from BDCarthage with confidence within the framework of our objective of providing a large-scale model of bank retreat.

Tableau 5.8: Mean, median (weighted by the stream length) and standard deviation of the parameters vegetation, floodplain, and flood discharge, and for the bank retreat rate for each *HER*. Highest mean and median values are highlighted in bold characters, and lowest values in italic characters

	Minimal bank retreat ($cm.yr^{-1}$)			Maximal bank retreat ($cm.yr^{-1}$)		
	mean	median	std	mean	median	std
Massif Central sud	0.13	**3.23 10^{-2}**	0.46	0.40	**9.78 10^{-2}**	1.39
Massif Central nord	0.08	2.06 10^{-2}	0.27	0.24	6.26 10^{-2}	0.80
Cévennes	**0.15**	3.07 10^{-2}	0.46	**0.46**	9.29 10^{-2}	1.38
Dépressions sédimentaires	*0.05*	6.76 10^{-3}	0.30	*0.15*	2.05 10^{-2}	0.92
Tables calcaires	0.08	*6.40 10^{-3}*	0.59	0.24	*1.94 10^{-2}*	1.78
Côtes calcaires	0.06	1.11 10^{-2}	0.29	0.19	3.37 10^{-2}	0.87
Dépôts argilo-sableux	0.07	1.17 10^{-2}	0.29	0.21	3.55 10^{-2}	0.89
Massif Armoricain	0.10	2.91 10^{-2}	0.42	0.31	8.83 10^{-2}	1.26

The total sediment supply to rivers from the Carthage stream sections ranges from 1.30 * 10^5 to 3.93 * 10^5 $t.yr^{-1}$ and thus represents a minor contribution of 14.85% to the total load eroded on the banks in the *LBRB*. The fine particles represent 45% of the total load in this area.

5.3.2.2 Global contribution of bank erosion to sediment budget

All bank retreat rates were considered to provide a final estimation of the contribution of the banks due to fluvial entrainment in streams of Strahler order 1 to 3. In general, the contribution from the Carthage stream sections is low and ranges from 4.13% (from minimum bank retreat) to 12.50 (from maximal bank retreat) in average. Table 5.9 gives the contribution from bank erosion to the sediment budget of the 77 catchments, the percentage of streams for which a bank erosion rate is available (streams of a Strahler order ≤ 3) and the percentage of the stream network coming from both database.

Tableau 5.9: Total contribution from the banks to sediment budget of the 77 catchments and the percentage of the total stream network (all Strahler order) covered by the bank retreat modelling and the proportion of streams from the two database used in this study

Station code	Name	Area	SSY	Bank contribution (%)		Percentage of stream network		
		(km^2)	($t.km^{-2}.yr^{-1}$)	Min	Max	Strahler $\leq 3^{rd}$	Carthage	$SYRAH_{CE}$
K2090810	Allier [1]	518.69	4.71	79.54	241.03	99.05	41.37	58.63
K2330810	Allier [2]	2260.13	5.50	57.10	173.04	98.88	44.86	55.14
K3650810	Allier [3]	14347.44	12.22	17.26	52.30	97.40	48.97	51.03
k3153010	Andelot	209.20	13.51	12.19	36.94	99.11	39.26	60.74
K1173210	Arconce	591.25	14.91	14.20	43.04	93.66	43.62	56.38
K1773010	Aron	1465.53	19.65	15.87	48.08	96.05	60.20	39.80
K5383010	Aumance	927.18	11.92	12.61	38.22	98.14	50.14	49.86
N5101710	Autise	244.16	13.52	32.78	99.33	100.00	36.17	63.83
M6014010	Beuvron	38.26	32.44	9.87	29.91	95.50	67.44	32.56
K3373010	Bouble	560.77	18.32	7.16	21.70	97.87	49.31	50.69
K1363010	Bourbince [1]	338.77	18.75	9.62	29.14	96.19	69.37	30.63
K1383010	Bourbince [2]	818.93	17.67	12.17	36.88	97.02	60.83	39.17
K4873110	Brenne	261.16	10.43	8.26	25.04	98.21	59.40	40.60
K5490910	Cher [3]	4520.05	8.26	20.90	63.34	95.64	48.81	51.19
K6720910	Cher [4]	13677.97	12.27	14.60	44.26	93.76	51.45	48.55
J7083110	Chevré	151.28	12.70	32.98	99.94	99.37	44.00	56.00
L2501610	Clain	2852.91	6.02	34.77	105.37	91.98	32.71	67.29
J0201510	Couesnon	856.07	16.03	15.00	45.45	95.61	53.63	46.37
L4220710	Creuse	1233.23	7.41	26.08	79.02	97.47	47.95	52.05
K2821910	Dore	105.20	7.27	28.63	86.75	100.00	38.74	61.26
K0454010	Dunière	217.46	3.16	112.53	340.99	100.00	47.96	52.04
J4742010	Ellé	574.59	11.45	23.46	71.10	94.94	51.53	48.47
J3413020	Elorn	200.66	15.57	19.22	58.25	100.00	43.12	56.88
M6323010	Erdre [1]	98.72	13.17	15.84	47.99	95.29	60.60	39.40
M6333020	Erdre [2]	464.64	7.40	79.74	241.62	100.00	45.05	54.95
J1324010	Evron	139.42	9.93	41.10	124.54	100.00	46.01	53.99
J7214010	Flume	91.69	10.12	31.31	94.88	95.45	30.60	69.40
K0614010	Furan	174.53	29.09	9.38	28.42	98.01	41.04	58.96
L0914020	Gorre	180.03	16.42	16.72	50.68	100.00	58.17	41.83
J1313010	Gouessant	244.05	7.18	34.76	105.34	89.49	39.74	60.26
J1513010	Gouët	135.68	10.41	22.47	68.09	100.00	33.01	66.99
J4014010	Goyen	88.87	5.19	56.56	171.38	86.44	20.57	79.43
N3001610	Grand Lay [1]	129.53	25.25	15.54	47.10	100.00	37.79	62.21
J2034010	Guindy	121.82	14.42	14.27	43.23	100.00	21.23	78.77
J3014310	Horn	50.49	12.82	13.51	40.94	96.16	30.41	69.59
M0421510	Huisne	1910.77	11.51	10.51	31.86	93.62	54.87	45.13
J7103010	Ille	102.60	2.94	78.13	236.76	100.00	67.75	32.25
J7114010	Illet	111.22	7.12	41.91	127.00	91.25	49.85	50.15
J2023010	Jaudry	165.13	13.36	14.68	44.50	94.23	41.53	58.47
J4902011	Laïta	851.71	11.36	26.16	79.27	94.68	46.03	53.97
M5222010	Layon	918.76	12.69	33.22	100.65	97.87	47.36	52.64
J1813010	Leff [2]	341.49	9.02	21.29	64.50	98.05	33.80	66.20
J8133010	Lié	298.65	13.03	19.49	59.07	100.00	48.62	51.38
N3024010	Loing	121.85	19.79	17.77	53.84	100.00	44.05	55.95
M1041610	Loir	1156.86	4.94	33.01	100.03	96.46	67.76	32.24
K0550010	Loire [1]	3249.13	8.98	41.01	124.27	99.50	45.51	54.49
L8000010	Loire [4]	80999.34	9.07	22.80	69.08	95.15	51.15	48.85
M3340910	Mayenne [2]	2901.17	14.42	18.52	56.12	96.17	57.52	42.48
M0114910	Merdereau	118.40	16.24	14.86	45.02	99.17	86.25	13.75
K4094010	Nohain	475.82	5.01	38.28	116.01	100.00	35.27	64.73
J4211910	Odet	202.72	15.37	29.54	89.51	100.00	49.20	50.80
M3711810	Oudon [1]	133.33	6.62	73.21	221.84	100.00	43.60	56.40
M3861810	Oudon [2]	1416.85	11.12	45.76	138.67	100.00	45.83	54.17
M3514010	Ouette	118.62	8.72	37.10	112.44	100.00	38.52	61.48
J8002310	Oust [1]	28.42	13.22	14.41	43.66	100.00	33.06	66.94
L4411710	Petite Creuse	853.13	15.85	10.66	32.30	95.72	53.04	46.96
J2614020	Queffleuth	95.29	11.81	15.52	47.03	97.73	31.03	68.97
j0611610	Rance	143.46	14.04	23.26	70.49	100.00	20.97	79.03
J1114010	Rosette	113.29	6.26	28.17	85.36	100.00	23.31	76.69
M0050620	Sarthe	906.05	14.90	6.65	20.16	93.04	62.99	37.01
J5102210	Scorff	299.48	13.59	20.62	62.50	96.03	48.41	51.59
N3222010	Smagne	184.87	11.92	44.93	136.15	100.00	39.09	60.91
K5183010	Tardes	859.17	5.73	55.95	169.54	100.00	43.97	56.03
M0674010	Taude	45.93	10.46	19.91	60.33	100.00	25.69	74.31
J1721720	Trieux	413.85	12.55	9.89	29.96	89.25	44.61	55.39
M0653110	Vaige	238.11	12.79	44.73	135.53	100.00	41.30	58.70
M0583020	Vègre	400.01	11.66	44.83	135.86	100.00	44.11	55.89
L7000610	Vienne [2]	19817.31	11.41	18.00	54.53	95.61	49.81	50.19
L0700610	Vienne [21]	3387.16	14.07	19.10	57.86	98.19	53.13	46.87
J7000610	Vilaine [1]	56.82	11.17	22.05	66.83	97.90	34.42	65.58
J7010610	Vilaine [2]	146.79	9.43	58.99	178.76	100.00	39.32	60.68
J7060620	Vilaine [3]	566.97	8.21	51.54	156.18	100.00	55.18	44.82
J7700610	Vilaine [4]	4146.39	11.86	30.19	91.49	94.56	46.46	53.54
L5223020	Vincou	285.55	11.91	26.72	80.96	100.00	43.60	56.40
L2253010	Vonne	304.41	7.51	56.63	171.60	98.82	26.35	73.65
J2314910	Yar	58.50	13.28	10.48	31.76	100.00	40.81	59.19
N3403010	Yon	40.55	17.33	23.13	70.08	100.00	22.43	77.57

The highest minimal contribution from the Carthage stream sections ($> 10\%$) are found for three catchments that already displayed medium to high contribution from the banks. Two are located in the *Massif Armoricain*, the *Evron* ($SYRAH_{CE}$ min contribution = 29.48%, Carthage min contribution = 11.62%), and the *Ille* ($SYRAH_{CE}$ min contribution = 50.89%, Carthage min contribution = 27.24%). The third one, the *Dunière* ($SYRAH_{CE}$ min contribution = 83.83%, Carthage min contribution = 28.69%) is located at the south east of the *Massif Central sud*. The *Ille* and *Dunière* have the lowest SSY in the $LBRB$ (2.94 and 3.16 t.km^{-2}.yr^{-1}, respectively) while the *Evron* displays a medium SSY value of 9.93 t.km^{-2}.yr^{-1}.

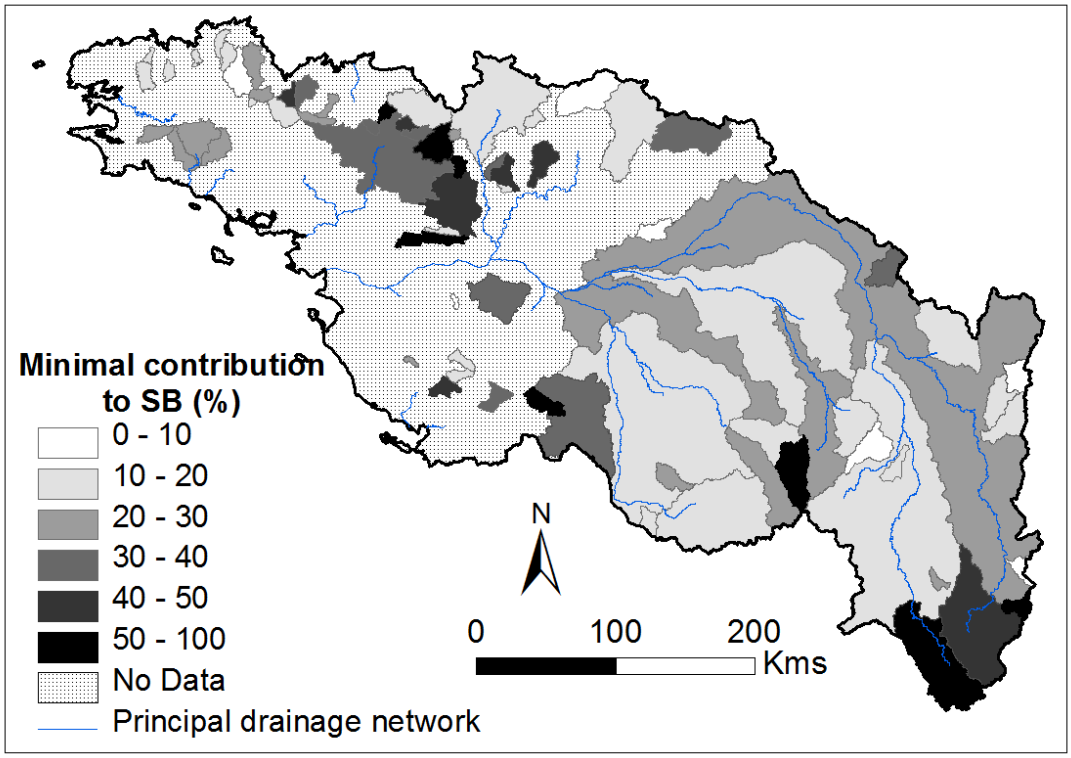

FIGURE 5.12 – Minimal contribution from the banks to the sediment budget from the modelling of bank retreat on the BD Carthage and $SYRAH_{CE}$

The inverse relation previously observed between the percentage of bank contribution and SSY is confirmed ($R^2 = 0.57$). It is important to note that the low contribution from the banks in the *Furan* catchment while the SSY is one of the highest value, is due to the importance of urban areas (30% of the catchment) where the soil information is a "NoData" value (and erodibility is put to 0). Our choice to not give these areas a mean erodibility value is a first step to include man interventions on the landscape. Indeed, in large urban area of the $LBRB$, riverbanks are constrained by concrete constructions such as dikes and very little erosion is possible. However, the case of the *Furan* is isolated as for the other catchments, the mean percentage of urban area is of 2.04%.

Figure 5.12 provides the spatial distribution of the contribution of banks to sediment budget. As previously highlighted in Section 5.3.1.4, higher contributions are found in the upstream parts of the *Allier* and *Loire* rivers and at the limits between the *Massif Armoricain* and *Tables calcaires*. The addition of the contribution from the Carthage stream sections on the *Loire [4]*, the largest catchment in the $LBRB$, has slightly increased the contribution from banks, rising from 19.03% to 22.80% (minimal contribution). A similar increase is observed for the *Cher [3]* catchment, with a contribution rising from 16.91% to 20.90% with the inclusion of the Carthage stream network.

5.4 Conclusion

The importance of bank erosion in lowland areas and the contribution from this source to the sediment budget can be significant and should not be neglected. In the Loire and Brittany river basin, to our knowledge, no quantification of such process exists. Still, evidence of river clogging by excess of fine sediment exist and are not explained by hillslope erosion models. Therefore, **in this study, we use a large-scale model of bank retreat due to fluvial entrainment to evaluate the sediment supply from the banks. We adapted equation taken from the literature to better take into account the effect of the vegetation and the bank erodibility.** The model is then applied over the entire $LBRB$ territory and contribution of fine particles to the sediment budget of 77 catchments is evaluated.

The mean rates of bank retreat vary from 0.42 to 1.29 cm.yr^{-1} on the entire study site. Higher values of bank retreat are found at the south east of the *Massif Armoricain* and in the *Cévennes* while low values are found in the forested floodplains of the surrounding of the mid-Loire basin. The absence of spatial organisation of the different parameters used in the equation, especially in lowland managed area, and the resulting patterns in stream bank erosion, indicate that bank retreat and contribution to sediment budget cannot be inferred using basic assumptions on site global characteristics. From the sensitivity analysis, it is clear that the **flood discharge is the driving parameter of the outputs of the bank retreat equation** and reflects the predominant role we first gave to it in this equation. Vegetation appears as the second most important parameter. The values of bank retreat rates calculated for the study area are in the range of values found for large temperate catchments of Australia but no comparable data exist for European streams. Finally, we provide an **estimation of the contribution from the banks to the sediment budget of 77 small to large catchments within the study area. The minimal sediment supply from the banks range from 6.6% to 122.5%**, which is consistent with literature data. These contributions are high in catchments with low sediment yields and lower for high suspended sediment exports catchments, without any correlation with the drainage area.

The model used in this study presents interesting perspectives for the assessment of bank retreat at large spatial scale. Indeed, the low number of required data allows for simple implementation of the model for a first quantitative and qualitative assessment

of bank retreat. However, further researches are needed to spatially quantify and qualify human impacts on the stream water regime and thus on fluvial bank erosion and to integrate this factor into fluvial bank retreat modelling. Furthermore, estimations of in-stream sediment deposition should help to better understand the net contribution from the banks to the sediment budget.

Troisième partie

Prise en compte de la connectivité dans le transfert de particules

Chapitre 6

Connectivité des milieux tempérés et agriculturaux de plaine : synthèse sur l'état des connaissances

---

Dans les précédents chapitres, différentes sources de particules ont été identifiées et quantifiées et les exports de sédiments à l'exutoire de bassins versants ont été calculés. Cependant, les caractéristiques morphologiques, topographiques ou climatiques des bassins versants ne permettent pas d'expliquer les flux de sédiments en sortie. Il est donc nécessaire de prendre en compte la distribution spatiale des paramètres et processus de transfert, via l'introduction de la connectivité pour faire le lien entre source et dépôt.

Cependant, l'essor récent et l'engouement autour de la connectivité ont multiplié les définitions, concepts et approches. Afin de mieux comprendre les différents enjeux de la connectivité pour l'utilisation que nous souhaitons en faire au regard de notre objectif de bilan sédimentaire, un bref état de l'art de la connectivité est proposé dans ce chapitre. Nous mettons plus particulièrement l'accent sur les paramètres et processus en jeu dans les milieux agriculturaux de plaine sous climat tempéré.

Sommaire

6.1 Introduction

Because they represent major environmental issues, sediment transfers have been widely studied since the 1960s. Numerous studies have attempted to provide a qualitative and quantitative insight into sediment transfer through experiments in the field and modelling approaches. A recent alternative to the different terms and concepts used so far in sediment transfer researches has emerge through the concept of connectivity.

The increasing use of the concept of "connectivity" in the field of environmental researches has led to an increase in the number of definitions, conceptual frameworks, field monitoring techniques and model developments, which will be briefly described further in the text. Several reviews have flourished on these different topics (*e.g.*, Bracken and Croke, 2007 [23]; Ali and Roy, 2009 [3]; Gumiere *et al.*, 2011 [117]; Bracken *et al.*, 2013 [25] and 2015 [24]; Fryirs, 2013 [93]; Golden *et al.*, 2014 [108]). Moreover, working groups, from the COST Connecteur action started in 2014, are currently working to provide the scientific community with a homogeneous set of definitions and methodologies to measure and model hydrological and sediment connectivity.

These recent works provide an important basis for our work on sediment connectivity and the present brief overview. One aspect that has been highlighted by Bracken *et al.* [25] in their 2013 paper, is the importance of taking into account site location and specificity for the comprehension and description of connectivity. The authors indicate that forested catchments in steep areas concentrate much of the research efforts on connectivity while developed approaches may not be transposed to other areas.

From our research, we confirm this concentration of attention on steep catchments (*e.g.*, Harvey, 2001 [121]; D'Haen *et al.*, 2013 [72]; Foerster *et al.*, 2014 [88]; Meßenzehl [185]), and we also add badlands (*e.g.* Faulkner, 2008 [86]; Godfrey *et al.*, 2008 [107]) or semi-arid to arid areas (*e.g.*, Cammeraat, 2004 [31]; Mueller *et al.*, 2007 [203]; Reaney *et al.*, 2007 [237]; Lesschen *et al.*, 2009 [166]) at the top of the list of studied areas for connectivity. However, much less attention has been paid to lowland areas. Still, unexpected connectivity, and the combination of increase in hillslope connectivity and in stream disconnectivity induced by land management decisions (Foucher *et al.*, 2015 [90]) may also cause severe damage in these areas. From the studies available on the topic, it seems that processes have been left aside in favour of investigations on landscape elements that enhance or impede sediment connectivity (*e.g.*, Fryirs *et al.*, 2007 [94]; Gascuel-Odoux *et al.*, 2011 [102]; Gumiere *et al.*, 2011 [117]). Whereas in mountainous areas overland flow is topographically driven, in flat areas process-based connectivity is a key to understanding the connections that arise from sources to sinks.

In this context, the aim of this chapter is to present briefly the different concepts that have emerged around the topic of connectivity. We build on existing works and concepts and do not aim at providing a new look at the sediment connectivity. However, we want to bring into light the importance of processes in the generation of connectivity within lowland areas and the gaps that should be bridged in the integration of landscape elements in the connectivity assessment of such landscapes. At some point we may not agree with previous statements on sediment connectivity that have emerged. Our motivations on rejecting the proposed hypothesis are exposed. At no time, our position on sediment connectivity calls into question the statement from other researchers. The first part of this review is dedicated to pure concepts and definitions. In the second and third parts, we select and describe the different parameters and processes that we believe to be the most important drivers of connectivity in lowland temperate areas.

6.2 General definitions and concepts of connectivity

6.2.1 A brief history of the origins of the word "connectivity" and its evolution

The term of connectivity first appeared in the 1990s in ecology management to characterize "the degree to which the landscape facilitates or impedes movement between resource patches" (Taylor *et al.*, 1993 [270]). Of course, this definition fits cases in which the movement is insured by living creatures. The word connectivity has thus been recycled and adapted to suit the water and sediment cycles.

Since then, the use of the word "connectivity" has spread considerably. As a consequence, the number of publications in geosciences mentioning connectivity as a basis for investigations on water and sediment movement, has increased exponentially (Figure 6.1). If at the early stage, the concept of connectivity may have appeared as a surrogate to the source-to-sink concept, and many definitions have flourished depending on the purpose of each study, it is starting to be a full-fledged concept that has its own

specificities, approaches and communities.

First, studies primarily focused on hydrological connectivity and the development of investigations around this topic have been initiated by the hydrogeologists (*e.g.*, Bour and Davy, 1998 [22]) and the hydrologists (*e.g.*, Western *et al.*, 1998 [312]). In comparison, the sediment connectivity has emerged later, introduced in the early 2000s (Hooke, 2003 [126]). The concept has then gained increasing attention from the active community of geomorphologists of Australia (*e.g.*, Brierly *et al.*, 2006 [26]; Fryirs *et al.*, 2007 [95]). There may exist several reasons for the observed time lapse between the emergence of both connectivity concepts. One of them is probably linked to the fact that sediment transfer can be triggered by water movement. Thus, the generation of hydrological connectivity represents a preliminary condition to sediment connectivity and constitutes a basis for its understanding.

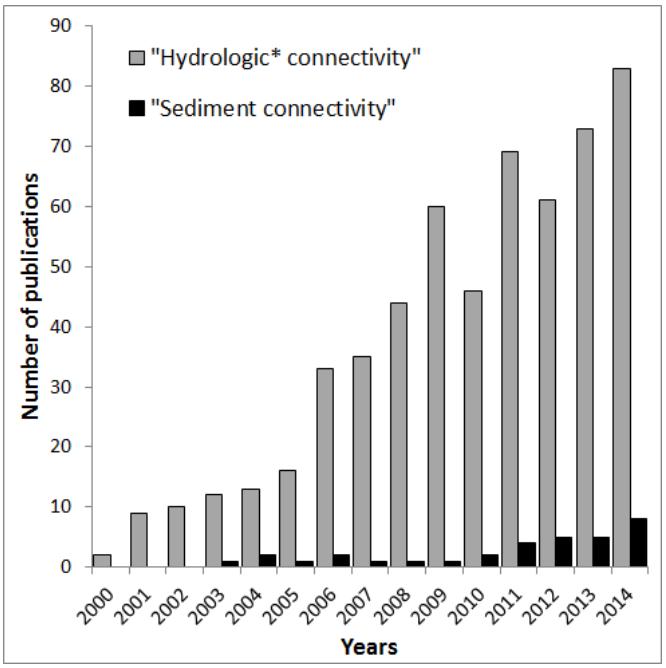

FIGURE 6.1 – Evolution of the number of papers dealing with hydrologic or sediment connectivity from 2000 to 2014

The vision of each community on the connectivity concept has direct consequences on the spatial scale of the studies. Indeed, in surface hydrology, connectivity has been investigated at the plot scale (Antoine *et al.*, 2009 [5]), field scale (Appels *et al.*, 2011 [6]), and catchment scale (Jencso *et al.*, 2009 [134]). While sediment connectivity assessment could have first been supported by the community of erosion modellers and experimenters, and benefit from their knowledge on sediment movement at the plot to catchment scale, the topic has gained interest among the community of geomorphologists, whom approach is more oriented towards the global comprehension of sediment dynamics within the landscape. As a consequence, the smallest unit considered in studies is either a small catchment or a compartment of the catchment (river/hillslope).

The use of the term connectivity within geomorphologic approaches has changed the focus from a sediment-based approach where the major question to be answered is "Will the particles stay in this place and if so, is it a permanent or a temporary state?" to a landscape oriented approach where the sediment is considered as an element that participates in landscape evolution. These changes of focus may certainly benefit the growing partnerships between scientists and land managers, who are trying to develop holistic approaches in order to understand the functioning entire catchments and not just part of it.

6.2.2 Definitions and concepts from literature

6.2.2.1 A set of definitions from Ali and Roy, 2009 [3]

Ali and Roy, 2009 [3] provide a synthesis of definitions of hydrological connectivity from prior works (Table 6.1). Though the question of sediment connectivity is not addressed by the authors, most of definitions provided apply to sediment connectivity and/or include a sediment dimension. The authors have grouped the definitions according to five connectivity classes depending on the spatial scale considered (hillslope *vs* watershed) and the integration of landscape features and their patterns versus processes. From this classification, it is clear that two different approaches of connectivity have emerged, one based on the opposition of static and dynamic connectivity (or structural *vs* functional), and the other one related to the connectivity within the three dimensions of the landscape. Both approach types are described in the next two sections.

Another definition of the connectivity can be seen in the approach developed by Borselli *et al.* (2008) [21]. The authors proposed an index of connectivity which is based on "the probability that a given part of the landscape transfer its contribution elsewhere in the catchment", a probability that depends on the landscape elements.

At present, there is no real consensus on the definition of connectivity and each and every scientist takes on board the definition that suits its applications best. A working group of the COST Action is currently working on a new definition/set of definitions to provide a homogeneous understanding of the different aspects of connectivity.

6.2.2.2 3D connectivity

One approach developed by the geomorphologist community consists of dividing the catchment into three compartments to which corresponds different processes and parameters (Brierley *et al.*, 2006 [26]). The connectivity is defined in the three spatial dimensions:

- **Lateral connectivity** refers to slope to channel connectivity *via* overland flow and/or flows in the subsurface zone and to channel floodplain interactions.
- **Vertical connectivity** refers to surface-subsurface interactions. As underlined by Duvert *et al.*, 2011 [80], vertical connectivity is particularly important in

regions where the surface and subsurface are highly connected, *e.g.* in alluvial plains.

– **Longitudinal connectivity** refers exclusively to in-channel connectivity with upstream to downstream material transfer and interactions between the trunk and its tributaries.

Tableau 6.1: Definitions of hydrological and sediment connectivity (from Ali and Roy, 2009 [3])

Connectivity type	Scale	Definition	Source
Water cycle	Watershed	An ecological context to refer to water-mediated transfer of matter, energy and/or organisms within or between elements of the hydrological cycle	Pringle, 2003
Landscape features	Watershed	All the former and subsequent positions, and times, associated with the movement of water or sediment passing through a point in the landscape	Bracken and Croke, 2007
		Flows of matter and energy (water, nutrients, sediment, heats, etc.) between different landscape compartments	Tetzlaff *et al.*, 2007
		The extent to which water and matter that move across the catchments can be stored within or exported out of the catchment	Lane *et al.*, 2004
	Hillslope	Physical linkage of sediment through the channel system, which is the transfer of sediment from one zone or location to another and the potential for a specific particle to move through the system.	Hooke, 2003
		The physical coupling between discrete units of the landscape, notably, upland and riparian zones, and its implication for runoff generation and chemical transport	Stieglitz *et al.*, 2003
		The internal linkages between runoff and sediment generation in upper parts of catchments and the receiving waters [Ě] two types of connectivity: direct connectivity via new channels or gullies, and diffuse connectivity as surface runoff reaches the stream network via overland flow pathways.	Croke *et al.*, 2005
Spatial patterns	Watershed and hillslope	Hydrologically relevant spatial patterns of properties (e.g. high permeability) or state variables (e.g. soil moisture) that facilitate flow and transport in a hydrologic system (e.g. an aquifer or watershed)	Western *et al.*, 2001
		Spatially connected features wich concentrate flow and reduce travel times	Knudby and Carrera, 2005
Flow processes	Hillslope	The condition by which disparate regions on a hillslope are linked via lateral subsurface water flow	Hornberger *et al.*, 1994; Creed and Band, 1998
		Connection, via the subsurface flow system, between the riparian (near stream) zone and the upland zone (also known as hillslope) occurs when the water table at the upland-riparian zone interface is above the confining layer	Vidon and Hill, 2004; Ocampo *et al.*, 2006

6.2.2.3 Structural versus process-based connectivity

As underlined previously, another understanding of connectivity has emerged and seems to be coming the most popular way to approach connectivity: static *versus* dynamic connectivity.

The static part also known as *structural connectivity* refers to the "continuum properties of state variables in space" (Antoine *et al.*, 2009 [5]), in other words, "the extent to which landscapes units are contiguous or physically linked to one another" (Wainwright *et al.*, 2011 [296]). Structural connectivity relates to the landscape features, and organisation, that may enhance of impede sediment transfer if such phenomenon is to appear. In all cases, a triggering agent (of a process-based kind) is needed for this structural connectivity to be effective. The different elements defining structural connectivity in the landscape (*e.g.*, topography, vegetation, *etc.*) are in general easily identifiable and quantifiable (slope, density of vegetated features, *etc.*). Yet, there efficacy under connectivity conditions or the part they play in connectivity remain less well understood such that assumptions have to be made.

The *functional connectivity* accounts for the dynamic part of connectivity. It is defined as "the capacity of water and associated particles to move in the system in response to a boundary stimulus" (Antoine *et al.*, 2009 [5]). Since the term "functional" has other meanings in hydrology, Bracken *et al.* (2013) [25] have proposed to name this functional connectivity *process-based connectivity* in order to avoid confusion. Therefore, in this chapter, we use the words process-based connectivity to relate to dynamic processes.

6.2.2.4 Structural and process-based feedbacks

As underlined by Bracken and Croke (2007) [23], the connectivity concept is the combination of both static and dynamic connectivities. The limit between structural and process-based connectivities is often unclear. The classification of one element in one or the other type of connectivity generally depends on the purpose of the study. For example, the development of a gully during a rainfall event through the concentration of water can be viewed as a process-based form of connectivity (Katz *et al.*, 2013 [138]). As the gully develops and becomes a stable permanent feature in the landscape, this element is part of the structural connectivity by linking two distant areas (Croke *et al.*, 2005 [51]). Similarly, vegetation is considered as a a physical barrier to sediment which also plays a role in process-based disconnectivity by increasing soil infiltration capacity (Sandercock and Hooke, 2007 [253]).

In 2011, Wainwright *et al.* [296] have provided an interesting framework in which structural and process-based connectivities and the feedbacks between both are clearly identified regarding the three compartments of the 3D connectivity. The approach proposed by the authors allows for the consideration of the system response at various spatial scales. Prior work from Lexartza-Artza and Wainwright (2009) [167] had already conceptualized the feedbacks and interactions that exist between features-features,

processes-processes and processes-features elements. These interactions are described in Figure 6.2.

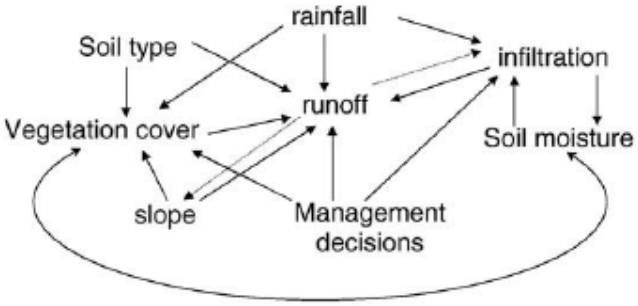

FIGURE 6.2 – Interactions and feedbacks between structural components and process-based connectivity from Lexartza-Artza and Wainwright (2009) [167]

Another major outcome of the study from Wainwright *et al.* (2011) [296] is the highlighting of the non-linearity of the feedbacks. The non linearity of hydrological and sediment connectivity in response to the structural complexity of the landscape (Baartman *et al.*, 2013 [9]), to process-based connectivity induced by rainfall (Tetzlaff *et al.*, 2014 [272]), or both aspects (Coulthard and Van De Wiel, 2007 [47]) is fundamental for the understanding of the overall catchment connectivity and the spatial and temporal variability of this response. However, the hydrological and sediment catchment responses to various *stimulii* are still misunderstood and further researches are needed at different spatial and temporal scales.

6.2.3 Space, time and forcing issues

Spatial and temporal scales have always been key issues in sediment transfer investigations. Indeed, the structural elements of the landscapes as much as its properties that determine process-based connectivity are under constant evolution. Before the rainfall event, the catchment is considered under its natural connectivity which could be comparable to a static structural connectivity. As overland flow is generated and new connections arise, a modified connectivity is generated and can be assimilated to functional connectivity. Therefore, connectivity has to be assessed at each time step throughout the period under consideration. At the event time scale, modified catchment properties that might affect connectivity are mainly soil saturation and runoff generation. At the seasonal time scale, changes in land use and land cover may affect the amount of sediment available and the landscape connectivity. At annual to decadal time scales, the structural landscape connectivity might be modified from its original point by natural processes such as progressive hillslope revegetation (land abandonment) or the result of connectivity events (landslides). The consideration of structural and process-based connectivity and of the feedbacks is always dependent on the spatial and temporal scales and Turnbull *et al.*, 2008 [280] have provided a framework for the conceptual understanding of these interactions (see Figure 6.3).

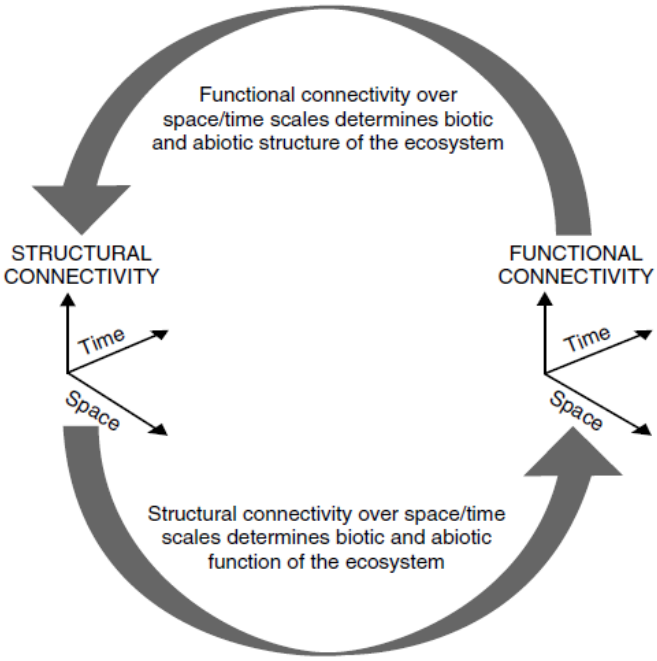

FIGURE 6.3 – Connectivity framework, interactions between structural and process-based (functional) connectivity, Turnbull *et al.*, 2008 [280]

The changes undergone at different type steps and scale resolutions depend on the magnitude of the force exerted on the landscapes. Pressures exerted on the system can either be of a natural kind (*e.g.*, rainfall) or of an anthropic kind (*e.g.*, management decisions).

Studies at the catchment scale have already indicated that the amount of sediment transported to the outlet vary throughout the time. At the inter-annual time scale, it is not during the wettest years but during years with higher number of rainfall events that sediment productivity is at its highest point. At the intra-annual time scale, Meybeck *et al.*, 2003 [189] show that most of the annual sediment load of rivers is scoured in less than 25% of the time. These variations in sediment connectivity and shaping of the landscape have been conceptualized through the "time compression" introduced by Gonzalez-Hidalgo *et al.* (2012) [110] and (2013) [109]. According to the authors "time compression means that most of the geomorphic work (particularly sediment transport) is produced in very short temporal intervals (*i.e.* in few events)". From their investigations, the authors state that geomorphic changes in the landscape are supported by a very few number large events, regardless of their magnitude. As a consequence, feedbacks in structural and process-based connectivity (and between them) should be linked to the number of large event that control the generation of connectivity.

Another issue related to spatial and temporal scales is the up-scaling of connectivity. While connectivity is important at fine to broad scales, the variations in the controlling factors and of thresholds operating at the different scales and the non linearity of connectivity response and feedbacks does not allow for up-scaling (Cammeraat, 2004

[30]). Therefore, studies at different spatial and temporal resolutions are needed to understand connectivity at each and every scale.

6.2.4 Degrees of connectivity and sediment typology

The notion of degrees of connectivity was introduced to add other levels in the binary approach, presence or absence, of connectivity (Western *et al.*, 2001 [313]). On the basis of the works from Wemple *et al.* (1996) [310], Croke *et al.* (2005) [51] added a third degree to the structural connectivity of the landscape so that features, *e.g.*, gullies, may be "partially" connected to the permanent drainage network. However, this new degree is a static characterisation of the landscape and does not account for the progressive changes in the landscape induced by and throughout rainfall events.

In 2003, Hooke [126] had proposed five classes of connectivity to juggle with static and dynamic connectivities by introducing the notion of the magnitude and recurrence of flood events. The different degrees proposed are briefly presented in Table 6.2. The notion of degrees of connectivity might be useful to characterize the different states the catchment is experiencing at various time steps and temporal scales.

Tableau 6.2 Degrees of connectivity according to Hooke, 2003 [126]

Degree of connectivity	Sediment supply availability	Channel competence for sediment transport
Unconnected	Yes	No
Partially connected	Yes	Only during extreme flood events
Potentially connected	No	Yes
Connected	Yes	Yes
Disconnected	Yes	Previously connected, now obstructed

This description of the degrees of connectivity is also based on the sediment supply availability which appears as a preliminary condition to connectivity. However, it is our understanding that the amount of sediment available within a given landscape and for a special rainfall event and the detachment processes should not be considered as a factor influencing connectivity. This statement is based on two premises.

First, the climatic change that affects our environments is likely to modify the sediment availability without altering the connectivity pathways that already exist or the process-based ensured by the different elements in the landscape. The underlying risk of considering the sediment stock as part of the connectivity is to devote more attention to areas where this stock is readily available in great quantities (mountainous areas) or with drastic consequences for local populations (semi-arid and arid environments) than to areas where this stock is far less important but unexpected connectivity can cause serious damages (*e.g.*, lowland areas).

Second, if the connectivity concepts is to be used in studies to evaluate the potential sediment transfer, landscape evolution, *etc.* it is our duty to provide researchers with broadlines on concepts, methods and models regardless of the sediment stock

availability which may very through time and from one site to another.

However, the sediment amount can be considered within the connectivity framework as an element that may shape the landscape (*e.g.* alluvial fans, Brierley *et al.*, 2006 [26]) or, once in movement, can participate in process-based connectivity, for example by increasing flow turbidity (*e.g.*, debris flows).

One point that is clearly neglected in sediment connectivity researches is the sediment type. As underlined by Hooke (2003) [126], the particle fraction has to be considered if sediment connectivity is to be assessed. While the connectivity of dissolved solids resemble hydrological connectivity, processes and parameters involved in cohesive, fine, and coarse particles transfers, if not much different, may have to vary over several orders to produce the same output. Indeed, a structural feature may be enough to disconnect one area from the others when considering coarse particles but not enough to fully or partially disconnect the area if fine particles are considered. Similarly, flow processes might be sufficient to hydrologically connect two areas but not for the transfer of sediment or at most the finest fraction. Concerning cohesive sediment connectivity, one may want to attach importance to other parameters generally not taken into account in sediment connectivity, such as water salinity, for example, relating to the strong affinity of cohesive particles with dissolved salts (Teisson *et al.*, 1993 [271]).

While some studies on coarse sediment clearly outline the type of sediment targeted (Hooke (2003) [126]; Reid *et al.*, 2007 [239]; Reid *et al.*, 2007 [240]), most studies on sediment connectivity do not clearly specify the type of sediment that is examined. We thus need to be more specific about the type of sediment considered.

6.2.5 Modelling sediment connectivity

In hydrological connectivity, significant progress have been realised to understand, monitor in the field, and model connectivity at various spatial and temporal scales. The concepts of "volume to breakthrough" and "fill and spill" have been largely investigated as they both include process-based runoff and to some extent, the structure of the landscape. Moreover, these concepts include the notion of exceeds in threshold depending on storage capacity and water inputs from rainfall event. Different methodologies are used to represent both concepts such as functions (Antoine *et al.*, 2009 [5]; Harel and Mouche [120]), indicators (Western *et al.*, 1998 [312]; Darboux *et al.*, 2001 [56]; Appels *et al.*, 2011 [6]), or distributed modelling (Golden *et al.*, 2014 [108]).

While sediment connectivity is primarily dependant on hydrological connectivity, and should benefit from the progress achieved in hydrological connectivity modelling, it seems that such advances have yet not reached the sediment connectivity assessment and major setbacks are being recorded. Indeed, sediment connectivity modelling builds on existing indices that have been developed in the framework of sediment transport assessment. However, most of these indices are either based on the absence of consideration of structural and process-based connectivity within the catchment or focus on the structural elements of the landscape and do not take into account the generation of process-based hydrological and sediment connectivity.

The *Sediment Delivery Ratio* (SDR), for example, was introduced in the 1950s (Glymph, 1954; Maner, 1958; Roehl, 1962 in Walling, 1983 [298]) to link local hillslope erosion to sediment yield at the outlet of catchments. Though it has been highly criticized for its "black box" nature, the index experiences a renewed interest with the expansion of the use of the connectivity concept, due to the very few amount of required data. The SDR gives a first estimation of connectivity at the catchment scale (*e.g.*, Brierley *et al.*, 2006 [26]; Baartman *et al.*, 2013 [9]; Minella *et al.*, 2014 [194]) without considering processes or features involved in the transfer of water and sediment.

To the contrary, the *Index of connectivity* (Borselli *et al.*, 2008 [21]) offers a more distributed approach of water and sediment connectivity with a strong structural connectivity background. Based on the similar topographic parameters as the index proposed by Pelacani *et al.* (2008) [218] (flow accumulation along the slope and length to the river network), it also integrates land characteristics such as a land use management factor. This index has met with great success in the scientific community for its easy handling, the very few data needed for the implementation, and its flexibility to the addition of other parameters (Cavalli *et al.*, 2013 [34]; D'Haen *et al.*, 2013 [72]). In addition, the authors provide an index of connectivity based on field observations and can be used as a complementary approach to the GIS index.

Still, there is some progress done for the consideration of process-based hydrologic connectivity in the sediment connectivity assessment, for example, by taking into account saturated areas *via* a wetness index (*e.g.*, Tetzlaff *et al.*, 2009 [273]; Cavalli *et al.* (2013) [34]). However, these indices are also based on topography and thus cannot reflect processes of involved in overland flow due to soil saturation in lowland areas.

One of the major issues in sediment connectivity modelling is to link the sediment source to the potential sinks. However, with the current available indices, one area is linked to one other by the probability that both features (source and sink) are (or become) connected during a rainfall event. Alternative pathways are thus not evaluated. Therefore, there exist a need to identify all potential sinks or storage zone (depending on time-scale issues) for each source area within a catchment. The recent use of the graph theory in sediment connectivity (Heckmann and Schwanghart, 2013 [122], Heckmann *et al.*, 2014 [123]) seems a promising tool to investigate alternative pathways for sediment connectivity.

The purpose of the present study is not to review all indices of modelling approaches on water and sediment connectivity that exist. However, we want to draw the attention of the scientific community on the lack of consideration of process-based sediment connectivity in the approaches developed which constraints their use to areas where overland flow is governed by the structure of the landscape.

6.3 Process-based and structural connectivity of lowland agricultural areas

In lowland area, process-based hydrological connectivity is the first condition to sediment connectivity whilst in steeper areas, structural connectivity can be the cause of sediment transfer. Indeed, in hilly environments, the slope is often the driver of the generation of hydrological connectivity. But in flat areas, the overland flow is controlled by the excess of water in soils and is associated with process-based connectivity. Different elements or other processes also play a part in the final lowland catchment connectivity. From their work on floodplain areas, Fryirs *et al.* (2007) [94] identified different natural or anthropogenic features that they named "Buffers", "Barriers" and "Blankets", that disrupt connectivity in the three dimension of the landscape.

The spatial distribution of the different elements in the landscape may completely transform the connectivity patterns within a catchment (Gumiere *et al.*, 2011 [117]). There exist a spatial optimization for each features/process to increase or reduce sediment connectivity. This concern also applies to the spatial organisation of the different features among themselves. Indeed, while a hedgerow placed downstream a hillslope may limit the connectivity between different landscape compartments (between two fields or from field to river network), its efficacy in trapping sediment if placed uphill may be close to zero. Moreover, if other features known to increase connectivity (*e.g.*, drain tiles) are placed in that same area, downstream hedgerows will offer no benefit in sediment trapping or water infiltration as the hydrological and sediment connectivity is insured in the subsurface zone. Therefore, it is important not to consider each feature independently but as part of a more complex system.

In this part, we present the different elements that are involved in sediment connectivity of lowland agricultural areas (see Figures 6.4 and 6.5). No clear classification between the structural function or process function of each identified element is given as one element may support both structural and process-based connectivities.

6.3.1 Soil moisture and water table

Soil moisture is one of the drivers of the generation of overland flow. Indeed, moisture content influences the rainfall-runoff response of the landscape. Soil moisture is highly variable in both time and space (Western *et al.*, 2001 [313]; Appels *et al.*, 2011 [6]). The understanding of this spatial and temporal variability may help in the comprehension of the non-linear response observed between rainfall and runoff patterns. In turn, the moisture conditions depend on antecedent condition and on the rainfall amount.

Different concepts (*e.g.*, volume to breakthrough) have helped in the development of functions to capture the hydrological connectivity induced by soil moisture content (Western *et al.*, 2001 [313]; Knudby and Carrera, 2005 [145]; Antoine *et al.*, 2009 [5]; Harel and Mouche, 2014 [120]) and models (Kirkby, 2014 [143]) have been developed to capture the hydrological connections that arise from the saturation of soils.

FIGURE 6.4 – Examples of hillslope (dis)connectivity features with. Artificial furrow created by farmers to evacuate water from the field A) prior to rainfall event and B) during important rainfall event, C) Outlet of burried drain tile, D) Flooded road and connections with ditches, E) Hedgerow network, and F) Development and persistence of a rill network leading to bank cutting

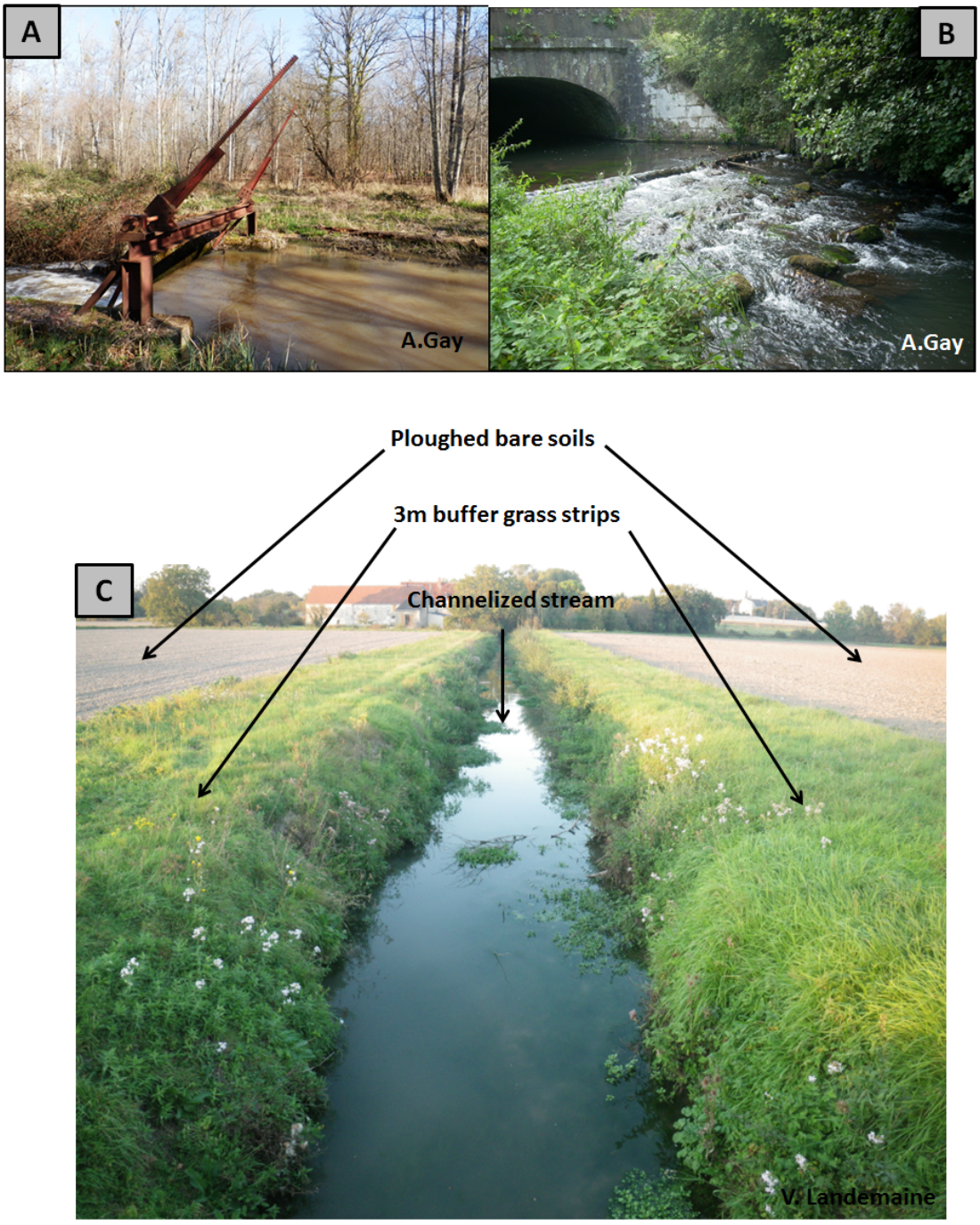

FIGURE 6.5 – Examples of channel (dis)connectivity features with A) Spillway B) Weir, C) and of the succession of (dis)connectivity features

In lowland environments, the shallow ground water table linked to the bedrock properties (*e.g.*, presence of an impervious layer) and shallow subsoil structure deterioration by soil compaction (Appels *et al.*, 2011 [6]) can offer a support to surface flow connectivity by increasing the surface flow connections that arise during a rainfall event.

Moreover, the existence of shallow groundwater flows at some times of the year may help to connect remote areas to the river system (Ocampo *et al.*, 2006 [214]; Tromp-van Meerveld *et al.*, 2006 [279]).

6.3.2 Land management and agricultural connectivity features

In agricultural catchments, anthropogenic land management affect the landscape structural sediment connectivity through water and soil conservation practices (Callow and Smettem, 2009 [29]). The exploitation of lands for agricultural purposes has clearly changed the landscapes and with it the connectivity at the plot to the landscape scale. In general, enhanced connectivity from agricultural practices takes a linear form such as tractor wheel marks (Le Bissonnais *et al.*, 2005 [158]; Boardman *et al.*, 2009 [20]), or furrows from tillage (Takken *et al.*, 2001 [269]). The latter is said to affect flow direction and soil redistribution as much as topographic slope does (Couturier *et al.*, 2013 [49]). Moreover, farmers often create a furrow at the field edge to avoid field water logging (Figure 6.4 A and B). Taken individually, these features may not have a strong impact on the catchment-scale connectivity. However, it is not unusual to find all of these features concentrated in one small area. In such case, the connectivity can be significantly increased at the field to catchment scale.

In this section, we briefly mentioned some of the practices that may enhance or impede connectivity but we do not provide an exhaustive list. The Sections 6.3.3 and 6.3.5 are specifically dedicated to two agricultural practices that we believe are important but are not enough considered in the evaluation of catchment connectivity.

6.3.3 Vegetation: hedgerows and grass strips

Vegetation is certainly the most studied feature in structural connectivity researches and one of the first land management practices recommended to limit water and sediment transfers. Vegetation acts in the three connectivity dimensions of the landscape but also participate in process-based connectivity. On hillslopes, vegetation represents an obstacle to lateral connectivity by the presence at the interface between soil and atmosphere of root-dams (Poeppl *et al.*, 2012 [225]), and by the increase of the vertical connectivity resulting from high water infiltration capacity. In stream vegetation also acts as a barrier to sediment connectivity by trapping fine particles (Rodrigues *et al.*, 2006 [247]). Its role in hydrological connectivity is less clear, but it is assumed that in stream vegetation reduces flow velocity and thus temporizes the hydrological connectivity through time.

The tricky part with the role played by the vegetation in disrupting hydrological and sediment connectivity is the number of parameters that seem to act on sediment trapping regardless of the spatial scale of the study: the type of vegetation (Gumiere *et al.*, 2011 [117]), the percentage of cover (López-Vicente *et al.*, 2013 [173]), the spatial distribution in the landscape (Lesschen *et al.*, 2009 [166]; Sandercock and Hooke, 2011 [253]; Foerster *et al.*, 2014 [88]) and the height (Rey, 2003 [242]).

In agricultural lands, tree hedgerows (Figure 6.4 E) and grass strips (Best Management Practices, Koiter *et al.*, 2013 [146]; Rittenburg *et al.*, 2015 [244]) are becoming common riparian features implemented to reduce lateral connectivity from field to river systems and thus input of nutrients, pesticides and sediment to rivers (Figure 6.5 C). Several studies have highlighted the importance the buffer strips in reducing direct (Blanco-Canqui *et al.*, 2006 [17]) or diffuse (Lee *et al.*, 1998 [162]) sediment connectivity.

Moreover, in their 2006 paper, Follain *et al.* [89] present ambiguous results on the effect of hedgerow on soil redistribution patterns. Indeed, the authors indicate higher soil thickness in uphill position of hedges, that corresponds to soil aggradation due to sediment trapping, and higher soil erosion rates in downslope position of the hedge. In the framework of hydrological and sediment connectivity, the question then arise of whether this downhill effect results from a new connectivity type induced by the presence of the hedge or if it consists of a resumption of lost connectivity.

However, as underlined by Van Oost *et al.* (2000) [285], "the behavior of the water erosion process at a field boundary is complex and characterized by a high spatial and temporal variability". Little quantifications of the reduction of sediment transfer and of hydrological and sediment process-based connectivity in the riparian area exist. There is a real need to investigate the effect of buffer strips on sediment connectivity over long time periods (at the decadal time scale) and at the field to catchment scale, to integrate this features in connectivity modelling approaches.

6.3.4 Roads and urbanisation

Linear elements are generally considered as preferential pathways as flow and sediment concentrate in such features with no (or very few) obstacles. Placed at the field edge to allow for mechanical engines to come, roads receive sediment-laden runoff from adjacent fields. In unsealed lanes of forested catchments (Figure 6.4 D; Thompson *et al.*, 2008 [275]) and sunken lanes (Boardman, 2013 [19]), roads are not only a vector for water and sediment but can also be an important sediment supplier (Reid and Dunne, 1984 [238]; van Meerveld *et al.*, 2014 [284]). The proximity with the drainage network has also a great influence on the flow and sediment catchment response. Thompson *et al.* (2008) [275] identify a critical distance of 40m between roads and drainage network under which, and for a 10-year recurrence interval rainfall event, both features are connected and muddy flows are likely to reach a permanent stream.

From being structural connectivity features, roads move on to being a real actor in process-based sediment connectivity. Wemple *et al.* (1996) [310] propose a conceptual model to investigate the influence of roads on the increase in the volume of water available for transport and the generation of direct (or concentrated) connectivity through the development of a gully network at the road culverts. The creation of these new features increases the drainage density (Croke *et al.* (2005) [51]) of the catchments as temporary gullies become stable. Katz *et al.* (2013) [138] determine a slope-area threshold at the interface between roads and the surrounding valley for the development of gullies.

Metalled roads, without supplying sediment, enhance the hydrological and sediment connectivity from sources to the drainage network. The increase in land artificialisation and thus of impervious areas have clearly modified the hydrologic response of urbanised catchments (Barron *et al.*, 2009 [11]). The failure to infiltration in urban areas directly induces increase in the volumetric runoff and in the transfer of sediment to the catchment outlet. To prevent the direct connection of pollutants contained in water and sediment from metalled roads to river system, pond retentions allow for the delaying of flow and sediment connection to permanent drainage network (Lee *et al.*, 1997 [163]).

6.3.5 Drainage tiles and ditches network

Artificial underground drainage networks (buried pipes) have been massively implemented in the 1970s to allow for the drainage of new lands for agricultural purposes (Figure 6.4 C). At first, the purpose was to increase the field hydrological connectivity in the subsurface zone to evacuate excess of water from overland flow. Nowadays, it is increasingly recognised that drain tiles participate not only in hydrological connectivity but also in sediment connectivity. Evidence of sediment transfer via the subsurface network (*e.g.*, Laubel *et al.*, 1999 [155]; Deasy *et al.*, 2009 [66]) indicate that at least 25 % of the sediment yield at the catchment outlet is transported through drain pipes. Moreover, the fact that direct connection occurs through the drainage network without any obstacles (except in case of sealed pipes) leaves little room for management practices to counteract the transfer of sediment.

Apart from a process-based view point, the hydrological and sediment connectivity at the field to catchment scale may not be clearly modified. Water and sediment that were originally connected at the surface by overland runoff are currently connected by runoff in the subsurface area. However, drain tiles certainly play a major role in the sorting by grain size of sediment connectivity. Only the finest fraction of sediment is likely to pass through the drain pores (Sogon *et al.*, 1999 [262]). This leaching of fine particles from soils is detrimental to soil fertility and thus represents a major issue for the sustainability of agricultural lands. However, subsurface sediment connectivity through the underground drainage network remains a complex process that needs further researches and quantifications.

In association with artificial drainage, the digging of branched networks of ditches at the field borders has modified the drainage density of the catchments (Lenhart *et al.*, 2012 [165]) leading to higher channel connectivity. This temporary channel network allows for water and sediment to pass into the permanent river network through direct connections. Moreover, ditches also play an important part in process-based connectivity through the diverse interactions with the level of the water table (Figure 6.6; Carluer and DeMarsily, 2004 [33]).

Agricultural practices of the 1970s include also channelization works of the streams and ditches. These modifications have resulted in a decrease in channel complexity and in water regime causing disequilibrium in the sediment connectivity balance of fluvial systems (*e.g.*, Landemaine *et al.*, 2015 [151]). The constraints exerted on the

channel bed and banks does not allow for the different steps of the sediment connectivity cycle erosion-deposition (*sediment continuity*, Hooke, 2003 [126]) to happen. Instead, the channelization of streams create a straightforward feature without meandering possibilities and where permanent sediment storage is likely to occur.

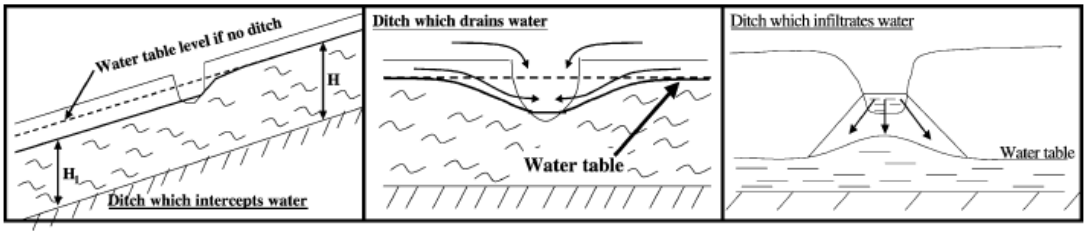

FIGURE 6.6 – Interactions between ditches and the surface and subsurface zones (Carluer and DeMarsily, 2004 [33])

6.3.6 Lakes, dams and knickpoints

Numerous studies have investigated the impact of large dams on sediment disconnectivity. Because of their size, the costs of their maintenance and the benefits from their use for electricity production and water retention purposes, large dams have received much attention in the past decades. One of the most famous dam is certainly the Three Gorges Dam in China (*e.g.*, Luo *et al.*, 2012 [175]; Dai and Liu, 2013 [53]; Gao *et al.*, 2013 [98]). Its recent construction and the size of the project has been a motivation for scientists to follow the morphological evolution of the stream and associated changes in stream connectivity.

Much less attention has been paid to smaller knickpoints such as weirs, mills, and spillways (Figure 6.5 A and B) that have been erected in small agricultural watersheds. Yet, their presence and their use create a strong (dis)connectivity for water and sediment flows (Eekhout *et al.*, 2014 [81]). During low flows, weirs are closed to increase groundwater levels leading to a physical and functional disconnectivity between upstream and downstream parts as flow velocity decreases and sediment is being deposited on the bed (*e.g.*, Landemaine *et al.*, 2015 [151]). To the contrary, during high flows, weirs are opened and the channel water and sediment connectivity is being drastically increased: the deposited sediment upstream from the weir is resuspended and transferred downstream where the sudden increase in flow velocity and supply of sediment causes bed incision.

By breaking connectivity and being a receptacle for sediment, natural and anthropic reservoirs (*e.g.*, Lexartza-Artza and Wainwright, 2011 [168]; Foucher *et al.*, 2015 [90]) are valuable records of sediment. Therefore, they represent interesting features to evaluate variations in sediment supply amount and changes in sediment connectivity associated with land use changes throughout and across the years.

6.4 Conclusion

In this chapter, **we give a quick overview of the different definitions and concepts that have emerged around the term of sediment connectivity. One of the most popular way to approach connectivity is to consider structural elements of the landscape (static connectivity) and flow processes (dynamic connectivity).** Most of the elements involved in both types of connectivity have already been identified and received attention. Challenges still remain to better understand the interactions between both connectivities and associated elements within the three dimensions of the landscape and across time scale. So far, hydrological connectivity has already been largely investigated at the local to broad scales and considerable progresses in quantification and modelling have been achieved. Further researches are needed to better understand the sediment connectivity and include processes and parameters involved in such connectivity in our modelling. **Moreover, attention needs to be paid to the conditions by which connectivity is generated (triggering agent) and the associated thresholds.** Defining the connectivity and the methodologies to measure, quantify and model, is still an on-going process.

Feeling that lowland areas have so far been neglected, while unexpected connectivity in these areas may cause severe damages both on hillslope and in-stream (Foucher *et al.*, 2015 [90]), we have provided a non exhaustive overview of the different connectivity elements that may be found in these areas or are characteristics of such landscapes. Whilst considerable work is required to improve our understanding of the functioning of lowland areas and of these elements within the sediment connectivity framework, such investigations need to be undertaken in conjunction with efforts to improve data quality and monitoring.

Chapitre 7

Modification et application d'un indice de connectivité

Le chapitre 2 de calculs de flux à l'exutoire des bassins versants et le chapitre 6 de synthèse bibliographique sur les aspects de la connectivité ont mis en évidence la nécessité d'utiliser un modèle distribué pour une meilleure prise en compte de l'hétérogénéité spatiale des processus dans la modélisation du transfert de particules.

Dans ce chapitre, nous proposons une application d'un indice topographique récemment publié comme première approche semi-distribuée de la connectivité. Afin de prendre en compte les propriétés infiltrantes/ruissellantes des sols au sein du bassin Loire-Bretagne, et donc des processus de connectivité hydrologique, un indice de développement et persistence des réseaux ($IDPR$) est inclu dans le modèle. Une approche qualitative est mise en place afin de mettre en exergue les zones à forte ou faible connectivité à l'échelle des masses d'eau.

Les résultats obtenus indiquent que l'introduction de l'$IDPR$ dans les zones de plaine ou collineuses (pentes $< 7\%$) permet de prendre en compte les processus de ruissellement liés aux caractéristiques topographiques et/ou lithologiques des différentes zones du bassin. Ainsi, la connectivité est augmentée dans les zones où le ruissellement par saturation est prépondérant et où le soutien à la connectivité est assuré par la présence d'une couche argileuse ou d'un aquifère peu profond. D'autre part, la connectivité est diminuée dans certaines zones montagneuses fortement fracturées ou dans les zones karstifiées. L'utilisation de cet indice modifié présente de nombreux avantages de par le peu de données d'entrée nécessaires et une implémentation facile du modèle.

Les résultats de ce chapitre font l'objet d'une publication dans la revue Journal of Soils and Sediments (Gay A., Cerdan O., Mardhel V., Desmet M., Accepted minor corrections. Application of an index of connectivity in a lowland area).

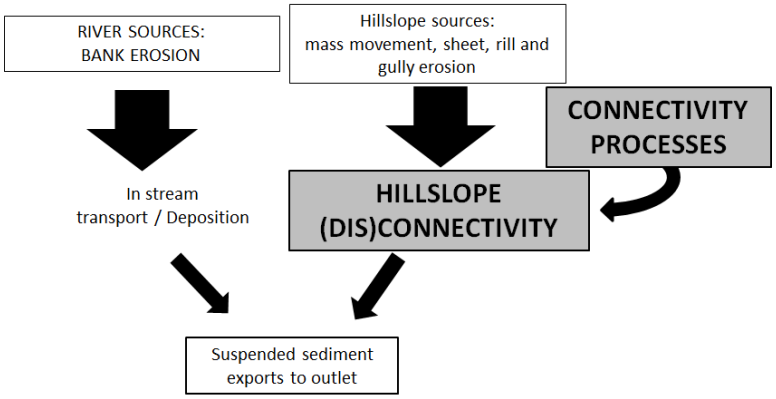

Application of an index of connectivity in a lowland area

Sommaire

Abstract

Purpose Sediment connectivity at the landscape scale has gained interest in the last decades. Distributed approaches, such as topographic indices, are widely used to evaluate this connectivity. However, most of the research efforts are concentrated in mountainous areas while little work has been done in lowland areas where evidence of high connectivity have been reported. The objectives of this study are i) to integrate landscape infiltration/runoff properties in the assessment of connectivity to account for lowland processes, and ii) to apply this approach to a large territory showing both mountainous and lowland areas.

Material and Methods The topographic index of connectivity (IC) of Borselli *et al.* (2008) [21] is computed on the Loire and Brittany river basin ($\geq 10^5$ km^2). A distributed parameter ($IDPR$) that reflects landscape infiltration and saturation properties due to underlying geological formations characteristics is introduced. We integrated this parameter in a revised index ($IC_{revised}$) as an indicator of landscape hydrologic connectivity. Results at the pixel-scale are aggregated at the watershed scale.

Results and Discussion Two maps of connectivity are produced, considering the initial IC and the revised form. As expected, the IC gives the highest connectivity in the steepest areas and does not reflect the existing connectivity in lowland areas. On the contrary, the $IC_{revised}$ computed in this study profoundly modifies the sediment connectivity values. These changes are evenly distributed over the entire territory and affected 51.5% of the watersheds. As a result, we obtained a better correlation between

calculated connectivity and the observed drainage density (which reflects the actual connections between hillslopes and rivers), in areas where slopes are gentle ($< 7\%$).

Conclusion and perspectives Topographic indices do not reflect the real sediment connectivity in lowland areas. But their adaptation by considering runoff processes of such areas is possible. The $IC_{revised}$ presents interesting perspectives to define other highly connected areas at the country scale as 17% of the French territory is characterised by very gentle slopes with high runoff capacity.

Keywords $IDPR$; Connectivity ; Lowland areas ; Loire river

7.1 Introduction

Sediment and flow connectivity, i.e. "the internal linkages between runoff and sediment generation in upper parts of catchments and the receiving waters" (Croke *et al.*, 2005 [51]), is a key attribute in the study of sediment redistribution within the landscape. Because on-site and off-site effects of such redistribution are detrimental to environmental systems and populations, the comprehension and assessment of the spatial variability of soil erosion and sediment delivery processes is a long standing effort and is still today a central topic of researches (Haregeweyn *et al.*, 2013 [119]; Bisantino *et al.*, 2015 [15]). The recent emergence of the connectivity framework and associated tools has provided a new framework for the study of landscapes and soil redistribution processes (Bracken *et al.*, 2013 [25] and 2015 [24]) and for the implementation of effective sediment trapping measures (Mekonnen *et al.*, 2014 [183]). As a consequence, considerable progress in quantifying connectivity at various spatial scale has been achieved and different methodologies have been developed. For example, at the plot to hillslope scale, functions (Western *et al.*, 2001 [313]) and indicators (Darboux *et al.*, 2001 [56]; Antoine *et al.*, 2009 [5]) have been developed to assess connectivity. At the hillslope to the catchment scale, the sediment connectivity can be inferred using conceptual frameworks such as: the Sediment Delivery Ratio (SDR, Walling, 1983 [298]) is the ratio between gross and net erosion and has been used to provide a first evaluation of the catchment connectivity (Brierley *et al.*, 2006 [26]; Baartman *et al.*, 2013 [9]). Sediment budgets (Bracken and Croke, 2007 [23]; Walling and Collins 2008 [303]) and indicators, e.g. the drainage density (Delmas *et al.*, 2009 [71]), the wetness index (Ali *et al.*, 2013 [4]), can also be used to provide finer insight into the catchment connectivity. However, to evaluate the sediment contribution from the different areas of the catchment, more distributed approaches are needed, e.g. the graph theory (Heckmann and Schwanghart, 2013 [122]), and topographic indices (*e.g.* Lane *et al.*, 2009 [153]). The latter have been widely used (*e.g.* Reid *et al.*, 2007 [240]; Lane *et al.*, 2009 [153]) as they require very few data allowing to evaluate connectivity where field campaigns are not easy to realize as in remote areas or for large territories.

Recently, Borselli *et al.* (2008) [21] have developed a GIS-based index relying on topography derived from a Digital Terrain Model, and on Land Use. The index provides information on the potential connections between source areas and local sinks.

Generally, this index has met with great success in the scientific community for its easy handling, the very few data needed for the implementation, and its complementarity with field observations. The index has been successfully applied to medium-size catchments ($\leq 10^2$ km^2) in Italy by the same authors, and has been used by other authors for similar-size catchments and for different purposes: to assess the influence of landuse change on connectivity in Spain (López-Vicente *et al.*, 2013 [172]; Foerster *et al.*, 2014 [88]), to track contaminated sediment dispersion in Japan (Chartin *et al.*, 2013 [38]), or to identify hot spots of primary sediment sources to permanent sinks in an Australian semi-arid areas (Vigiak *et al.*, 2012 [293]), and in the Mediterranean basin (*e.g.*, Sougnez *et al.*, 2011 [264]).

Nevertheless, Borselli *et al.* (2008) [21] stressed that soil surface characteristics that influence runoff processes within a watershed or a hillslope should be also considered. To this purpose, adjustments have been proposed by Cavalli *et al.* (2013) [34] in order to account for i) soil surface characteristics, by introducing a roughness index as weighing factor, and ii) for mountainous transfer properties such as debris flows and channelized sediment transfers. Such modifications allowed to consider different types of sediment transport processes that may be hydrologically controlled or not (Bracken *et al.*, 2015 [24]). This new version of the index and has been applied in Italy by the same authors, in Turkey (D'haen *et al.*, 2013 [72]) and in Switzerland (Meßenzehl *et al.*, 2014 [185]).

By definition, topographic indices are based on the concept that the routing of the sediment is driven by the slope steepness and direction. In Borselli's index of connectivity, the probability that sediment arriving in point A will reach point B via overland flow processes is based on upstream and downstream characteristics of point A. The index combines both perspectives in a fraction in which the slope parameter plays a role in each of the upstream and downstream characteristics. In contrasted catchments, the application of such index will reveal high connectivity in the hilly areas whereas in the valleys, the connectivity will be low. However, in flat areas (e.g. large floodplains, lowland catchments), the use of an index exclusively based on topography may not reveal hot spots of connectivity because other factors than topography control the (dis)connectivity between the different points (Fryirs *et al.*, 2007 [94]; Ali *et al.*, 2013 [4]).

Yet, most of the studies dealing with connectivity have been achieved in catchments where sediment is transported rapidly during a rainfall event, where the runoff is hortonian-type (Horton, 1945 [130]), and where human intervention on landscape is negligible (e.g. mountainous areas, semi-arid areas). This concentration of research efforts on connectivity in these particular areas has already been highlighted by Bracken *et al.* (2013) [25] and the main reason for this interest in these catchments is their high sediment yield. In contrast, in lowland areas where sediment yields are often lower (Gay *et al.*, 2014 [104]), where intensive agriculture is predominant and runoff can be generated by soil saturation, little work has been done to incorporate these characteristics in the sediment connectivity assessment. Still, the clogging of numerous French lowland rivers and lakes (*e.g.*, Foucher *et al.*, 2015 [90]; Landemaine *et al.*, 2015 [151]) points out that connectivity between sediment sources and rivers is a key

component in soil redistribution.

In this context, the objective of the present paper is to provide an evaluation of sediment connectivity for a lowland territory. The assessment of the hillslope sediment connectivity is achieved through the use of a sediment connectivity index, based on the one proposed by Borselli *et al.* (2008) [21], with processes and scale constraints: i) landscape infiltration and saturation properties of lowland areas are integrated in the index, and ii) the assessment is done over a large river basin ($\sim 10^5$ km^2) showing both mountainous and lowland areas.

7.2 Material and Methods

7.2.1 Study area

The French metropolitan territory is divided into six river basin districts, and for each district, a river basin agency is in charge of the water resources. The Loire Brittany river basin (named *LBRB* hereafter) is one of the districts and represents 28% of the territory ($\sim$ 155,000 km ^{2}). From an hydrological and administrative viewpoint, the basin is divided into 2122 small watersheds. Their areas vary from 0.3 km^2 for a lake and its close surroundings to 1492.9 km^2 for the Conie river and its tributaries (Beauce region). This division is generally used for decision making. Therefore, the results are presented at this spatial scale (Degan *et al.*, *in prep.* [67]).

Figure 7.1 displays the slopes and landuse characteristics and geological regions of the study area. From a geological viewpoint, the centre of the *LBRB* lies on the sedimentary formations of the Parisian basin and the Aquitaine basin. This area is primarily dominated by croplands, dedicated to intensive farming, on gentle slopes (maximum = 66.2%, mean = 3.1%). The eastern and western parts of the study area lie on old granitic formations. To the east, the Massif Central includes a mountainous area with steep slopes (maximum = 134.7%, mean = 10.5%) dominated by pastures and forests, the highest point of the study site (1849 m), and a gentler area with croplands, the Limagne basin. In contrast, the Armorican basin in the western part of the *LBRB* is a rolling landscape (maximum altitude = 385 m) and displays gentler slopes (maximum = 86.9%, mean = 4.5%) and is dominated by croplands and pastures.

7.2.2 Index of hillslope sediment connectivity

7.2.2.1 Database and pretreatments

In order to compute the Index of Connectivity of Borselli *et al.* (2008) [21], we used three types of data:

The surface water network is provided by the BDCarthage 2013 ® (available at http://services.sandre.eaufrance.fr/telechargement/geo/BDCarthage/FXX/). This database is a GIS vector layer which provides information on all surface waters within

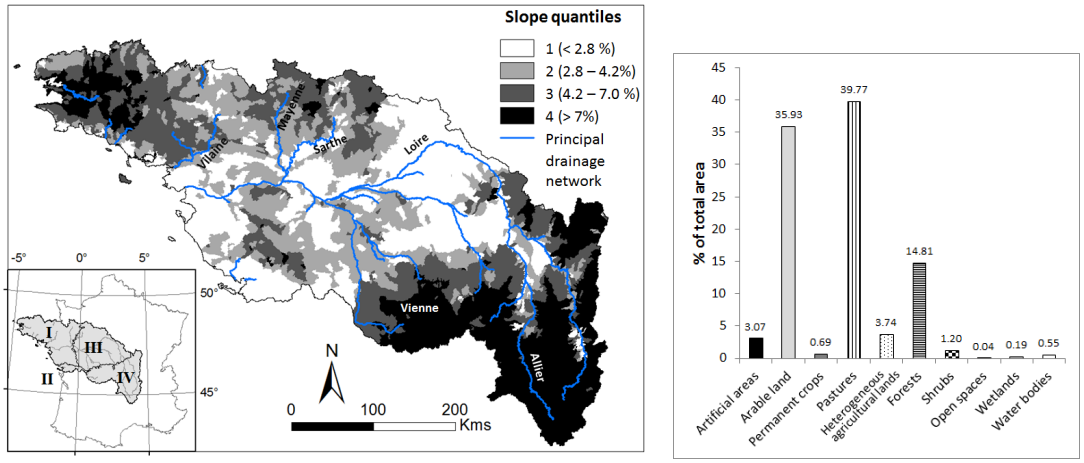

(a) (b)

FIGURE 7.1 – Characteristics of the Loire and Brittany river basin. a) Mean slopes values per watershed and location of the study area. Roman numerals indicate the four geological regions: I Armorican basin, II Aquitaine basin, III Parisan basin, and IV Massif Central. b) Land use statistics from the combination of the CLC2006 and the RPG 2010 (Degan et al. *in prep.* [67]), see text

the French territory. It covers both the entire river network and lakes/ponds and these two data were transformed into rasters (cells of 50 ∗ 50m).

The topographic data *i.e.* the slope, the contributing area and the length to the river network, are calculated using the digital elevation model at a 50m resolution from the BD Alti ® IGN. This DEM is derived from the digitalisation of contour lines taken from maps at 1:25,000 1:50,000 and aerial photographs at 1:20,000, 1:30,000 and 1:60,000. In order to ensure the continuity of flow through the landscape, the depressions are filled using the Spatial Analyst algorithm. Moreover, as in some flat areas, the real and theoritical drainage networks do not strictly coincide, we force the flow direction of the DEM using the raster of the real drainage network and then calculate the values of the contributing area and the length to the river network from this forced-DEM.

The landuse type is determined using the map from Degan *et al.* (*in prep.*) [67] who combined information from the Référentiel Parcellaire Graphique 2010 (RPG2010 available at https://www.data.gouv.fr/fr/datasets/registre-parcellairegraphique-2010-contours-des-ilots-culturaux-et-leur-groupe-de-culturesmajorita/) and Corine Land Cover 2006. The RPG2010 is a GIS vector layer computed from farmers declaration on the location of their farms and the type of crops. The precision is of 1:5,000. The layer is rasterized (cells of 50 ∗ 50m) and superimposed with the Corine Land Cover raster in order to complete missing data (*e.g.* urban areas, forests, etc.).

7.2.2.2 Computation of the index of connectivity

Our approach of hillslope connectivity mapping is based on the index of connectivity developed by Borselli *et al.* (2008) [21]. The IC is pixel-based and represents the probability that sediment within an area will reach a defined target (sinks). The target is defined by the users and can either be the outlet of a catchment or water systems. In this paper, we only consider the sediment connectivity from hillslopes to river channels/lakes. A mask is thus applied on rivers and lakes. The index is computed on ArcGIS10 using the Spatial Analyst extension. The index takes the form (Equation 7.1):

$$IC = log10\left(\frac{D_{up}}{D_{dn}}\right) \tag{7.1}$$

with D_{up} the upslope component and D_{dn} the downslope component. The Index of Connectivity IC is a dimensionless measure within the $[-\infty; +\infty]$ range.

The upslope component represents the potential for downward routing of the sediment produced in the upslope contributing area of each cell, and is calculated as follows (Equation 7.2):

$$D_{up} = \overline{W}.\overline{S}.\sqrt{A} \tag{7.2}$$

where $\overline{W}$ is an average weighing factor of the upslope contributing area (dimensionless), $\overline{S}$ is the average slope gradient of the upslope contributing area ($m.m^{-1}$) and A is the upslope contributing area (m^2). The downslope component D_{dn} represents the weighted flow path length of the transported sediment to the nearest sink targeted by the users (water systems in our case) and is calculated as in Equation 7.3.

$$D_{dn} = \sum_i \frac{d_i}{W_i S_i} \tag{7.3}$$

where d_i is the length of the ith cell along the downslope path (in m), W_i is the weight of the ith cell (dimensionless), and S_i is the slope gradient of the ith cell.

The weighing factor W is introduced in the index by Borselli *et al.*, 2008 [21] to account for the local condition of the landscape. The authors set its value according to the C-factor of USLE/RUSLE models (Wischmeier and Smith, 1978 [318]; Renard *et al.*, 1997 [241]) that is the crop/vegetation and management factor used to determine the relative effectiveness of crop management systems in terms of soil loss. We use the same values as the ones proposed by these authors for the different landuse types.

7.2.3 Adaptation of the index of connectivity for lowland area

At the watershed scale, the hydrologic connectivity can be inferred from the drainage density (Delmas *et al.*, 2009 [71]). This parameter is calculated as the ratio between the length of the hydrographic network to the watershed area and is expressed in $km.km^{-2}$. In this study, we introduce a pixel-based parameter ($IDPR$) related to the drainage density and which accounts for hydrological connectivity. This parameter

characterises the landscape in terms of soil infiltration/runoff. In this section, we describe the computation of the $IDPR$, the rescaling of the values and the integration of the parameter in the original index of connectivity as a weighing factor.

7.2.3.1 Hillslope hydrologic connectivity parameter

The index of development and persistence of the drainage network ($IDPR$, *Indice de Développement et Persistance des Réseaux*) was developed by Mardhel *et al.* in 2004 [179] and has been recently modified. This index supports the assumption that the organisation of the drainage network is dependent on the underlying geological formations. In a homogeneous environment, only the slope and relief forms guide the development of the hydrographic network while in natural landscapes, the geological formations play an important role in the development of this hydrographic network. Indeed, lands overlying permeable material display a sparse hydrographic network (and thus a low drainage density) as water infiltrates, while in lands overlying impermeable rocks, the hydrographic network is important and the drainage density is high.

The $IDPR$ allows to compare the theoretical river network established due to morphological parameters only (homogeneous environment) and the real river network that has developed under heterogeneous geological conditions. This distributed index characterises each landscape unit (raster cell in this study) in terms of its distance to the theoretical river network and to the real river network along the flow path. The distance to the theoretical river network is calculated using the raw-DEM and the network of talweg is extracted automatically thanks to an algorythm (Mardhel and Gravier, 2006 [180]). The distance to the real river network is calculated using the river network from the BDCarthage and the DEM. In order to ensure the continuity of the flow through the landscape, the depressions of the DEM are filled.

Finally, the $IDPR$ is calculated according to equation 7.4.

$$IDPR = \frac{\begin{array}{l}\text{The least cumulative cost distance for each cell to}\\ \text{the nearest theoretical water course over the slope}\\ \text{surface}\end{array}}{\begin{array}{l}\text{The least cumulative cost distance for each cell to}\\ \text{the nearest cell real water course over the slope}\\ \text{surface}\end{array}} * 1000 \tag{7.4}$$

The $IDPR$ values range from 0 to $+\infty$. Values under 1000 suggest that waters running off the slopes reach a theoritical network before they reach the real hydrographic network. This result thus indicates that the underlying rock formations are permeable and that infiltration is the dominant process. On the contrary, values above 1000 indicate a denser real river network than the theoretical one. This implies that runoff is the dominant process. A value of 1000 represents a strict balance between infiltration and runoff as there exist a compliance between the disponibility of the real and theoretical hydrographic networks. In order to simplify this index, the values are

arbitrarily limited to 2000. Lands with $IDPR$ values above 2000 are assimilated to wetlands.

In mountainous areas, the drainage density and the $IDPR$-values are very high. In these regions, runoff is important and is mostly governed by the steep slopes. Therefore, the $IDPR$ parameter is redundant with the slope information already contained in the IC. Thus, we chose not to take this parameter into account in these areas. For pixels with a steeper slope than 7% (Delmas, 2011 [68]), the $IDPR$ was not taken into account into the calculation of the Index of Connectivity.

The use of the $IDPR$ as an indicator of hydrologic connectivity presents several advantages. First, it is a distributed parameter, that can be integrated directly into the IC as its resolution corresponds to the same cell-size as the two other input data (DEM and landuse map). Secondly, it allows for the substitution of numerous data on geological and soil/subsoil properties while taking these parameters into account in the evaluation of connectivity. Thirdly, it is not only topography-based and can reflect flat areas prone to rapid soil saturation. Finally, the $IDPR$ has proven to be a good indicator of hydrologic connectivity at the catchment scale in the Loire Brittany river basin and in France (Dupas *et al.*, 2014 [78]).

7.2.3.2 Reclassification values of the $IDPR$

In the same way as the $\overline{W}$ factor displays values between 0 and 1, the hydrologic connectivity factor, the $IDPR$, should display the same range of values. Therefore, the initial $IDPR$ values are rescaled to the range [0,1] with values of 1 representing full connectivity due to high runoff, and 0 as low connectivity du to high infiltration properties. In order to avoid zeros and infinite values in Equation 7.6, we set a threshold of 0.1 to null $IDPR$ values. The frequency of occurrence of the $IDPR$-values takes a trimodal distribution form with peaks at the extreme values 0 and 2000 and a third peak centred on the 1000 value. Two types of rescaling are investigated.

First, we rescaled the $IDPR$ values according to the 1:1 line into $IDPR_{linear}$ (Equation 7.5, Figure 7.2). Second, in order to stretch the extreme values of the $IDPR$ and thus highlight areas characterized by high infiltration or saturation properties, we rescaled the values according to a sigmoid curve into $IDPR_{sigmoid}$ (Equation 7.5, and Figure 7.2).

$$\begin{cases} IDPR_{linear} = \frac{IDPR}{2000} \\ IDPR_{sigmoid} = \frac{1}{1+e^{-a(IDPR-c)}} \end{cases} \tag{7.5}$$

where a is a lumped parameter, which we arbitrarily set to 0.035. Assuming that the 1000 value of the $IDPR$ (corresponding to infiltration/runoff of same importance) represents the mean connectivity, we assigned a hydrologic connectivity value of 0.5 to it in both cases.

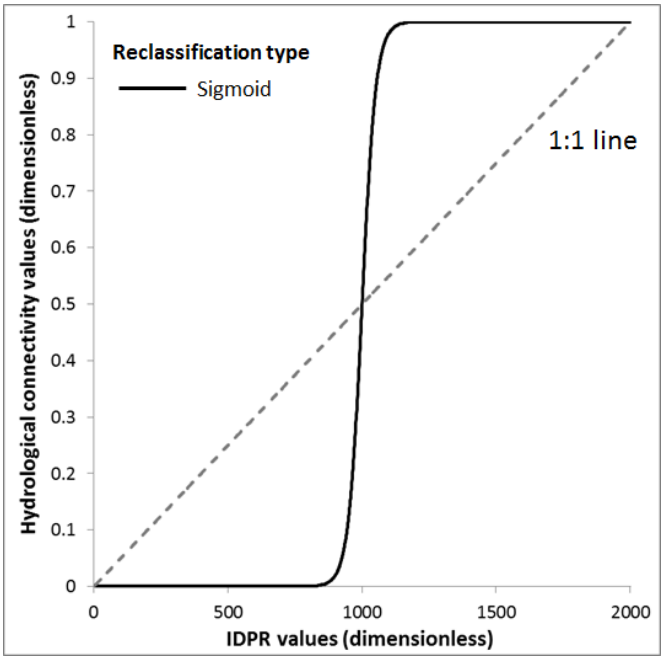

FIGURE 7.2 – Hydrologic connectivity values from the reclassification of the $IDPR$ according to a sigmoid function and to the 1:1 line

Finally, we included the resampled values of the $IDPR$ in a $IC_{revised}$ as in Equation 7.6.

$$IC_{revised} = log10\left(\frac{\overline{W}.\overline{IDPR}.\overline{S}.\sqrt{A}}{\sum_i \frac{d_i}{W_i.IDPR_i.S_i}}\right) \tag{7.6}$$

where $\overline{IDPR}$ is the average weighing factor of the upslope contributing area and $IDPR_i$ is the weight of the ith cell.

7.3 Results and discussion

Generally, the IC and $IC_{revised}$ are adimensional estimations of the basin connectivity. The values obtained via the computation of both indices are provided for infor-

mation purpose only. Both indices were applied on the entire Loire and Brittany river basin, considering the permanent channel network and lakes as targets for sediment. The results are presented both at the pixel-scale and at the watershed-scale.

7.3.1 Modelling results from Borselli's index

The pixel values of connectivity range from -12.61 to 1.31 (mean = -6.04, std = 1.92) and the mean connectivity values per watershed range from -10.02 to -3.87. Figure 7.3(a) displays the map of mean connectivity values for each watershed, for which the values are ranked in four classes according to quartiles boundaries, and a zoom on a certain region at the pixel scale is proposed. At both scales, important regional differences exist. Indeed, the highest mean connectivity values are observed in the eastern and western parts of the territory and the lowest values in the centre. The limits between these three areas correspond to those of the geological formations (see Figure 7.1(a)) and of the slopes. Figure 7.3(b) presents the relationship between the mean connectivity values and the mean slope values. A weak but significant correlation ($p - value < 0.0001$) is found between both variables. This relation takes a logarithmic form. As expected, the steepest the slopes are, the higher the connectivity is. In contrast, no correlation is found between the mean connectivity values of the watersheds and their drainage density (Figure 7.3(c)).

As expected at the pixel scale, on the entire $LBRB$, the highest values of connectivity are found close to the river network while the lowest values are found in more distant regions. Finer variations in connectivity patterns can also be observed. Indeed, the area north of the Loire river and corresponding to the Beauce region appears more connected than the area south of the river which corresponds to the Sologne region. These two regions display similar mean slope values ($< 2\%$) and the driving factor for connectivity differences between both areas is the landuse type (W factor) as the Beauce region is primarily agricultural while the Sologne region is dominated by forests.

From these results, two conclusions may be drawn. Firstly, to our knowledge, it is the first time that the IC is computed on such a large territory. Indeed, in other studies, the order of magnitude of catchment size do not exceed 10^3km^2 and the DEM resolution is fine (from 2.5m to 20m grid). In our case, the computation is done with a lower resolution DEM (50m grid) over more than 10^5 km^2. Despite those two constraints, the IC is applicable and allows to discriminate some areas that are supposed to be more connected than others.

Secondly, as expected, steeper areas appear more connected than those of lowland. However, some regions such as the Sologne are primarily composed of wetlands with an important network of ditches. In these places, hillslopes are therefore highly connected to the main channel system. However, their connectivity values from the IC are the among lowest ones of the $LBRB$. Similarly, pond and river clogging are evidence of the high connectivity in upstream areas and deposition in downstream parts.

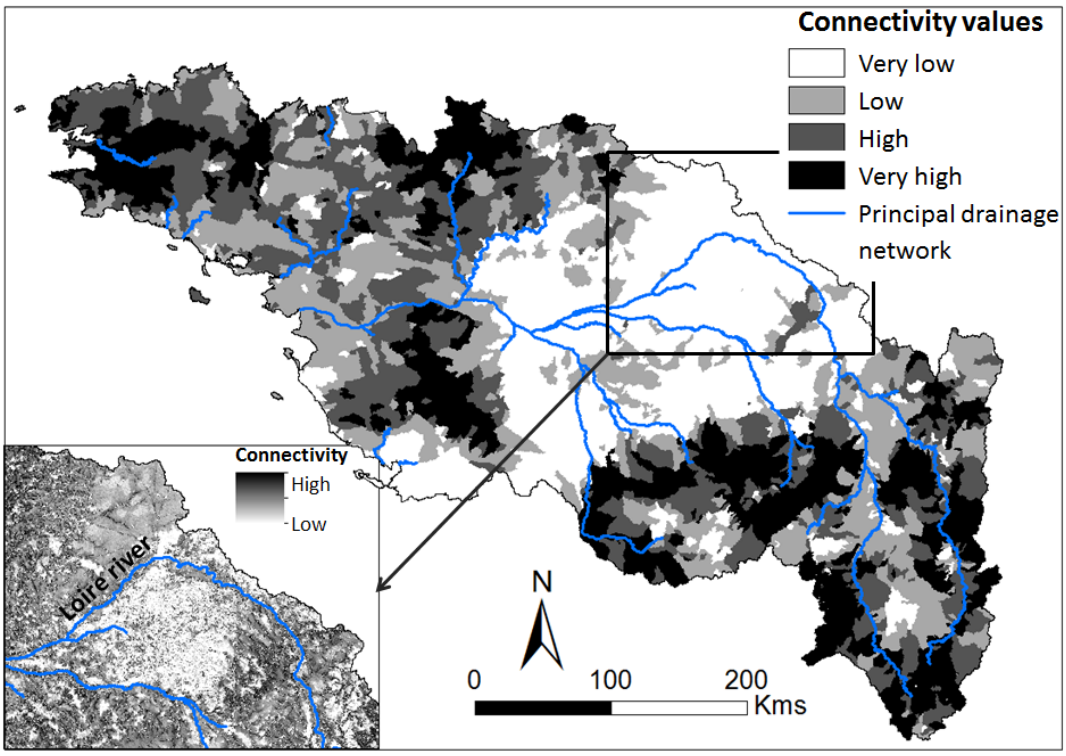

(a)

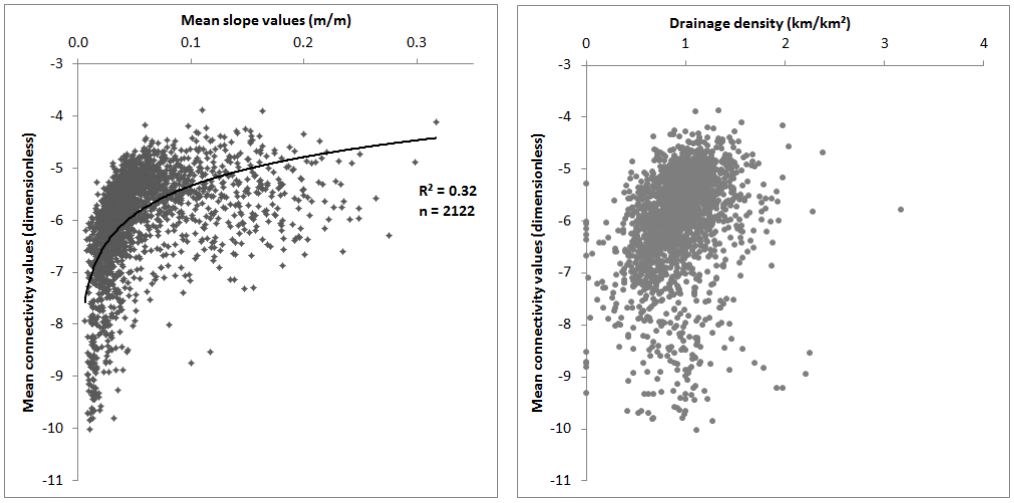

(b) (c)

FIGURE 7.3 – Sediment connectivity from hillslope to water system according to the *IC* (Borselli *et al.*, 2008 [21]). a) Map of the mean connectivity for each watershed, the values are ranked according to quartiles classes, and zoom at the pixel size on the Beauce and Sologne regions (see text) b) Relationship between the mean connectivity and the mean slope per watershed, and c) Relationship between the mean connectivity and the drainage density per watershed

Several problem of such clogging have been reported by the River Basin Agency (Bourrain, *personal communication*, 2014) in areas where the connectivity is given by the IC as low. Of course, these results do not call into question the efficiency of the IC, which can be used directly as a first approach for connectivity assessment, but clearly highlights the lack of consideration of lowland processes in sediment transfers.

7.3.2 Connectivity from the revised index and comparison with initial index

A distributed parameter, the $IDPR$, accounting for landscape infiltration and saturation properties is introduced as one of the weighing factors in the IC (see Section 7.2). Two rescaling of this parameter are proposed taking a linear ($IDPR_{linear}$) and a sigmoid form ($IDPR_{sigmoid}$). We first present the results obtained at the pixel and watershed scale in the $IC_{revised}$ when introducing the $IDPR_{sigmoid}$. We then discuss these results and differences obtained with $IC_{revised}$ when introducing the $IDPR_{linear}$.

7.3.2.1 Connectivity at the pixel scale

At the pixel-scale, the connectivity values from the $IC_{revised}$ range from -42.89 to 1.31, with a mean value of -13.58 (std = 10.07) representing a decrease by -7.54 of the mean value. As expected, for most cells, the connectivity has decreased due to the introduction of the $IDPR$ values in the range of]0,1]. For a very few cells (0.21%), the connectivity has increased.

Figure 7.4 presents the frequency of connectivity values using a step of 0.5. While the IC curve displays a single and high peak around the -6.0 value, the $IC_{revised}$ curves display two peaks. For the $IC_{revised}$ with $IDPR_{sigmoid}$, the first peak is high and around -6.0, while the second is smoother and around -23.0. Similarly, for the $IC_{revised}$ with $IDPR_{linear}$ values according to the 1:1 line, the first peak is around -6.5 and the second around -10.5. In all three cases, the peak around -6.0 and -6.5 corresponds to cells close to the channel network (within a distance of $\sim$ 500m around the river), while in the case of a second peak, it corresponds to areas further away from rivers or to very small subcatchments directly (dis)connected to the river system. Therefore, the introduction of the $IDPR_{sigmoid}$ strongly modifies the distribution of the connectivity values. Moreover, when looking at the zoom on Figure 7.5, we note that the trend in connectivity has reversed: the cells in the Beauce region with high infiltration properties, due to underlying karstified limestones, are less connected than the ones in the Southern region, the Sologne where the drainage density is high as soils are easily saturated due to an impermeable layer of clay. Therefore, for the same slope values, while the dominant factor for connectivity in the IC is the landcover in this area, the $IDPR_{sigmoid}$ takes over this factor in the $IC_revised$.

Table 7.1 presents some connectivity values (minimum, maximum, mean, and standard deviation) mapped with the IC, the $IC_{revised}$, and from the difference between both, for different landuse types (arable land, pastures, and forests) and slope classes.

The three landuse types presented correspond together to 90% of the area of the entire territory. The most representative combination is the arable lands on slopes <2% which corresponds to 15.66% of the $LBRB$ followed by pastures on slope from 2 to 5% (12.36% of the territory).

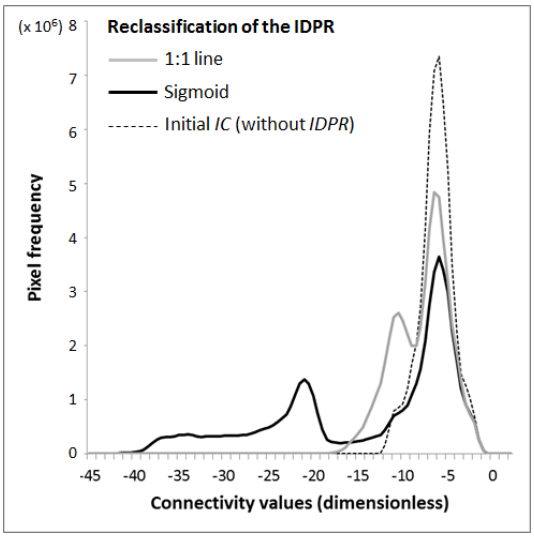

FIGURE 7.4 – Comparison of the frequency of connectivity values at the pixel scale from the initial IC and the $IC_{revised}$ using a sigmoidal rescaling of the $IDPR$ values or a linear rescaling (1:1 line)

When looking at IC and $IC_{revised}$ values, we note that independently from the landuse type, the connectivity increases as the slope increases in both cases. This result highlights the importance of the slope factor in the calculation of the indices. However, if the std values for the IC remain stable independently from the landuse type and the slope steepness (comprised between 1.17 and 1.43), the range of std values for $IC_{revised}$ is wider (between 6.05 and 11.55). In general, the variations decrease as the slope increases. This is primarily due to the fact the $IDPR$ is not taken into account in cells with slopes >7%. These results confirm that in flat areas, for similar slopes and landuse types, the introduction of the $IDPR_{sigmoid}$ leads to strong differences in connectivity values according to soil properties.

More specifically, great differences between the connectivity from both indices exist as the values obtained with the $IC_{revised}$ may be up to 3 times smaller than the ones obtained with the initial IC. This highest variability between both values is observed for arable lands on very gentle slope (<2%) with a mean difference of -12.54 (std =10.96).

Tableau 7.1: Connectivity values per landuse type and slope classes according to the initial IC and the $IC_{revised}$ with the $IDPR_{sigmoid}$ and the differences between both

	Slope classes											
	< 2%			**2 to 5 %**			**5 to 7 %**			**> 7%**		
	IC	$IC_{revised}$	Difference	IC	$IC_{revised}$	Difference	IC	$IC_{revised}$	Difference	IC	$IC_{revised}$	Difference
Arable lands (%)		**15.66**			**11.60**			**3.40**			**4.06**	
min	-10.85	-41.04	-30.70	-10.28	-39.77	-30.40	-9.75	-39.77	-30.40	-9.32	-25.05	-19.13
max	-0.88	-1.58	3.55	-0.91	-1.00	4.22	-0.89	-1.01	4.51	-0.02	-0.02	3.66
mean	-6.77	-19.31	-12.54	-5.84	-15.03	-9.19	-5.23	-12.12	-6.89	-4.75	-8.96	-4.20
std	1.21	11.55	10.96	1.17	10.25	9.63	1.17	8.97	8.39	1.28	6.88	6.17
Pasture (%)		**10.74**			**12.36**			**5.36**			**11.52**	
min	-10.55	-40.48	-31.09	-10.18	-39.54	-30.40	-9.6	-39.19	-30.40	-9.57	-24.9	-17.62
max	-0.93	-1.20	4.12	0.04	-0.04	4.09	-0.05	-0.56	3.95	0.23	0.18	4.95
mean	-5.00	-14.05	-8.05	-5.25	-12.03	-6.78	-4.77	-10.50	-5.73	-4.29	-7.65	-3.36
std	1.32	9.85	9.41	1.26	8.94	8.43	1.27	8.24	7.71	1.40	6.45	5.72
Forests (%)		**4.61**			**3.05**			**1.20**			**5.95**	
min	-12.61	-42.89	-30.99	-12.00	-42.22	-30.40	-11.48	-41.20	-30.40	-11.16	-27.68	-19.50
max	-3.23	-3.36	3.50	-2.94	-3.13	2.66	-2.66	-2.76	2.91	-1.88	-1.90	3.11
mean	-10.08	-19.38	-9.29	-9.10	-17.52	-8.42	-8.41	-15.32	-6.91	-7.31	-10.18	-2.86
std	1.26	10.13	9.79	1.30	9.60	9.14	1.33	8.90	8.41	1.43	6.05	5.41

The lowest variability is observed for forests on steep slopes (> 7%) where connectivity values from $IC_{revised}$ are 0.4 times smaller than the ones obtained with the IC. The lowest connectivity values are observed for forests on slopes <2% with a minimum of -12.61 with the IC and -42.89 with the $IC_{revised}$. The highest mean connectivity value (-1.31) per landuse type obtained with both indices correspond to inland marshes (not shown in the Table).

In general, the introduction of the $IDPR$ has induced more variation and differences in connectivity values in flat areas than in steep ones, and especially in agricultural lands (arable lands and pastures) than in forested areas. However, other processes than soil saturation may induce variations in sediment and flow connectivity but are not reflected by the $IDPR$ or within the IC. First, soil crusting can induce high runoff and can thus increase the connectivity of the soil surface (Le Bissonnais *et al.*, 2005 [158], Kirkby, 2014 [143]). Second, land management practices such as the implementation of drainage tiles networks in agricultural lands in the 1970s has provided arable land with subsurface pathways for water and sediment. Several studies indicate that the contribution of drain tiles to the sediment budget can be up to 15% in a German catchment (Kiesel *et al.*, 2009 [142]) and 55% in a British catchment (Russell *et al.*, 2001 [250]). However, the contribution of such features to sediment connectivity remains unclear, and their inclusion in models is a difficult task that needs great attention (Kiesel *et al.*, 2010 [140]). In the low connectivity belt at the centre of the $LBRB$, arable lands are the dominant landuse type (up to 90% of the surface area) and the percentage of those lands implemented with drained tiles can reach 85.5% (statistics from the French Ministry for Agriculture, available online at http://agreste.agriculture.gouv.fr/enquetes/recensements-agricoles/recensement-agricole-2010/resultats-donnees-chiffrees/). This area is also prone to soil crusting (Le Bissonnais *et al.*, 2005 [159]). Therefore, the connectivity in this area might be much more important than exposed by the $IC_{revised}$ and researches are needed to take the described processes into account in the connectivity assessment. Furthermore, land use type (Novara *et al.*, 2011 [213]; Gao *et al.*, 2014 [100]), land management practices such as crop rotation (Gabriels *et al.*, 2003 [96]; Foerster *et al.*, 2014 [88]) and tillage (Van Oost *et al.*, 2000 [285]), and wildfires (Cerdà and Doerr, 2010 [35]) may participate in the variation of connectivity throughout the year by influencing soil conservation and moisture conditions. At present, no fine distinction is made between the different land use types within the arable land or forest classes. Further researches should therefore concentrate on integrating these agricultural practices and seasonal variations of land cover to provide a finer insight into sediment connectivity during the year.

7.3.2.2 Connectivity at the watershed scale

Figure 7.5 presents the map of mean connectivity per watershed obtained with the $IC_{revised}$. In the same way as beforehand (Section 7.3.1), values are ranked in four classes according to quartiles boundaries, and a zoom on the same region at the pixel scale is provided. Mean connectivity values per watershed range from -34.87 to -4.44 (mean = -12.30, std = 4.32). The decrease in mean connectivity values per

watershed has changed the boundaries of the quartile classes. From the new map of mean connectivity, we notice that the four classes are homogeneously distributed over the entire territory. Still, the three areas previously described (Eastern, centre and Western parts) remain identifiable with clear lithological limits and may be explained by the strong relationship between the $IDPR$ values and the underlying lithology.

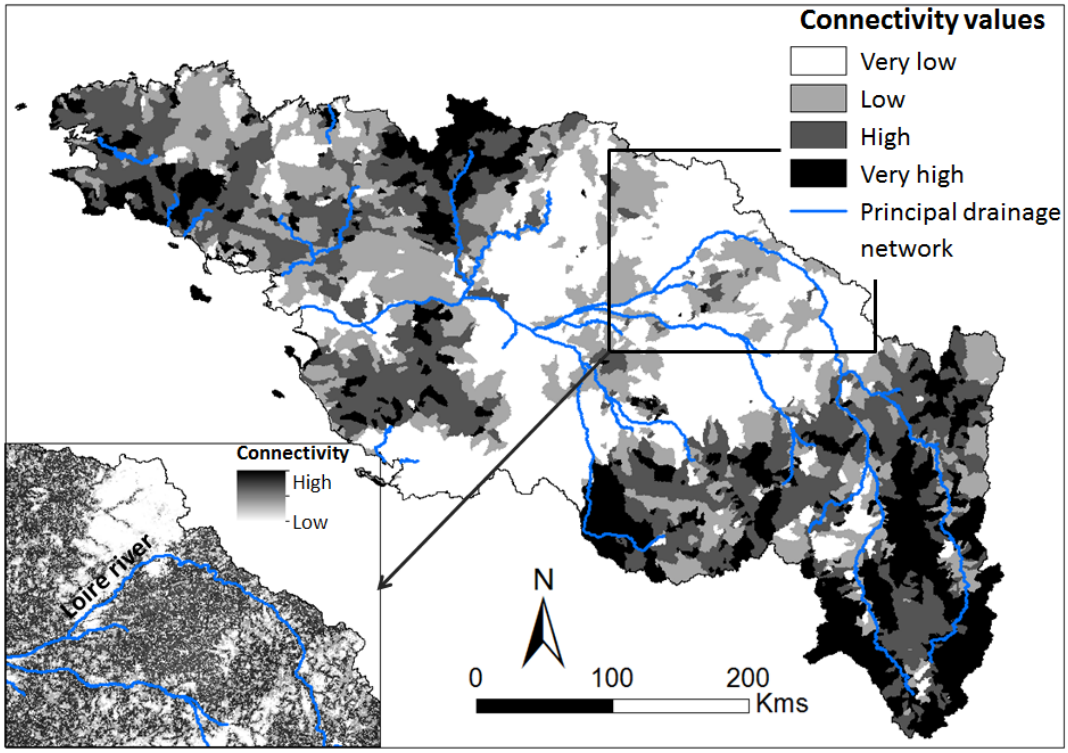

FIGURE 7.5 – Map of mean connectivity for each watershed (classification of mean values in quartiles)

From Figure 7.6(a), it is clear that a correlation exists ($R^2 = 0.52$) between the mean connectivity values from the $IC_{revised}$) and the drainage density. This result was expected as the drainage density strongly depends on the lithology and reflect soil infiltration (Vogt *et al.*, 2007 [294]) and connectivity (Delmas *et al.*, 2009 [71]). Moreover, a strong correlation ($R^2 = 0.69$, not shown on the graph) between mean $IDPR$ values and the mean connectivity values and between the the mean $IDPR$ values and the drainage density ($R^2 = 0.53$, Figure 7.6(b)). This result confirm the interesting potential of the $IDPR$ to reflect connectivity in lowland areas.

Figure 7.7 presents the map of the class differences between the initial IC and the $IC_{revised}$ for each watershed. The mean connectivity class remains unchanged for 48.5% of the watersheds. For 61.3% of them, the connectivity values were already in the highest or the lowest class with the IC. In these areas, the $IDPR$ confirmed the low connectivity of the landscape, e.g. in karstified limestones of the Beauce regions, or the high connectivity of the landscape, e.g. on the volcanic formations at the east of

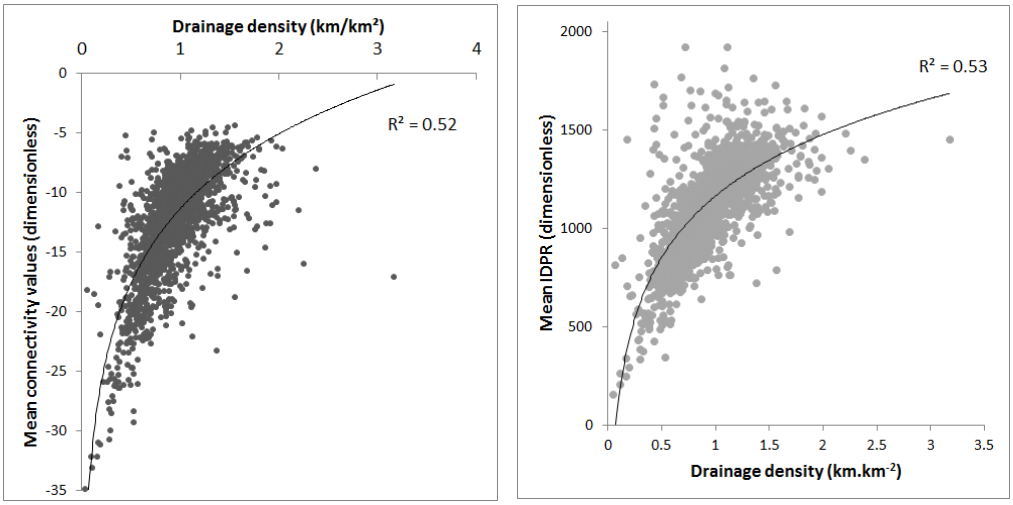

(a) (b)

FIGURE 7.6 – Relationships per watershed between the drainage density and (a) the mean connectivity values, and (b) the mean $IDPR$ values

the upstream part of the Allier river.

In contrast, the introduction of the $IDPR$ in the $IC_{revised}$ changed the mean connectivity classes for 51.5% of the watersheds. Even though the positive (increase in connectivity for 24.1% of the watersheds) and negative (decrease in connectivity for 27.4% of the watersheds) changes in class difference are evenly distributed in the Loire Brittany river basin, some patterns can be distinguished which are closely related to the underlying geological formation characteristics. Indeed, in Vendée at the south of the Loire outlet, the $IDPR$ is very high and express the existence of a shallow aquifers and the low infiltration capacity of soils. Moreover, in the Sologne region, or in the Limagne basin at the centre of the Massif Central, the high $IDPR$ values are related to the presence of impermeable geological formations, respectively clays of the cenomanian period and sedimentary formations on a granitic basement with low permeability. In these areas, the connectivity has been increased by two to three classes. On the other hand, the decrease of connectivity corresponds to low values of the $IDPR$ which are related to high infiltration due to a high permeability in the fractured bedrock in the north of the Armorican basin or to intense karstification of the sedimentary formations *e.g.* in the upstream part of the Loir river basin, at the south east of the Parisan basin. There is therefore a great benefit to incorporate factors like the $IDPR$ that can account for the nature of the lithology, as all of these changes of connectivity induced by the landscape ability to infiltrate (or not) potential overland flow, and that cannot

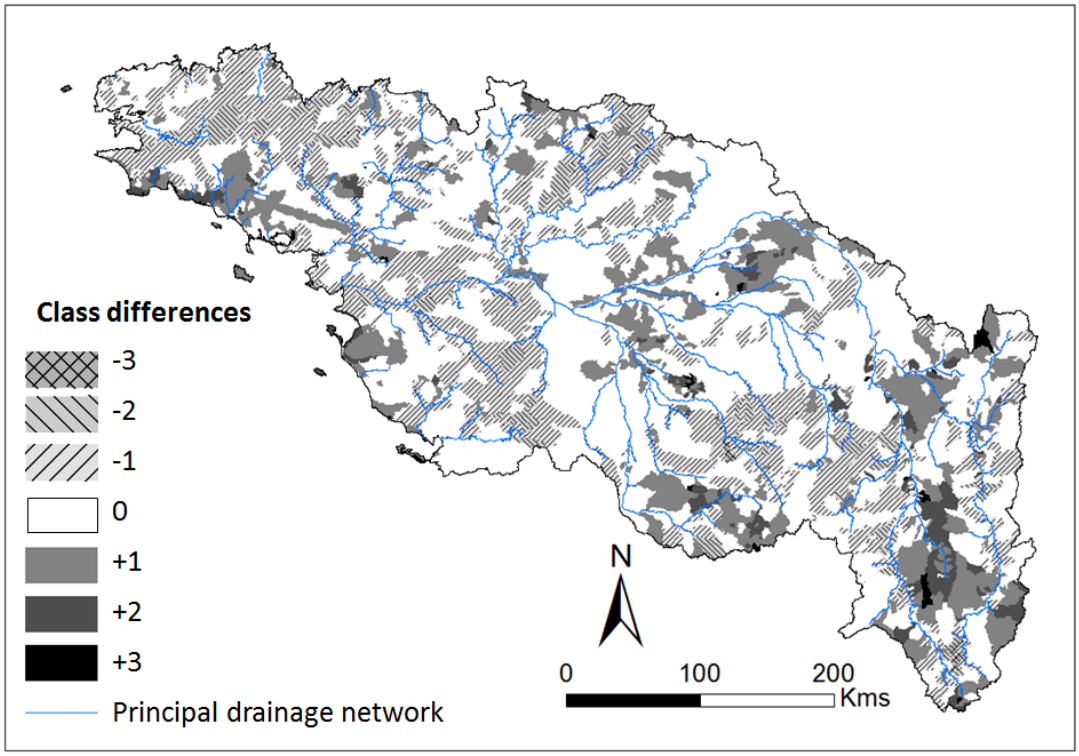

FIGURE 7.7 – Map of the class differences between the initial IC and the $IC_{revised}$ with $IDPR_{sigmoid}$

be detected by an index solely dependent on topography.

The relationship between the mean connectivity values from initial IC and $IC_{revised}$ is presented in Figure 7.8. The correlation between the mean values from initial IC and $IC_{revised}$ is weak ($R^2 = 0.33$). The dispersion of the dots takes a conic form with mean connectivity values relatively similar between both variables when the connectivity is high and a widening scattering when the connectivity decreases. Indeed, the mean value from $IC_{revised}$ with $IDPR_{sigmoid}$ can be five times less than the mean value obtained from IC. In contrast, when the $IDPR_{linear}$ values are considered in the calculation of the connectivity, a correlation exists between mean connectivity values from the IC and the ones from the $IC_{revised}$ ($R^2 = 0.79$). The fact that such a correlation exists clearly indicates that the introduction of the $IDPR_{linear}$ values or raw $IDPR$ values in the index, would just correspond to the addition of an adjustment factor and will not represent the described properties of lowland areas. The rescaling of the $IDPR$ values according to a sigmoid curve allows to give more weight to areas where the infiltration or the saturation is medium to high.

Finally, as discussed at the end of Section 7.3.2, the $IDPR$ reflects one of the processes characteristics of lowland areas, the soil saturation due to certain underlying lithology. However, in a man-maid landscape, such as intensive cultivated areas,

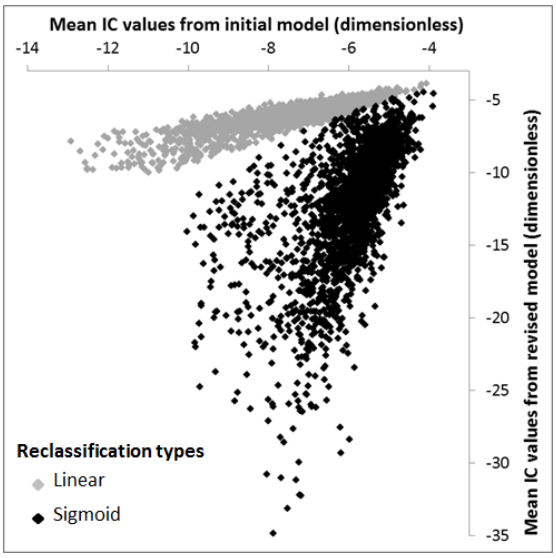

FIGURE 7.8 – Relationship between mean connectivity values from the $IC_{revised}$ with $IDPR_{sigmoid}$ and the initial IC

anthropic factors play a role in connectivity and their integration is necessary. Still, the assessment of sediment connectivity over the $LBRB$ has helped us to identify hot spots for sediment transfers. The proposed revised index of connectivity at the pixel scale and aggregation of results at the watershed scale shows interesting potentials to i) define priority zones for financial support from stakeholders to implement land and water conservation practices, and ii) determine the appropriate location for sediment trapping measures (Gumiere *et al.*, 2011 [117]; Mekonnen *et al.*, 2014 [183]).

7.4 Conclusion, applications and perspectives

In this paper, **we present the application of the sediment index of connectivity (IC) of Borselli *et al.* 2008 [21] to a large territory, the Loire and Brittany river basin, and its adaptation to take into account lowland runoff processes.** A distributed parameter, the $IDPR$, that reflects landscape infiltration and saturation properties is added into a revised index $IC_{revised}$. The index of connectivity is used in qualitative way to compare mean connectivity values at the watershed scale.

In this large territory characterised by diverse landscape types, the IC reflects only the high connectivity from hillslope to river network in steep areas while lowland areas appear to be barely connected to the river network. In these areas where hillslope

runoff also depends on the soil saturation, a topographic index does not reflect the real sediment connectivity induced by lithological properties. The introduction of the $IDPR$ in the $IC_{revised}$ allowed us to consider runoff processes both in steep and flat areas. **Changes in connectivity classes induced by this modification affected 51.5 % of the watersheds with 24.1% of connectivity being increased corresponding to clay-dominated areas, low-permeability areas of the granitic bedrock, and areas with shallow aquifers, and 27.4% of connectivity being decreased in intensively fractured bedrock areas and karstified sedimentary formations. Our results also suggest that the $IDPR$ cannot be directly used into the model but needs to be first rescaled to give more weight to the areas characterized by each process.** The addition of the $IDPR$-values rescaled according to a sigmoid curve has led to a severe decrease in connectivity values in certain regions and to the reclassification of the mean connectivity values (from low to high) of the watersheds. A new map of hillslope connectivity is proposed. The $IC_{revised}$ presents interesting perspectives to define other highly connected areas at the country scale. Indeed, the French territory is a very contrasted landscape which presents 29% of its surface area with slope $< 2\%$, in which 58% of the area presents more runoff properties than infiltration ones ($IDPR$-values > 1000).

The flexibility of the index of connectivity seems very promising to take into account other distributed parameters such as rainfall intensity or drain tiles. Further research is needed on the connectivity of lowland areas and the hillslope revised index of connectivity proposed in the present study should be coupled to a river index of connectivity and to existing erosion maps (*e.g.* Cerdan *et al.*, 2010 [37]) and compared to suspended sediment fluxes on the same territory (Gay *et al.*, 2014 [104]). Finally, the choice was made to aggregate cells into larger units (watersheds). However, other divisions (*e.g.*, Homogeneous Response Units (Bracken *et al.*, 2013 [25])), administrative regions (Le Bissonnais *et al.*, 2002 [160]) can be used to provide other insight into (dis)connected areas according to the stakeholders decision.

Chapitre 8

Intégration du réseau de haies dans un indice de connectivité

Dans le Chapitre 7, les processus de saturation et infiltration ont été pris en compte dans un indice de connectivité particulaire. Dans ce chapitre, la connectivité structurale des paysages (réseau bocager) est ajoutée dans l'indice précédemment utilisé et permet de mieux prendre en compte les propriétés d'occupation du sol dans le bassin Loire-Bretagne. Cependant, si les processus mis en jeu dans le transfert particulaire en zone bocagère sont bien documentés dans la littérature, cette étude est limitée par la connaissance de la distribution spatiale des haies et de leurs propriétés (espèces végétales, présence de talus...) sur l'intégralité du territoire. L'indice de connectivité n'est donc appliqué que sur les trois quart du territoire où des données sont disponibles. De plus, l'accent est mis sur la compréhension de l'influence de l'intégration des haies sur les sorties du modèle.

Les résultats indiquent bien une diminution de la connectivité dans les zones où le réseau de haies est présent. Les propriétés et l'influence de la distribution spatiale des haies sur le transfert particulaire sont donc bien reflétées par le modèle. Dans l'indice, l'IDPR exerce une influence plus forte sur les sorties du modèle que la présence de haies et traduit ainsi la hiérarchisation des processus et paramètres mis en jeu dans ce transfert et par lesquels le ruissellement constitue la première condition au transport.

Une nouvelle carte de connectivité sédimentaire à l'échelle de la masse d'eau est proposée, et est combinée avec une carte d'érosion de versant pour estimer l'érosion connectée sur le site d'étude. Cette carte finale permet d'identifier de manière qualitative les masses d'eau pour lesquelles l'érosion de versant apporte une part plus significative au bilan sédimentaire en sortie que les autres.

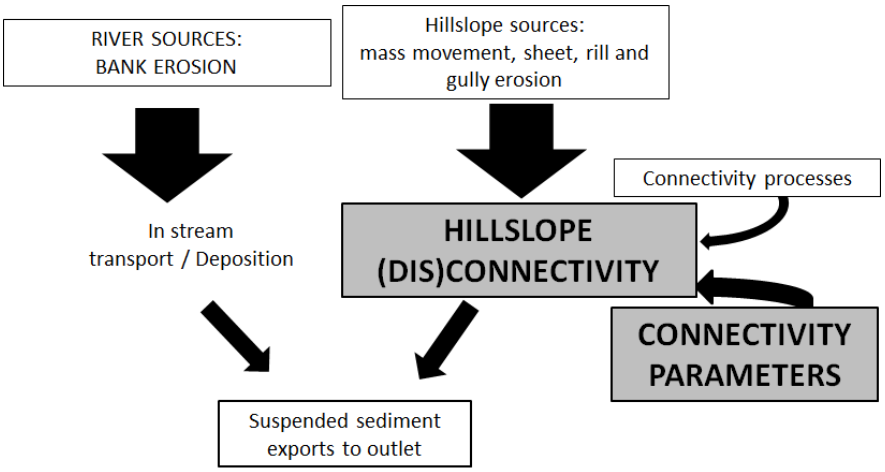

Sommaire

8.1 Introduction

Natural and anthropogenic linear elements such as rills, gullies (Poesen *et al.*, 2003 [226]; Croke *et al.*, 2005 [51]) and field borders have been identified as preferential flow and sediment pathways. In Europe, changes in agricultural practices have strongly modified the landscapes and led to the creation or destruction of different linear features that enhanced or impeded sediment transfers. Indeed, in the 1970s, the conversion into intensive farming was associated with the implementation of drain tiles and the creation of high density ditches networks (Kiesel *et al.*, 2010 [140]; Viel *et al.*, 2014 [291]) that have been set up to evacuate excess of water from the fields. These practices have thus increased the connectivity from the field to the permanent drainage network through an artificial subsurface network. Land reparcelling also resulted in the decimation or abandonment of non-crop features such as hedgerows (Stoate *et al.*, 2001 [265]) and the creation of large cultivated open fields with no, or few, barriers to sediment transfers. Nowadays, measures are oriented towards soil conservation practices and limitation of sediment connectivity from fields to rivers by, for example, the restoration of the hedgerow network.

Baudry *et al.* 2000 [14] define a hedgerow as "a linear feature composed of shrubs and/or trees that forms part of a management unit". The term "bocage" is also used but specifically refers to the diversity of the tree species and to a certain spatial organisation of the landscape in which the agricultural fields are enclosed by a hedgerow network (Mérot, 1999 [184]). If the initial functions of a hedgerow were to define field edges, be a shelter for livestock, a wind breaker, a corridor for wildlife (Marshall and Moonen, 2002 [181]), and provide farmers with wood (Baudry *et al.*, 2000 [14]), present-day functions put forward for the restoration of such features include: the decrease of soil erosion, buffer of pesticide drifts, aesthetic services (Marshall and Moonen, 2002 [181]), and carbon sequestration (Walter *et al.*, 2003 [306]; Dabney *et al.*, 2006 [52]). Recent policies

have therefore encouraged the development of management practices that reduce solid and chemical fluxes from hillslopes to water systems through the setting-up of grass strips at field borders and hedgerow replanting, especially in riparian areas.

Much attention has been paid to grass strips effects on sediment transport reduction and sediment trapping, facing interill or concentrated flow (Blanco-Canqui *et al.*, 2006 [17]) according to the strip width or the grass species (Lee *et al.*, 1998 [162]) and sediment size (Gumiere *et al.*, 2011 [117]). However, less studies have been conducted to understand the efficacy of hedgerows in sediment trapping. This lack of information is primarily due to the difficulty of measuring this efficacy in the field. Indeed, most of the field experiments are carried out at the plot scale and thus cannot reflect the role of hedgerows that act as barriers at the landscape scale. Another reason for this lack of knowledge is that this feature is generally considered in association with grass strip buffers (Daniels and Gilliam, 1996 [55]) and the differentiation between the efficacy of both vegetated filters is hard to quantify. Yet, Yuan *et al.*, 2009 [322] indicate that both buffers may offer the same efficacy in regards of sediment trapping. However, too few studies on hedgerows were considered by the authors to provide a strict comparison of both buffers.

From the existing studies on hedgerows, it appears that the spatial distribution and orientation of the features in the field is an important factor in sediment trapping (Polyakov *et al.*, 2005 [230]; Follain *et al.*, 2006 [89]; Ouvry *et al.*, 2012 [216]). There exists an optimal hedgerow spatial distribution to reduce water runoff and trap sediment. Moreover, the efficacy of hedgerow varies across time-scale: at the event scale, from 31% to 76% (Hai *et al.*, 2000 [118]) and up to 95% (Lee *et al.*, 2003 [161]) of the sediment may be stopped by the presence of a buffer. However, the authors also indicate that the proportion of trapped sediment strongly varies with the intensity and duration of the storm event. At the decadal time-scale, the efficacy of hedgerows in sediment trapping has, to our knowledge, never been studied because i) the topic is too recent in the geomorphologist community to allow for long-term studies, and ii) the efficacy increases within the first years as the hedgerow grows, widens and roots stabilize (Hai *et al.*, 2000 [118]). From their two-years study, Daniels and Gillian (1996) [55] concluded that the reduction in sediment load was of $\sim$ 80% thanks to vegetated filters.

Despite these different issues on the knowledge of hedgerow efficacy, several studies have attempted to integrate the spatial distribution and properties of hedgerows into sediment connectivity and soil redistribution modelling at the small catchment scale (Carluer and Marsily, 2004 [33]; Follain *et al.* 2006 [89]; Gascuel-Odoux *et al.*, 2011 [102]; Lacoste *et al.*, 2014 [149]; Viel *et al.*, 2014 [291]). Results from these investigations indicate that the consideration of hedgerows strongly modifies the sediment and flow volumes and direction, and thus the outputs of the models.

However, at a larger spatial scale, consideration of the hedgerow networks in the sediment connectivity assessment is limited by the large number of required data or by the poor resolution of available data. In such cases, the sediment connectivity assessment may be based on semi-distributed to distributed approaches or empirical equations in which the presence of hedgerows is implicitly taken into account through

management practices factors. For example, the $P - factor$ of the USLE (Wischmeier and Smith, 1978 [318]) refers to the practices used to control erosion and the value is affected according to the combination of different parameters such as land slope, strip cropping, land contouring, and terraces (Blanco-Canqui and Lal, 2008 [18]). In their 2011 paper, Gumiere *et al.* [117] combined the land slope and percentage of strip grass cover to provide different $P - factor$ values. However, as stated by these authors, this factor is more of a sediment production term in the USLE than related to sediment transfer itself: the $P - factor$ is not sensitive to the location of the land management practices and as to whether grass-strips are placed upslope or downslope the field. Nonetheless, the $P - factor$ can present advantages to reflect hedgerow properties in reducing soil erosion.

In France, strong spatial discrepancies in the hedgerow density exist. For example, the Brittany region is well-known for its dense "bocage" while cereal crop areas, such as the *Beauce* region, has very few hedgerows. Even if more than 200,000 km of hedgerows have disappeared between 1950 and 2000 in Brittany (Mérot *et al.*, 1999 [184]), this region still displays the denser hedgerow network in Europe together with the Massif Central (Van der Zanden *et al.*, 2013 [283]). A recent study from Pointereau *et al.*, 2007 [227] based on data acquired between 2000 and 2008 confirms these trends at the national scale. In the Loire river basin, the authors indicate that, in grain culture areas, primarily in the Parisian basin and in the Limagne plain, the hedgerow density is very low (see Appendix E).

In a previous work, Gay *et al., accepted* [105] (see Chapter 7) proposed a map of connectivity for the Loire and Brittany river basin, using a modified index of sediment connectivity from Borselli *et al.* (2008) [21]. In this approach, process-based connectivity of overland flow in lowland areas is taken into account through a index of hydrological connectivity that reflects soil infiltration/saturation properties. This index of hydrological connectivity also takes into account implicitly the artificial drainage network (drain tiles and ditches) in the catchment. However, some parameters of the initial index of connectivity have been introduced as such in the modified index ($C - factor$) while differences in cropping and management practices exist between study areas (*e.g.*, ploughing, nature of crops). Therefore, when using the index of connectivity, there is a need to refine values of such parameters to better suit the characteristics of each study area. Furthermore, the structural connectivity is only reflected by the slope steepness while the spatial organisation of the landscape and associated features are not considered. Therefore, there is a need to take into account the structural connectivity of this lowland area imposed by the presence of hedgerows that are characteristic elements of the $LBRB$.

In this context, the objective of this study is to incorporate the properties and spatial distribution of hedgerows in the hillslope sediment connectivity assessment of the $LBRB$. To this aim, the hedgerow network is included in the modified index of connectivity previously described in Chapter 7. Moreover, values of the *C-factor* are modified according to literature data to better fit the cover properties of the landuse types of the $LBRB$. Section 8.2 presents the data used and how we incorporated them

into the index of connectivity. The results are presented and discussed in Section 8.3.

8.2 Material and methods

In this study, we add to the modified index of Borselli (see page 158), the hedgerow data in both the upslope and downslope components. Moreover, the values of the *C-factor* are also modified according to literature data to better fit the cover properties of the landuse types of the *LBRB*.

8.2.1 Database and pretreatments

8.2.1.1 Landuse and *C-factor*

Tableau 8.1 Values of the $C-factor$ for landuse types from CLC and RPG, defined for the *LBRB*. In the code columns, bold numbers refer to the CLC map, other numbers refer to the RPG data

Code	Landuse type	Percentage in *LBRB*	$C-factor$	Reference
0 - 15, 24, 25, 28 and **2.1**	Arable lands	35.29	0.4	Wischmeier and Smith, 1978 [318]; Jordan *et al.*, 2005 [137]; Yoshikawa *et al.*, 2004 [321]
18 and **2.3.1**	Permanent pastures	20.39	0.1	Jordan *et al.*, 2005 [137]
19	Temporary pastures	19.39	0.15	This study
3.1	Forests	14.81	0.001	Borselli *et al.*, 2008 [21]
2.4.2	Complex cultivation patterns	2.63	0.2	Bakker *et al.*, 2008 [10]
2.4.3	Land principally occupied by agriculture, with significant areas of natural vegetation	1.11	0.3	Bakker *et al.*, 2008 [10]
3.2.4	Transitional woodland-shrubs	0.82	0.04	Bakker *et al.*, 2008 [10]
21 and **2.2.1**	Vineyards	0.52	0.5	Borselli *et al.*, 2008 [21] ; Angeli, 2004 in Diodato *et al.*, 2011 [75]
17 and **3.2.1**	Natural grasslands	0.39	0.05	Bakker *et al.*, 2008 [10]
3.2.2	Moors and heathland	0.32	0.01	Bakker *et al.*, 2008 [10]
16	Fodder crop	0.29	0.15	This study
20, 22, 23, 27, and **2.2.2**	Orchards	0.17	0.3	Jordan *et al.*, 2005 [137]
1.4	Artificial, non-agricultural vegetated areas	0.16	0.05	Borselli *et al.*, 2008 [21]
1.3	Mine, dump and construction sites	0.09	1	Borselli *et al.*, 2008 [21]
3.3	Open spaces with little or no vegetation	0.04	0.9	Borselli *et al.*, 2008 [21]

The landuse map is taken from Degan *et al., in prep* [67] who combined information from the Corine Land Cover 2006 and the RPG 2010. $C-factor$ values presented in

(Table 8.2.1.1) are attributed to each landuse type according to literature data and expert-based knowledge.

In order to investigate the effect of the modification of the values of the $C-factor$ in the IC as proposed by Borselli *et al.* (2008) [21], this intial index is computed in the $LBRB$ with the new values of the $C-factor$. In a second step, the $IC_{revised}$ is computed with the new C values.

8.2.1.2 Hedgerows

The BDTopo ® IGN provides for each department of the French territory, a GIS vector layer of hedgerows in the form of polygons. In the $LBRB$, this information is available for 22 out of 36 departments (Figure 8.1). The polygons are mapped using orthophotographies and ground surveys and the planimetric precision is of 2.5 to 5m. Both field campaigns are realised every ten years at most per department to ensure the validity of the final data. Hedgerow data for departments within the $LBRB$ result from field campaigns carried out between 2007 and 2011 (Figure 8.2). Considering the planimetric precision of the data and the resolution of the landuse map (50m cell-size), we chose to transform the polygons into a raster of 5*5m cell size.

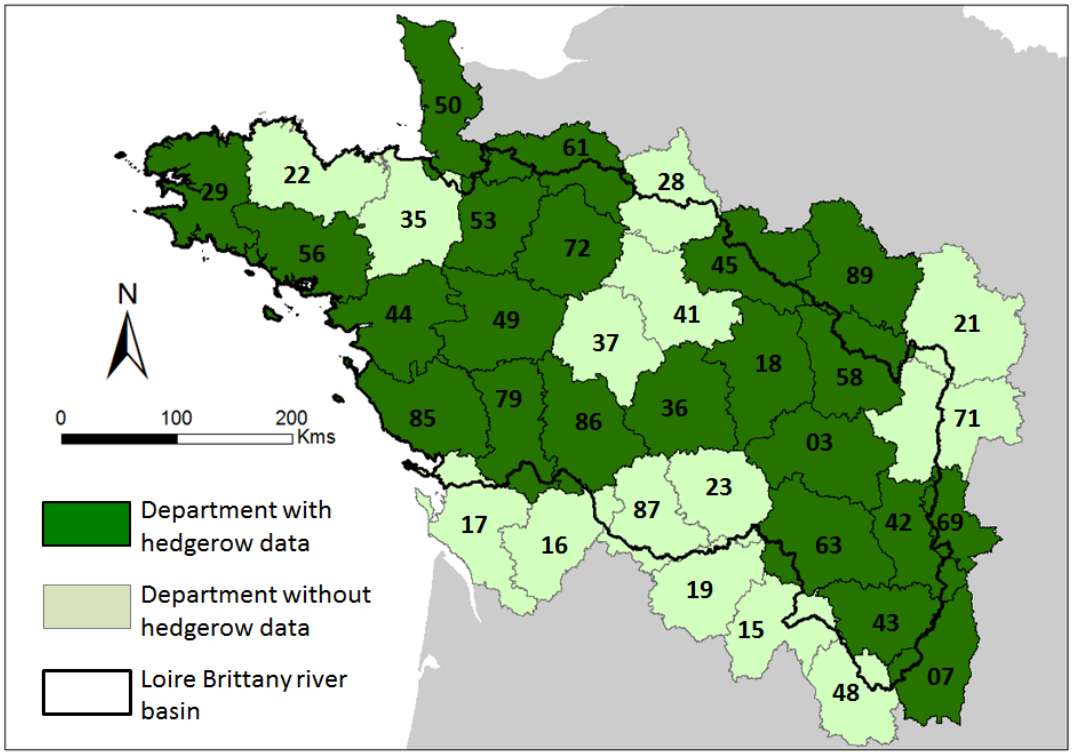

FIGURE 8.1 – The 36 departments of the Loire Brittany river basin and availability of the hedgerow data for each department from the field "NATURE" of the VEGETATION layer of the BDTopo ® in February 2015

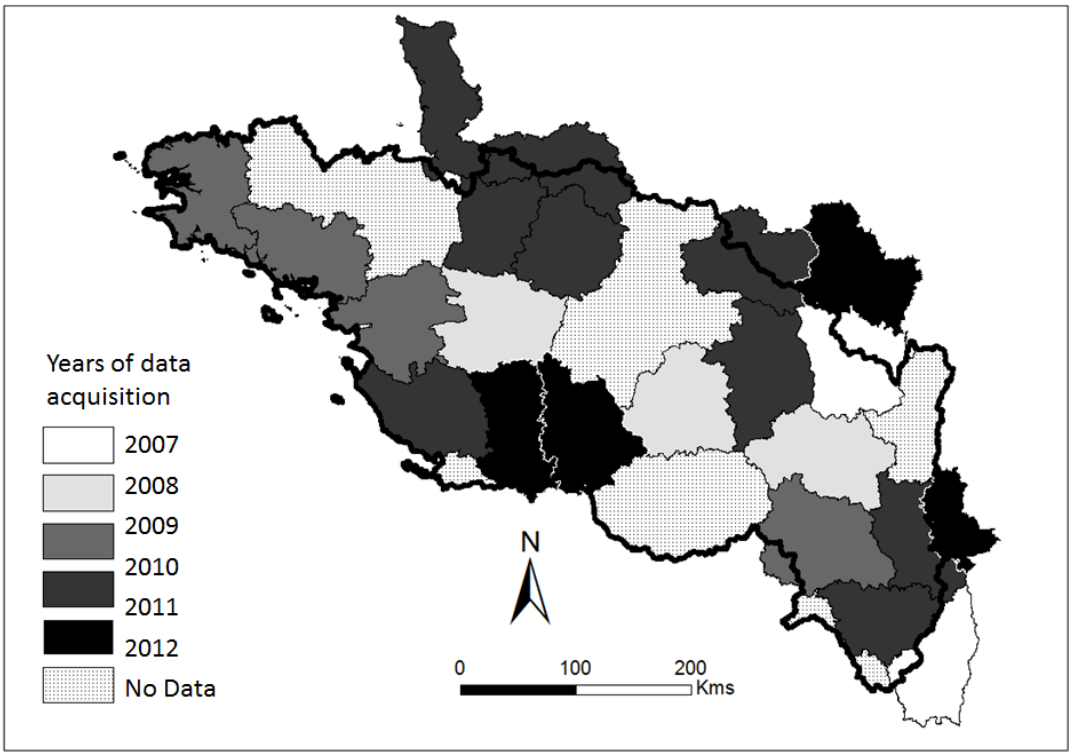

FIGURE 8.2 – Yeras of hedgerow data aquisition (BDTopo ®) for the 22 departments of the Loire Brittany river basin

8.2.2 Inclusion of hedgerows in the index of connectivity

In the initial IC presented by Borselli et al. in 2008 [21], topography and landuse type (*via* the *C-factor*) are the only weighing factors of the flow and sediment connectivity. Recently, Gay *et al., accepted* [105] also added a landscape parameter, the $IDPR$, which accounts for infiltration/saturation properties in both the upslope and downslope components of an $IC_{revised}$. In the present study, the hedgerows data are incorporated to reflect the hedgerow properties in the upslope component, and the influence of their spatial distribution in the downslope component.

8.2.3 $P - factor$ values

The presence and properties of hedgerows is taken into account by including a support practice factor ($P-factor$ of the USLE, Wischmeier and Smith, 1978 [318]) according to the percentage of hedgerows cover (5*5m cells) in each landuse cell (50*50m cells). In $\sim$ 25% of cases, the cover of hedgerows does not exceed 6% and corresponds, in general, to a hedgerow end. In $\sim$ 25% of cases, the percentage of cover is higher than 25 and corresponds to complex patterns such as large hedgerows or corners of

field enclosed by hedgerows. For a hedgerow cover below 25%, the $P-factor$ values are affected according to the percent of hedgerow cover in each cell of the landuse map (Figure 8.3). In case of a hedgerow cover higher than 25%, we consider the pixel as a forested area. These cells are thus given the $C-factor$ value (W factor in the index of connectivity) of "forest" land use type ($C-factor=0.001$) and the $P-factor$ is not taken into account.

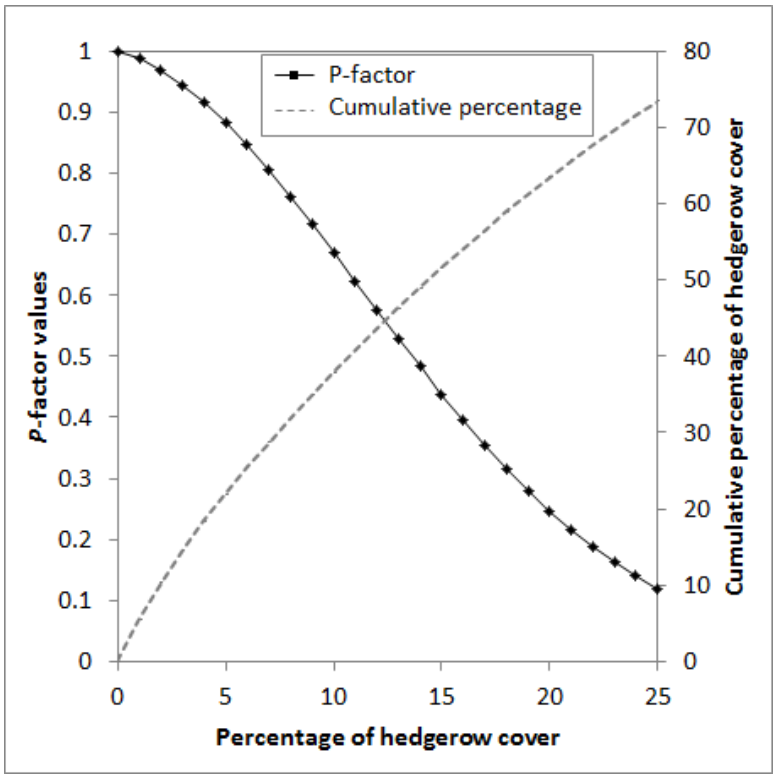

FIGURE 8.3 – $P-factor$ values according to the percentage of hedgerow cover in land use cells

8.2.4 Inclusion of the $P-factor$ in the $IC_{revised2}$

The $P-factor$ is included in the upslope component as in Equation 8.1.

$$D_{up2}=\overline{W.P}.\overline{S}.\sqrt{A} \tag{8.1}$$

where $\overline{W.P}$ is an average weighing factor of the upslope contributing area (dimensionless) reflecting the cropping management and conservation practices, $\overline{S}$ is the average slope gradient of the upslope contributing area ($m.m^{-1}$) and A is the upslope contributing area (m^2). For more details on the factors, please refer to page 156 to 159.

The downslope component consists of weighing each surface down the pathway from cell i to the nearest sink with different characteristics. In the present study, the flow length is also weighed by the presence of hedges on the way from each cell to the river system. Even though the $P-factor$ is not sensitive to the location of land management

practices (Gumiere *et al.* (2011) [117]), the downslope component already accounts for the spatial distribution of elements in the landscape. Therefore, the $P - factor$ is included in the D_{dn} component as in Equation 8.2 and the distance to the river is increased by a wall function at the edge of the hedgerow pixel or is not modified if no hedgerow exits on the way.

$$D_{dn2} = \sum_i \frac{d_i}{W_i \; S_i \; IDPR_i \; P_i} \tag{8.2}$$

Finally, the new index of Borselli $IC_{revised2}$ is computed as in Equation 8.3 over the departments where the hedgerow network is available.

$$IC_{revised2} = log10 \left(\frac{\overline{W.P}.\overline{IDPR}.\overline{S}.\sqrt{A}}{\sum_i \frac{d_i}{W_i.IDPR_i.S_i.Hedge_i}} \right) \tag{8.3}$$

8.3 Results and discussion

In this section, we present and discuss the results of the influence of the modification of the $C - factor$ values on the sediment connectivity values, and the influence of the inclusion of the hedgerows as barriers to sediment on the connectivity patterns. We want to draw the attention of the reader on the fact that our reasoning is based on a qualitative rather than quantitative approach of the connectivity at the pixel and watershed scale. Our aim is thus to highlight areas displaying extreme values of connectivity within the $LBRB$ and the watershed breakdown of the Basin Agency presented in Chapter 7 is used for the representation of the results. Due to the lower availability of the hedgerow data, only 1350 out of 2122 watersheds are considered in the analysis of the sediment connectivity at this resolution.

8.3.1 Changes induced by the modification of the *C-factor*

In this study, we have modified the values of the $C - factor$ (W factor in the index of connectivity) in order to better suit the characteristics of the study site. The choice of one value for one defined landuse type results from a compromise between the information contained in our database and values found in the literature. For example, in forested areas, $C - factor$ values range from 0.001 to 0.003 depending on forest-tree type in the Mediterranean area (Angeli, 2004 in Diodato *et al.*, 2011 [75]) and from 0.02 to 0.06 depending on forest density in tropical monsoon catchments (Ghosh, 2013 [106]). However, if all agree about the protective nature of forests that are generally given very low values of $C - factor$ in comparison with arable lands, the effect of pastures in terms of soil protection is rather controversial. Indeed, while Borselli *et al.* (2008) [21] and Pelacani *et al.* (2008) [218] affected a higher $C - factor$ value to pastures than to

arable lands, other authors give pastures from 3.6 to 15 times lower values than that of arable lands (Jordan *et al.*, 2005 [137] and Bakker *et al.*, 2008 [10], respectively). In the $LBRB$, arable lands are generally ploughed and primarily dedicated to cereal cropping. In these circumstances, we believe that the practices in arable lands lead to less soil conservation than in pastures and we gave a higher $C-factor$ values to arable lands. Similarly, heterogeneous agricultural lands (HAL) of the $LBRB$ mostly concentrate in Brittany and are a mixture of crop areas and dense hedgerow network. In order to avoid taking into account the effect of hedgerows twice, the HAL have been given a higher $C-factor$ value than in the original IC.

As a result, at the pixel scale, the modification of the $C-factor$ values in the index of connectivity induced an increase in connectivity in 57.69% of the $LBRB$ area, a decrease in connectivity in 25.39% and no changes in 16.92% of the area. The spatial distribution of such changes are very localised in three different areas. The decrease in connectivity values is almost exclusively observed in the Massif Central due to the presence of permanent pastures for which the $C-factor$ is 0.05 less than the one proposed by Borselli *et al.* (2008) [21]. Connectivity is being increased in the Limagne plain of the Massif Central and over the rest of the study area, except in the Sologne region which endures no modification due to the presence of forests for which the $C-factor$ values have not been modified.

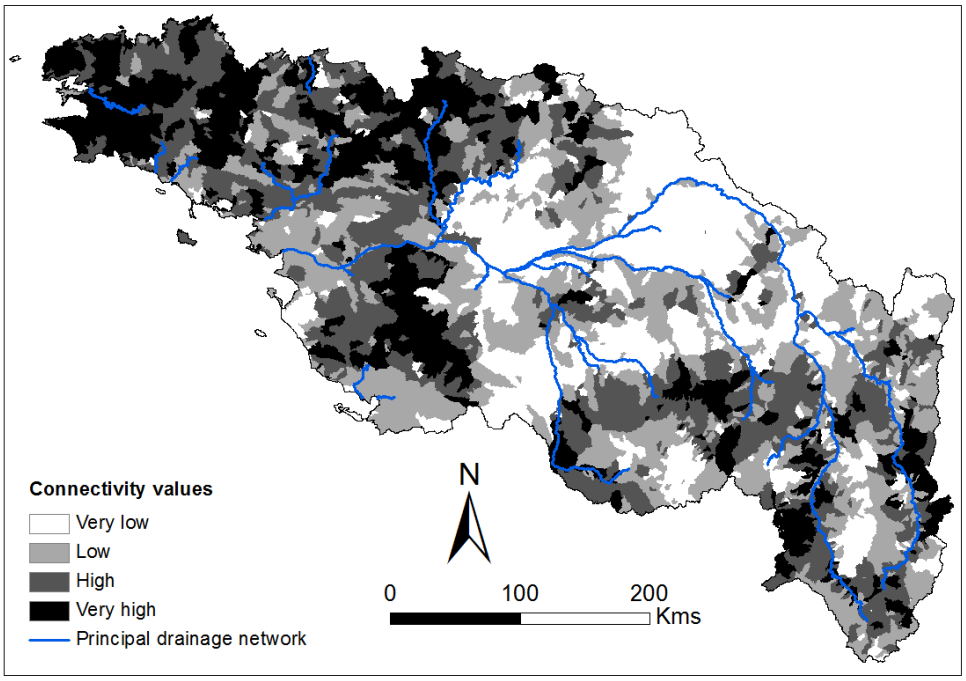

FIGURE 8.4 – Map of the mean sediment connectivity for each watershed according to the IC (Borselli et al. 2008 [21]) with values of $C-factor$ defined in Section 8.2.1.1. The values are ranked according to quartiles classes.

Figure 8.4 presents the map of mean connectivity values per watershed obtained

from the computation of the initial IC (from Borselli *et al.*, 2008 [21]) with the new $C-factor$ values. For 38.7% of the watersheds, connectivity has been decreased by one to two classes (410 watersheds out of 2122) and increased by one to two classes (411 watershed out of 2122) and the spatial distribution of such changes corresponds to changes observed at the pixel scale.

Lithological and slope boundaries are less evident than in the map of connectivity produced when using the initial $C-factor$ values in the IC (see Figure 7.3(a), page 161). In the Massif Central, the lower $C-factor$ values for pastures counteract the effect of steep slopes while in the Armorican basin, the combination of steep areas and higher $C-factor$ values for the arable lands and HAL has led to an increase in connectivity. As a consequence, the Armorican basin concentrates most of the watersheds displaying the highest mean connectivity values. The connectivity of the Sologne and Beauce regions taken as example of lowland saturation and infiltration processes (see page 168) remains unchanged and confirms the importance to take into account an index that reflect such processes ($IDPR$).

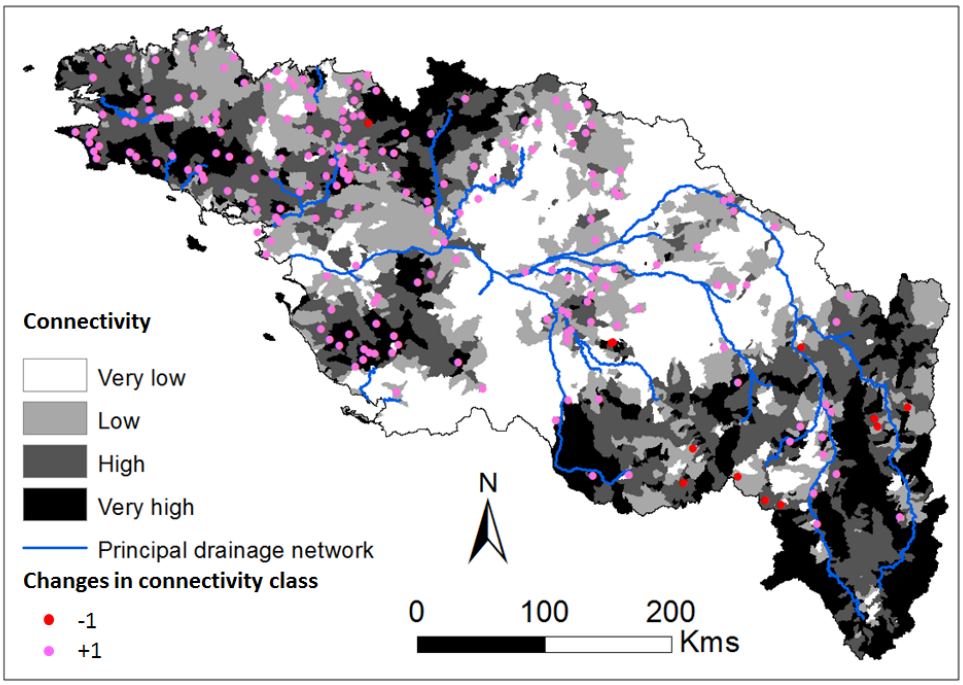

FIGURE 8.5 – Map of the mean sediment connectivity for each watershed according to the $IC_{revised}$ (Gay *et al., accepted*) [105] and $C-factor$ values defined in Section 8.2.1.1. Dots represent Changes in connectivity class induced by the modification of $C-factor$ values. The values of the boundaries of the classes correspond to those of the $IC_{revised}$ with the initial $C-factor$ values, as presented in Chapter 7, Figure 7.5

The modification of the values of the $C-factor$ in the $IC_{revised}$ (as defined in Chapter 7) induces little changes, with an increase or decrease of at most one class. These changes affected 216 watersheds out of 2122 (Figure 8.5). Positive changes

(increase of connectivity by one class) affect 204 watersheds and are evenly distributed in the Armorican basin, the Parisian basin and the Limagne plain. The connectivity of 12 watersheds has been decreased by one class and are primarily located in the Massif Central with one exception for a very small watershed dominated by pastures in Brittany. The connectivity of the extensively and intensively cropped areas of the Parisian belt remain among the lowest values of $LBRB$ due to the high infiltration properties of this area.

From these results, it is clear that the weight given to the $IDPR$ as an indicator of hydrologic connectivity is preponderant in the final outputs of the index of sediment connectivity. While the modification of the $C - factor$ seems to strongly modify the initial IC values, its influence in the $IC_{revised}$ is much less evident. Moreover, the connectivity values are still very high in the Brittany region. However, this area is characterised by a high erosion risk (Le Bissonnais *et al.*, 2002 [160]; Degan *et al., in prep.* [67]) while very little sediment is found in the rivers. Two possibilities exist to explain this phenomenon: either the sediment is rapidly evacuated from the rivers to the sea and is not deposited on the way, or the sediment never reaches the rivers as deposition areas exist on hillslopes, at the hedgerow borders for example. It is thus necessary to include the structural elements of the landscape in the connectivity assessment.

In the remainder of this study, the comparisons and analysis are based on the $IC_{revised}$ and $IC_{revised2}$ considering the $C - factor$ values proposed in the present study.

8.3.2 Connectivity changes induced by the introduction of hedgerows

The introduction of the presence of a hedgerow network in the $IC_{revised2}$ induced modifications in the values and patterns of the D_{up2} and D_{dn2} components and resulted in lower values of connectivity at the watershed scale. These changes are described and discussed hereafter.

8.3.2.1 Modification induced in the downslope and upslope components

In order to provide an understanding of the changes in outputs induced by the integration of the hedgerow network, we present in this section, the differences between i) D_{dn} and D_{dn2} outputs, and ii) D_{up} and D_{up2} outputs, in terms of changes in values and patterns. The patterns of the values of the proper D_{dn2} and D_{up2} rasters are not analysed here.

The inclusion of the hedgerow network as barriers to sediment in the D_{dn2} component of the $IC_{revised2}$ has led to an increase in the D_{dn2} values. Such an increase is linked to the reorientation of the flow path and thus to the increase in the distance from cell i down to the river network. In the study area, 67.9% of the pixels have undergone such changes while for 32.1% of the pixels the D_{dn2}, no changes in values is observed.

Concerning the patterns of the differences between the D_{dn} and D_{dn2}, the hedgerow network contributes to isolating entire subcatchments from the river network. There exist an inverse relation between the distance to the river and the percentage of changes in the D_{dn2} component such that, the closest to the river network, the highest the changes induced by the introduction of the hedgerows. Indeed, the important riparian vegetation leads to severe increase in the distance from close-by cells to the drainage network. While in the $IC_{revised}$ riparian cells are directly connected to the rivers, the integration of the hedgerow networks has increased by up to 1000% the length from these cells to the river network corresponding to increase of the distance to sink by 20 times. In remote areas, the percentage of changes induced by the downstream presence of hedgerows is not so important as the initial distance to the river network is higher.

The introduction of the $P - factor$ in D_{up2} has induced decreases in values of this component by up to 100% of the initial values. Indeed, the $P - factor$ comprised between $\sim$ 0.1 and 1 decreases the connectivity values of upstream cells converging into cell i. Changes affected only 30.9% of cells while 69.1% remain unchanged. Spatial patterns of the differences between D_{up} and D_{up2} differ from the ones observed for the D_{dn} components. Indeed, changes in values concentrate along the flow path given by the flow accumulation raster rather than on an entire subcatchment.

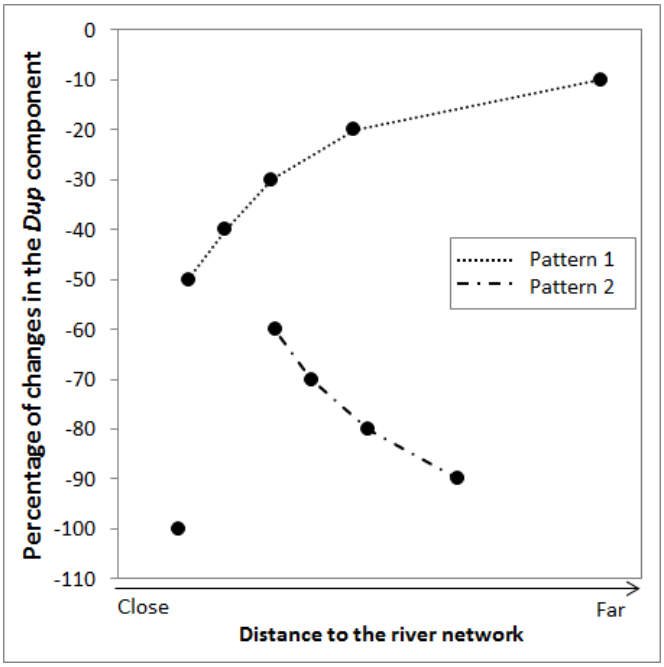

FIGURE 8.6 – Percentage of changes in the D_{up} component values according to the distance to the river network. See text for explanation of the Pattern 1 and Pattern 2

Complex patterns between of changes induced by the introduction of the hedgerow network and the distance to the river are observed (Figure 8.6). As the distance to the river network decreases, Pattern 1 and 2 display opposite trends. Indeed, Pattern 1 corresponds to the "dilution" of the effect of the hedgerow as the upstream catchment size increases and more adjacent cells contribute to connectivity. At the pixel scale,

this pattern is reflected by a decrease in percentage of changes with the increase of the upstream surface area (thus with a decrease of the length from cell i to the river network). Pattern 2 displays an increase of percentage of changes with the decrease of the length from cell i to the river network. There are two possible explanations for this trend. First, the density of the hedgerow network is more important in riparian areas than in upper parts of the landscape and contributes to lowering the connectivity in these riparian areas. Second, as the flow of sediment progresses downstream the hillslope, the presence of new hedgerow on the path will lead to a new decrease of connectivity and thus to an increase in the difference between D_{up} and D_{up2} values. In this respect, Pattern 1 corresponds to cells upstream the hedgerow while Pattern 2 corresponds to cells downstream the hedgerow.

However, a sudden jump in percentages of changes is observed between nearby areas, where the percentage is the highest (-100%), and the next closest area where changes do not exceed -50% of the initial values of the D_{up}. This result can be explained by the dense riparian vegetation but also because the flow accumulation in riparian areas may be very low. Indeed, in 41% of cases, cells displaying a number of accumulated cells smaller or equal to 2 are located within 300 metres around the river network and are associated with very gentle slopes. The remainder 59% of cells are located around the ridges. Cells downstream very small catchments are thus strongly affected by the presence of hedgerows and thus by changes in connectivity values.

At the watershed scale, there exists a strong correlation between the hedgerow density ($km^2.km^{-2}$) and the percentages of changes between D_{up} and D_{up2} values per watershed ($R^2 = 0.96$). Yet, absolutely no relation is found between the hedgerow density and the percentages of changes between the D_{dn} and D_{dn2} per watershed. Such findings confirm the fact that the $P - factor$ is not sensitive to the location of the hedgerow within the landscape (Gumiere *et al.*, 2011 [117]) nor to the orientation of the hedgerow (in the D_{up2}). Conversely, the spatial distribution of the hedgerow network taken into account by the D_{dn2} component greatly influences the model outputs even in the case of a poor hedgerow density.

8.3.2.2 Connectivity at the pixel and watershed scale

As a consequence of the decrease in the values of the numerator, D_{up2}, and increase in the values of the denominator, D_{dn2}, the connectivity values at the pixel scale have strongly decreased.

The minimal connectivity value has not been modified as it corresponds to forested areas. 71% of the pixels have undergone a decrease in sediment connectivity values. Such changes are localised in cells close to the channel network and correspond to disconnection from the river by riparian vegetation. Riparian cells, in the 300m around the river network, display the highest changes and patterns such as the ones described in the differences between D_{dn} and D_{dn2}: entire subcatchments are being disconnected from the channel network. On average, the pixels have undergone a decrease by 18.2% of their initial values due to the introduction of the hedgerow network. Such changes

affect both remote areas and close-by areas from the river network.

The decrease of connectivity values resulted in the decrease of mean values at the watershed scale and in the modification of watersheds being the most connected. For 365 out of the 1350 watersheds, the connectivity has decreased by one class and by two classes for 3 watersheds. These changes especially concern watersheds that initially displayed from high (149 watersheds) to very high (150 watersheds) connectivity values. In all, 26% of the changes of watersheds connectivity are located in the Massif Central while the Massif Armorican concentrates most of the connectivity class changes (59%). The remaining 15% of watersheds that have changed of connectivity class following the inclusion of the hedgerow in the $IC_{revised2}$ are located at the edges of the Parisian basin (Figure 8.7).

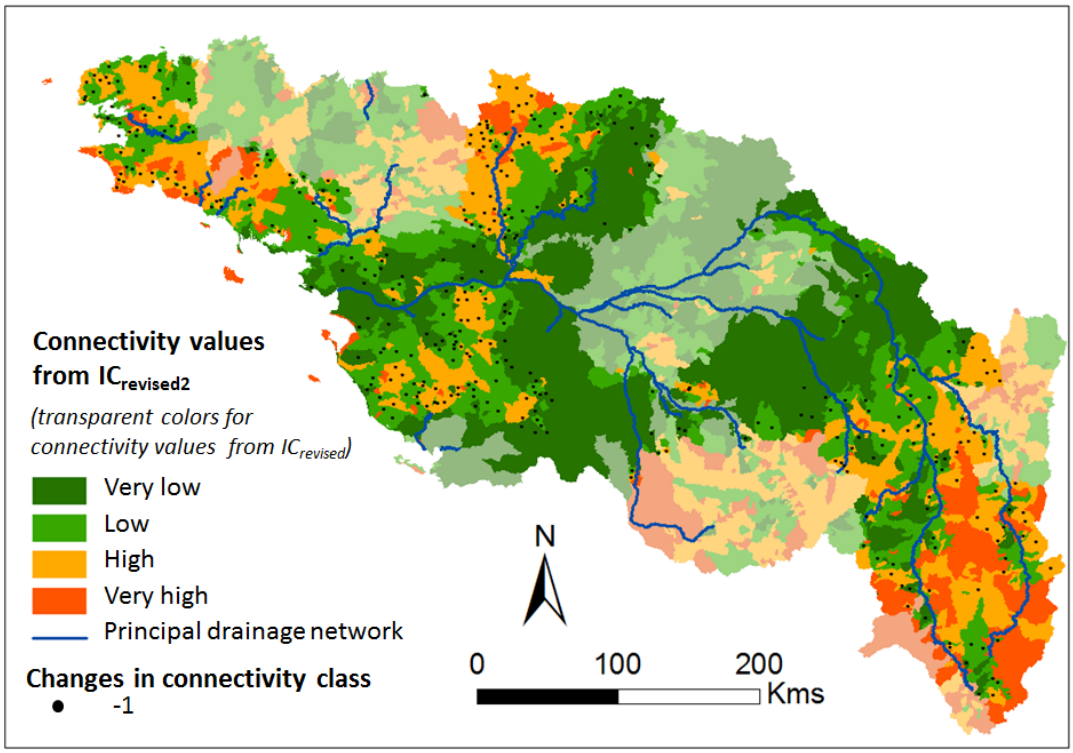

FIGURE 8.7 – Map of the sediment connectivity from the $IC_{revised2}$ for the 1350 watersheds and location of the changes in connectivity class. The class boundaries corresponds to quartiles values of the sediment connectivity from the $IC_{revised}$ displayed in the background as transparent layer.

As a consequence of the strong correlation between hedgerow density and the percentage of changes between D_{up} and D_{up2}, a medium correlation ($R^2 = 0.66$) between hedgerow density and differences in connectivity values between $IC_{revised2}$ and $IC_{revised}$ per watershed is observed (Figure 8.8).

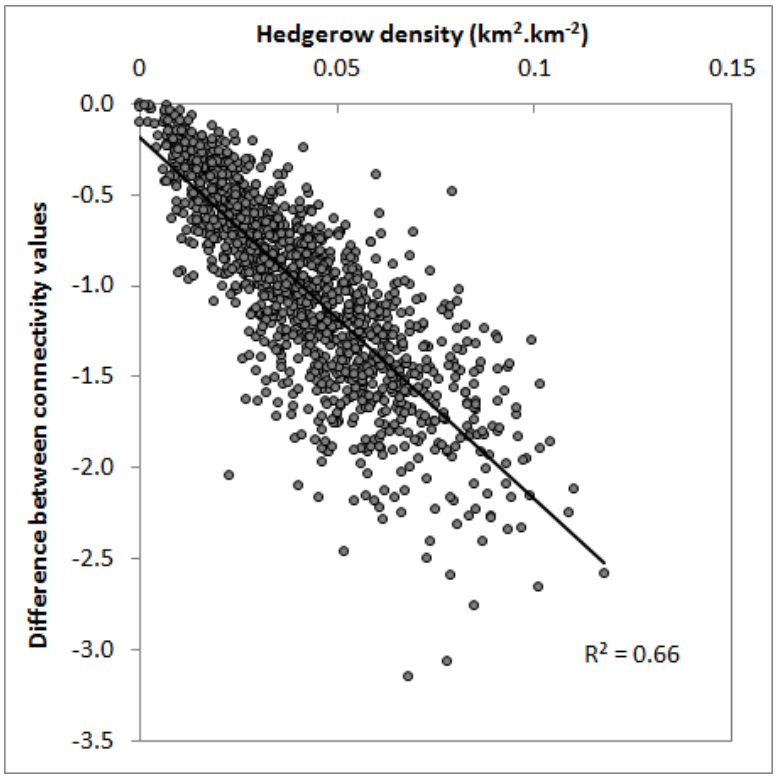

FIGURE 8.8 – Relation between hedgerow density and differences in connectivity values between $IC_{revised2}$ and $IC_{revised}$

In general, the results on the sediment connectivity including both process-based ($IDPR$) and structural (hedgerows) connectivity dimensions indicate that the pixels and watersheds are much less impacted by the presence of the hedgerows than by the infiltration or saturation properties of the landscape. In the field, together with the slope steepness, the infiltration or soil saturation (and thus, the $IDPR$) is the first condition to sediment connectivity, while the absence or presence of a hedgerow network constitutes a secondary condition to the sediment transfer. This grading of the importance of processes and landscape organisation are thus well reflected in the index of connectivity.

Moreover, it appears that at the watershed scale, the hedgerow density is low in areas with high infiltration rates and *vice versa* (Figure 8.9). In this context, the lack of hedgerow data in different departments of the $LBRB$ constitue a major limit in areas where the connectivity is high due to steep slopes or high soil saturation (*e.g.*, at the confluence of the *Cher* and *Loire* rivers), and a minor limit in areas where the connectivity is low due to gentle slopes and high infiltration properties such as in the belt of the sedimentary Parisian basin. Still, the spatial organisation of both process-based connectivity and structural elements needs to be considered at the pixel scale for a full understanding of the sediment connectivity within the $LBRB$.

In this study, no increase in connectivity is generated by the presence of a hedgerow

as we affected connectivity values to these features such that the sediment is being stopped by their presence. However, in certain cases – *e.g.*, if hedgerow and slope are in the same direction – the presence of a hedgerow may increase connectivity by concentrating the flow and sediment fluxes along the edges.

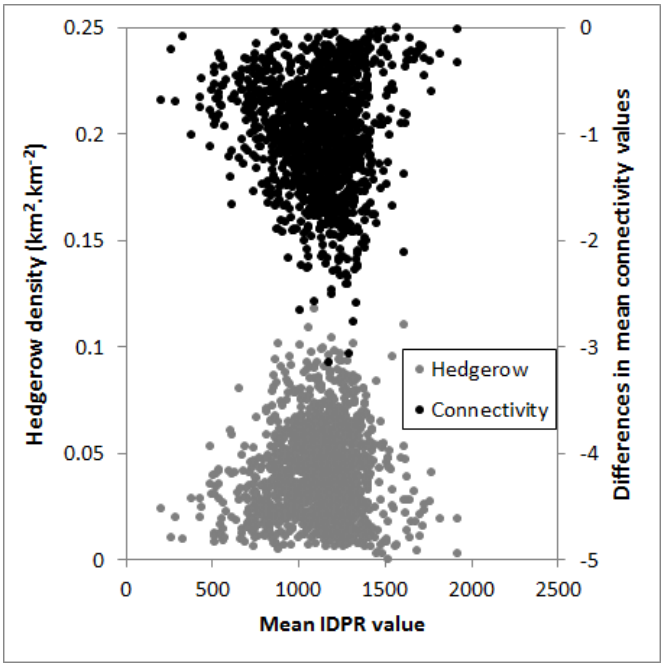

FIGURE 8.9 – Relation at the watershed scale between hedgerow density and mean $IDPR$ values and differences in connectivity and $IDPR$ values

8.3.3 Connected erosion from hillslopes to water systems

The map of rill and interill erosion from Cerdan *et al.* (2010) [37] provides a quantification of hillslope erosion in Europe (see page 85). At the pixel scale, in order to obtain values of connected erosion, the values of gross erosion are multiplied by the hybrid map of sediment connectivity resulting from the computation of $IC_{revised2}$ where the hedgerow data are available and of the $IC_{revised}$ over the rest of the territory. In order to have positive values of connected erosion, the connectivity values at the pixel scale are first resampled between 0 (no connectivity) and 1 (full connectivity). The map of connected erosion at the pixel scale is proposed in Appendix F. We want to draw the attention of the reader on the fact that the provided quantitative values of connected erosion are indicative of magnitude only and should be taken with caution.

In this study, the focus is put on the qualitative analysis of potential connected erosion and the comparison between watersheds. The map of mean connected erosion per watershed (Figure 8.10) helps to answer the question "which of the watersheds within the $LBRB$ deserve more attention in terms of protective measures against soil erosion and on-land sediment transfers?". From this Figure, it appears that most of the watersheds displaying medium to high connected erosion rates are located at the centre

and to the west of the *LBRB* and in the surroundings of the *Allier* river.

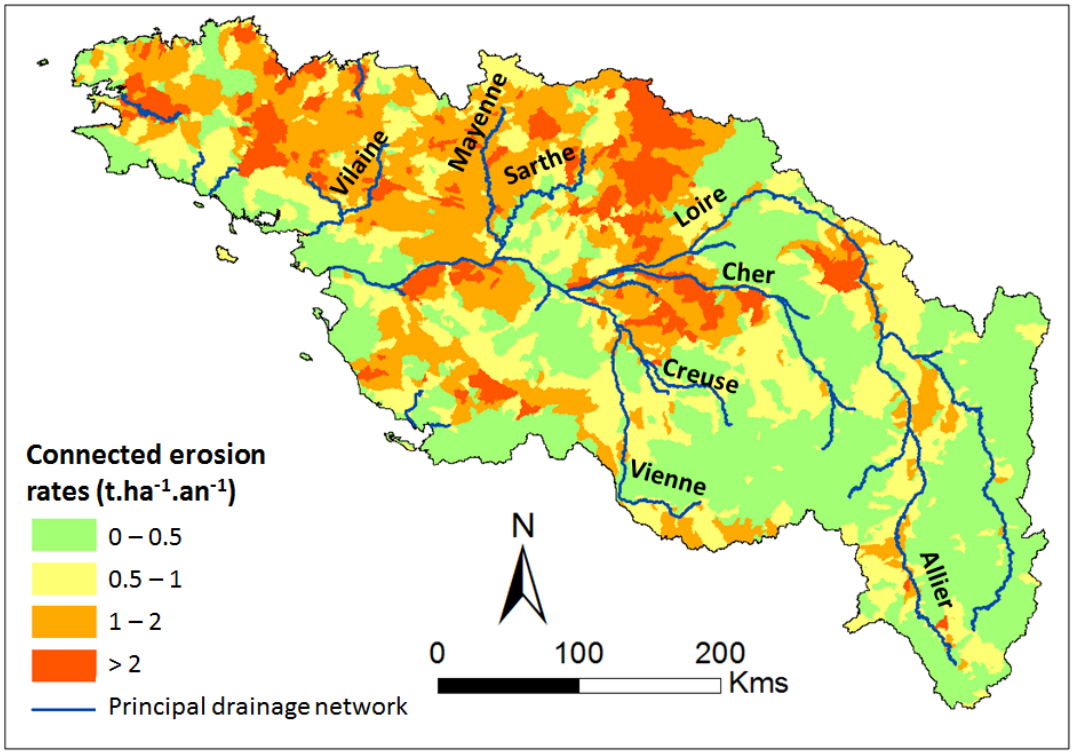

FIGURE 8.10 – Map of hillslope connected erosion rates (particule sources: rill and interill erosion) from the combination of rill and interill erosion (Cerdan *et al.*, 2010 [37]) and connectivity from $IC_{revised}$ and $IC_{revised2}$ (this study)

Considering the maps of connectivity, erosion and connected erosion, one can notice that three combinations may be possible. First, high sediment connectivity combined with low erosion rates, *e.g.* in the Massif Central, result in low connected erosion values as little sediment is available for transport. Second, high erosion rates combined with low sediment connectivity results in low to medium connected erosion. This combination is observed in the Beauce region, downstream from the confluence of the *Loire* and *Allier* rivers or to the East of the *Vienne* river. Finally, the combination of high erosion rates and low sediment connectivity can result in high connected erosion rates, *e.g.* to the north of the Brittany region or in the Parisian basin, to the east of the *Sarthe* river.

The resulting connected erosion from the first two combinations is rather obvious and indicate that little erosion combined with high connectivity can have the same influence in the hillslope sediment budget than high erosion combined with low connectivity. Concerning the third combination, the most likely explanation is linked to the spatial scale of the considered maps: at the pixel scale, the spatial distribution of high erosion rates and low connectivity values, observed at the watershed scale, do not coincide. In these watershed, the combination of high erosion rate and high connectivity

may represent a small fraction of a watershed area but are enough to explain the mean values of connected erosion of the watershed.

From this result, it is clear that maps of erosion and connectivity cannot be considered separately in decision making. Furthermore, the combination of distributed erosion rates and distributed connectivity values at the pixel scale is primordial to define mean connected erosion rates or classes at the watershed scale.

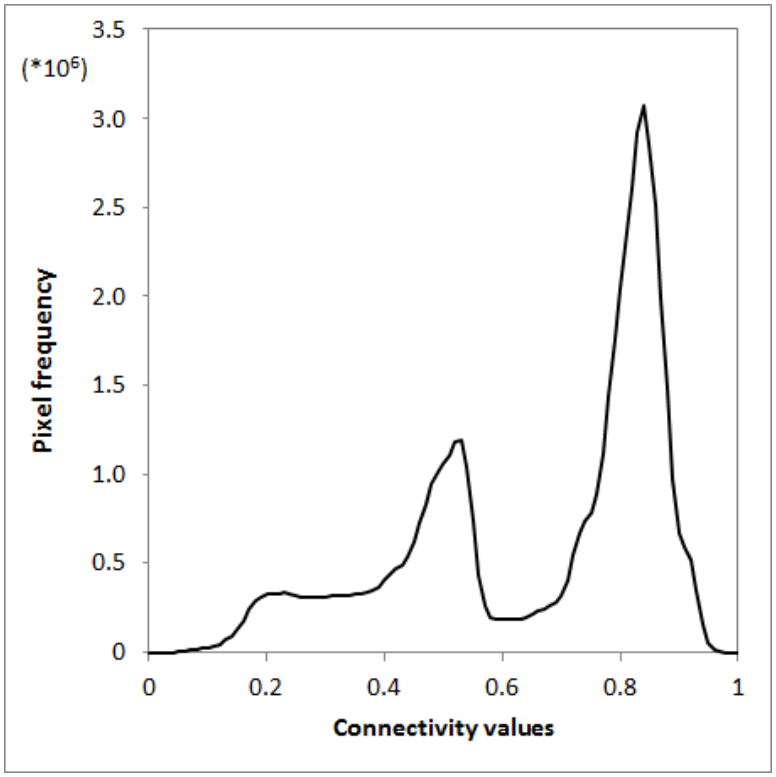

FIGURE 8.11 – Frequency of connectivity values resampled between 0 and 1 at the pixel scale

The resampling of connectivity values between 0 and 1 allowed us to provide a preliminary insight in patterns of connected erosion. Still, this approach corresponds to a worst case scenario as i) the lack of hedgerow data in some departments of the *LBRB* (north of Brittany) may induce overestimation of connectivity in these areas, and ii) the proposed resampling of $IC_{revised2}$ values implies that in more than half of the pixels, 75% of the material available is transported to the river system (Figure 8.11). However, in-zone deposition and in field deposition generally exceed sediment transfer to rivers (Walling and Collins, 2008 [303]). Further researches are thus needed to calibrate the resampling of the connectivity values.

Furthermore, in the present study, the potential given to the hedgerow network to stop particles is very low and corresponds to a low hypothesis of the effect of hedgerows. Indeed, while very fine particles may not be stopped by hedgerows, between 70 and 90% of fine particles (and up to 99% for coarse particles) may be deposited at the hedgerow

edge (Ouvry *et al.*, 2012 [216]). In the present study, less than 40% of particles are being stopped by the presence of such obstacle. Therefore, there is also a need to calibrate the values given to the $P - factor$ (Figure 8.3, page 178) in order to increase the role of hedgerows. This stage cannot be realised without calibration and validation data on sediment transport for the study area and the knowledge of the spatial distribution of hedgerows and of some properties of such features (*e.g.*, presence of an embankment to support the hedgerow, age of the hedgerow).

8.4 Conclusion and perspectives

The inclusion of two factors, the $IDPR$ (see Chapter 7) and the hedgerow network in this study, has allowed to take into account three major characteristics of lowland areas. On the one hand, the $IDPR$ accounts for landscape process-based overland flow through infiltration and saturation properties but also implicitly for the presence of drain tiles and ditches network and constitutes a first condition to sediment movement and thus to the sediment connectivity. On the other hand, the hedgerow network allowed us to consider barriers to sediment from hillslopes to water systems as a secondary condition to sediment transfers.

The introduction in the $IC_{revised2}$ of hedgerow properties and location in the landscape has led to a decrease in connectivity values and disconnection of entire areas from the river network. Though our study is limited by the spatial availability of the hedgerow data, the availability in both densely and poorly covered areas with hedgerow networks, allowed us to draw comparison between model outputs. At the watershed scale, a new map of hillslope connectivity is proposed. Most of the changes in connectivity classes are located in the Massif Armoricain and correspond to the extensively developed bocage in this region. Nonetheless, **our results indicate that the hedgerow location has greater influence in sediment transfers than hedgerow density.** Therefore, there is a need to take into account the presence of hedgerow in the sediment connectivity assessment even in case of low hedgerow density.

Finally, **we propose a map of connected erosion by combining hillslope erosion and sediment connectivity**. Our results emphasise the importance of taking both parameters into account in decision making and not just one or the other. Especially, the spatial distribution of both parameters has to be evaluated before aggregating values at larger spatial scale.

Once more, the index of connectivity has proved to be highly flexible and a promising tool in the sediment connectivity assessment. Still, studies need to be conducted to improve our understanding of hedgerow efficacy at the catchment scale and to integrate such properties into the model. Indeed, in this study, we considered hedgerows as barriers to sediment disregarding the amount of sediment arriving at the edge of the hedgerow or the magnitude and duration of the rainfall events. Further researches on this topic may help to fix a percentage of sediment and water trapped and that may reflect an average situation over several years (Van Oost *et al.*, 2000 [285]). Moreover,

crop rotations should also be taken into account in the $C - factor$ values (Gabriels *et al.*, 2003 [96]) as they are likely to modify the connectivity throughout the year.

In the present study, only the transfer of the particulate phase is considered. However, hedgerows play an important role in the reduction of excess of nitrates (Grimaldi *et al.*, 2012 [113]) and phosphorus (Lee *et al.*, 1998 [162]) to rivers. As an interesting perspective, the index of connectivity combined with the spatial distribution of the hedgerow network may help to estimate the inputs of nutrients from land to rivers in the $LBRB$.

Chapitre 9

Conclusion générale et perspectives

9.1 General conclusion

The main purpose of this study was to propose a sediment budget for the Loire and Brittany river basin, and to take into account the spatial distribution of processes and parameters involved in the different aspects of the sediment cycle. Our approach is built around the three main components of the sediment budget: the identification and quantification of sediment supply sources, their transfer (in)to water systems, and their exports to the catchment outlet. The originality of this study lies in the viewpoint we adopted which consists on giving an overview of the functioning of a very large territory rather than focusing on highly detailed processes involved in the sediment cascade. In this respect, the outcomes of this study open new opportunities of researches both at the Loire river basin and world-wide scales.

9.1.1 Outcomes of the present study and direct applications

A global contribution from this work is related to the fact that **we consider a lowland area and the associated specificities** of this landscape. Indeed, research efforts have mostly focused on very specific small areas within catchments or a certain type of catchments, primarily mountainous and (semi)-arid. However, in the context of climate change and sustainable development, sediment redistributions are becoming a key issue in agricultural lands of temperate areas.

In this context, we have provided a certain number of data, propositions and applications for the evaluation of the aspects of the sediment budget for one lowland area. In general, our study has highlighted the strong spatial variability that exists in all three components of the sediment budget within this area. This unexpected variability emphasizes the need for a better understanding of the functioning of flat agricultural lands. We hope that such contribution will promote research efforts on the sediment cycle in other lowland landscapes.

The second outcome of this study is **the development of a large database of suspended and dissolved sediment yields**. This work constitutes a basis for the comparison with other rivers exports but also for further analysis of the sediment production and transfer within each catchment. This database can be used as a calibration/validation dataset for the development of complete models of sediment re-

distribution. Nested catchments seem particularly promising for investigations on the sediment dynamics and evaluate transfers at different spatial scales.

The dual approach combining solid and dissolved exports at the outlet of 52 catchments underlines the predominant contribution of the dissolved loads in total exports. This work constitutes a basis for a finer understanding of the physical and chemical processes of the biogeochemical cycle and in the soil denudation rates.

The consideration of the **different sources of sediment**, namely sheet and rill erosion, gully erosion, mass movement, and bank erosion, provides an overall picture of the sediment availability in the $LBRB$. The major progress provided by this study is the **development of a methodology to quantify mass movements and the application of a global model for the estimation of bank erosion** on a large territory.

Though the $LBRB$ is less prone to mass movements than mountainous catchments and this form of erosion represents less contribution to the sediment budget than other sources, it is our concern to evaluate the entire potential sediment supply. In this respect, we have developed a method for the quantification of the detachment of particles through mass movement. This method is rather simple, allows for the production of hazard maps as much as cubing of sediment removed, and is easily repeatable due to the low number of required data.

So far, less attention has been paid to bank erosion processes and quantifications than to hillslope erosion. In this study, we apply a simple model of bank retreat to provide quantified erosion rates from banks. Despite the low contribution of banks to the overall sediment supply of detached particles, the direct connections between this source and the river system suggest that bank erosion cannot be neglected in the sediment budget and may contribute significantly to the suspended load at the catchment outlet.

Based on previous works taken from the literature, **a semi-distributed index of connectivity is adapted from our understanding of the dominant processes and parameters involved in sediment transfers in lowland areas.** The new index allows for the consideration of the process-based connectivity through the generation of overland flow by the topography in steep areas, and by soil saturation in flat areas. This tool seems really promising for application over the French territory where all input data are available and flat areas represent 29% of the country. Due to the easy handling of the index and calculation of the $IDPR$, other applications in European countries can be achieved.

Moreover, the integration of the hedgerow network as structural element of the connectivity has confirmed the flexibility of the index. In this way, the final index of connectivity can be used for conservation practices purposes by using different *scenarii* of landuse cover and help to promote the implementation of hedgerows in highly connected areas.

In fine, this index of connectivity helps in the identification of the hotspots of hillslope connectivity. Coupled with the hillslope sediment sources, it provides an estimation of the connected erosion that reach the stream network.

Finally, throughout this study we have provided **various spatial representations and aggregations of our results** on sediment sources and transfers. Each of these representations results from a compromise between the information at the local scale (pixel, stream section) which may not be relevant if considered alone, and the $LBRB$ scale. By these different representations, we have aimed at targeting different communities.

On the one hand, the catchment is generally considered as the fundamental unit of studies on sediment dynamics. Therefore, the different components of the sediment budget are evaluated and provided at this spatial resolution. The choice of this working scale also results from the constraints linked to the calculation of suspended sediment yields and from the data availability for this work.

On the other hand, stakeholders generally use other geographic (hydrologic) breakdowns in the decision-making process. The considered units are smaller than the catchment scale as defined in this study. We have thus aimed, when possible, at providing a decision support tool using different spatial aggregation of our results. We believe that stakeholders are starting to play an important part in the research activities. Hence, it is our responsibility to provide them with suitable tools.

The use of homogeneous database and models over the entire study area allows for a strict comparison of the trends observed at the different spatial scales. Most of these database are available at the national scale and for some of them, at the European scale. Thus, direct applications of the proposed models can be realised on the five other hydrographic basins of the French metropolitan territory.

9.1.2 A glimpse to the sediment budget of the Loire river

The quantifications provided by the individual sources of sediment and their connectivity have been synthesized to establish an annual sediment budget for the Loire river basin (Figure 9.1). Despite the limits inherent to the quantification of processes at large spatial scales and the missing information on some sediment sources (field drain tiles and stream bed incision) or deposition (overbank and in channel) in the proposed budget, which are discussed hereafter, we are confident on the trends and the proportion of each of the compartments. The proposed sediment budget is the first one of the sort in the Loire river basin and gives an insight into sediment supply and deposition within this area.

The proportion of the contribution of each source to the sediment supply is consistent with the data found in the literature (*e.g.*, Walling and Collins, 2008 [303]). Several elements, especially in-channel sources and deposition, have not been estimated yet (see next section for the limits of the present study). A sediment budget is established

for each of the 77 catchments within the Loire and Brittany river basin (see Table in Appendix G). Very slight differences in the contribution from each source exist. But in general, similar trends as the one proposed here are observed, *i.e.* highest contribution to sediment supply from the sheet and rill erosion.

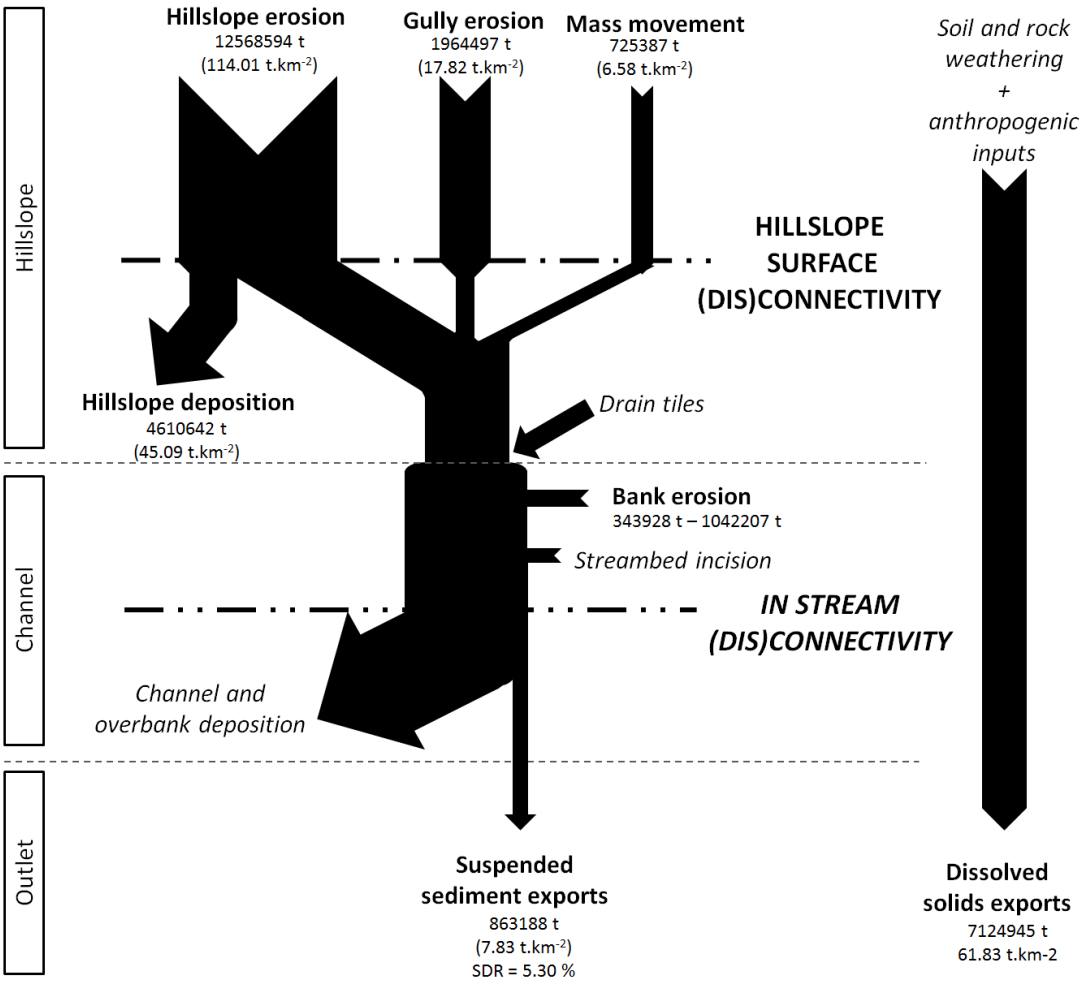

FIGURE 9.1 – The suspended sediment and dissolved solids budget of the Loire river basin. Italic characters indicate sources, sinks and connectivity processes that have not been considered in the present study and remain to be quantified

Limits of the approach and perspectives

In this section, we give the different limits of the present study in order to provide the reader with a full understanding of the benefits and drawbacks of the developed approaches. Some perspectives of research on sediment transfers in the *LBRB* follow on logically from these limits and from the gaps in the proposed sediment budget. Several

achievable goals in an immediate future (regarding data availability) are identified and proposed along with other perspectives in the medium to long term. Besides, we point out the researches that need to be carried out at broader scales.

From a qualitative view point, we have proposed a comparison of erosion, transport and deposition patterns at different spatial scales. The modelling of each of these three aspects results from the combination of our understanding of parameters and processes involved, our knowledge on the functioning of the study area from field observations, and a compromise between the data availability and the ability of our models to reflect these driving processes/parameters. For all these reasons, we are confident in the general trends provided for the different compartments of the sediment budget.

From a quantitative viewpoint, **one of the major limit of the outcomes of the present work is the lack of terrain data to calibrate and validate the proposed models, namely bank erosion and hillslope sediment connectivity.** In-field data acquisition and a study of the uncertainties of both models are needed to provide a confidence interval for the quantified rates. Though the sediment yield database provided in this study may help in the calibration and validation of the different compartment of a *complete* sediment budget, all sources, transfers and deposition areas have not yet been quantified (see further in the text). The use of fallout radionuclide (^{137}Cs) and other tracing techniques that have emerged during the last decade should help to define the proportion of sediment delivered from hillslope surface and subsurface/bank compartments (*e.g.*, Walling, 2005 [302]). A study has already been undertaken for 6 small catchments within the study area. Yet, the results do not allow for a strict comparison of bank and surface sources. Further investigations and terrain data may contribute to clarify these contributions.

Three components of the sediment budget, that we believe to be the next most important aspects to take into account, have not been estimated yet. These are related to i) the supply of fine sediment *via* the networks of buried drain tiles, ii) the stream sediment connectivity which could help in the prediction of in-channel and overbank deposition, and iii) the incision of the streambeds.

At present, there have been some evidence of hillslope surface sediment transfers through the network of buried pipes (Cooper *et al.*, 2015 [46]). However, the proportion of particles transported in this subsurface area results from complex processes that have not all been quantified yet. Still, the consideration of drain tiles in sediment budgeting is a crucial issue as water and sediment are no more under the influence of surface (dis)connectivity and can thus be directly transferred to the stream network. Moreover, the drains may also participate as a supplier of sediment (Sogon *et al.*, 1999 [262]) through the leaching of the finest fraction of soils and their transfer through the drainage network. We have proposed a map of probability of the presence of drain tiles in agricultural lands. However, if this map can be used to predict the hydrological connectivity of a catchment, it does not allow for an evaluation of the sediment connectivity in buried pipes. **Field experiments are needed to evaluate the contribution of field drain tiles both as source and vector of particles.** In 2015, a project has been launched to evaluate the supply of sediment that flows through

the drain tiles in the intensively drained catchment of the *Bonnée* river, a right bank small tributary of the mid-Loire river (length = 27km). Results from these experiments should help to understand the dynamics of sediment in the buried drainage network.

In the river, **the sediment disconnectivity that knickpoints cause upstream the features and streambed incision and enhanced connectivity downstream** has been highlighted at fine spatial scales (*e.g.* study of the *Ligoire river*, Appendix D). In the *LBRB*, the ROE database (*Référentiel des Obstacles à l'Ecoulement*) indicates that 20688 obstacles of various types (dams, weirs, locks, spillways, *etc.*) are present. This database provides information on the nature of the knickpoints and the height of waterfall downstream. However, **their impacts on the channel morphology, on the sediment (dis)connectivity, and their storage capacity remain to be evaluated with quantitative tools.** A stream sediment connectivity index partly based on the presence or absence of such features and their sediment storage capacity (*e.g.*, SedNet model, Prosser *et al.*, 2001 [233]), and on flow discharge should provide a first evaluation of the sediment transfers within river systems.

As for streambed incision, the study on the *Ligoire* indicates that such process can be found downstream knickpoints but also participate in the headwater stream retreat. However, incision remains clearly understudied and poorly understood at broad spatial scales and should deserve more attention from the scientific community.

Finally, one aspect that has been left aside by the connectivity community and in this study is the forcing exerted on the landscape. In Western Europe, this involves **pressures on soils from agricultural practices and the climatic disparities that exist between regions, primarily linked to the total rainfall and the rainfall intensity.** For example, the climate of the Brittany region is very wet but for the same amount of rainfall, the intensity is far less beyond that of the Massif Central. The integration of rainfall intensity would certainly modify the patterns of connectivity within the *LBRB*. In lowland areas, we suggest that the time lapse between rainfall events has also to be considered for the evaluation of soil infiltration capacity (due to antecedent soil moisture) and thus, the generation of overland flow due to saturation. The SAFRAN database provides information on daily rainfall amount that should help in the introduction of this parameter in a dynamic index of connectivity. Moreover, this rainfall forcing is also to be considered in the light of changes in land cover and crop rotation throughout the year in agricultural lands (Degan *et al., in prep* [67]).

From a broader perspective, throughout this study, we have attempted to highlight the lack of consideration of lowland areas in studies on sediment dynamics and of the impact of inherent properties of this particular landscape on sediment transfers. *There is a real need for a better understanding of the sediment production, storage and transfers within lowland areas at the local and the catchment scales.* Two other major points should also be considered in further researches. The first one concerns the magnitude of the forcing exerted on the system and the identification and quantification of such forces. Research efforts should help to define thresholds in the generation of process-based (dis)connectivity. Secondly, stakeholders are increasingly taking part in research activities and are also direct users of results of sediment transfers works and in the

financial support of such studies. Therefore, they should be included in our research works to bring alternative dimensions, applications and perspectives to the works on connectivity.

Annexe A

Characteristics of the 77 catchments

Code station (BANQUE HYDRO)	Mean slope (%)	Maximum slope (%)	Maximum altitude (m)	Mean altitude (m)	% de slope < 2%	Area (km^2)	Perimeter (km)	Gravelius index	Drainage Density ($km.km^{-2}$)	Mean IDPR (-)	Median IDPR (-)	Mean flow discharge ($L.s^{-1}$)	Utilised Agricultural Land (UAL, %)	Percentage of UAL with drain tiles	Urban areas (%)	Arable land (%)	Mean annual rainfall (mm)	Specific sediment yield ($t.km^{-2}.yr^{-1}$)	Specific sheet and rill erosion ($t.km^{-2}.yr^{-1}$)
J0201510*	4.18	54.40	245	100.25	26.23	856.07	177.22	1.71	1.15	1227.16	1056	7722.16	93.46	3.84	2.46	42.27	876.75	16.03	140.85
J0611610*	4.36	21.00	310	148.99	15.40	143.46	74.29	1.75	0.65	861.59	905	1219.20	93.75	11.47	1.20	52.59	891.01	14.04	211.27
J1114010*	3.79	38.20	186	96.97	32.46	113.29	69.83	1.85	0.43	736.29	756	744.45	86.34	5.13	2.23	54.76	835.01	6.26	191.01
J1313010*	3.31	34.30	337	100.44	35.08	244.05	85.74	1.55	0.73	936.07	967	1442.69	89.40	4.24	2.81	58.57	828.13	7.18	153.10
J1324010*	5.54	41.20	339	128.79	20.25	139.42	65.63	1.57	0.95	1099.43	1000	1068.99	94.62	0.44	1.86	52.33	884.34	9.93	174.20
J1513010*	6.14	38.70	322	213.16	8.95	135.68	62.01	1.50	0.81	1004.65	992	1671.13	86.09	0.97	2.32	45.35	1098.64	10.41	141.27
J1721720*	6.36	49.40	307	180.18	14.55	413.85	121.29	1.68	0.81	1015.83	1000	5264.39	85.49	7.85	3.21	40.85	1074.00	12.55	76.57
J1813010*	3.70	39.10	284	115.63	38.31	341.49	111.04	1.70	0.73	960.41	966	2720.40	89.88	41.11	1.97	55.95	963.48	9.02	159.70
J2023010*	4.63	35.50	301	121.04	27.67	165.13	64.51	1.42	0.86	1074.06	1000	1730.67	93.82	7.32	2.15	47.70	975.84	13.36	65.51
J2034010*	3.81	34.20	301	83.50	31.57	121.82	72.76	1.86	0.87	1072.27	1000	1224.74	97.40	22.01	1.40	56.40	959.76	14.42	209.66
J2314910*	6.64	35.50	258	145.54	14.59	58.50	45.88	1.69	0.93	1178.84	1028	793.96	86.75	0.00	0.60	35.87	1054.84	13.28	47.78
J2614020*	7.85	42.10	367	165.62	11.16	95.29	50.68	1.46	0.80	1035.99	1000	1670.63	79.07	0.00	1.87	34.68	1273.66	11.81	163.40
J3014310*	3.63	22.10	128	84.17	31.62	50.49	37.04	1.47	0.87	1076.65	1000	700.32	95.95	47.95	2.54	68.68	1043.30	12.82	207.71
J3413020*	6.55	50.90	382	138.21	12.26	200.66	75.31	1.50	0.90	1102.39	1000	4333.99	84.06	0.00	4.25	42.14	1223.57	15.57	140.23
J4014010*	6.37	40.20	167	80.08	14.71	88.87	65.63	1.96	0.95	1078.68	1000	1414.78	95.84	0.00	1.17	50.15	1012.52	5.19	70.23
J4211910*	7.27	65.80	294	144.16	8.02	202.72	82.56	1.64	0.95	1105.63	1000	4774.77	93.27	0.00	1.93	43.53	1276.77	15.37	209.14
J4742010*	7.32	56.60	309	163.40	11.48	574.59	144.70	1.70	1.13	1250.60	1085	9372.37	86.48	0.00	1.29	41.84	1228.95	11.45	120.93
J4902011*	7.06	56.60	309	151.23	12.75	851.71	162.20	1.57	1.10	1222.01	1064	13570.57	86.80	0.13	2.01	43.16	1226.37	11.36	105.56
J5102210*	7.45	79.50	272	143.67	8.79	299.48	114.23	1.86	1.22	1290.82	1121	4767.34	81.84	0.00	0.95	39.00	1226.46	13.59	134.32
J7000610*	4.69	29.70	224	157.03	20.26	56.82	34.58	1.29	1.09	1303.57	1122	465.63	97.06	0.00	0.56	40.86	898.41	11.17	188.70
J7010610*	5.08	39.20	223	138.29	18.50	146.79	79.15	1.84	1.04	1261.60	1087	1246.01	94.81	0.43	2.60	40.18	900.47	9.43	207.93
J7060620*	4.29	72.10	224	116.29	25.05	566.97	141.53	1.68	0.98	1234.03	1068	4228.67	90.84	2.47	3.40	44.21	875.41	8.21	214.60
J7083110*	3.98	50.20	138	96.68	26.69	151.28	71.46	1.64	1.00	1200.79	1023	1102.92	91.27	0.00	2.37	37.84	868.34	12.70	154.79
J7103010*	2.20	24.30	119	77.55	59.37	102.60	59.25	1.65	1.14	1141.35	1016	641.76	84.42	19.81	1.35	40.31	798.15	2.94	65.71
J7114010*	3.63	21.30	121	82.17	30.50	111.22	55.69	1.49	1.06	1201.57	1029	732.77	77.86	0.00	2.35	27.61	844.13	7.12	70.88
J7214010*	3.39	14.40	152	96.25	25.21	91.69	44.90	1.32	0.89	1120.03	1026	520.07	95.75	0.00	2.79	55.67	781.86	10.12	165.71
J7700610*	3.57	72.10	272	81.02	31.53	4146.39	481.86	2.11	0.91	1140.20	1010	25704.28	87.06	7.19	4.98	44.72	806.29	11.86	161.18
J8002310*	5.71	24.60	316	218.65	13.00	28.42	23.99	1.27	0.92	1131.04	1012	390.95	97.51	22.91	0.12	44.29	1126.48	13.22	320.06
J8133010*	6.68	44.00	336	198.19	7.85	298.65	84.22	1.37	0.89	1105.91	1000	3445.41	86.82	9.30	1.02	42.50	949.69	13.03	133.17
K0454010*	15.81	72.40	1384	951.48	2.09	217.46	85.16	1.63	1.03	1185.25	1036	3226.55	49.23	0.00	1.48	9.84	824.50	3.16	33.05
K0550010*	14.09	110.60	1725	965.99	4.11	3249.13	368.50	1.82	0.96	1128.54	1000	36386.12	67.18	0.30	1.12	10.30	824.40	8.98	49.74
K0614010*	16.91	88.20	1304	658.26	4.45	174.53	94.86	2.03	1.10	1127.57	1000	2398.32	50.19	0.21	28.45	8.45	797.80	29.09	24.47
K1173210*	7.92	53.60	754	357.51	7.29	591.25	151.39	1.76	0.85	1066.71	1000	5611.53	79.34	4.18	0.84	14.66	874.91	14.91	23.25
K1363010*	7.56	66.10	651	340.30	9.06	338.77	99.33	1.52	1.00	1163.66	1028	3271.14	70.11	4.33	13.16	14.59	884.90	18.75	15.35
K1383010*	6.11	66.70	651	316.19	14.02	818.93	176.66	1.74	1.06	1188.50	1037	7613.23	74.31	6.74	7.30	14.04	866.31	17.67	18.88
K1773010*	7.51	63.90	838	297.80	15.03	1465.53	209.88	1.55	1.13	1190.63	1034	17458.75	74.27	9.40	0.52	10.86	943.84	19.65	39.10
K2090810*	15.44	83.70	1500	1127.41	3.30	518.69	132.28	1.64	1.15	1234.64	1062	11402.90	59.36	0.00	0.52	24.70	865.88	4.71	53.68
K2330810*	16.17	119.40	1549	1042.42	3.60	2260.13	300.95	1.79	1.06	1208.64	1037	29204.75	66.71	0.00	0.36	21.17	752.24	5.50	53.60

Code station (BANQUE HYDRO)	Mean slope (%)	Maximum slope (%)	Maximum altitude (m)	Mean altitude (m)	% de slope <2%	Area (km^2)	Perimeter (km)	Gravelius index	Drainage Density ($km.km^{-2}$)	Mean IDPR (-)	Median IDPR (-)	Mean flow discharge ($L.s^{-1}$)	Utilised Agricultural Land (UAL, %)	Percentage of UAL with drain tiles	Urban areas (%)	Arable land (%)	Mean annual rainfall (mm)	Specific sediment yield ($t.km^{-2}.yr^{-1}$)	Specific sheet and rill erosion ($t.km^{-2}.yr^{-1}$)
K2821910*	12.64	67.70	1137	941.77	2.45	105.20	61.63	1.70	0.98	1185.44	1001	1119.98	30.84	0.00	0.11	6.00	894.46	7.27	19.96
K3153010*	3.84	45.60	591	349.38	45.60	209.20	82.92	1.62	0.83	984.00	985	970.70	90.46	54.04	3.25	60.11	772.48	13.51	100.51
K3373010*	7.25	58.80	766	438.31	11.48	560.77	141.56	1.69	0.89	1096.32	1000	3930.02	83.24	6.18	1.12	18.84	775.88	18.32	61.02
K3650810*	11.68	134.70	1847	658.06	15.08	14347.44	953.37	2.25	0.98	1133.51	1000	123982.70	71.24	10.61	2.19	20.53	826.91	12.22	67.22
K4094010*	4.71	39.00	382	236.10	23.70	475.82	114.81	1.48	0.34	532.44	425	3345.89	76.27	2.70	0.58	62.53	828.43	5.01	115.10
K4873110*	2.14	27.20	171	130.25	66.06	261.16	104.34	1.82	0.97	1198.19	1042	1279.82	87.58	44.86	1.90	81.28	701.55	10.43	191.07
K5183010*	6.68	65.00	830	506.77	15.89	859.17	921.05	8.86	1.04	1231.60	1068	8744.95	89.22	1.38	0.56	8.36	917.07	5.73	20.06
K5383010*	5.66	48.00	649	341.73	13.56	927.18	160.92	1.49	0.93	1136.18	1000	6737.29	91.80	4.62	0.95	11.45	775.92	11.92	50.66
K5490910*	5.93	75.50	830	360.14	21.90	4520.05	531.25	2.23	0.91	1095.46	1000	33841.84	85.07	7.83	1.73	19.56	810.01	8.26	46.30
K6720910*	3.76	75.50	830	230.42	42.62	13677.97	921.05	2.22	0.80	983.41	1000	96346.00	77.20	28.42	2.21	39.06	781.82	12.27	112.54
L0700610*	9.87	78.70	952	472.53	5.19	3387.16	338.09	1.64	0.94	1139.71	1011	59410.64	64.86	0.19	2.81	8.99	1112.91	14.07	81.78
L0914020*	6.12	39.40	516	314.48	6.73	180.03	66.88	1.41	1.16	1353.15	1166	1901.95	81.75	1.40	0.54	15.79	1056.65	16.42	117.24
L2253010*	3.36	31.80	270	167.98	37.85	304.41	100.37	1.62	0.66	826.10	880	3070.14	89.34	25.79	0.90	47.19	877.59	7.51	167.12
L2501610*	2.72	41.30	270	140.29	53.03	2852.91	365.63	1.93	0.45	601.81	430	22322.75	85.22	37.85	3.34	59.72	802.25	6.02	162.42
L4220710*	9.87	69.30	950	534.61	5.38	1233.23	255.76	2.05	0.91	1120.20	1000	15633.65	74.47	0.00	1.24	24.98	1003.42	7.41	37.79
L4411710*	6.44	53.70	655	392.03	8.18	853.13	174.84	1.69	1.04	1187.92	1031	8410.17	92.93	0.00	0.61	17.59	886.74	15.85	28.40
L5223020*	7.57	79.50	585	323.02	11.41	285.55	99.12	1.65	0.98	1201.42	1047	3486.58	69.30	0.00	1.75	40.78	1085.59	11.91	20.77
L7000610*	5.61	79.50	952	266.05	27.27	19817.31	907.30	1.82	0.82	1037.89	1000	192796.49	80.10	15.47	1.81	25.98	894.67	11.41	92.76
L8000010*	6.80	134.70	1847	359.78	30.73	80999.34	2047.84	2.03	0.88	1062.18	1000	608935.36	74.22	19.65	2.34	42.50	823.93	9.07	89.73
M0050620*	4.44	51.80	410	184.04	33.72	906.05	158.36	1.48	0.99	1127.14	1000	7076.81	85.04	23.67	2.35	25.70	809.49	14.90	146.36
M0114910*	6.32	51.20	362	213.96	10.64	118.40	57.65	1.49	1.05	1193.85	1002	1173.44	76.36	0.00	1.91	40.34	894.82	16.24	223.68
M0421510*	5.62	42.80	311	163.96	20.65	1910.77	293.83	1.90	0.76	951.31	972	13094.73	84.24	28.83	1.77	46.92	766.45	11.51	338.63
M0583020*	4.60	36.90	299	121.33	22.67	400.01	118.36	1.67	0.90	1018.95	1000	3185.14	92.05	8.79	1.26	46.78	774.58	11.66	118.61
M0653110*	2.86	21.20	136	84.65	43.20	238.11	100.45	1.84	0.87	1072.27	1000	1490.30	96.91	40.86	1.27	51.43	771.77	12.79	160.90
M0674010*	3.43	21.50	121	83.49	31.01	45.93	34.77	1.45	0.83	1137.14	1028	276.25	94.10	28.37	1.63	48.14	766.05	10.46	230.50
M1041610*	1.77	19.60	285	175.70	73.70	1156.86	214.11	1.78	0.71	873.74	916	3412.59	92.27	68.53	1.20	85.08	664.92	4.94	258.81
M3340910*	5.04	49.90	416	177.92	18.67	2901.17	379.09	1.99	1.18	1268.90	1084	29582.45	91.29	1.71	2.17	41.61	897.23	14.42	147.63
M3514010*	3.40	30.40	137	90.38	33.78	118.62	74.03	1.92	1.03	1239.81	1056	692.94	96.96	31.54	1.04	47.34	782.01	8.72	195.14
M3711810*	3.47	19.70	193	109.23	26.42	133.33	58.53	1.43	1.07	1275.94	1082	889.07	97.30	6.55	1.01	54.54	828.05	6.62	226.26
M3861810*	3.12	35.70	193	73.44	36.18	1416.85	254.44	1.91	0.91	1161.03	1018	7364.11	93.72	12.13	1.72	45.85	763.86	11.12	205.51
M5222010*	2.98	51.30	216	93.33	45.56	918.76	167.10	1.56	0.74	929.12	969	4095.06	94.48	33.76	2.11	33.59	718.63	12.69	215.68
M6014010*	3.01	21.30	140	106.10	38.80	38.26	33.97	1.55	1.13	1302.41	1108	298.22	91.39	4.38	6.89	38.38	762.39	32.44	49.27
M6323010*	2.41	13.60	96	60.74	50.79	98.72	68.83	1.95	0.69	957.67	1000	980.37	96.81	0.57	1.54	32.22	759.98	13.17	123.85
M6333020*	3.08	28.50	96	53.92	40.42	464.64	157.14	2.06	0.79	1024.28	1000	2634.50	89.92	7.58	1.72	34.77	810.76	7.40	161.46
N3001610*	5.97	33.80	276	151.33	10.33	129.53	64.85	1.61	1.06	1258.01	1087	1353.10	94.72	16.84	3.97	36.41	936.28	25.25	173.02
N3024010*	4.80	32.70	231	105.17	14.63	121.85	57.68	1.47	0.94	1179.46	1032	1100.27	95.97	21.60	1.95	46.92	909.29	19.79	196.76
N3222010*	3.46	25.90	136	67.12	28.26	184.87	77.70	1.61	0.88	1014.86	1000	1540.41	88.83	21.72	2.37	65.65	869.86	11.92	185.06
N3403010*	2.71	18.30	108	89.87	47.46	40.55	33.86	1.50	0.93	1328.00	1220	401.60	95.97	32.25	0.62	39.61	899.84	17.33	63.99
N5101710*	5.60	35.00	254	121.13	16.68	244.16	90.97	1.64	0.82	984.55	1000	2509.37	94.19	24.41	1.40	46.26	887.65	13.52	342.77

Annexe B

Equations of bank erosion due to hydraulic forces

Equation	Reference	Parameters
Equations of bank retreat based on stream power		Q_{Bf} the bankfull discharge
$M = 0.025\,(\rho\, g\, Q_{Bf}\, S_x)^{0.53}$	Walker and Rutherfurd 1999 [311]	ρ the water density
$BE = 0.00002\,\rho\, g\, Q_{Bf}\, S_x\,(1 - PR)(1 - e^{-0.008 F_x})$	Bartley *et al.*, 2004 [12]	g the acceleration due to gravity S_x the energy slope (channel gradient) F_x the floodplain width
$LBE = 2.16\, log_e(BA) + 0.31\, log_e PH + 0.77\, OH - 0.016\, VCOV - 6.94$	Laubel *et al.*, 2003 [162]	LBE the log_e-transformed mean bank erosion rate BA the bank angle PH the height specific stream power OH the overhanging bank (0 = no; 1 = yes) $VCOV$ the total vegetation cover
Equations of bank retreat based on mean annual flood discharge		
$M = 0.0435\, Q^{0.6008}$	Rutherfurd (2000) [256]	Q the mean annual flood discharge $Q_{1.58}$ the discharge of 1.58 years recurrence interval flood event assumed to represent bankfull discharge
$BE = 0.016\, Q_{1.58}^{0.6}$	Rutherfurd (2000) [256]	
$BE = 0.008\, Q_{1.58}^{0.6}(1 - PR)$	Prosser *et al.*, 2001 [237]	PR the proportion of riparian vegetation
Equations of (cohesive) bank retreat based on excess shear stress		τ the applied shear stress by flow
$E = k\,(\tau - \tau_c)$	Julian and Torres 2006 [140]; Wynn and Mostaghimi 2006 [338]	τ_c the critical shear stress for entrainment

Annexe C

Probability density function of parameters of the bank retreat model and of bank retreat values

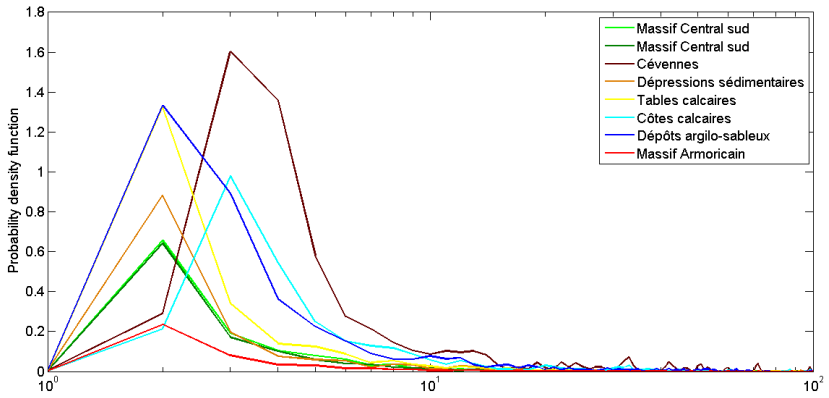

Figure C.1 – Probability density function (kernel density estimator) of the flood discharge values for each *HER*

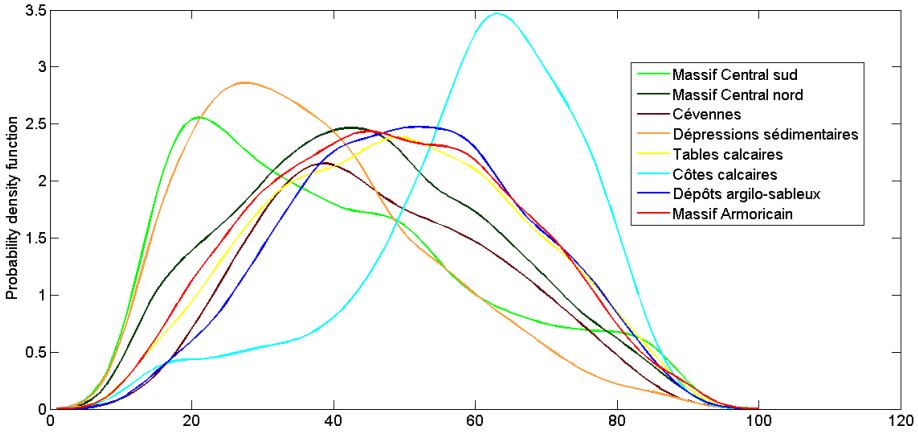

Figure C.2 – Probability density function (kernel density estimator) of the vegetation factor values for each *HER*

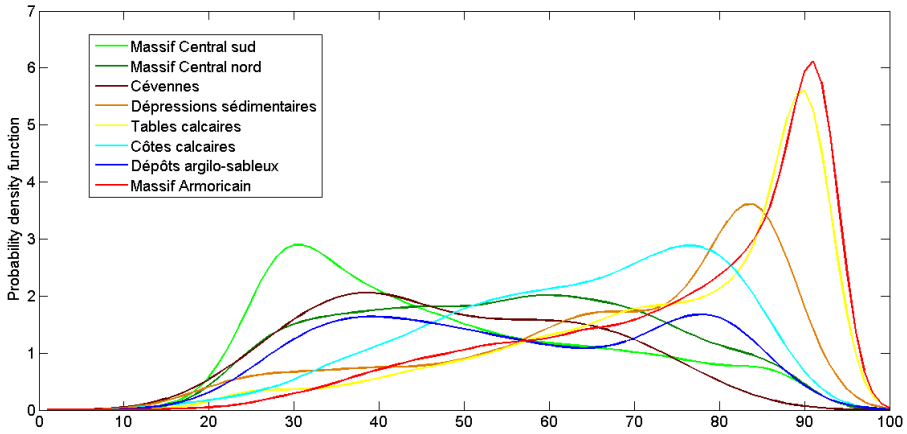

FIGURE C.3 – Probability density function (kernel density estimator) of the floodplain factor values for each *HER*

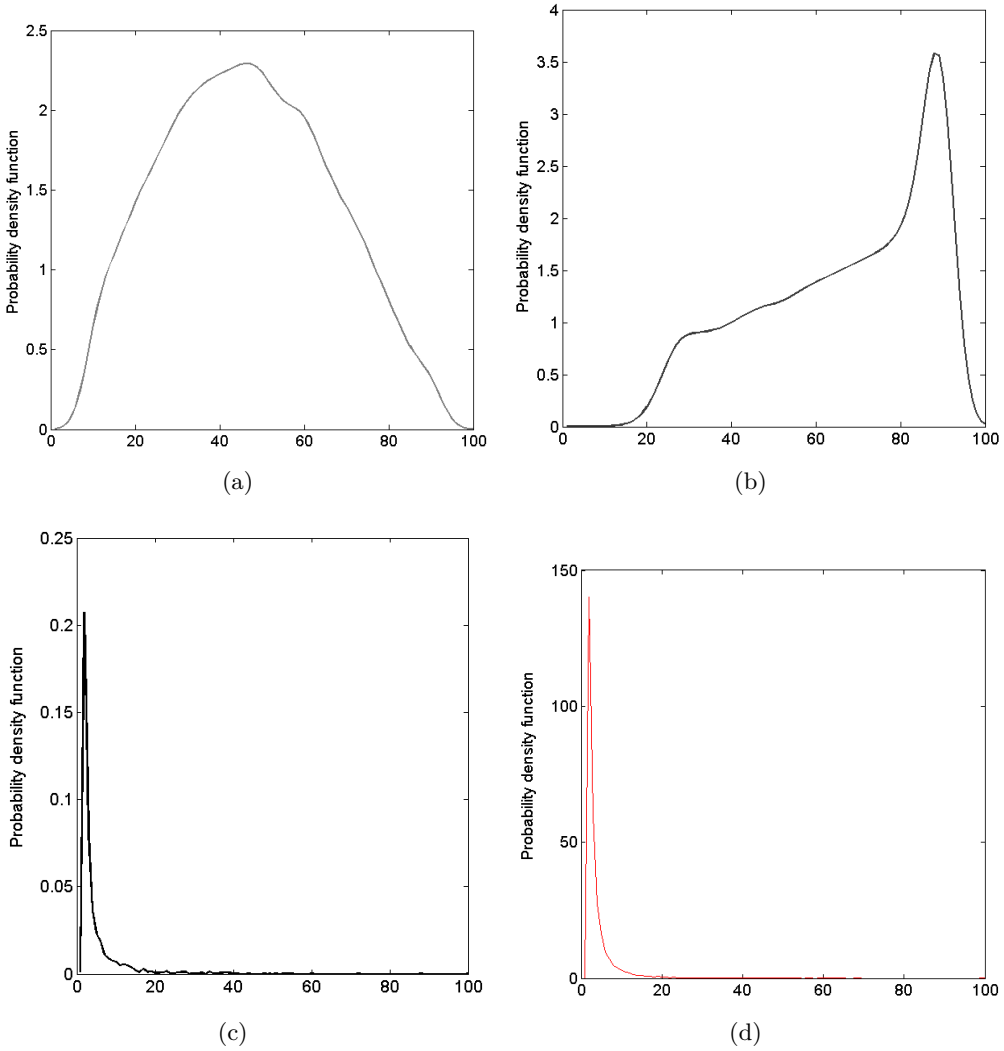

FIGURE C.4 – Probability density function (kernel density estimator) for (a) the vegetation factor, (b) the floodplain factor, (c) the flood discharge, and (d) the bank retreat values

Annexe D

Evolution morphologique après chenalisation d'un cours d'eau de tête de bassin en zone agricole

En parallèle de la modélisation de l'érosion de berges réalisée à large échelle sur le bassin Loire Bretagne (Chapitre 5), une étude sur un petit cours d'eau de plaine a été réalisée afin d'apporter des connaissances sur le fonctionnement des cours d'eau au sein de notre site d'étude.

L'érosion de berges résulte de différents paramètres (endogènes et exogènes) et processus (gravitaires, fluviaux, subaériens). Dans cette étude, un des paramètres exogènes est illustré, la chennalisation dans les années 1970 d'un cours d'eau de plaine en contexte agricole, la Ligoire, ainsi que ses conséquences sur la dynamique hydromorphologique et sédimentaire du cours d'eau. Des documents historiques ainsi qu'une campagne de mesures ont été nécessaires pour évaluer, d'une part, l'impact des opérations sur la morphologie même du cours d'eau juste après les travaux, et d'autre part, sur les réajustements du cours d'eau pour atteindre un état d'équilibre.

Les apports de cette étude sont doubles et concernent, d'une part, la quantification à moyen terme (40 ans) du retrait de berges et des volumes de sédiments exportés et, d'autre part, une spatialisation des zones de dépôt dans le lit du cours d'eau ainsi que des volumes retenus. De plus, l'étude propose une évaluation de la part de la contribution de l'érosion de berges et de l'incision du lit dans le bilan sédimentaire du cours d'eau ainsi qu'une analyse et quantification des incertitudes associées. L'une des principales conclusion de ce chapitre indique que la Ligoire n'est, à l'heure actuelle, pas encore revenue à un état d'équilibre et d'autres réajustements morphologiques du lit et des berges du cours d'eau sont possibles.

Bien que les résultats issus de cette étude ne puissent être valorisés à l'échelle de notre site d'étude, ils apportent des perspectives d'amélioration de la prise en compte des paramètres mis en jeu dans l'érosion de berges dans les modèles. Les résultats ont été publiés dans Geomorphology (Landemaine V., Gay A., Cerdan O., Salvador-Blanes S., and Rodrigues S. 2015. Morphological evolution of a rural headwater stream after channelisation. Geomorphology, 230, 125-137).

Geomorphology 230 (2015) 125–137

Contents lists available at ScienceDirect

Geomorphology

journal homepage: www.elsevier.com/locate/geomorph

Morphological evolution of a rural headwater stream after channelisation

Valentin Landemaine [a], Aurore Gay [a,*], Olivier Cerdan [a], Sébastien Salvador-Blanes [b], Stéphane Rodrigues [b]

[a] BRGM, 3 avenue Claude Guillemin, BP6009, 45060 Orléans Cedex 2, France
[b] GéHCO, Université François Rabelais, Parc de Grandmont – 37200 Tours, France

ARTICLE INFO

Article history:
Received 19 May 2014
Received in revised form 14 November 2014
Accepted 18 November 2014
Available online 22 November 2014

Keywords:
Channelisation
Historical cross sections
Sediment budget
Fine sediment
Uncertainties

ABSTRACT

In recent decades, stream valleys have been profoundly modified by the construction of weirs and dams and by channelisation. Channelisation modifies the morphology of streams and induces changes in their energy regime and sediment transport capacity. These types of changes in the channel morphology have to be quantified to allow the implementation of management strategies to regulate sediment transfer. However, studies over an entire stream using historical comparisons remain scarce, and the associated uncertainties have not yet been resolved.

In this study, the sedimentary response to channelisation on a medium time scale (42 years) of a French river known as the Ligoire is investigated. This river is the main channel of a small rural headwater catchment that has been channelised over 21 km. We have used the historical cross sections before and after channelisation and the current ones, and the objectives of this study were as follows: (1) to develop a methodology of cross section superposition and the associated uncertainties; (2) to quantify the erosion and aggradation processes in the bed and on the banks along the bed profile; and (3) to calculate a sediment budget for the entire stream and determine the relative contributions of the banks and the streambed to this budget.

A comparison of the cross sections before and after the channelisation shows that the morphology of the stream has been completely altered: the main channel length was reduced by 10%, the bankfull width was increased on average by 63%, and the slopes were smoothed. A total of 60,000 m^3 of sediments was excavated during the channelisation works.

Our results indicate that erosion is the dominant process: over 63% of its length, the streambed was incised by 0.41 m on average; and over 60% of its length, the banks were eroded by 0.20 m on average. The successive patterns of erosion and deposition along the stream are the result of the cumulative effects of channelisation and of the presence of weirs and artificial knickpoints in the Ligoire channel.

The vertical uncertainty of the elevation of the historical cross section is an important parameter for controlling the areas and sediment budget values. Using Monte Carlo methods, we found that 1000 sediment budgets from different profile shiftings are necessary to obtain a variation coefficient below 0.1%. The overall mean stream sediment budget for the period 1970–2012 is -9358 ± 412 m^3, with 66% originating from the banks and 34% from the streambed. Relative to the Ligoire watershed surface, the stream sediment yield is 2.71 ± 0.12 $m^3.km^{-2}.y^{-1}$. The approach developed in this study is easily replicable and relatively cheap and provides an integrated quantified, overview of the morphological adjustments after channelisation works on a stream.

1. Introduction

To allow for the transformation of extensive agriculture into intensive agriculture, most rural watersheds in lowland areas of Europe have been completely remodelled since the early twentieth century (Stoate et al., 2001). Changes generally included reparcelling of the land, modification of the drainage, and elimination of landscape elements (such as hedges and wetlands) that had dampened liquid and solid fluxes (De Groot et al., 2002; Van der Zanden et al., 2013). Stream valleys have been profoundly modified through the construction of weirs and dams and by channelisation. The latter process modifies the morphology of a stream to reduce the frequency and magnitude of floods, drain new agricultural land, favour navigation, and reduce erosion in the channel (Brookes et al., 1983). The different methods of channelisation include the recalibration, realignment, or rectification of meanders, damming, or levee construction, bank protection, and bed cleaning (Brookes, 1985).

In the 1980s, certain studies (Brookes, 1985; Simon and Hupp, 1987) mentioned that channelisation operations can cause serious and almost systematic morphosedimentary dysfunctions. Indeed, increasing the slope gradient and associated transport capacity of a stream (Wilcock, 1991) leads to bed scouring and bank erosion in the high-energy sections (Surian and Rinaldi, 2003; Simon and Rinaldi, 2006), resulting in

* Corresponding author. Tel.: +33 238 644 794.
E-mail address: aurore.gay73@gmail.com (A. Gay).

http://dx.doi.org/10.1016/j.geomorph.2014.11.011
0169-555X/

the transport of eroded sediment downstream and its accumulation in low-energy reaches (Nakamura et al., 1997; Kroes and Hupp, 2010). This aggradation primarily involves fine sediment, which may clog the streambed (Landwehr and Rhoads, 2003), deteriorate the physico-chemical water quality (Shields et al., 2010), and degrade aquatic habitats (Steiger et al., 2005). In addition, changes in land use can result in an increasing supply of fine sediment and, thus, accentuate the aggradation phenomenon (Walling and Amos, 1999; Collins and Walling, 2007). Moreover, the suspended sediment deteriorates water quality though pollutants adsorbed on the fine fractions, such as heavy metals, nutrients, organic contaminants, or pesticides (Kronvang et al., 2003; Walling et al., 2003; Ballantine et al., 2009).

These environmental problems have led to the development of different approaches to quantifying the production, transport, and deposition rates in each of the geomorphological units of a watershed. One of the most frequent approaches is the sediment budget, which has been widely employed as a sediment management tool (Dietrich et al., 1982). These budgets help establish sustainable management strategies for sediment transfer (Walling and Collins, 2008). Furthermore, these budgets show that the sediment contribution from the banks of a channel on a decadal time scale in temperate rural catchments is ~10% in the case of streams slightly impacted by human influence (Walling et al., 2002) but can reach more than 50% in channelised streams (Wilson et al., 2008; Day et al., 2013; Palmer et al., 2014). Thus, the sediment emanating from a channelised river can represent a large proportion of the total sediment yield from a landscape (Simon and Rinaldi, 2006). This contribution varies with the size and extension of the modifications to the fluvial corridor (Malavoi and Adam, 2007), but it also varies based on changes to the watershed (Schilling et al., 2011).

This type of dysfunction has been observed over almost 300,000 linear kilometres in the USA (Schoof, 1980), 40,000 km of streams in Great Britain (Brookes et al., 1983), and tens of thousands of kilometres of streams in France (Malavoi and Adam, 2007). Nevertheless, the quantification of the morphosedimentary impact of channelisation on such streams and the contribution of the channels to the sediment budget commonly remain underdocumented (Heitmuller, 2014). Moreover, although most qualitative studies dealing with the impact of channelisation only focus on the channelised reach, channelisation also causes morphological readjustments in upstream and downstream adjacent reaches.

In fact, regular and comprehensive monitoring of the morphology of a stream is difficult (Sear and Newson, 2003), as it requires the deployment of high-spatial-resolution instrumentation over several decades, which limits the number of available studies (Gomez et al., 2007; Heitmuller, 2014). To overcome this lack of monitoring, the impact of channelisation on the stream banks and bed morphology is commonly quantified by retrospective studies. The pre-works morphology is generally extracted from aerial photographs (or occasionally from historical cross sections) and then compared to the current morphology by means of recent aerial photographs (Kesel and Yodis, 1992; Sipos et al., 2007; Segura-Beltrán and Sanchis-Ibor, 2013), newly measured cross sections (Terrio and Nazimek, 1997; Rinaldi and Simon, 1998; Kiss et al., 2008; Heitmuller, 2014), or airborne LiDAR topographic surveys (Rhoades et al., 2009; De Rose and Basher, 2011; Day et al., 2013; Kessler et al., 2013). Still, retrospective studies based on airborne methods are mostly restricted to evaluating morphological changes in stream banks and do not provide the three-dimensional morphology of the channel. Therefore, Gregory (2006) recommends the use of cross sectional surveys at different time steps for the quantification of changes affecting the river bed and banks. However, in many cases, the uncertainties of the measurements are not clearly defined, and furthermore, the use of historical cross sections over a medium time scale remains scarce.

In this context, the objective of this study is to investigate the morphosedimentary response to channelisation on a medium time scale (42 years) of a stream in a small headwater within a lowland catchment that has been strongly impacted by agricultural practices. The main objectives of the investigation consist of (i) developing a methodology for comparing cross sections and assessing the associated uncertainties; (ii) quantifying erosion and aggradation processes in the bed and on the banks along the channel profile; and (iii) calculating the sediment budget for the entire stream and determining the relative contribution of the banks and the streambed to this budget.

2. Study area

The Ligoire drainage basin is an 82-km^2 watershed located in the southwestern part of the Paris sedimentary basin; its length is 19 km from southwest to northeast, and its elongation ratio is 0.52 (Fig. 1). The area is hilly, but it has a moderate relief. The slopes have an average gradient of 5%, and elevations range from 60 m asl at the catchment outlet to 143 m asl, which is the highest point of the divide at the northeastern edge of the basin.

The geology of the Ligoire basin is characterised by an east–west trending anticline. The incision of the anticline during the Quaternary period led to the outcropping of Cretaceous rocks. In the Ligoire valley, these geological formations are represented in the stratigraphic order by micaceous chalks including flintstones (middle Turonian, C3b), by early Turonian argillaceous chalk with flints (C3a), and by late Cenomanian marlstone (C2). These formations are overlaid by sandy micaceous limestone with flints (late Turonian), Senonian clays and flints, Tertiary sandy-clay deposits, and Quaternary aeolian loess. Land use consists mainly of intensive agriculture, and 75% of the basin surface is covered by crops (corn, wheat, and rapeseed).

The drainage network comprises 107 km of streams. The two main streams are the Ligoire trunk channel and its main tributary: the Riolle. The Ligoire is 21 km long, issues from a spring in the northeast of the basin at an elevation of 131 m asl and joins the Esves River at an elevation of 58 m. In 1970, to enable the transformation from extensive agriculture into intensive agriculture, the main channel of the Ligoire was entirely straightened and resectioned over 21 km, and artificial knickpoints have been implemented along the stream. The longitudinal profile of the channel bed is punctuated by several artificial knickpoints, such as masonry weirs, riprap infill of fords, and bridge pillars (Fig. 2). The most remarkable is found at the Verger mill, where a dam impedes sediment transfer to the downstream reach and enhances sediment deposition along a 1200-m reach upstream. Except for this 2-m-high dam, the drops over most of the obstacles do not exceed a few tens of centimetres.

Many of the morphological, sedimentary, biological and chemical dysfunctions described in the introduction are observed in the Ligoire River.

3. Material and methods

In France, many stream channelisation projects were carried out in the first half of the twentieth century (Bravard et al., 1999). Usually, the stream morphology was surveyed by means of cross sections, longitudinal profiles, and linear drawings on the cadastral maps of the period. These morphological data were used as a basis for designing the new morphology of the channelised stream. Information of this type shows strong potential to provide accurate data, and these data were used in the present study to quantify the hydraulic, morphologic, and sedimentary impact of the realignment and resectioning of the main stream. In this study, we analysed the changes in the stream morphology for two periods: (i) before and after the channelisation and (ii) after the channelisation and currently.

3.1. Stream morphology before and after the channelisation

Topographical data before and after the channelisation were extracted from surveys of the stream cross section carried out by the Public Works Department of the Indre-et-Loire province. A total of 135 cross sections were measured along the main channel. These data were

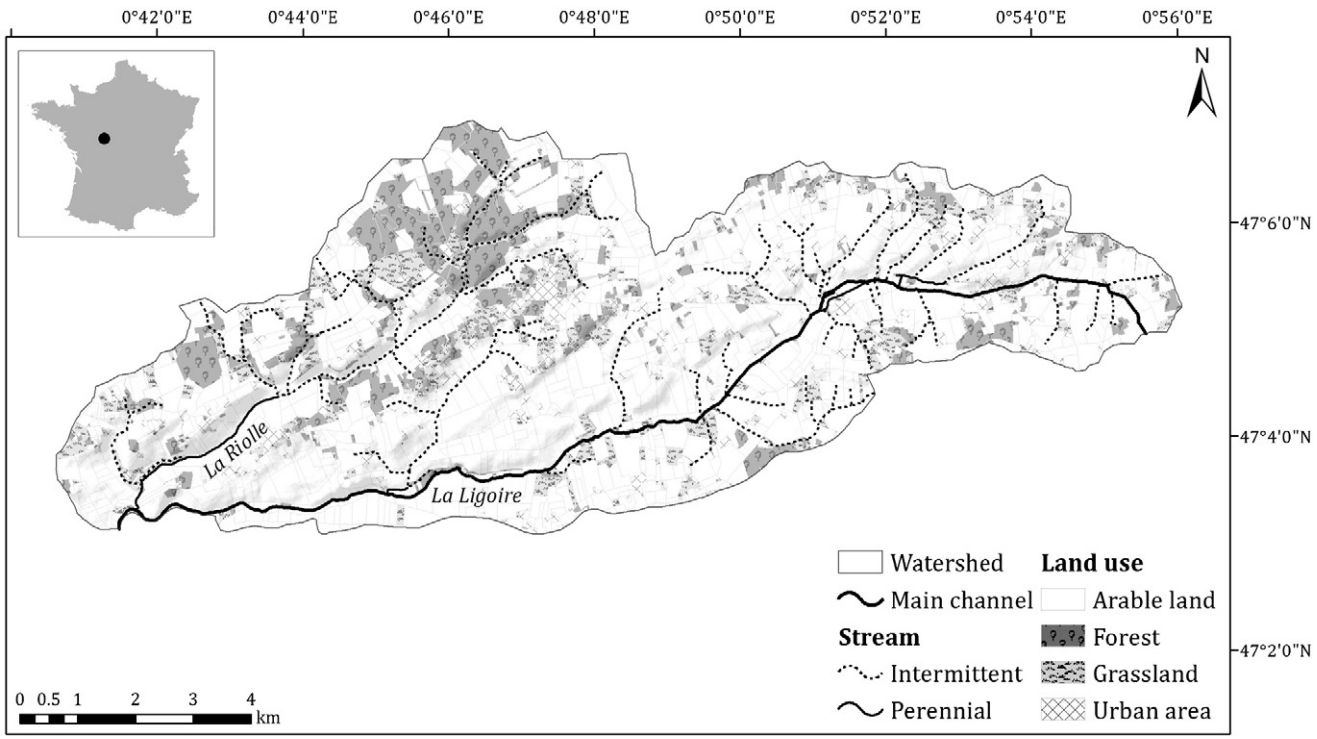

Fig. 1. Maps of the Ligoire watershed showing the land use and the drainage network.

used to design the new trapezoidal profiles. The distances between the cross sections are known, and each cross section was plotted on cadastral maps. Thus, the location of the historical cross sections was not referred to using a coordinate system. To allow comparisons of the topographic data, we georeferenced the historical cadastre in the Lambert-93 coordinate system, and then we extracted the centroid of all the historical cross sections.

3.2. Current stream morphology

A cross section was measured for each of the 135 georeferenced stations. The sections were measured using a DGPS (Differential Global Positioning System) Magellan Proflex 500, which has a post-processing accuracy of 1 cm in the *Z* direction and 0.5 cm in the *X* and *Y* directions. To identify relations between the stream morphology and the sediment deposition, we measured the sediment thickness and grain size within the streambed at each station.

The sediment thickness was obtained in two steps. First, we measured the bed-surface elevation. Second, the DGPS rod was driven into the streambed until it became blocked for a second elevation measurement (Lisle and Hilton, 1999). Then, the thickness was obtained by subtracting both values.

Finally, a visual estimate was made of the grain size at each topographic measuring point in the streambed using Wentworth's grain size classification as well as the sediment thickness.

3.3. Superposition of stream morphologies and associated uncertainties

To compare the morphology of the channel for the two periods, the cross sections are superposed. The cross sections from before

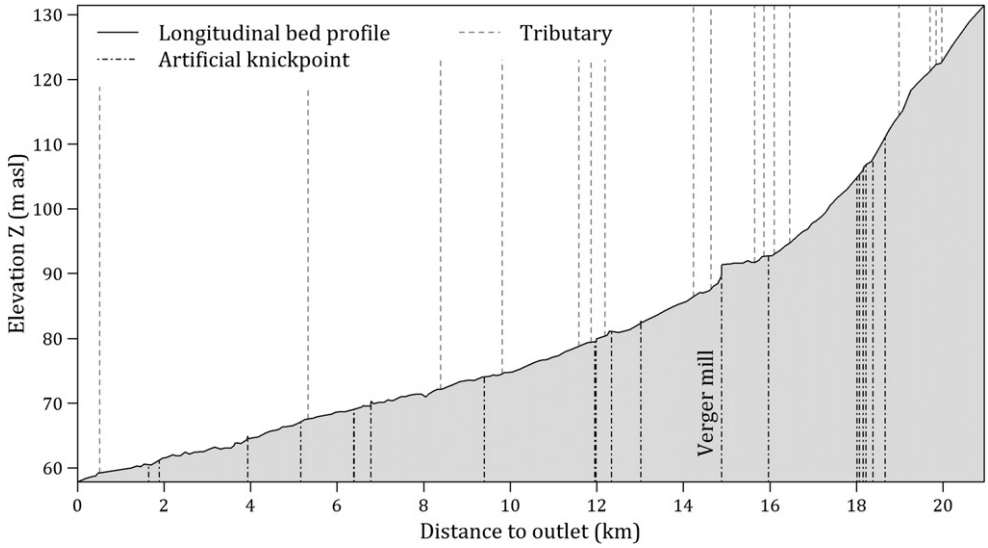

Fig. 2. Current longitudinal bed profile of the main channel of the Ligoire with its tributaries and artificial knickpoints.

and after the channelisation were directly superposed because the cross sections after the channelisation were based on the ones that had existed before it (Fig. 3). In this case, the uncertainties can be considered negligible.

Because the superposition of the current cross sections and the cross sections after channelisation is more complex, a specific method was developed. In our process, the superposition is realised based on the topographic data available for the current cross sections and the centroid of the cross sections after the channelisation. At first, the most adequate superposition is to centre both data. More precisely, (i) the historical bed-surface elevation and the current bed-surface elevation are superposed on the elevation axis, and (ii) both axes of symmetry are superposed on the station axis (Fig. 4A).

Furthermore, vertical and lateral potential uncertainties caused by the superposition of both cross sections were considered. First, with respect to the vertical uncertainties, we consider the uncertainty in the elevation measurements using the DGPS to be negligible, but this error is not negligible for the historical elevation data. Given the instrument used in the past, namely, a levelling rod, the uncertainty in the elevation Z can be estimated as $\sigma = \pm 5$ cm. Therefore, we shift each after-channelisation cross section vertically according to the established uncertainty in the Z direction (Fig. 4A). Second, for the lateral uncertainties, each cross section after channelisation is shifted laterally to the left bank (Fig. 4B) and to the right bank (Fig. 4C) of the current cross section. For both shifts, the uncertainty σ is also considered.

Therefore, nine positions of the historical cross sections after channelisation are considered according to different combinations of lateral and vertical shifting.

3.4. Quantification of changes in the stream morphology

The calculation of the net surface difference (m^2) between the superposed cross sections allows us to quantify the changes in the channel morphology for the two periods.

For the first period (before and after the channelisation), the areas between the cross sections are calculated for the entire channel (the banks and the streambed). The values of the channel areas are negative, and these areas correspond to the sediment areas extracted during the channelisation works. As stated in Section 3.3, the lateral and vertical uncertainties are considered negligible. A channel area is calculated per station, giving a total of 135 channel areas.

For the second period (after channelisation to today), which corresponds to the adjustment period of the Ligoire River, the values of the areas can be either positive or negative based on the type of processes involved: deposition and erosion, respectively. To provide more spatial insight into those processes, the channel was separated into the streambed (dark grey in Fig. 4) and the banks (light grey in Fig. 4). We calculated the areas for the streambed and the entire channel. The difference between the two areas gives the area for the banks according to Eq. (1):

$$Area_{channel} = Area_{streambed} + Area_{banks} \quad (1)$$

To take into account the lateral and vertical uncertainties, nine shifts were considered in the calculations of the areas. For each station, this process resulted in nine areas for the channel, nine for the streambed, and nine for the banks. Thus, for the 135 stations, $135 \times 9 = 1215$ areas were computed for the channel, 1215 were computed for the streambed and 1215 were computed for the banks.

Moreover, the sensitivity of lateral and vertical shifting in the calculation of the nine channel areas per station is studied. Initially, we calculated the mean area and its variation coefficient for each of the 135 nine-value series. Then, each of the series was reclassified into three sets of three values. The first set comprises the centred area values of the cross sections after the channelisation, the second set comprises the right-bank-shifted cross sections, and the third set comprises the corresponding cross sections of the left bank. For each three-value set, the variation coefficient and the mean were calculated.

The erosion and deposition processes in the streambed and along the banks can also be quantified by distance measurements. The maximum distance D_{bed} separating the minimum elevation of the cross section after channelisation and the minimum elevation of the current bed gives a numerical value for the incision of the bed or the sediment deposition. The uncertainty of $\sigma = \pm 5$ cm is utilised in the calculation of this distance.

With respect to the banks, the ratio between the area of the banks and their current developed length (the wetted perimeter minus the width of the minor bed) gives the eroded or deposited distance D_{banks} (Eq. (2)):

$$D_{banks} = \frac{Area_{banks}}{Wetted\ \ perimeter - Streambed\ \ width} \quad (2)$$

For each station, this distance is calculated nine times, or once from each of the nine areas identified as the bank positions, and we use these distances to calculate the mean values and their uncertainties. Finally, we deduce the erosion or deposition rates for the bed or the banks by dividing by 42 years (which is time elapsed since channelisation, 1970–2012).

3.5. Sediment budget

We recognised that each cross section is representative of half of the distance to the previous cross section and to the next cross section. The volume of the channel reach (in m^3) that is represented by a given cross section is determined by Eq. (3). The sum of the volumes of each station gives the overall sediment budget of the Ligoire channel (Eq. (4)):

$$Volume\left(m^3\right) = Area\left(m^2\right) \times \left(\frac{1}{2}\ upstream\ \ distance + \frac{1}{2}\ downstream\ \ distance\right) \quad (3)$$

$$Sediment\ \ budget\left(m^3\right) = \sum_{i=1}^{135} Volume\ \ (Site\ \ i) \quad (4)$$

For the first period, the sediment budget is negative and corresponds to the extraction of sediment during the works. During the adjustment period of the stream (1970–2012), whereas a negative budget indicates that the dominant process was erosion of the channel sediment, a positive budget indicates that the dominant process

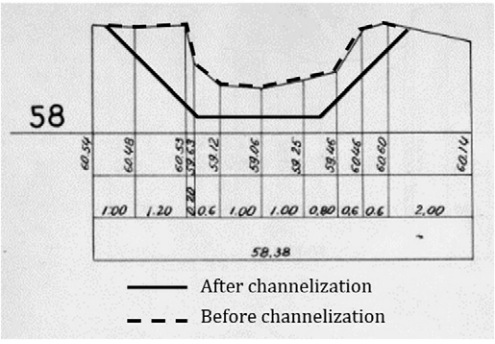

Fig. 3. Example of a cross section before and after channelisation. The cross section after the channelisation was designed based on the cross sections found before the channelisation.

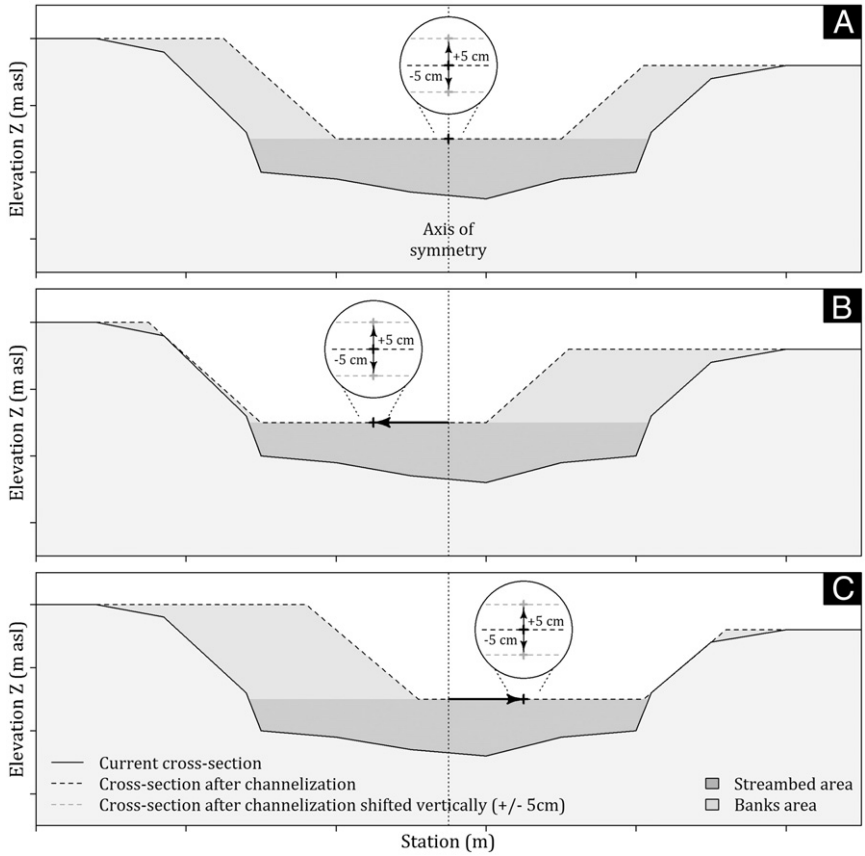

Fig. 4. Schematic representation of the adequate superposition of the cross sections after the channelisation and the current cross sections with the associated uncertainty $\sigma = \pm 5$ cm on the elevation *Z*. The superposition is carried out by considering the coincidence of (A) the axis of symmetry, (B) the left bank, and (C) the right bank. For each shift, the area between the cross sections after the channelisation and the current cross sections is calculated for the channel, the streambed, and the banks.

was sediment deposition. Moreover, the value of the sediment budget compared to the Ligoire watershed surface and to the study period gives the specific rate of erosion or deposition (in $m^3.km^{-2}.y^{-1}$).

However, as nine channel areas are available for each of the 135 stations, 9^{135} sediment budget values are possible. As a result, Monte Carlo methods were used to examine these possibilities. At each station, we randomly selected one of the nine channel areas, and then the sediment budget of the channel was calculated as described previously (Eq. (4)). Based on the results from employing 2, 5, 10, 20, 50, 100, 200, 500, 1000, 2000, 5000, 10,000, 20,000, and 50,000 budgets, we calculated a mean sediment budget. Subsequently, the associated uncertainty (standard deviation) was calculated from each set of selections, which ranged from 2 to 50,000. The convergence of the sediment budget values from this method was studied to determine the optimum number of selections needed to calculate a mean reliable and stable sediment budget and its value.

3.6. Hydraulic variables

The measured erosion and deposition processes indicated the morphosedimentary response of the energetic disequilibrium imposed by channelisation of the Ligoire River. To study this relationship, hydraulic variables (Table 1) were calculated for each cross section and for each time step (i.e., before the channelisation, after the channelization, and currently), and these variables were linked with D_{bed}, D_{banks}, the channel areas, the streambed areas, the banks area, the streambed grain size, and the sediment thickness. The longitudinal slope was calculated at each cross section by performing a linear regression between the minimal elevation values for the cross section and the upstream and downstream cross sections.

4. Results and discussion

4.1. Channelisation of the Ligoire: the creation of a disequilibrium

The different hydraulic variables measured before and after the channelisation show a drastic modification in the morphology of the Ligoire channel:

- Horizontally: the cutting of meanders and displacement of the stream reduced the main channel length by 10%: it shrank from 20,843 to 18,903 m.
- Transversally: the bankfull width grew on average by 63% (from 5.0 to 8.2 m), and the bankfull height grew by 57% on average (from 1.0 to 1.61 m).
- Longitudinally: the slope distribution before and after the channelisation (Fig. 5B) clearly shows that the variability of the

Table 1
The different morphologic and hydraulic variables measured for each cross section before and after channelisation and currently.

Variables	Name	Unit
i	*Longitudinal slope*	$m.km^{-1}$
L	*Top width*	*m*
l	*Water surface*	*m*
H	*Full channel depth*	*m*
β	*Aspect ratio*	-
C	*Conveyance*	$m^3.s^{-1}$
Wp	*Wetted perimeter*	*m*
Wa	*Wetted area*	m^2
Rh	*Hydraulic radius*	-
P	*Specific stream power*	$W.m^{-2}$

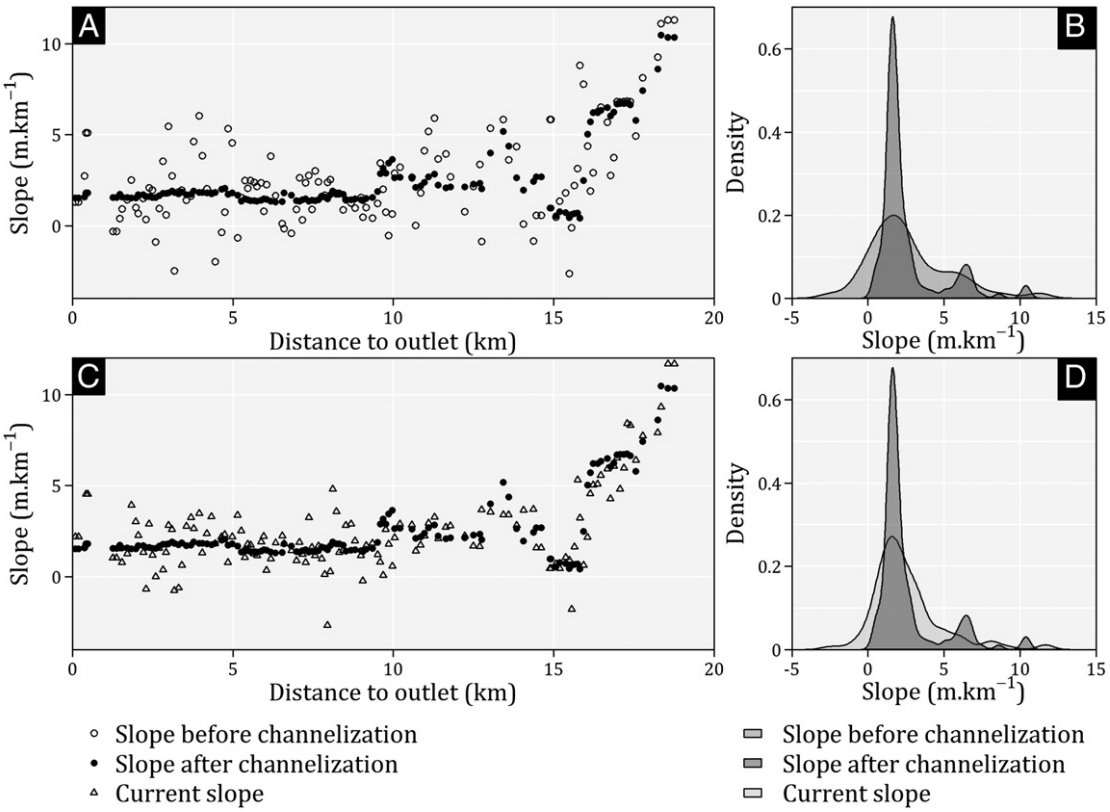

Fig. 5. Evolution of the longitudinal slopes of the streambed for period 1 (before and after the channelisation) (A) and period 2 (after the channelisation to the present) (B). Corresponding evolution of the probability density function of longitudinal slopes for period 1 (C) and period 2 (D).

longitudinal slopes (Fig. 5A) strongly decreased, resulting in an almost continuous longitudinal cross section.

Thus, our results show how the channelisation completely altered the morphology of the stream. A total of 60,000 m^3 of sediments was excavated during the works. The conveyance increased on average by 316% (from 3.8 to 15.9 m^3.s^{-1}), and the specific stream power increased by 80% (from 28.0 to 50.4 W.m^{-2}).

4.2. Morphological adjustments over the study period (1970–2012)

Currently, the slopes have greater variability (Fig. 5C and D) than they did just after the channelisation, which is caused by morphological readjustments during the period from 1970 to 2012.

The distance measurements D_{bed} and D_{banks} show that the channelisation mostly led to erosion of the main Ligoire channel. In fact, the streambed was incised by 0.41 m and the banks eroded by 0.20 m on average over 63% and 60% of the length of the entire channel, respectively (Table 2). Still, the sediment deposition was not negligible, as it occurred in 37% of the streambed and 40% of the banks.

The distribution of channel areas is very close to the distribution of the bed and the banks. In over 61% of the channel length, the net erosion is on average −1.05 m^2. Conversely, in over 39%, the net deposition is on average +1.40 m^2 (Fig. 6). This result is explained by the fact that for a given cross section, the processes affecting the bed and the banks act similarly. Indeed, for 46% of the stations, the bed and the banks have been affected by net erosion; and for 30% of the stations, they are both subject to deposition (Table 3).

From a longitudinal viewpoint, these erosion and deposition processes occurred successively along the stream. Therefore, five reaches can be identified, where three are dominated by erosion and two are dominated by aggradation (Fig. 6). Understanding these processes requires an upstream-downstream analysis of their hydraulic and morphologic characteristics (Table 3).

Reach 5, which is very upstream from the Ligoire channel, has the highest energy; and this fact has remained true even after the channelisation when the slope became 7.25 m.km^{-1}. Increasing the slope, width, and bankfull height (1.5%, 102%, and 66%, respectively) caused an increase in the specific power of the reach by 423%: it increased from 25 to 131 W.m^{-2}. As a consequence, the channel was subsequently strongly eroded (Fig. 7A), with an average incision in the bed of 0.38 m and a mean bank erosion of 0.15 m, creating a narrow and deep section with an aspect ratio of 3.62. In the upper part of this reach, the incision reaches 0.86 m and is locally blocked by micaceous chalk including flintstone (middle Turonian, C3b) outcrops (Fig. 7C). Therefore, the erosion power of the water is transferred laterally, which induces the undercutting of the banks over a height of more than 2 m (Simon and Hupp, 1987). This pattern has led locally to major bank failures that created reaches with streambed incision and accretion on the banks. Nevertheless, the influence of five weirs (Fig. 7A) of heights of a few tens of centimetres around the village of Mouzay (kilometre 18.0) is not negligible. In spite of strong longitudinal slopes, these weirs limit the incision of the stream in this area.

Reach 4, in contrast, has the lowest energy because of a gentle slope after channelization of 1.28 m.km^{-1} and a specific power of 13 W.m^{-2}. This area corresponds to the sediment deposition zone caused by the

Table 2
Stream lengths affected by erosion and deposition processes in the streambed and on the banks.

	Mean erosion (−) or deposition (+) (m)	Mean rate of erosion or deposition (m.y^{-1})	Affected length of the Ligoire River (%)
Streambed	−0.41 ± 0.06	−0.010	63
	+0.28 ± 0.06	+0.007	37
Banks	−0.20 ± 0.04	−0.050	60
	+0.90 ± 0.04	+0.020	40

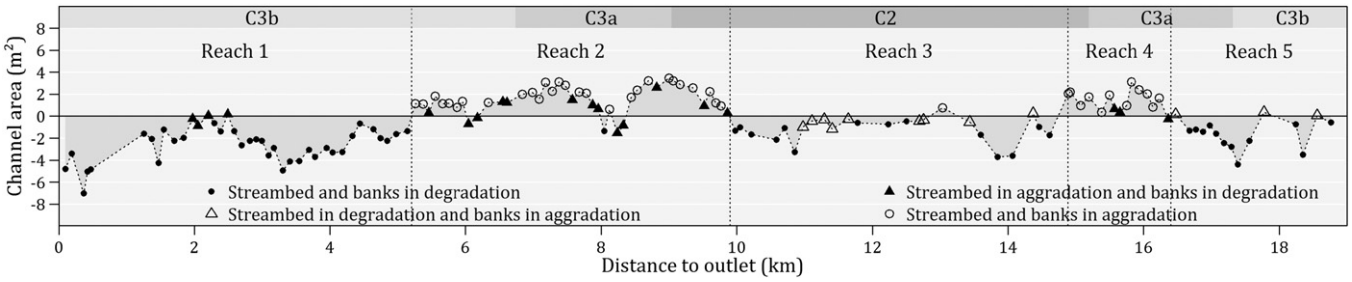

Fig. 6. Estimated channel area along the longitudinal profile of the river: (+) is aggradation and (−) is erosion. (C3b): Micaceous chalks including flintstones; (C3a): argillaceous chalk with flints; (C2): marlstone.

Verger mill (kilometre 14.9) (Fig. 7A). In this reach, the initial stream section was wide and shallow, but during the channelisation, it was further widened by 52% (from 4.99 to 7.58 m) (Fig. 7B). Currently, the channel is in a state of net aggradation (with a channel area of 1.71 m^2), and it has a mean deposit thickness in the bed of 0.20 m and a bank accretion of 0.05 m. The configuration of this reach is ideal for this aggradation phenomenon, as the erosion in reach 5 supplies a large quantity of sediment downstream. In reach 4, the drop in slope of 82% (from 7.36 to 1.28 $m.km^{-1}$) and the widening of the bankfull width by 33% have caused a drastic reduction in the carrying capacity of the water flow, with the consequent deposition of sediments. The formation of a deposit with a thickness of over 1 m at the beginning of this reach clearly shows this phenomenon (Fig. 7A).

Reach 3, which is downstream from the Verger mill, was historically a high-energy section with a slope of 2.86 $m.km^{-1}$ (Fig. 8A). Following channelisation, its specific power increased by 39% from 26 to 36 $W.m^{-2}$. Moreover, the retention of a solid load upstream from the mill further modifies the solid-transport capacity of the Ligoire waters downstream of this knickpoint. Thus, we observe an average bed incision of 0.42 m and strong erosion of the channel (the mean channel area is -0.97 m^2). As a result, the reach has been mostly deepened, with an average increase in the bankfull height of 41% and narrow and deep sections with an aspect ratio of 4.50. Downstream of the dam, in the area of energy dissipation, the bed was deepened by a maximum of 1 m, but incision is now blocked by the outcrop of nonerodible clay (late Cenomanian, C2) (Fig. 8C). The erosion products are transferred downstream where they accumulate upstream from the Roche mill (kilometre 13.0). Downstream from this knickpoint, the presence of three weirs at the Montfouet ford (kilometres 12.3–11.9) further limits bed incision, and sediment deposits exist for ~10 m behind each weir. In this area, many of the stations exhibit accreting banks caused by bank failures. Finally, downstream from this stretch, the absence of natural or artificial knickpoints is conducive to the resumption of complete erosion of the channel.

Reach 2 was the most extensively modified section during the channelisation process: the bankfull width and the height increased on average by 96% and 95%, respectively (Fig. 8B). Notwithstanding gentle slopes (1.56 $m.km^{-1}$ after the channelisation), the oversizing of the section caused a 306% increase in its specific power from 8 to 32 $W.m^{-2}$. Currently, this reach is in net aggradation, with a mean thickness of bed deposits of 0.34 m and a bank accretion of 0.04 m. This reach has the same functioning as reach 4. In fact, the passage from reach 3 to reach 2 is shown by an abrupt drop in slope angles of 43% (from 2.75 to 1.56 $m.km^{-1}$) and an increase in the bankfull width of 36%. Although the specific power of the reach increased, the widening of the water surface has led to a decreased sediment transport capacity and an aggradation of the bed surface of 0.67 m on average (Fig. 8A). The presence of weirs at the Arche ford (kilometre 9.4), at Joubardes (kilometre 6.4), and at the Gruteau mill (kilometre 5.1) locally amplifies the aggradation phenomenon.

Table 3
Average morphologic, hydraulic and sedimentary characteristics of the five identified reaches.

		Reach 1		Reach 2		Reach 3		Reach 4		Reach 5	
Length (m)		5.14		4.11		4.63		1.35		2.39	
Streambed area (m^2)		−0.92		1.22		−0.94		0.93		−0.54	
D_{bed} (m)		−0.31		0.26		−0.42		0.20		−0.38	
Banks area (m^2)		−1.04		0.34		−0.05		0.25		−0.62	
D_{banks} (m)		−0.22		0.04		0.00		0.05		−0.15	
Channel area (m^2)		−2.23		1.32		−0.97		1.71		−1.26	
Number of cross sections		39		42		24		14		16	
Streambed and banks in erosion		35		1		14		0		12	
Streambed in erosion and banks in aggradation		0		0		9		0		3	
Streambed in aggradation and banks in erosion		4		13		0		2		1	
Streambed and banks in aggradation		0		28		1		12		0	
Top width (m)	before	5.10		4.72		5.94		4.99		2.82	
	after	7.49	47%	9.23	96%	6.78	14%	7.58	52%	5.69	102%
	current	7.80	4%	7.64	−17%	6.86	1%	7.62	0%	5.80	2%
Top depth (m)	before	1.09		0.99		1.35		1.16		0.69	
	after	1.39	27%	1.93	95%	1.17	−13%	1.26	9%	1.14	66%
	current	1.56	12%	1.66	−14%	1.64	41%	1.31	4%	1.72	51%
Aspect ratio (−)	before	4.79		5.51		4.66		4.57		4.57	
	after	5.41	13%	4.80	−13%	5.78	24%	6.44	41%	5.00	9%
	current	5.15	−5%	4.50	−6%	4.50	−22%	5.95	−8%	3.62	−28%
Longitudinal slope ($m.km^{-1}$)	before	1.63		1.52		2.86		2.59		7.25	
	after	1.70	4%	1.56	3%	2.75	−4%	1.28	−51%	7.36	2%
	current	1.65	−3%	1.58	1%	2.76	0%	1.46	14%	7.29	−1%
Specific stream power ($W.m^{-2}$)	before	11.4		7.90		25.8		27.7		25.7	
	after	22.2	95%	32.2	306%	35.8	39%	13.3	−52%	134.4	423%
	current	23.9	7%	18.7	−42%	25.0	−30%	5.80	−56%	150.6	12%

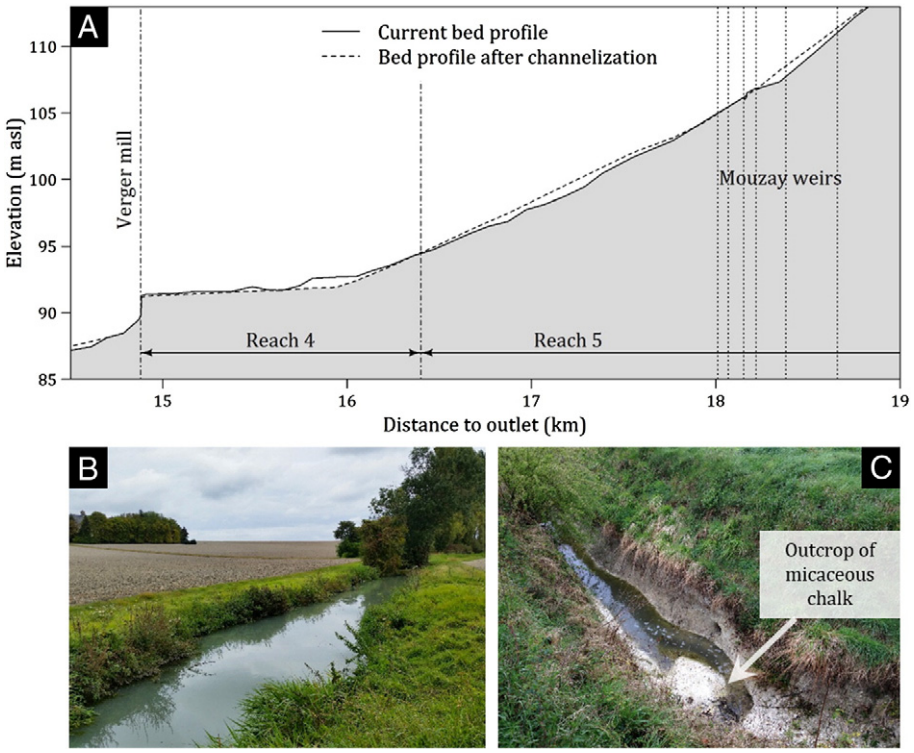

Fig. 7. (A) Longitudinal profile after channelisation and today. (B) In reach 4, the energy within the channel was not sufficient to transport all sediments coming from reach 5 and caused aggradation. (C) In reach 5, the steep slopes caused an erosion of the main channel and the incision reached micaceous chalks.

Reach 1 begins downstream from the Gruteau mill and ends at the Ligoire watershed outlet. During the channelisation, the bankfull slope, width, and height were increased by 4.3%, 47%, and 27%, respectively. This change in morphology led to an increase in the specific power of 95%: the power increased from 11 to 22 $W.m^{-2}$. Currently, the channel is strongly eroded, with a channel area of -2.23 m^2. This erosion affects both the streambed and the banks, as the mean bed incision is -0.31 m and the average erosion of the banks is −0.22 m. The sedimentary functioning of reach 1 is similar to the functioning of reach 3. A massive sediment deposition upstream from reach 1 modifies the

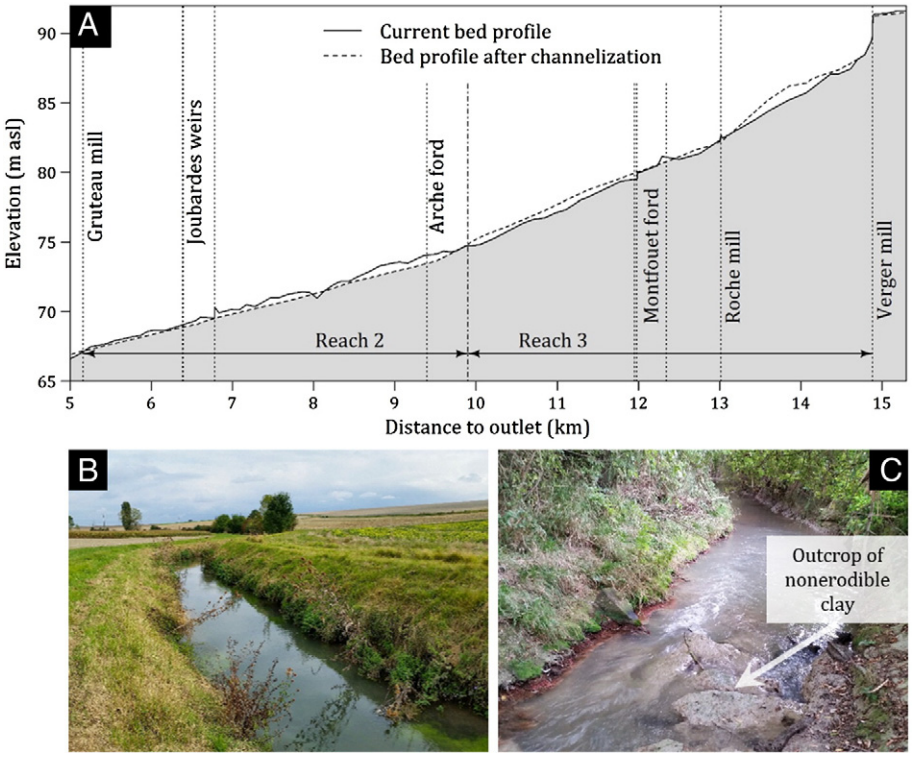

Fig. 8. (A) Current and after-channelisation bed profiles. (B) The low energy, combined with sediments supplied from reach 3, resulted in aggradation in reach 2. (C) The steep slopes in reach 3 and the modification of the solid-transport capacity of the stream by the Verger mill involved the incision of the channel and the outcropping of nonerodible clay.

transport capacity of the waters and, thus, provokes sediment removal from the streambed and the banks of the reach. The intensity of this uptake increases from the Gruteau mill until kilometre 3.3, where the incision can reach 1.16 m and the bank erosion is 0.50 m. Beyond this maximum, sediment removal decreases until the Saint-Paul mill (kilometre 2.6) and the RD 101 road (kilometre 1.9). These two knickpoints again prevent further deepening of the bed and favour sediment deposition in this section. Finally, below this reach, the channel is completely eroded and incision is mostly blocked by paving of the streambed.

This detailed descriptive analysis of the different channelised reaches helps us understand the active processes, as it clearly shows that the morphologic adjustments measured in a reach are governed not only by the human modifications in this reach (channelisation and artificial knickpoints) but also by the human modifications that have been made upstream and downstream from this reach. Moreover, this analysis illustrates the common patterns observed in channelised streams, i.e., erosion of the high-energy reaches and aggradation of the low-energy ones (Simon and Hupp, 1987).

Still, the generalisation of the intensity of morphologic readjustments with respect to the channel geometry is not possible. Additionally, no significant correlation could be established between the morphologic, hydraulic, and sedimentary variables regardless of the study period considered (before and after the channelisation and today). The relationships between the channel areas and the longitudinal slopes after the channelisation illustrate this complexity (Fig. 9). For a same-slope value after the channelisation, the section today may be erosional or depositional. Other parameters — such as bed roughness (Simon and Thorne, 1996), bank-sediment grain size distributions (Couper, 2003), aquatic and terrestrial vegetation (Rodrigues et al., 2006; Heppell et al., 2009), or the activity of vermin such as coypus (Ford and Grace, 1998) — locally complicate the reaction of a section to an energy disequilibrium.

Only an exact description of the channel allows an overall interpretation of the morphologic evolution of the channelised stream. In this case, erosion is observed not only in a reach with steep slopes (reach 5) but also in reaches with gentler slopes (reaches 1 and 3). In the first case, the high transport capacity of the stream causes erosion of the channel. In the second case, the retaining effect of the weir(s) upstream creates a lack of suspended sediment load and erosion. Conversely, aggradation is commonly observed in reaches with gentle slopes, which can be either natural (reach 2) or man-made through the sediment deposition zone behind a dam (reach 4). Aggradation is also observed in reaches with strong longitudinal slope, but this phenomenon is very localised. Thus, from our study, the distribution of erosion and deposition processes following the channelization clearly corresponds to the cumulative effects of such modifications and the presence of knickpoints along the Ligoire channel.

The important rate of fine sediment observed in certain reaches is influenced by the current geometry of the channel. In fact, certain trends become clear when comparing the current longitudinal slope, the current surface-water width, and the sediment thickness (Fig. 10A) and grain size for each station (Fig. 10B). Fine sediment will preferentially be deposited in sections with a longitudinal slope <4 m.km^{-1} and a surface width >2 m. The widening of the surface width observed in reaches 2 and 4 reduces the stream velocity, decreases the transportation capacity, and causes deposition of the sediment load. Conversely, the erosional power of the water in sections with a strong slope and a narrow channel (reaches 1, 3, and 5) will only allow the deposition of thin beds and coarse-grained sediments.

4.3. Sensitivity of the channel area calculation method

We studied the influence of the vertical and lateral shifting on the dispersion of the 135 sets of nine values of the channel area. The dispersion within each set is moderate, as the mean variation is 33.5% (Fig. 11A). Still, the median of 16.6% indicates that this mean is strongly influenced by high dispersion values, with a variation coefficient of up to 675%. This dispersion increases when the unit-area value approaches zero, and *vice versa*.

When a distinction is made between lateral and vertical shifting, the dispersion is mainly caused by vertical shifting. The reason is that although the mean value of the dispersion is 38.6%, it is only 2.7% for the lateral shifting (Fig. 11B). Thus, the uncertainties of the areas are mainly associated with the vertical shifting of the historical cross sections compared to the corresponding shifting of the current cross sections.

Consequently, the validity of the uncertainty on Z of $\sigma = \pm 5$ cm can be questioned. However, this figure can be verified by quantifying the longitudinal variability of the bed elevations Z of the cross sections after the channelisation based on the distances and slopes between these cross sections. More precisely, the uncertainty σ was applied to the bed-elevation value Z of each cross section to calculate the longitudinal distance by integrating over the interval $[Z\text{-}\sigma; Z + \sigma]$. For 81% of the cross sections, the interval $[Z\text{-}\sigma; Z + \sigma]$ incorporates a distance of at least 25 m. Hence, within a radius of 12.5 m around a given cross section, the average bed elevation of the cross sections falls between Z-5 cm and $Z + 5$ cm.

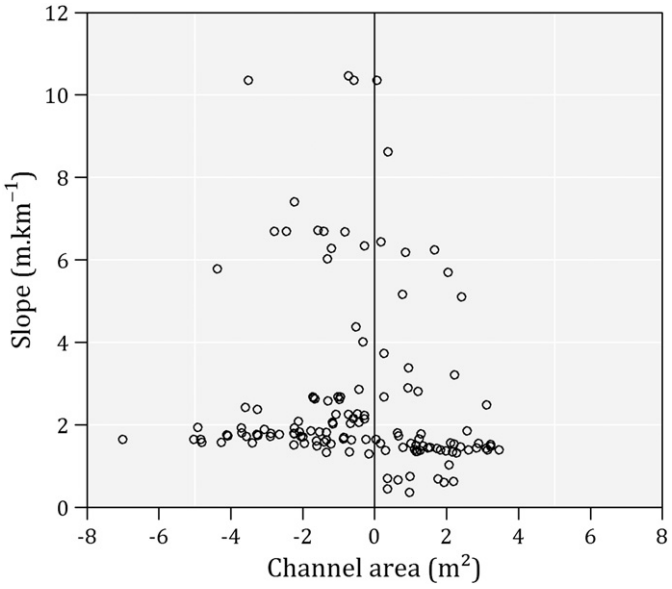

Fig. 9. Relationship between the longitudinal slopes after the channelisation and the channel areas. For a given slope value, the area can be positive (an erosional cross section) or negative (a depositional cross section).

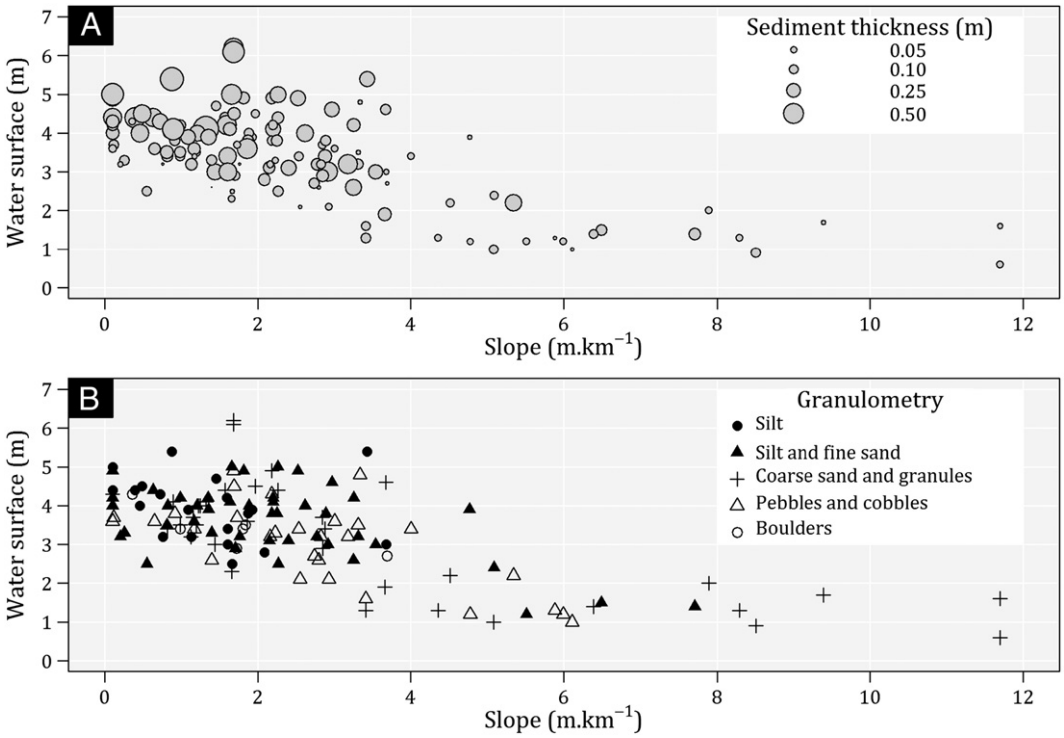

Fig. 10. Relationships between the current water surface, the current longitudinal slope, (A) the sediment thickness, and (B) the dominant sediment grain size.

4.4. Sediment budget of the Ligoire channel

4.4.1. Sensitivity of the sediment-budget calculation method

We used Monte Carlo methods to determine the optimal number of sediment budgets for calculating an overall sediment budget. The mean sediment budget progressively converges with the increase in the number of budgets used (Fig. 12A) from −9302 m^3 for two budgets to −9359 m^3 for 50,000 budgets. This stabilisation can be observed, as (if we use 1000 sediment budgets) the mean volume is −9358 m^3.

The larger the number of overall sediment budgets is, the smaller the variation coefficient of the iterations will be. For example, this coefficient is 5.3% when two sediment budgets are used and 0.02% for

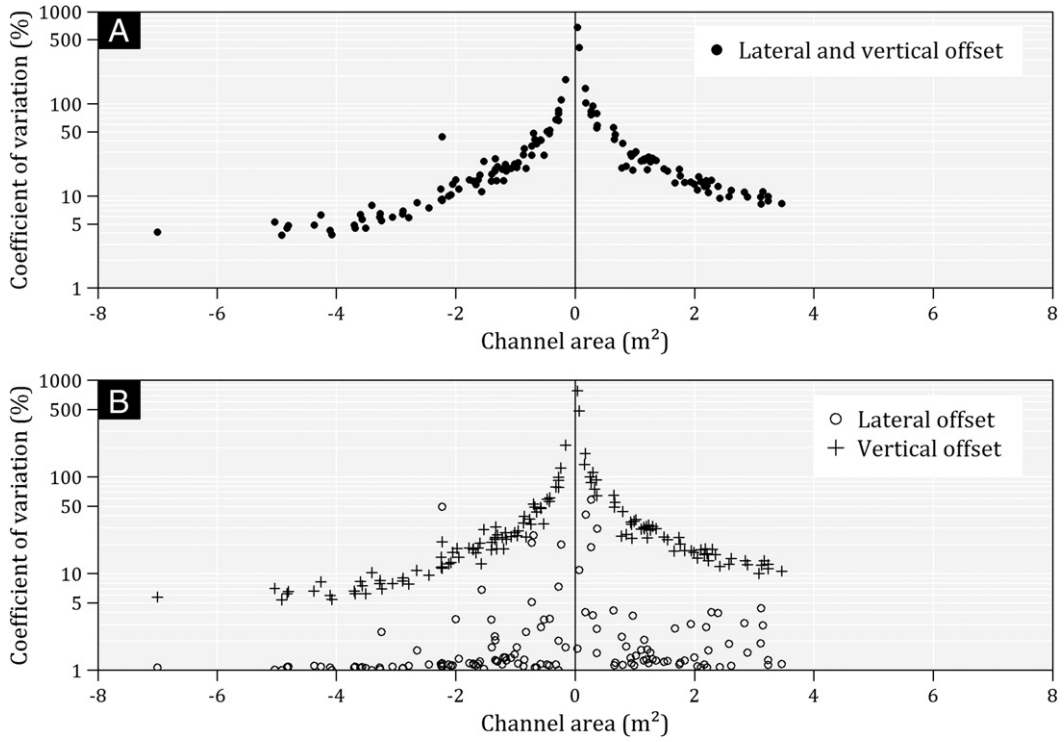

Fig. 11. The variation coefficient in terms of the mean channel area of each set: (A) of each of the 135 nine-value sets of channel areas (with no distinction between lateral and vertical shifting); (B) of each of the 135 × 3 value sets of three channel areas (which make a distinction between lateral and vertical shifting).

50,000 budgets. Similarly, this stabilisation appears when 1000 budgets are used, and the variation coefficient of the iterations is only 0.1%.

The same descriptive approach is valid for the mean standard deviation (Fig. 12B). Similar to the mean sediment budget, the mean standard deviation converges to 412 m^3 when 1000 standard deviations are used. The iteration variation coefficient associated with this value is low at 2.3%, and it decreases from 61.8% when two standard deviations are used to 0.3% for 50,000 standard deviations. Therefore, we utilised 1000 sediment budgets to calculate the mean sediment budget and the mean standard deviation.

4.4.2. Mean sediment budget of the Ligoire channel

The sediment budget of the main Ligoire channel can be calculated with the method developed in our study. The results are a sediment volume eroded from the channel of 19,358 ± 329 m^3 and a sediment deposition of 10,178 ± 243 m^3. Thus, the mean sediment budget is −9358 ± 412 m^3 (Fig. 13), of which 3121 ± 228 m^3 came from the bed and 6237 ± 412 m^3 came from the banks. These figures imply that during the period from 1970 to 2012, ~9400 m^3 of sediment was removed from the Ligoire basin; and whereas 66% came from the banks, 34% came from the streambed.

Relative to the Ligoire watershed surface of 82 km^2 and the study period of 42 years, the specific erosion rate (or the contribution of the main channel to the sediment budget) is $Y^* = 2.71 \pm 0.12$ $m^3.km^{-2}.y^{-1}$. We use a bulk density to provide a value for sediment export (Lick and McNeil, 2001), and it represents between 3.4 and 5.7 $t.km^2.y^{-1}$.

Finally, after adding this overall sediment budget of the channel to the volume of sediment excavated during channelisation, the main channel in 2012 clearly had a sediment deficit of almost 70,000 m^3, illustrating the profound sedimentary impact of channelisation on a stream.

5. Conclusion

The morphologic, hydraulic, and sedimentary impact of channelisation in the Ligoire River (France) was recorded over 42 years. The aim of this work was to develop a method for quantifying such changes and to assess the associated uncertainties and their influence on the calculated values of the erosion, aggradation, and sediment budget.

To this end, we compared cross sections of the stream before and after the channelisation based on historical documents, and we measured new cross sections during recent fieldwork. This study required the development of methods for superposing historical and current cross sections and for integrating the uncertainties related to errors in the measurements used in our calculation. The vertical uncertainty of the elevation of historical cross sections is an important parameter for controlling the area and sediment budget values. In addition, the use of Monte Carlo methods indicates that 1000 overall sediment budgets must be calculated to obtain a variation coefficient below 0.1% for the mean channel sediment budget.

During the channelisation work, the trace of the main channel was straightened and 60,000 m^3 of sediment were excavated. This alteration caused a serious energy disequilibrium and morphologic readjustments of the stream through erosion and aggradation processes. After the work, the Ligoire was affected by net erosion processes in 61% of its length. This erosion mostly occurred in the high-energy stretches of the channel. Thickness and grain size measurements of the sediments show that general widening of the channel caused deposition of fine-grained sediments in the low-energy stretches where the water surface was widest. The present study clearly shows that the distribution of erosion/aggradation phenomena is the result of the cumulative effects of the channelisation and of the presence of natural and artificial knickpoints in the Ligoire channel. However, in view of the imposed disturbance, such readjustments were insufficient to allow for a return to the initial state of the streambed as it was before the 1970s. An important implication is that the present hydromorphological functioning of the stream is still under the influence of the channelisation, and therefore it cannot be explained by topographical or hydrologic parameters. Thus, the use of historical information is crucial for understanding the likely evolution of these types of altered streams. Overall, between 1970 and 2010, ~9400 m^3 of sediment was removed from the main

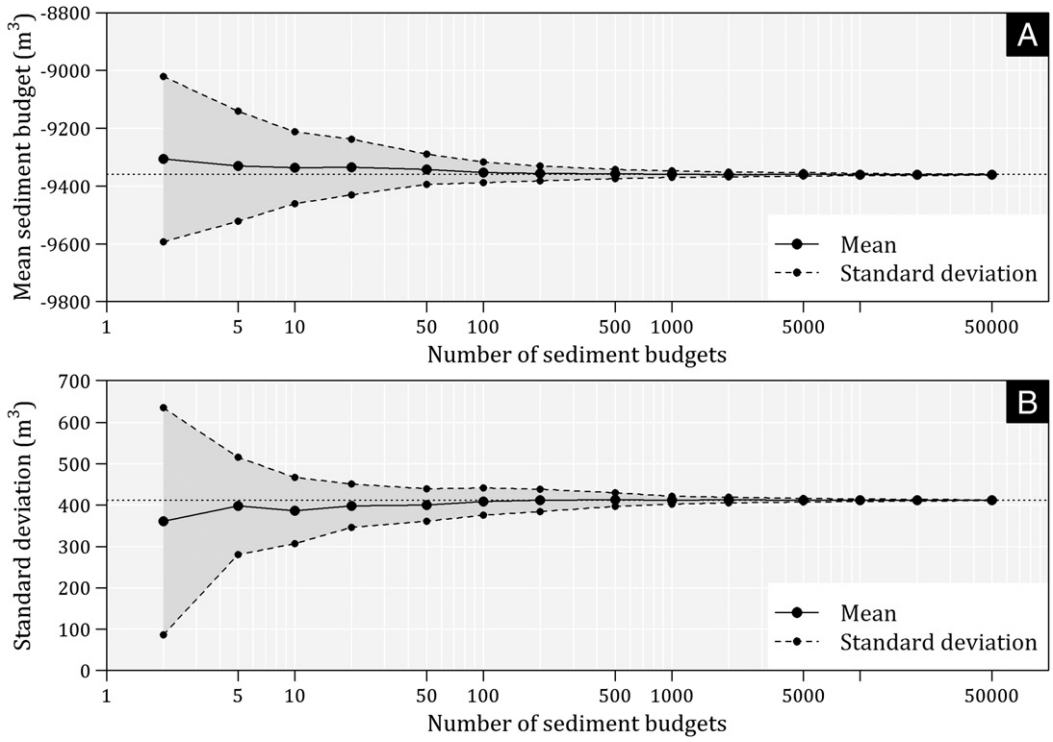

Fig. 12. From 2 to 50,000 sediment budgets are considered for the calculation of (A) a mean sediment budget, and (B) the associated standard deviation. For each number of sediment budgets, the mean sediment budget and the standard deviation are iterated 50 times, and the mean and the standard deviation from these calculations are extracted.

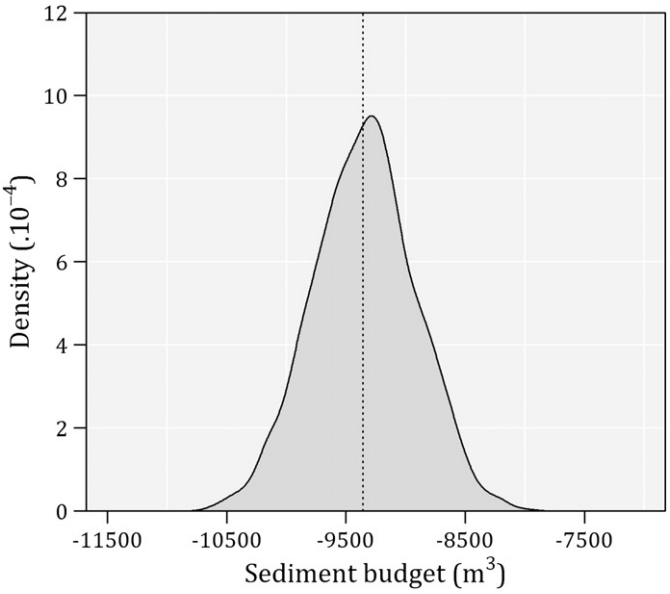

Fig. 13. Probability density function of the case of 1000 sediment budgets of the Ligoire channel. The mean sediment budget and its associated uncertainty are derived from this distribution.

channel by stream action. This figure represents an annual yield of 2.71 ± 0.12 m^3.km^{-2}.y^{-1} (between 3.4 and 5.7 t.km^2.y^{-1}), including 66% of the bank sediments and 34% of the sediments that come from the streambed. Compared to the total sediment flux exported from watersheds of a similar size in the Loire Basin (Gay et al., 2014), the Ligoire may contribute a significant part of the sediment budget of the catchment area drained by the stream (the minimum figure is 20%).

Finally, our approach of comparing historical documents with modern high-resolution field data is easily replicable and relatively cheap to implement, and it provides a quantified overview of the re-equilibration phenomena after modification work is performed on a stream. Monitoring and sampling of so-called natural streams can take place yearly or every few years, and such work is promising for drawing up sediment budgets of rivers on a regional scale.

Acknowledgements

This work is supported by the Loire Brittany river basin agency (AELB), and the authors would like to thank Xavier Bourrain and Jean-Noël Gautier for funding the VERSEAU project 'Transfert de particules des VERSants aux masses d'EAU'. The authors also thank the editor and two anonymous reviewers for their helpful suggestions and corrections to the paper.

References

Ballantine, D.J., Walling, D.E., Collins, A.L., Leeks, G.J.L., 2009. The content and storage of phosphorus in fine-grained channel bed sediment in contrasting lowland agricultural catchments in the UK. Geoderma 151, 141–149. http://dx.doi.org/10.1016/j.geoderma.2009.03.021.

Bravard, J.P., Landon, N., Peiry, J.L., Piegay, H., 1999. Principles of engineering geomorphology for managing channel erosion and bedload transport, examples from French rivers. Geomorphology 31, 291–311.

Brookes, A., 1985. River channelization: traditional engineering methods. Prog. Phys. Geogr. 9, 44–73.

Brookes, A., Gregory, K.J., Dawson, F.H., 1983. An assessment of river channelization in England and Wales. Sci. Total Environ. 27, 97–111.

Collins, A.L., Walling, D.E., 2007. Sources of fine sediment recovered from the channel bed of lowland groundwater-fed catchments in the UK. Geomorphology 88, 120–138. http://dx.doi.org/10.1016/j.geomorph.2006.10.018.

Couper, P., 2003. Effects of silt–clay content on the susceptibility of river banks to subaerial erosion. Geomorphology 56, 95–108. http://dx.doi.org/10.1016/S0169-555X(03)00048-5.

Day, S.S., Gran, K.B., Belmont, P., Wawrzyniec, T., 2013. Measuring bluff erosion part 2: pairing aerial photographs and terrestrial laser scanning to create a watershed scale sediment budget. Earth Surf. Process. Landforms 38, 1068–1082. http://dx.doi.org/10.1002/esp.3359.

De Groot, R.S., Wilson, M.A., Boumans, R.M.J., 2002. A typology for the classification, description and valuation of ecosystem functions, goods and services. Ecol. Econ. 41, 393–408. http://dx.doi.org/10.1016/S0921-8009(02)00089-7.

De Rose, R.C., Basher, L.R., 2011. Measurement of river bank and cliff erosion from sequential LIDAR and historical aerial photography. Geomorphology 126, 132–147. http://dx.doi.org/10.1016/j.geomorph.2010.10.037.

Dietrich, W.E., Dunne, T., Humphrey, N.F., Reid, L.M., 1982. Construction of sediment budgets for drainage basins. Sediment budgets and routing in forested drainage basins: proceedings of the symposium; 31 May - 1 June 1982; Corvallis, Oregon. Gen. Tech. Rep. PNW-141. Pacific Northwest Forest and Range Experiment Station, Forest Service, U.S. Departm, Portland, Oregon, pp. 5–23.

Ford, M.A., Grace, J.B., 1998. Effects of vertebrate herbivores on soil processes, plant biomass, litter accumulation and soil elevation changes in a coastal marsh. J. Ecol. 86, 974–982. http://dx.doi.org/10.1046/j.1365-2745.1998.00314.x.

Gay, A., Cerdan, O., Delmas, M., Desmet, M., 2014. Variability of suspended sediment yields within the Loire river basin (France). J. Hydrol. 519, 1225–1237. http://dx.doi.org/10.1016/j.jhydrol.2014.08.045.

Gomez, B., Coleman, S.E., Sy, V.W.K., Peacock, D.H., Kent, M., 2007. Channel change, bankfull and effective discharges on a vertically accreting, meandering, gravel-bed river. Earth Surf. Process. Landforms 785, 770–785. http://dx.doi.org/10.1002/esp.

Gregory, K.J., 2006. The human role in changing river channels. Geomorphology 79, 172–191. http://dx.doi.org/10.1016/j.geomorph.2006.06.018.

Heitmuller, F.T., 2014. Channel adjustments to historical disturbances along the lower Brazos and Sabine Rivers, south-central USA. Geomorphology 204, 382–398. http://dx.doi.org/10.1016/j.geomorph.2013.08.020.

Heppell, C.M., Wharton, G., Cotton, J.A.C., Bass, J.A.B., Roberts, S.E., 2009. Sediment storage in the shallow hyporheic of lowland vegetated river reaches. Hydrol. Process. 23, 2239–2251. http://dx.doi.org/10.1002/hyp.

Kesel, R.H., Yodis, E.G., 1992. Some effects of human modifications on sand-bed channels in southwestern Mississippi, U.S.A. Environ. Geol. Water Sci. 20, 93–104. http://dx.doi.org/10.1007/BF01737876.

Kessler, A.C., Gupta, S.C., Brown, M.K., 2013. Assessment of river bank erosion in Southern Minnesota rivers post European settlement. Geomorphology 201, 312–322. http://dx.doi.org/10.1016/j.geomorph.2013.07.006.

Kiss, T., Fiala, K., Sipos, G., 2008. Alterations of channel parameters in response to river regulation works since 1840 on the Lower Tisza River (Hungary). Geomorphology 98, 96–110. http://dx.doi.org/10.1016/j.geomorph.2007.02.027.

Kroes, D.E., Hupp, C.R., 2010. The effect of channelization on floodplain sediment deposition and subsidence along the Pocomoke River, Maryland. J. Am. Water Resour. Assoc. 46, 686–699.

Kronvang, B., Laubel, A., Larsen, S.E., Friberg, N., 2003. Pesticides and heavy metals in Danish streambed sediment. Hydrobiologia 494, 93–101.

Landwehr, K., Rhoads, B.L., 2003. Depositional response of a headwater stream to channelization, East Central Illinois, USA. River Res. Appl. 19, 77–100. http://dx.doi.org/10.1002/rra.699.

Lick, W., McNeil, J., 2001. Effects of sediment bulk properties on erosion rates. Sci. Total Environ. 266, 41–48.

Lisle, T.E., Hilton, S., 1999. Fine bed material in pools of natural gravel bed channels. Water Resour. Res. 35, 1291–1304. http://dx.doi.org/10.1029/1998WR900088.

Malavoi, J.-R., Adam, P., 2007. Les interventions humaines et leurs impacts hydromorphologiques sur les cours d'eau. Ingénieries 50, 35–48.

Nakamura, F., Sudo, T., Kameyama, S., Jitsu, M., 1997. Influences of channelization on discharge of suspended sediment and wetland vegetation in Kushiro Marsh, northern Japan. Geomorphology 18, 279–289. http://dx.doi.org/10.1016/S0169-555X(96)00031-1.

Palmer, J.A., Schilling, K.E., Isenhart, T.M., Schultz, R.C., Tomer, M.D., 2014. Streambank erosion rates and loads within a single watershed: Bridging the gap between temporal and spatial scales. Geomorphology 209, 66–78. http://dx.doi.org/10.1016/j.geomorph.2013.11.027.

Rhoades, E.L., O'Neal, M.A., Pizzuto, J.E., 2009. Quantifying bank erosion on the South River from 1937 to 2005, and its importance in assessing Hg contamination. Appl. Geogr. 29, 125–134. http://dx.doi.org/10.1016/j.apgeog.2008.08.005.

Rinaldi, M., Simon, A., 1998. Bed-level adjustments in the Arno River, central Italy. Geomorphology 22, 57–71. http://dx.doi.org/10.1016/S0169-555X(97)00054-8.

Rodrigues, S., Bréhéret, J.-G., Macaire, J.-J., Moatar, F., Nistoran, D., Jugé, P., 2006. Flow and sediment dynamics in the vegetated secondary channels of an anabranching river: The Loire River (France). Sediment. Geol. 186, 89–109. http://dx.doi.org/10.1016/j.sedgeo.2005.11.011.

Schilling, K.E., Isenhart, T.M., Palmer, J.A., Wolter, C.F., Spooner, J., Keith, E., 2011. Impacts of land-cover change on suspended sediment transport in two agricultural watersheds. J. Am. Water Resour. Assoc. 47, 672–686. http://dx.doi.org/10.1111/j.1752-1688.2011.00533.x.

Schoof, R., 1980. Environnemental impact of channel modification. JAWRA J. Am. Water Resour. Assoc. 16, 697–701.

Sear, D.A., Newson, M.D., 2003. Environmental change in river channels: a neglected element. Towards geomorphological typologies, standards and monitoring. Sci. Total Environ. 310, 17–23. http://dx.doi.org/10.1016/S0048-9697(02)00619-8.

Segura-Beltrán, F., Sanchis-Ibor, C., 2013. Assessment of channel changes in a Mediterranean ephemeral stream since the early twentieth century. The Rambla de Cervera, eastern Spain. Geomorphology 201, 199–214. http://dx.doi.org/10.1016/j.geomorph.2013.06.021.

Shields, F.D., Lizotte, R.E., Knight, S.S., Cooper, C.M., Wilcox, D., 2010. The stream channel incision syndrome and water quality. Ecol. Eng. 36, 78–90. http://dx.doi.org/10.1016/j.ecoleng.2009.09.014.

Simon, A., Hupp, C.R., 1987. Geomorphic and vegetative recovery processes along modified Tennessee streams: an interdisciplinary approach to distributed fluvial systems. Proceedings of the Vancouver Symposium, August 1987 (Actes Du Colloque de Vancouver, Août 1987). Forest Hydrology and Watershed Management (Hydrologie Forestière et Aménagement Des Bassins Hydrologiques), pp. 251–262 (IAHS-AISH, Publ. No. 167).

Simon, A., Rinaldi, M., 2006. Disturbance, stream incision, and channel evolution: The roles of excess transport capacity and boundary materials in controlling channel response. Geomorphology 79, 361–383. http://dx.doi.org/10.1016/j.geomorph.2006.06.037.

Simon, A., Thorne, C.R., 1996. Channel adjustment of an unstable coarse-grained stream: opposing trends of boundary and critical shear stress, and the applicability of extremal hypotheses. Earth Surf. Process. Landforms 21, 155–180. http://dx.doi.org/10.1002/(SICI)1096-9837(199602)21:2<155::AID-ESP610>3.0.CO;2-5.

Sipos, G., Kiss, T., Fiala, K., 2007. Morphological alterations due to channelization along the lower Tisza and Maros Rivers (Hungary). Geogr. Fis. Dinam. Quat. 30, 239–247.

Steiger, J., Tabacchi, E., Dufour, S., Corenblit, D., 2005. Hydrogeomorphic processes affecting riparian habitat within alluvial channel-floodplain river systems: a review for the temperate zone. River Res. Appl. 21, 719–737. http://dx.doi.org/10.1002/rra.879.

Stoate, C., Boatman, N.D., Borralho, R.J., Carvalho, C.R., De Snoo, G.R., Eden, P., 2001. Ecological impacts of arable intensification in Europe. J. Environ. Manag. 63, 337–365. http://dx.doi.org/10.1006/jema.2001.0473.

Surian, N., Rinaldi, M., 2003. Morphological response to river engineering and management in alluvial channels in Italy. Geomorphology 50, 307–326. http://dx.doi.org/10.1016/S0169-555X(02)00219-2.

Terrio, P.J., Nazimek, J.E., 1997. Changes in cross-section geometry and channel volume in two reaches of the Kankakee River in Illinois, 1959–94. Water-Resources Investig. Rep. USGS (96-4261. 45 pp.).

Van der Zanden, E.H., Verburg, P.H., Mücher, C.A., 2013. Modelling the spatial distribution of linear landscape elements in Europe. Ecol. Indic. 27, 125–136.

Walling, D.E., Amos, C.M., 1999. Source, storage and mobilisation of fine sediment in a chalk stream system. Hydrol. Process. 13, 323–340.

Walling, D.E., Collins, A.L., 2008. The catchment sediment budget as a management tool. Environ. Sci. Pol. 11, 136–143. http://dx.doi.org/10.1016/j.envsci.2007.10.004.

Walling, D.E., Russell, M.A., Hodgkinson, R.A., Zhang, Y., 2002. Establishing sediment budgets for two small lowland agricultural catchments in the UK. Catena 47, 323–353. http://dx.doi.org/10.1016/S0341-8162(01)00187-4.

Walling, D.E., Owens, P.N., Carter, J., Leeks, G.J.L., Lewis, S., Meharg, A.A., Wright, J., 2003. Storage of sediment-associated nutrients and contaminants in river channel and floodplain systems. Appl. Geochem. 18, 195–220.

Wilcock, D.N., 1991. Environmental impacts of channelization on the River Main, County Antrim, Northern Ireland. J. Environ. Manag. 32, 127–143.

Wilson, C.G., Kuhnle, R.A., Bosch, D.D., Steiner, J.L., Starks, P., Tomer, M.D., Wilson, G.V., 2008. Quantifying relative contributions from sediment sources in Conservation Effects Assessment Project watersheds. J. Soil Water Conserv. 63, 523–532.

Annexe E

Available data on hedgerows and comparison

The choice to use the hedgerow network from BDTopo is linked to the fact that the IGN provides spatially distributed data considering homogeneous methods of data acquisition and treatment over a large portion of the *LBRB*. However, several other data presenting other advantages and drawbacks are available on the *LBRB*. A brief description of database available and their characteristics is proposed here. They are grouped in two families: statistical data resulting from and surveys or statistical procedures and distributed data resulting from mapping procedures.

Statistical data

National study from Pointereau *et al.* (2007) [227] provides the most complete spatial information on hedgerows in the *LBRB* in the sense that it covers the entire French national territory. The data consist of values of kilometres of hedgerows per municipality. The raw data come from the IFN ("*Insventaire Forestier National*") and were acquired between 2000 and 2008. This large time lapse leads to great disparities between departments within the the *LBRB*. The most striking difference is found in Brittany where the department of the Morbihan (56, south Brittany) displays a much lower hedgerow density than in adjacent departments (Figure E.1). This clearly constitute a major drawback, together with the absence of spatial distributed data of the hedgerow network, to the use of the data in a distributed approach of connectivity.

European study from Van der Zanden *et al.* (2013) [283] provides information on the density of the hedgerow network (mentioned as "green lines" by the authors) using linear 250-m transects from the 2009 LUCAS database and interpolation procedures (Figure E.2). The advantage of such database is to provide a homogeneous trend of the hedgerow network and could provide , should the $IC_{revised2}$ be applied over the European territory. Moreover, the initial database, LUCAS, has been updated in 2009, and thus guarantees the homogeneity, in time, of the provided data. However, no information on hedgerow orientation in the field is available.

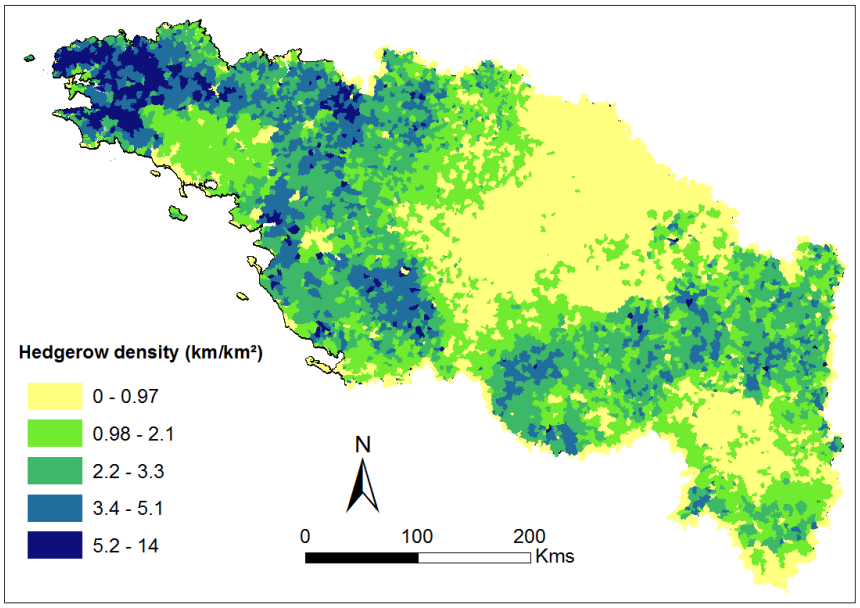

FIGURE E.1 – Hedgerow density (km.km^{-2}) per municipality. Data from SOLAGRO (Pointereau *et al.* (2007) [227]

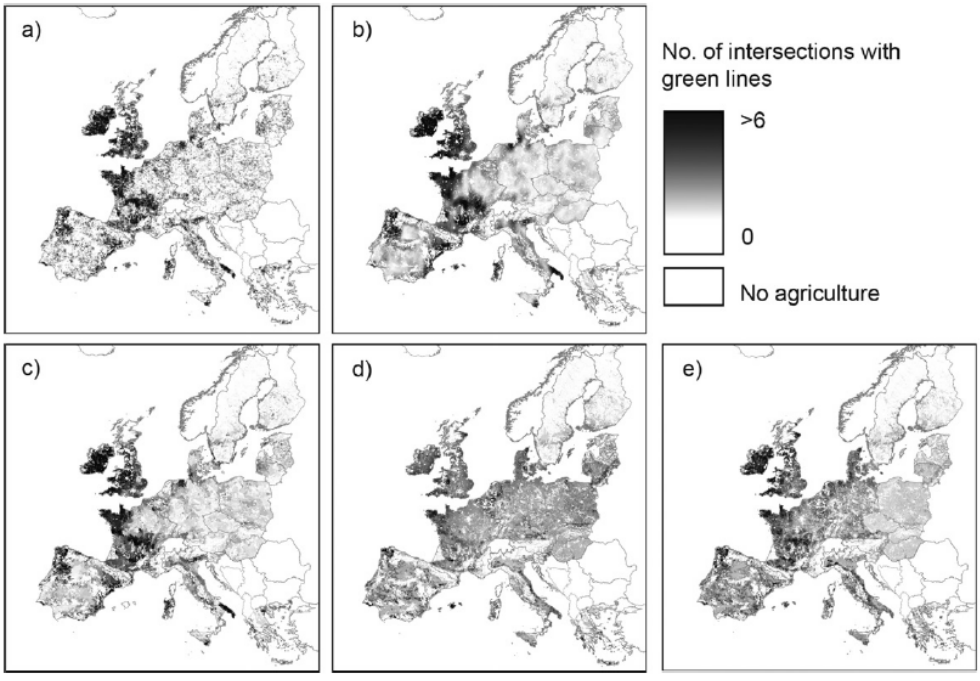

FIGURE E.2 – Modelled density of green lines (counts per 250-m transect) for different interpolation methods using data from LUCAS database: (a) inverse distance weights (IDW), (b) ordinary kriging (OK), (c) LANMAP interpolation, (d) ZINB regression for Europe, and (e) ZINB regression per region (taken from van der Zanden *et al.*, 2013 [283]

Distributed data

The BDTopo ® IGN provides for each department of the French territory, a GIS vector layer of hedgerows in the form of polygons. Though this information is not available for all of the 36 departments, this database constitute the more complete distributed information we know of. The polygon form of each entity allows for the consideration of hedge width and form. Similar trends exist between hedgerow density ($km^2.km^{-2}$) calculated per municipality from these data (Figure E.4) and from the SOLAGRO data. The discrepancy in hedgerow density observed in the data from SOLAGRO between the Morbihan and other departments is not evident in the IGN data. All ground surveys and orthophotographies for the 22 departments where the hedgerow data is available were realised after 2007.

Local studies from the Fishing Federation (Pays de la Loire Region), the Pays Vendômois, and the Breizh Bocage project (still in process), provide GIS vector layers in the form of polylines (Figure E.4). Though this information is very valuable as it is very recent, it could not be used in the present study due to the non-homogeneity of data between three sources, in terms of acquisition and treatment, and the poor cover rate over the $LBRB$. Data from the Breizh Bocage project can be found at :

http://geobretagne.fr/mapfishapp/map/6d97af9c102ccb5f3a2c85cd7dc3f644.

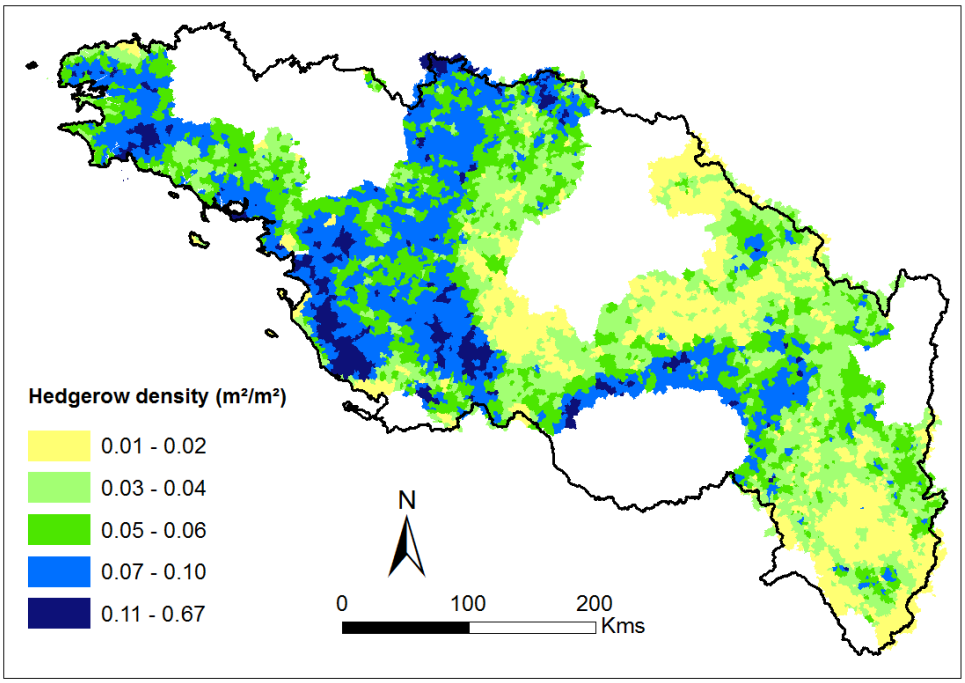

FIGURE E.3 – Hedgerow density ($km2.km^{-2}$) per municipality. Data from BDTopo ® IGN

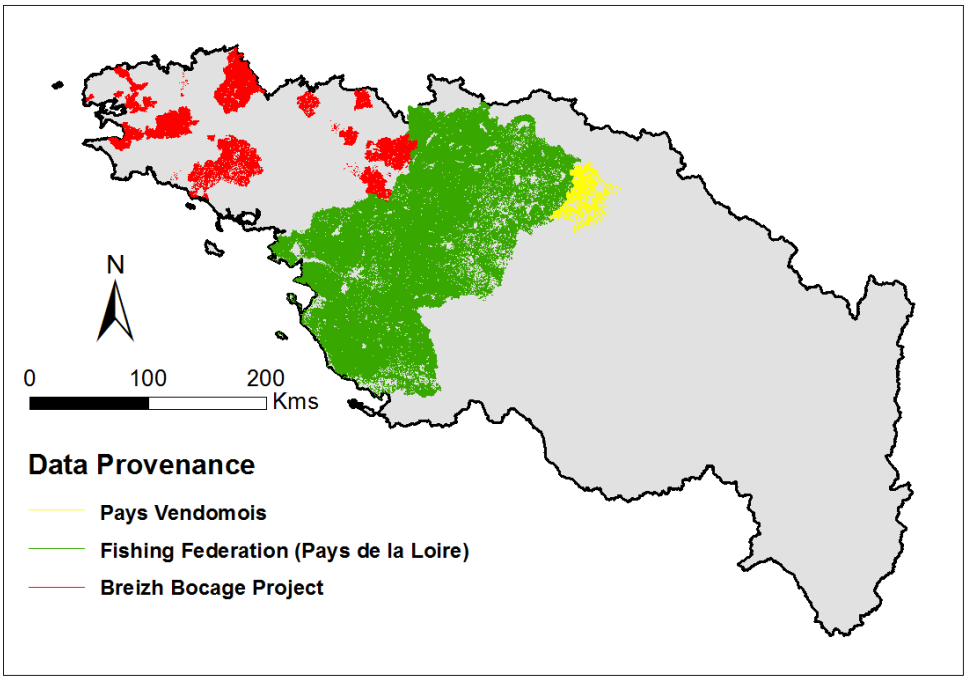

FIGURE E.4 – Hedgerow networks from the different data providers

Annexe F

Map of connected hillslope erosion

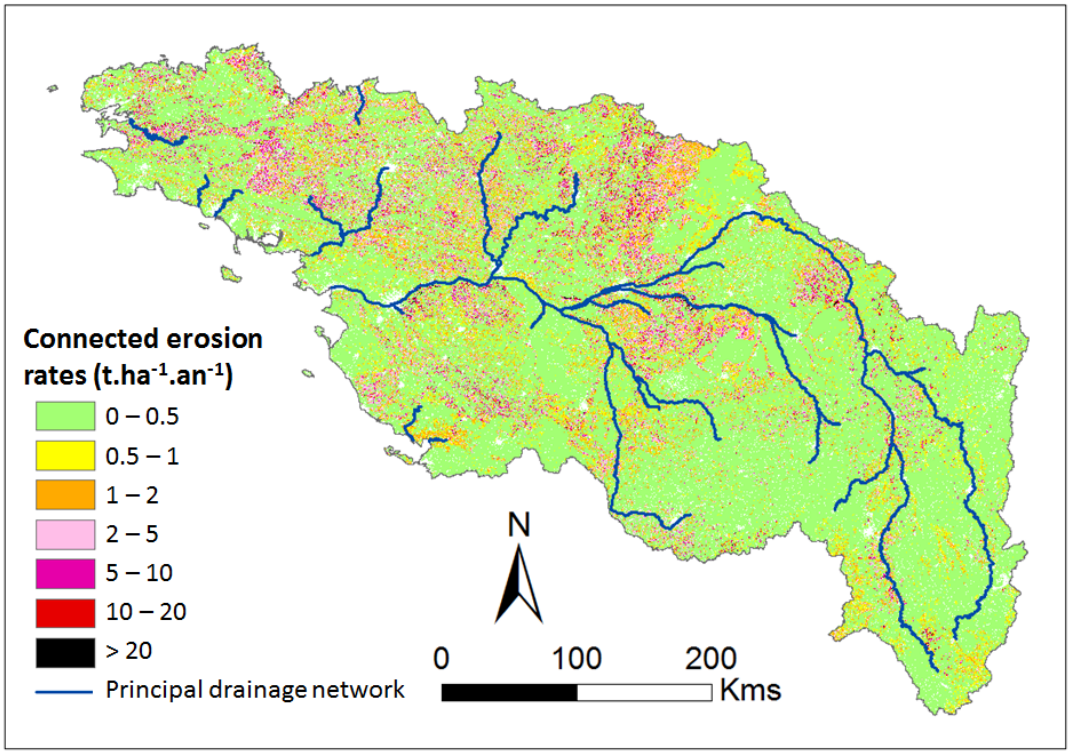

Figure F.1 – Map of rill and interill connected erosion rates

Annexe G

Sediment budget of the 77 catchments

Code station	River name	Area (km^2)	Suspended Sediment yield ($t.km^{-2}.yr^{-1}$)	Dissolved sediment yield ($t.km^{-2}.yr^{-1}$)	Sheet and rill erosion ($t.km^{-2}.yr^{-1}$)	Mass movement ($t.km^{-2}.yr^{-1}$)	Gully erosion ($t.km^{-2}.yr^{-1}$)	Maximum bank erosion ($t.yr^{-1}$)
J0201510	Couesnon	856.07	16.03	-	140.85	4.25	18.74	9367.07
J0611610	Rance	143.46	14.04	-	211.27	5.79	29.76	2457.43
J1114010	Rosette	113.29	6.26	-	191.01	3.94	23.56	1159.43
J1313010	Gouessant	244.05	7.18	-	153.10	3.98	26.81	2766.34
J1324010	Evron	139.42	9.93	-	174.20	4.84	39.03	2519.65
J1513010	GouÃńt	135.68	10.41	-	141.27	4.15	30.68	1551.21
J1721720	Trieux	413.85	12.55	-	76.57	6.79	17.36	2348.61
J1813010	Leff [2]	341.49	9.02	-	159.70	6.65	19.51	3092.07
J2023010	Jaudy	165.13	13.36	-	65.51	4.16	12.93	1416.28
J2034010	Guindy	121.82	14.42	78.72	209.66	6.06	21.12	1329.75
J2314910	Yar	58.50	13.28	66.65	47.78	4.61	21.98	402.88
J2614020	Queffleuth	95.29	11.81	64.97	163.40	5.22	34.38	820.65
J3014310	Horn	50.49	12.82	-	207.71	6.09	29.79	459.11
J3413020	Elorn	200.66	15.57	99.79	140.23	7.98	29.47	2770.31
J4014010	Goyen	88.87	5.19	77.04	70.23	4.46	29.95	1383.98
J4211910	Odet	202.72	15.37	84.87	209.14	5.58	34.24	4030.83
J4742010	EllÃĭ	574.59	11.45	51.8	120.93	5.32	25.89	6890.73
J4902011	LaÃŕta	851.71	11.36	78.16	105.56	5.06	24.73	11564.92
J5102210	Scorff	299.48	13.59	51.1	134.32	4.42	26.24	3708.52
J7000610	Vilaine [1]	56.82	11.17	48.01	188.70	3.73	22.66	792.38
J7010610	Vilaine [2]	146.79	9.43	69.07	207.93	4.13	25.86	3551.00
J7060620	Vilaine [3]	566.97	8.21	-	214.60	4.28	25.97	10247.71
J7083110	ChevrÃĭ	151.28	12.70	-	154.79	4.64	20.43	2971.40
J7103010	Ille	102.60	2.94	37.49	65.71	3.79	11.10	985.09
J7114010	Illet	111.22	7.12	-	70.88	3.89	13.65	1580.00
J7214010	Flume	91.69	10.12	39.14	165.71	3.76	24.17	1365.70
J7700610	Vilaine [4]	4146.39	11.86	49.01	161.18	4.94	21.18	68187.70
J8002310	Oust [1]	28.42	13.22	-	320.06	3.75	41.76	284.19
J8133010	LiÃĭ	298.65	13.03	52.95	133.17	5.26	30.38	3237.81
K0454010	DuniÃĺres	217.46	3.16	-	33.05	3.98	30.18	3261.52
K0550010	Loire [1]	3249.13	8.98	34.03	49.74	7.61	28.93	53920.70
K0614010	Furan	174.53	29.09	199.9	24.47	3.70	23.27	2023.96
K1173210	Arconce	591.25	14.91	-	23.25	11.33	11.74	5855.41
K1363010	Bourbince [1]	338.77	18.75	151.77	15.35	8.37	9.55	2623.02
K1383010	Bourbince [2]	818.93	17.67	69.34	18.88	8.70	9.31	7427.84
K1773010	Aron	1465.53	19.65	59.94	39.10	7.52	14.78	20767.00
K2090810	Allier [1]	518.69	4.71	26.34	53.68	4.64	36.95	9397.23
K2330810	Allier [2]	2260.13	5.50	25.56	53.60	4.34	36.04	32790.09
K2821910	Dore	105.20	7.27	-	19.96	4.25	23.81	977.59
K3153010	Andelot	209.20	13.51	-	100.51	6.26	15.17	1500.12
K3373010	Bouble	560.77	18.32	43.5	61.02	4.74	13.34	3452.85
K3650810	Allier [3]	14347.44	12.22	-	67.22	8.42	25.76	137539.79
K4094010	Nohain	475.82	5.01	-	115.10	7.55	20.25	4915.85
K4873110	Brenne	261.16	10.43	58.66	191.07	4.91	16.17	1036.16
K5183010	Tardes	859.17	5.73	26.67	20.06	4.35	9.82	12844.03
K5383010	Aumance	927.18	11.92	42.05	50.66	5.81	11.35	6221.83
K5490910	Cher [3]	4520.05	8.26	44.32	46.30	6.18	12.03	36042.08
K6720910	Cher [4]	13677.97	12.27	-	112.54	5.75	13.90	110377.58
L0700610	Vienne [1]	3387.16	14.07	29.27	81.78	5.38	15.74	39275.08
L0914020	Gorre	180.03	16.42	28.99	117.24	4.24	9.62	2168.80
L2253010	Vonne	304.41	7.51	-	167.12	5.77	18.76	5875.27
L2501610	Clain	2852.91	6.02	-	162.42	5.40	17.41	28087.16
L4220710	Creuse	1233.23	7.41	26.56	37.79	5.60	15.65	11213.75
L4411710	Petite Creuse	853.13	15.85	26.87	28.40	5.19	10.07	6492.47
L5223020	Vincou	285.55	11.91	20.63	20.77	5.33	11.28	4107.10
L7000610	Vienne [2]	19817.31	11.41	-	92.76	5.63	14.49	183802.96
L8000010	Loire [4]	80999.34	9.07	-	89.73	6.79	17.40	758136.38
M0050620	Sarthe	906.05	14.90	113.02	146.36	8.61	17.26	4122.09
M0114910	Merdereau	118.40	16.24	-	223.68	3.76	26.57	1053.98
M0421510	Huisne	1910.77	11.51	-	338.63	13.50	32.92	10019.53
M0583020	VÃĺgre	400.01	11.66	109.46	118.61	4.74	19.26	8757.84
M0653110	Vaige	238.11	12.79	-	160.90	3.98	19.59	6216.35
M0674010	Taude	45.93	10.46	-	230.50	3.69	26.10	502.78
M1041610	Loir	1156.86	4.94	-	258.81	4.40	18.47	8159.33
M3340910	Mayenne [2]	2901.17	14.42	-	147.63	4.29	20.46	33634.93
M3514010	Ouette	118.62	8.72	-	195.14	5.01	24.38	2066.83
M3711810	Oudon [1]	133.33	6.62	-	226.26	3.76	28.66	2978.47

Code station	River name	Area (km^2)	Suspended Sediment yield ($t.km^{-2}.yr^{-1}$)	Dissolved sediment yield ($t.km^{-2}.yr^{-1}$)	Sheet and rill erosion ($t.km^{-2}.yr^{-1}$)	Mass movement ($t.km^{-2}.yr^{-1}$)	Gully erosion ($t.km^{-2}.yr^{-1}$)	Maximum bank erosion ($t.yr^{-1}$)
M3861810	Oudon [2]	1416.85	11.12	-	205.51	4.52	23.94	33644.77
M5222010	Layon	918.76	12.69	33.7	215.68	4.30	17.18	17099.36
M6014010	Beuvron	38.26	32.44	63.6	49.27	4.46	9.92	627.99
M6323010	Erdre [1]	98.72	13.17	78.95	123.85	3.84	17.52	1065.22
M6333020	Erdre [2]	464.64	7.40	40.37	161.46	4.30	18.97	12241.03
N3001610	Grand Lay [1]	129.53	25.25	69.21	173.02	5.18	25.33	2322.80
N3024010	Loing	121.85	19.79	-	196.76	5.41	27.87	2012.13
N3222010	Smagne	184.87	11.92	104.18	185.06	4.62	19.88	4217.85
N3403010	Yon	40.55	17.33	-	63.99	4.02	16.01	920.79
N5101710	Autise	244.16	13.52	92.87	342.77	5.04	32.12	4735.27

Bibliographie

[1] B. Abernethy and I. D. Rutherfurd. Where along a river's length will vegetation most effectively stabilise stream banks? Geomorphology, 23(1):55–75, 1998. (Cité en page 96.)

[2] European Environment Agency. The European environment - state and outlook 2015: synthesis report. Technical report, Copenhagen, 2015. (Cité en pages xiii, 1, 2 et 98.)

[3] G. A. Ali and A. G. Roy. Revisiting Hydrologic Sampling Strategies for an Accurate Assessment of Hydrologic Connectivity in Humid Temperate Systems. Geography Compass, 3(1):350–374, 2009. (Cité en pages xxi, 130, 133 et 134.)

[4] G.A. Ali, C. Birkel, D. Tetzlaff, C. Soulsby, J. J. McDonnell, and P. Tarolli. A comparison of wetness indices for the prediction of observed connected saturated areas under contrasting conditions. Earth Surface Processes and Landforms, 39(3):399–413, 2013. (Cité en pages 152 et 153.)

[5] M. Antoine, M. Javaux, and C. Bielders. What indicators can capture runoff-relevant connectivity properties of the micro-topography at the plot scale? Advances in Water Resources, 32(8):1297–1310, 2009. (Cité en pages 132, 135, 139, 141 et 152.)

[6] W. M. Appels, P. W. Bogaart, and S. E.A.T.M. van der Zee. Influence of spatial variations of microtopography and infiltration on surface runoff and field scale hydrological connectivity. Advances in Water Resources, 34(2):303–313, 2011. (Cité en pages 132, 139, 141 et 143.)

[7] E. Armijos, A. Crave, P. Vauchel, P. Fraizy, W. Santini, J.-S. Moquet, N. Arevalo, J. Carranza, and J.-L. Guyot. Suspended sediment dynamics in the Amazon River of Peru. Journal of South American Earth Sciences, 44:75–84, 2012. (Cité en page 30.)

[8] N. E. M. Asselman. Fitting and interpretation of sediment rating curves. Journal of Hydrology, 234(3):228–248, 2000. (Cité en page 30.)

[9] J. E.M. Baartman, R. Masselink, S. D. Keesstra, and A. J.A.M. Temme. Linking landscape morphological complexity and sediment connectivity. Earth Surface Processes and Landforms, 2013. (Cité en pages 136, 140 et 152.)

[10] M. M. Bakker, G. Govers, A. van Doorn, F. Quetier, D. Chouvardas, and M. Rounsevell. The response of soil erosion and sediment export to land-use change in four areas of Europe: The importance of landscape pattern. Geomorphology, 98(3-4):213–226, 2008. (Cité en pages 175 et 180.)

[11] O. V. Barron, D. W. Pollock, and W. R. Dawes. Evaluation of catchment connectivity and storm runoff in flat terrain subject to urbanisation. Hydrology and Earth System Sciences Discussions, 6(5):6721–6758, 2009. (Cité en page 146.)

[12] R. Bartley, A. Henderson, G. Baker, M. Bormans, and S. Wilkinson. Patterns of erosion and sediment and nutrient transport in the Douglas Shire catchments

(Daintree, Saltwater, Mossman and Mowbray), Queensland. Technical report, CSIRO Land and Water, 2004. (Cité en pages 97, 104 et 120.)

[13] R. Bartley, R. J. Keen, A. A. Hawdon, P. B. Hairsine, M. G. Disher, and A. E. Kinsey-Henderson. Bank erosion and channel width change in a tropical catchment. Earth Surface Processes and Landforms, 33(14):2174–2200, 2008. (Cité en pages 97 et 105.)

[14] J. Baudry, R.G.H Bunce, and F. Burel. Hedgerows: An international perspective on their origin, function and management. Journal of Environmental Management, 60(1):7–22, 2000. (Non cité.) :$_2$0001722172*et* 172

[15] T. Bisantino, R. Bingner, W. Chouaib, F. Gentile, and G. Trisorio Liuzzi. Estimation of runoff, peak discharge and sediment load at the event scale in a medium-size mediterranean watershed using Annagnps model. Land Degradation & Development, 2015. (Cité en page 152.)

[16] S. Bizzi and D. N. Lerner. The use of stream power as an indicator of channel sensitivity to erosion and deposition processes. River Research and Applications, 2013. (Cité en page 104.)

[17] H. Blanco-Canqui, C. J. Gantzer, and S. H. Anderson. Performance of Grass Barriers and Filter Strips under Interrill and Concentrated Flow. Journal of Environment Quality, 35(6):1969, 2006. (Cité en pages 145 et 173.)

[18] H. Blanco-Canqui and R. Lal. Principles of Soil Conservation and Management. Springer edition, 2008. (Cité en page 174.)

[19] J. Boardman. The hydrological role of 'sunken lanes' with respect to sediment mobilization and delivery to watercourses with particular reference to West Sussex, southern England. Journal of Soils and Sediments, 13(9):1636–1644, 2013. (Cité en page 145.)

[20] J. Boardman, M. L. Shepheard, E. Walker, and I. D.L. Foster. Soil erosion and risk-assessment for on- and off-farm impacts: A test case using the Midhurst area, West Sussex, UK. Journal of Environmental Management, 90(8):2578–2588, 2009. (Cité en page 144.)

[21] L. Borselli, P. Cassi, and D. Torri. Prolegomena to sediment and flow connectivity in the landscape: A GIS and field numerical assessment. CATENA, 75(3):268–277, 2008. (Cité en pages xviii, 133, 140, 151, 152, 153, 154, 156, 161, 169, 174, 175, 176, 177, 179, 180 et 181.)

[22] O. Bour and P. Davy. On the connectivity of three-dimensional fault networks. Water Resources Research, 34(10):2611–2622, 1998. (Cité en page 132.)

[23] L. J. Bracken and J. Croke. The concept of hydrological connectivity and its contribution to understanding runoff-dominated geomorphic systems. Hydrological Processes, 21(13):1749–1763, 2007. (Cité en pages 130, 135 et 152.)

[24] L. J. Bracken, L. Turnbull, J. Wainwright, and P. Bogaart. Sediment connectivity: a framework for understanding sediment transfer at multiple scales. Earth Surface Processes and Landforms, 40(2):177–188, 2015. (Cité en pages 130, 152 et 153.)

[25] L. J. Bracken, J. Wainwright, G. A. Ali, D. Tetzlaff, M. W. Smith, S. M. Reaney, and A. G. Roy. Concepts of hydrological connectivity: Research approaches, pathways and future agendas. Earth-Science Reviews, 119:17 – 34, 2013. (Cité en pages 130, 135, 152, 153 et 170.)

[26] G. Brierley, K. Fryirs, and V. Jain. Landscape connectivity: the geographic basis of geomorphic applications. Area, 38(2):165–174, 2006. (Cité en pages 132, 133, 139, 140 et 152.)

[27] A. Brookes, K. J. Gregory, and F. H. Dawson. An assessment of river channelization in England and Wales. Science of the Total Environment, 27(2):97–111, 1983. (Cité en page 111.)

[28] L. J. Bull. Magnitude and variation in the contribution of bank erosion to the suspended sediment load of the River Severn, UK. Earth Surface Processes and Landforms, 22(12):1109–1123, 1997. (Cité en pages 97, 109 et 120.)

[29] J.N. Callow and K.R.J. Smettem. The effect of farm dams and constructed banks on hydrologic connectivity and runoff estimation in agricultural landscapes. Environmental Modelling & Software, 24(8):959–968, 2009. (Cité en page 144.)

[30] E. L. H. Cammeraat. A review of two strongly contrasting geomorphological systems within the context of scale. Earth Surface Processes and Landforms, 27(11):1201–1222, 2002. (Cité en page 138.)

[31] E. L.H. Cammeraat. Scale dependent thresholds in hydrological and erosion response of a semi-arid catchment in southeast Spain. Agriculture, Ecosystems & Environment, 104(2):317–332, 2004. (Cité en page 131.)

[32] M. Campy, J.-J. Macaire, and C. Grosbois. Géologie de la surface : érosion, transfert et stockage dans les environnement continentaux, 3e édition. Paris, dunod edition, 2003. (Cité en page 87.)

[33] N. Carluer and G. D. Marsily. Assessment and modelling of the influence of man-made networks on the hydrology of a small watershed: implications for fast flow components, water quality and landscape management. Journal of Hydrology, 285(1-4):76–95, 2004. (Cité en pages xvii, 146, 147 et 173.)

[34] M. Cavalli, S. Trevisani, F. Comiti, and L. Marchi. Geomorphometric assessment of spatial sediment connectivity in small Alpine catchments. Geomorphology, 188:31–41, 2013. (Cité en pages 140 et 153.)

[35] A. Cerdà and S. H. Doerr. The effect of ant mounds on overland flow and soil erodibility following a wildfire in eastern Spain. Ecohydrology, 3(4):392–401, 2010. (Cité en pages 84 et 165.)

[36] O. Cerdan, M. Delmas, P. Négrel, J.-M. Mouchel, E. Petelet-Giraud, S. Salvador-Blanes, and F. Degan. Contribution of diffuse hillslope erosion to the sediment export of French rivers. Comptes Rendus Geoscience, 344(11-12):636–645, 2012. (Cité en pages 59, 62, 68, 76 et 77.)

[37] O. Cerdan, G. Govers, Y. Le Bissonnais, K. Van Oost, J. Poesen, N. Saby, A. Gobin, A. Vacca, J. Quinton, K. Auerswald, A. Klik, F.J.P.M. Kwaad, D. Raclot, I. Ionita, J. Rejman, S. Rousseva, T. Muxart, M.J. Roxo, and T. Dostal.

Rates and spatial variations of soil erosion in Europe: A study based on erosion plot data. Geomorphology, 122(1-2):167–177, 2010. (Cité en pages xvi, xix, 3, 44, 53, 85, 98, 170, 187 et 188.)

[38] C. Chartin, O. Evrard, Y. Onda, J. Patin, I. Lefèvre, C. Ottlé, S. Ayrault, H. Lepage, and P. Bonté. Tracking the early dispersion of contaminated sediment along rivers draining the Fukushima radioactive pollution plume. Anthropocene, 1:23 – 34, 2013. (Cité en page 153.)

[39] C. Chartin, O. Evrard, S. Salvador-Blanes, F. Hinschberger, K. Van Oost, I. Lefèvre, J. Daroussin, and J.-J. Macaire. Quantifying and modelling the impact of land consolidation and field borders on soil redistribution in agricultural landscapes (1954–2009). Catena, 110:184–195, 2013. (Cité en page 92.)

[40] B. Cheviron, M. Delmas, O. Cerdan, and J.-M. Mouchel. Calculation of river sediment fluxes from uncertain and infrequent measurements. Journal of Hydrology, 508:364–373, 2014. (Cité en pages 30, 34, 35 et 63.)

[41] R. Ciampalini, S. Follain, and Y. Le Bissonnais. LandSoil - A model for analysing the impact of erosion on agricultural landscape evolution. Geomorphology, 175:25–37, 2012. (Cité en page 92.)

[42] D. Ciszewski and A. Czajka. Human-induced sedimentation patterns of a channelized lowland river. Earth Surface Processes and Landforms, 2014. (Cité en page 111.)

[43] A.L. Collins, D. E. Walling, and G. J. L. Leeks. Storage of fine-grained sediment and associated contaminants within the channels of lowland permeabe catchments in the U.K. In IAHS Publications., pages 259 – 268, 2005. (Cité en page 45.)

[44] M.B. Collins. Processes and controls involved in the transfer of fluviatile sediments to the deep ocean. Journal of the Geological Society, 143(6):915–920, 1986. (Cité en page 38.)

[45] European Commission. The European Soil Database distribution version 2.0. Technical Report EUR 19945 EN., 2004. (Cité en page 87.)

[46] R. J. Cooper, T. Krueger, K. M. Hiscock, and B. G. Rawlins. High-temporal resolution fluvial sediment source fingerprinting with uncertainty: a Bayesian approach. Earth Surface Processes and Landforms, 40(1):78–92, 2015. (Cité en page 197.)

[47] T. J. Coulthard and M. J. Van De Wiel. Quantifying fluvial non linearity and finding self organized criticality? Insights from simulations of river basin evolution. Geomorphology, 91(3-4):216–235, 2007. (Cité en page 136.)

[48] P. Couper. Effects of silt–clay content on the susceptibility of river banks to subaerial erosion. Geomorphology, 56(1-2):95–108, 2003. (Cité en page 97.)

[49] A. Couturier, J. Daroussin, F. Darboux, V. Souchère, Y. Le Bissonnais, O. Cerdan, and D. King. Improvement of surface flow network prediction for the modeling of erosion processes in agricultural landscapes. Geomorphology, 183:120–129, 2013. (Cité en page 144.)

[50] A. Coynel, J. Schafer, J. Hurtrez, J. Dumas, H. Etcheber, and G. Blanc. Sampling frequency and accuracy of SPM flux estimates in two contrasted drainage basins. Science of The Total Environment, 330(1-3):233–247, 2004. (Cité en page 30.)

[51] J. Croke, S. Mockler, P. Fogarty, and I. Takken. Sediment concentration changes in runoff pathways from a forest road network and the resultant spatial pattern of catchment connectivity. Geomorphology, 68(3-4):257–268, 2005. (Cité en pages 135, 138, 145, 152 et 172.)

[52] S. M. Dabney, M. T. Moore, and M. A. Locke. Integrated management of in-field, edge-of-field, and after-field buffer. JAWRA Journal of the American Water Resources Association, 42(1):15–24, 2006. (Cité en page 172.)

[53] Z. Dai and J. T. Liu. Impacts of large dams on downstream fluvial sedimentation: An example of the Three Gorges Dam (TGD) on the Changjiang (Yangtze River). Journal of Hydrology, 480:10–18, 2013. (Cité en page 147.)

[54] T. H. Dang, A. Coynel, D. Orange, G. Blanc, H. Etcheber, and L. A. Le. Long-term monitoring (1960–2008) of the river-sediment transport in the Red River Watershed (Vietnam): Temporal variability and dam-reservoir impact. Science of The Total Environment, 408(20):4654–4664, 2010. (Cité en page 29.)

[55] R. B. Daniels and J. W. Gilliam. Sediment and chemical load reduction by grass and riparian filters. Soil Science Society of America Journal, 60(1):246–251, 1996. (Cité en page 173.)

[56] F. Darboux, P. Davy, C. Gascuel-Odoux, and C. Huang. Evolution of soil surface roughness and flowpath connectivity in overland flow experiments. Catena, 46(2):125–139, 2001. (Cité en pages 139 et 152.)

[57] S. E. Darby, A. M. Alabyan, and M. J. Van de Wiel. Numerical simulation of bank erosion and channel migration in meandering rivers. Water Resources Research, 38(9):2–1, 2002. (Cité en page 97.)

[58] P. Davy, F. Guillocheau, B. Hamelin, and others. Géomorphologie: Processus et modélisation. Mémoire de Géosciences Rennes, 1997. (Non cité.) :$_1$997611161

[59] S. S. Day, K. B. Gran, P. Belmont, and T. Wawrzyniec. Measuring bluff erosion part 2: pairing aerial photographs and terrestrial laser scanning to create a watershed scale sediment budget. Earth Surface Processes and Landforms, 38(10):1068–1082, 2013. (Cité en page 97.)

[60] Comité de Bassin Loire-Bretagne. État des lieux du bassin Loire-Bretagne. 2013. (Cité en page 1.)

[61] R. C. De Rose and L. R. Basher. Measurement of river bank and cliff erosion from sequential LIDAR and historical aerial photography. Geomorphology, 126(1-2):132–147, 2011. (Cité en pages 120 et 121.)

[62] R. C. De Rose, I. P. Prosser, L. J. Wilkinson, A. O. Hughes, and W. J. Young. Regional patterns of erosion and sediment and nutrient transport in the Mary river catchment, Queensland. CSIRO Land and Water, 2002. (Cité en pages 110, 119 et 120.)

[63] J. de Vente and J. Poesen. Predicting soil erosion and sediment yield at the basin scale: Scale issues and semi-quantitative models. Earth-Science Reviews, 71(1-2):95–125, 2005. (Cité en page 29.)

[64] J. de Vente, J. Poesen, and G. Verstraeten. The application of semi-quantitative methods and reservoir sedimentation rates for the prediction of basin sediment yield in Spain. Journal of Hydrology, 305(1-4):63–86, 2005. (Cité en pages 29 et 40.)

[65] J. de Vente, J. Poesen, G. Verstraeten, A. Van Rompaey, and G. Govers. Spatially distributed modelling of soil erosion and sediment yield at regional scales in Spain. Global and Planetary Change, 60(3-4):393–415, 2008. (Cité en pages 86 et 105.)

[66] C. Deasy, R. E. Brazier, A. L. Heathwaite, and R. Hodgkinson. Pathways of runoff and sediment transfer in small agricultural catchments. Hydrological Processes, 23(9):1349–1358, 2009. (Cité en pages 90 et 146.)

[67] F. Degan, S. Salvador-Blanes, and O. Cerdan. Multifunctional map of soil erosion hazard: example in the Loire-Brittany region. In prep., 2015. (Cité en pages xiii, xvii, 19, 20, 53, 86, 91, 154, 155, 175, 182 et 198.)

[68] M. Delmas. Origine des exports de sédiments fluviatiles: Prise en compte de l'hétérogénéité spatiale des versants. PhD thesis, Université Paris VI, 2011. (Cité en pages xvi, 3, 54, 86, 87 et 158.)

[69] M. Delmas, O. Cerdan, B. Cheviron, and J. M. Mouchel. River basin sediment flux assessments. Hydrological Processes, 25(10):1587–1596, 2011. (Cité en pages 29, 30, 34 et 42.)

[70] M. Delmas, O. Cerdan, B. Cheviron, J.-M. Mouchel, and F. Eyrolle. Sediment export from French rivers to the sea. Earth Surface Processes and Landforms, 37(7):754–762, 2012. (Cité en pages 30, 31, 33, 38, 54, 59, 64 et 66.)

[71] M. Delmas, O. Cerdan, J.-M. Mouchel, and M. Garcin. A method for developing a large-scale sediment yield index for European river basins. Journal of Soils and Sediments, 9(6):613–626, 2009. (Cité en pages 38, 39, 53, 54, 87, 152, 156 et 166.)

[72] K. D'Haen, B. Dusar, G. Verstraeten, P. Degryse, and H. De Brue. A sediment fingerprinting approach to understand the geomorphic coupling in an eastern Mediterranean mountainous river catchment. Geomorphology, 197:64 – 75, 2013. (Cité en pages 131, 140 et 153.)

[73] E. Dhivert. Mécanismes et modalités de la distribution spatiale et temporelle des métaux dans les sédiments du bassin versant de la Loire. PhD thesis, Université François Rabelais-Tours, Tours, 2014. (Cité en pages xiii et 17.)

[74] W. E. Dietrich, T. Dunne, N. F. Humphrey, L. M. Reid, et al. Construction of sediment budgets for drainage basins. Sediment Budgets in Forested Drainage Basins. United States Forest Service Gen. Tech. Rep. PNW-141. p5-23, 1982. (Cité en page 3.)

[75] N. Diodato, M. Fagnano, and I. Alberico. Geospatial and visual modeling for exploring sediment source areas across the Sele river landscape, Italy. Italian Journal of Agronomy, 6(2):14, 2011. (Cité en pages 175 et 179.)

[76] J. Doherty. PEST - Model-Independant Parameter Estimation, User Manual. Watermark Numerical Computing., 2004. (Cité en page 34.)

[77] R. Dupas, F. Curie, C. Gascuel-Odoux, F. Moatar, M. Delmas, V. Parnaudeau, and P. Durand. Assessing N emissions in surface water at the national level: Comparison of country-wide vs. regionalized models. Science of The Total Environment, 443:152–162, 2013. (Cité en page 71.)

[78] R. Dupas, M. Delmas, J.-M. Dorioz, J. Garnier, F. Moatar, and C. Gascuel-Odoux. Assessing the impact of agricultural pressures on N and P loads and eutrophication risk. Ecological Indicators, 48:396–407, 2015. (Cité en pages 71 et 158.)

[79] R. Dupas, C. Gascuel-Odoux, N. Gilliet, C. Grimaldi, and G. Gruau. Distinct export dynamics for dissolved and particulate phosphorus reveal independent transport mechanisms in an arable headwater catchment. Hydrological Processes, 2015. (Cité en page 59.)

[80] C. Duvert, N. Gratiot, R. Anguiano-Valencia, J. Némery, M. E. Mendoza, T. Carlón-Allende, C. Prat, and M. Estèves. Baseflow control on sediment flux connectivity: Insights from a nested catchment study in Central Mexico. CATENA, 87(1):129–140, 2011. (Cité en pages 30 et 133.)

[81] J. P. C. Eekhout, A. J. F. Hoitink, J. H. F. de Brouwer, and P. F. M. Verdonschot. Morphological assessment of reconstructed lowland streams in the Netherlands. Advances in Water Resources, 2014. (Cité en page 147.)

[82] J.G. Estèves and W. Ludwig. Transfert de matière en suspension et de carbone particulate dans le bassin versant de la Têt (Sud de la France). IAHS Publications, 278, 2003. (Cité en page 30.)

[83] D.J. Evans, C.E. Gibson, and R.S. Rossell. Sediment loads and sources in heavily modified Irish catchments: A move towards informed management strategies. Geomorphology, 79(1-2):93–113, 2006. (Cité en page 97.)

[84] O. Evrard, G. Nord, O. Cerdan, V. Souchère, Y. Le Bissonnais, and P. Bonté. Modelling the impact of land use change and rainfall seasonality on sediment export from an agricultural catchment of the northwestern European loess belt. Agriculture, Ecosystems & Environment, 138(1-2):83–94, 2010. (Cité en page 44.)

[85] FAO/IIASA/ISRIC/ISS-CAS/JRC. Harmonized World Soil Database (version 1.2). Technical report, FAO, Rome, Italy and IIASA, Laxenburg, Austria., 2009. (Cité en pages 12, 102 et 105.)

[86] H. Faulkner. Connectivity as a crucial determinant of badland morphology and evolution. Geomorphology, 100(1-2):91–103, 2008. (Cité en page 131.)

[87] J. L. Florsheim, J. F. Mount, and A. Chin. Bank erosion as a desirable attribute of rivers. BioScience, 58(6):519–529, 2008. (Cité en page 96.)

[88] S. Foerster, C. Wilczok, A. Brosinsky, and K. Segl. Assessment of sediment connectivity from vegetation cover and topography using remotely sensed data in a dryland catchment in the Spanish Pyrenees. Journal of Soils and Sediments, 14(12):1982–2000, 2014. (Cité en pages 131, 144, 153 et 165.)

[89] S. Follain, B. Minasny, A. B. McBratney, and C. Walter. Simulation of soil thickness evolution in a complex agricultural landscape at fine spatial and temporal scales. Geoderma, 133(1-2):71–86, 2006. (Cité en pages 145 et 173.)

[90] A. Foucher, S. Salvador-Blanes, O. Evrard, A. Simonneau, A. Chapron, T. Courp, O. Cerdan, I. Lefèvre, H. Adriaensen, F. Lecompte, and M. Desmet. Increase in soil erosion after agricultural intensification: Evidence from a lowland basin in France. Anthropocene, 2015. (Cité en pages 131, 147, 148 et 153.)

[91] A. Foucher, S. Salvador-Blanes, R. Vandromme, O. Cerdan, and M. Desmet. Quantification of bank erosion in an agricultural lowland drained catchment. In prep., 2015. (Cité en page 97.)

[92] R. M. Frings, N. Gehres, M. Promny, H. Middelkoop, H. Schüttrumpf, and S. Vollmer. Today's sediment budget of the Rhine River channel, focusing on the Upper Rhine Graben and Rhenish Massif. Geomorphology, 2013. (Cité en page 3.)

[93] K. Fryirs. (Dis)Connectivity in catchment sediment cascades: a fresh look at the sediment delivery problem. Earth Surface Processes and Landforms, 38(1):30–46, 2013. (Cité en pages 3 et 130.)

[94] K. A. Fryirs, G. J. Brierley, N. J. Preston, and M. Kasai. Buffers, barriers and blankets: The (dis)connectivity of catchment-scale sediment cascades. CATENA, 70(1):49–67, 2007. (Cité en pages 131, 141 et 153.)

[95] K. A. Fryirs, G. J. Brierley, N. J. Preston, and J. Spencer. Catchment-scale (dis)connectivity in sediment flux in the upper Hunter catchment, New South Wales, Australia. Geomorphology, 84(3-4):297–316, 2007. (Cité en page 132.)

[96] D. Gabriels, G. Ghekiere, W. Schiettecatte, and I. Rottiers. Assessment of USLE cover-management C-factors for 40 crop rotation systems on arable farms in the Kemmelbeek watershed, Belgium. Soil and Tillage Research, 74(1):47–53, 2003. (Cité en pages 165 et 191.)

[97] J. Gaillardet, B. Dupré, P. Louvat, and C. J. Allegre. Global silicate weathering and CO2 consumption rates deduced from the chemistry of large rivers. Chemical Geology, 159(1):3–30, 1999. (Cité en pages 58, 59, 60, 67, 68, 77 et 80.)

[98] B. Gao, D. Yang, and H. Yang. Impact of the Three Gorges Dam on flow regime in the middle and lower Yangtze River. Quaternary International, 304:43–50, 2013. (Cité en page 147.)

[99] P. Gao and J. Puckett. A new approach for linking event-based upland sediment sources to downstream suspended sediment transport. Earth Surface Processes and Landforms, 37(2):169–179, 2011. (Cité en page 54.)

[100] X. Gao, P. Wu, X. Zhao, J. Wang, and Y. Shi. Effects of land use on soil moisture variations in a semi-arid catchment: implications for land and agricultural water management. Land Degradation & Development, 25(2):163–172, 2014. (Cité en page 165.)

[101] M. Garcin, N. Carcaud, E. Gautier, J. Burnouf, C. Castanet, N. Fouillet, et al. Impacts des héritages sur un hydrosystème: l'exemple des levées en Loire moyenne

et océanique. L'érosion entre société, climat et paléoenvironnement, pages 225–236, 2006. (Cité en page 31.)

[102] C. Gascuel-Odoux, P. Aurousseau, T. Doray, H. Squividant, F. Macary, D. Uny, and C. Grimaldi. Incorporating landscape features to obtain an object-oriented landscape drainage network representing the connectivity of surface flow pathways over rural catchments. Hydrological Processes, 25(23):3625–3636, 2011. (Cité en pages 131 et 173.)

[103] E. Gautier, H. Piégay, and P. Bertaina. A methodological approach of fluvial dynamics oriented towards hydrosystem management: case study of the Loire and Allier rivers. Geodinamica Acta, 13(1):29–43, 2000. (Cité en page 98.)

[104] A. Gay, O. Cerdan, M. Delmas, and M. Desmet. Variability of suspended sediment yields within the Loire river basin (France). Journal of Hydrology, 519:1225–1237, 2014. (Cité en pages 69, 77, 119, 121, 153 et 170.)

[105] A. Gay, O. Cerdan, V. Mardhel, and M. Desmet. Application of an index of connectivity in a lowland area. Journal of Soils and Sediments, 2015. (Cité en pages xviii, 174, 177 et 181.)

[106] K. Ghosh. Assessment of Soil Loss of the Dhalai River Basin, Tripura, India Using USLE. International Journal of Geosciences, 04(01):11–23, 2013. (Cité en page 179.)

[107] A. E. Godfrey, B. L. Everitt, and J. F. M. Duque. Episodic sediment delivery and landscape connectivity in the Mancos Shale badlands and Fremont River system, Utah, USA. Geomorphology, 102(2):242–251, 2008. (Cité en page 131.)

[108] H. E. Golden, C. R. Lane, D. M. Amatya, K. W. Bandilla, H. Raanan Kiperwas, C. D. Knightes, and H. Ssegane. Hydrologic connectivity between geographically isolated wetlands and surface water systems: A review of select modeling methods. Environmental Modelling & Software, 53:190–206, 2014. (Cité en pages 130 et 139.)

[109] J. C. Gonzalez-Hidalgo, R. J. Batalla, and A. Cerda. Catchment size and contribution of the largest daily events to suspended sediment load on a continental scale. CATENA, 102:40–45, 2013. (Cité en page 137.)

[110] J. C. Gonzalez-Hidalgo, R. J Batalla, A. Cerda, and M. de Luis. A regional analysis of the effects of largest events on soil erosion. Catena, 95:85–90, 2012. (Cité en page 137.)

[111] G. Govers, T.A. Quine, P.J.J. Desmet, and D.E. Walling. The relative contribution of soil tillage and overland flow erosion to soil redistribution on agricultural land. Earth Surface Processes and Landforms, 21(10):929–946, 1996. (Cité en page 92.)

[112] M. Granet, F. Chabaux, P. Stille, C. France-Lanord, and E. Pelt. Time-scales of sedimentary transfer and weathering processes from U-series nuclides: Clues from the Himalayan rivers. Earth and Planetary Science Letters, 261(3-4):389–406, September 2007. (Cité en page 68.)

[113] C. Grimaldi, M. Fossey, Zahra. Thomas, Y. Fauvel, and P. Merot. Nitrate attenuation in soil and shallow groundwater under a bottomland hedgerow in a European farming landscape. Hydrological Processes, 26(23):3570–3578, 2012. (Cité en page 191.)

[114] C. Grosbois, P. Negrel, C. Fouillac, and D. Grimaud. Dissolved load of the Loire River: chemical and isotopic characterization. Chemical Geology, 170(1):179–201, 2000. (Cité en pages 31, 58, 67 et 68.)

[115] C. Grosbois, P. Négrel, D. Grimaud, and C. Fouillac. An overview of dissolved and suspended matter fluxes in the Loire river basin: natural and anthropogenic inputs. Aquatic Geochemistry, 7(2):81–105, 2001. (Cité en pages 58, 59, 61 et 76.)

[116] J. R. Grove, J. Croke, and C. Thompson. Quantifying different riverbank erosion processes during an extreme flood event: Riverbank erosion from an extreme flood event. Earth Surface Processes and Landforms, 2013. (Cité en page 97.)

[117] S. J. Gumiere, Y. Le Bissonnais, D. Raclot, and B. Cheviron. Vegetated filter effects on sedimentological connectivity of agricultural catchments in erosion modelling: a review. Earth Surface Processes and Landforms, 36(1):3–19, 2011. (Cité en pages 130, 131, 141, 144, 169, 173, 174, 179 et 184.)

[118] P.S. Hai, T.D. Khoa, N. Dao, N.T. Mui, T.V. Hoa, P.D. Hien, and T.C. Tu. Application of Caesium-137 and Beryllium-7 to Assess the Effectiveness of Soil Conservation Technologies in the Central Highlands of Vietnam. Soil Conservation Measures on Erosion Control and Soil Quality, page 195, 2000. (Cité en page 173.)

[119] N. Haregeweyn, J. Poesen, G. Verstraeten, G. Govers, J. Vente, J. Nyssen, J. Deckers, and J. Moeyersons. Assessing the performance of a spatially distributed soil erosion and sediment delivery model (WATEM/SEDEM) in Northern Ethiopia. Land Degradation & Development, 24(2):188–204, 2013. (Cité en page 152.)

[120] M.-A. Harel and E. Mouche. Is the connectivity function a good indicator of soil infiltrability distribution and runoff flow dimension? Earth Surface Processes and Landforms, 2014. (Cité en pages 139 et 141.)

[121] A. M. Harvey. Coupling between hillslopes and channels in upland fluvial systems: implications for landscape sensitivity, illustrated from the Howgill Fells, northwest England. Catena, 42(2):225–250, 2001. (Cité en pages 97, 104 et 131.)

[122] T. Heckmann and W. Schwanghart. Geomorphic coupling and sediment connectivity in an alpine catchment — Exploring sediment cascades using graph theory. Geomorphology, 182:89–103, 2013. (Cité en pages 140 et 152.)

[123] T. Heckmann, W. Schwanghart, and J. D. Phillips. Graph theory — recent developments of its application in geomorphology. Geomorphology, 2014. (Cité en page 140.)

[124] A. J. Henshaw, C. R. Thorne, and N. J. Clifford. Identifying causes and controls of river bank erosion in a British upland catchment. CATENA, 100:107–119, 2013. (Cité en page 110.)

[125] J. N. Holeman. The sediment yield of major rivers of the world. Water Resources Research, 4(4):737–747, 1968. (Cité en page 38.)

[126] J. Hooke. Coarse sediment connectivity in river channel systems: a conceptual framework and methodology. Geomorphology, 56(1-2):79–94, 2003. (Cité en pages 132, 138, 139 et 147.)

[127] J. M. Hooke. Magnitude and distribution of rates of river bank erosion. Earth surface processes, 5(2):143–157, 1980. (Cité en pages 96 et 97.)

[128] A. J. Horowitz. An evaluation of sediment rating curves for estimating suspended sediment concentrations for subsequent flux calculations. Hydrological Processes, 17(17):3387–3409, 2003. (Cité en pages 29 et 30.)

[129] A. J. Horowitz, F. A. Rinella, P. Lamothe, T. L. Miller, T. K. Edwards, R. L. Roche, and D. A. Rickert. Variations in suspended sediment and associated trace element concentrations in selected riverine cross sections. Environmental science & technology, 24(9):1313–1320, 1990. (Cité en page 35.)

[130] R.E. Horton. Erosional development of streams and their drainage basins; Hydrophysical approach to quantitative morphology. Geological Society of America Bulletin, 56(3):275, 1945. (Cité en page 153.)

[131] A. O. Hughes and I. P. Prosser. Gully and riverbank erosion mapping for the Murray-Darling Basin. CSIRO Land and Water, 2003. (Cité en pages 97, 104 et 110.)

[132] A. O. Hughes, I. P. Prosser, P. J. Wallbrink, and J. Stevenson. Suspended sediment and bedload budgets for the Western Port Bay Basin. CSIRO Land and Water, 2003. (Cité en page 110.)

[133] I. M. L. Jansen and R. B. Painter. Predicting sediment yield from climate and topography. Journal of Hydrology, 21(4):371–380, 1974. (Cité en pages 29, 38 et 53.)

[134] K. G. Jencso, B. L. McGlynn, M. N. Gooseff, S. M. Wondzell, K. E. Bencala, and L. A. Marshall. Hydrologic connectivity between landscapes and streams: Transferring reach- and plot-scale understanding to the catchment scale. Water Resources Research, 45(4), 2009. (Cité en page 132.)

[135] P. K. Jha, V. Subramanian, and R. Sitasawad. Chemical and sediment mass transfer in the Yamuna River - a tributary of the Ganges system. Journal of hydrology, 104(1):237–246, 1988. (Cité en page 68.)

[136] K.-T. Jiann and L.-S. Wen. Intra-annual variability of distribution patterns and fluxes of dissolved trace metals in a subtropical estuary (Danshuei River, Taiwan). Journal of Marine Systems, 75(1):87–99, 2009. (Cité en page 63.)

[137] G. Jordan, A. van Rompaey, P. Szilassi, G. Csillag, C. Mannaerts, and T. Woldai. Historical land use changes and their impact on sediment fluxes in the Balaton basin (Hungary). Agriculture, Ecosystems & Environment, 108(2):119–133, 2005. (Cité en pages 175 et 180.)

[138] H. A. Katz, J. M. Daniels, and S. Ryan. Slope-area thresholds of road-induced gully erosion and consequent hillslope-channel interactions. Earth Surface Processes and Landforms, 2013. (Cité en pages 135 et 145.)

[139] A. C. Kessler, S. C. Gupta, and M. K. Brown. Assessment of river bank erosion in Southern Minnesota rivers post European settlement. Geomorphology, 201:312–322, 2013. (Cité en pages 97 et 109.)

[140] J. Kiesel, N. Fohrer, B. Schmalz, and M. J. White. Incorporating landscape depressions and tile drainages of a northern German lowland catchment into a semi-distributed model. Hydrological Processes, 24(11):1472–1486, 2010. (Cité en pages 90, 165 et 172.)

[141] J. Kiesel, B. Schmalz, G. L. Brown, and N. Fohrer. Application of a hydrological-hydraulic modelling cascade in lowlands for investigating water and sediment fluxes in catchment, channel and reach. Journal of Hydrology and Hydromechanics, 61(4), 2013. (Cité en page 97.)

[142] J. Kiesel, B. Schmalz, and N. Fohrer. SEPAL-a simple GIS-based tool to estimate sediment pathways in lowland catchments. Advances in Geosciences, 21:25–32, 2009. (Cité en page 165.)

[143] M. Kirkby. Do not only connect: a model of infiltration-excess overland flow based on simulation. Earth Surface Processes and Landforms, 2014. (Cité en pages 141 et 165.)

[144] M. J. Kirkby, B. J. Irvine, R. J. A. Jones, G. Govers, and PESERA team. The PESERA coarse scale erosion model for Europe. I. - Model rationale and implementation. European Journal of Soil Science, 59(6):1293–1306, 2008. (Cité en pages 3, 86 et 98.)

[145] C. Knudby and J. Carrera. On the relationship between indicators of geostatistical, flow and transport connectivity. Advances in Water Resources, 28(4):405–421, 2005. (Cité en page 141.)

[146] A. J. Koiter, D. A. Lobb, P. N. Owens, E. L. Petticrew, K. H. D. Tiessen, and S. Li. Investigating the role of connectivity and scale in assessing the sources of sediment in an agricultural watershed in the Canadian prairies using sediment source fingerprinting. Journal of Soils and Sediments, 13(10):1676–1691, 2013. (Cité en page 145.)

[147] D. E. Kroes and C. R. Hupp. The Effect of Channelization on Floodplain Sediment Deposition and Subsidence Along the Pocomoke River, Maryland1. JAWRA Journal of the American Water Resources Association, 46(4):686 – 699, 2010. (Cité en page 111.)

[148] B. Kronvang, H. E. Andersen, S. E. Larsen, and J. Audet. Importance of bank erosion for sediment input, storage and export at the catchment scale. Journal of Soils and Sediments, 13(1):230–241, 2013. (Cité en pages 97 et 120.)

[149] M. Lacoste, D. Michot, V. Viaud, O. Evrard, and C. Walter. Combining 137cs measurements and a spatially distributed erosion model to assess soil redistribution in a hedgerow landscape in northwestern France (1960–2010). CATENA, 119:78–89, 2014. (Cité en pages 92 et 173.)

[150] F. Lacquement, F. Prognon, S. Courbouleix, F. Quesnel, C. Prognon, G. Karnay, and E. Thomas. Carte géologique du régolithe de la France Métropolitaine,

Formations allochtones et autochtones. Technical report, BRGM, 2009. (Cité en page 87.)

[151] V. Landemaine, A. Gay, O. Cerdan, S. Salvador-Blanes, and S. Rodrigues. Morphological evolution of a rural headwater stream after channelisation. Geomorphology, 230:125–137, 2015. (Cité en pages 97, 111, 146, 147 et 153.)

[152] K. Landwehr and B. L. Rhoads. Depositional response of a headwater stream to channelization, East Central Illinois, USA. River Research and Applications, 19(1):77–100, 2003. (Cité en page 111.)

[153] S. N. Lane, S. M. Reaney, and A. L. Heathwaite. Representation of landscape hydrological connectivity using a topographically driven surface flow index: hydrological connectivity. Water Resources Research, 45(8):W08423, 2009. (Cité en page 152.)

[154] A. Latapie, B. Camenen, S. Rodrigues, A. Paquier, J.P. Bouchard, and F. Moatar. Assessing channel response of a long river influenced by human disturbance. CATENA, 121:1–12, 2014. (Cité en page 98.)

[155] A. Laubel, O. H. Jacobsen, B. Kronvang, R. Grant, and H. E. Andersen. Subsurface drainage loss of particles and phosphorus from field plot experiments and a tile-drained catchment. Journal of Environmental Quality, 28(2):576–584, 1999. (Cité en page 146.)

[156] A. Laubel, B. Kronvang, A. B. Hald, and C. Jensen. Hydromorphological and biological factors influencing sediment and phosphorus loss via bank erosion in small lowland rural streams in Denmark. Hydrological Processes, 17(17):3443–3463, 2003. (Cité en pages 97 et 109.)

[157] D. M. Lawler. The impact of scale on the processes of channel-side sediment supply: a conceptual model. IAHS Publications-Series of Proceedings and Reports-Intern Assoc Hydrological Sciences, 226:175–186, 1995. (Cité en page 96.)

[158] Y. Le Bissonnais, O. Cerdan, V. Lecomte, H. Benkhadra, V. Souchère, and P. Martin. Variability of soil surface characteristics influencing runoff and interrill erosion. CATENA, 62(2-3):111–124, 2005. (Cité en pages 144 et 165.)

[159] Y. Le Bissonnais, M. Jamagne, J.J. Lambert, C. Le Bas, J. Daroussin, D. King, O. Cerdan, J. Léonard, L.M. Bresson, and R. Jones. Pan-European soil crusting and erodibility assessment from the European Soil Geographical Database using pedotransfer rules. Advances in Environmental Monitoring and Modelling, 2:1 – 15, 2005. (Cité en page 165.)

[160] Y. Le Bissonnais, C. Montier, M. Jamagne, J. Daroussin, and D. King. Mapping erosion risk for cultivated soil in France. CATENA, 46(2):207–220, 2002. (Cité en pages 2, 86, 170 et 182.)

[161] K. H. Lee, T. M. Isenhart, and R. C. Schultz. Sediment and nutrient removal in an established multi-species riparian buffer. Journal of Soil and Water Conservation, 58(1):1–8, 2003. (Cité en page 173.)

[162] K. H. Lee, T. M. Isenhart, R. C. Schultz, and S. K. Mickelson. Nutrient and sediment removal by switchgrass and cool-season grass filter strips in Central

Iowa, USA. Agroforestry Systems, 44(2-3):121–132, 1998. (Cité en pages 145, 173 et 191.)

[163] P.-K. Lee, J.-C. Touray, P. Baillif, and J.-P. Ildefonse. Heavy metal contamination of settling particles in a retention pond along the A-71 motorway in Sologne, France. Science of the Total Environment, 201(1):1–15, 1997. (Cité en page 146.)

[164] J. Lefrançois, C. Grimaldi, C. Gascuel-Odoux, and N. Gilliet. Suspended sediment and discharge relationships to identify bank degradation as a main sediment source on small agricultural catchments. Hydrological Processes, 21(21):2923–2933, 2007. (Cité en pages 30 et 36.)

[165] C. F. Lenhart, E. S. Verry, K. N. Brooks, and J. A. Magner. Adjustment of prairie pothole streams to land-use, drainage and climate changes and consequences for turbidity impairment. River Research and Applications, 28(10):1609–1619, 2012. (Cité en page 146.)

[166] J.P. Lesschen, J.M. Schoorl, and L.H. Cammeraat. Modelling runoff and erosion for a semi-arid catchment using a multi-scale approach based on hydrological connectivity. Geomorphology, 109(3-4):174–183, 2009. (Cité en pages 131 et 144.)

[167] I. Lexartza-Artza and J. Wainwright. Hydrological connectivity: Linking concepts with practical implications. CATENA, 79(2):146–152, 2009. (Cité en pages xvii, 135 et 136.)

[168] I. Lexartza-Artza and J. Wainwright. Making connections: changing sediment sources and sinks in an upland catchment. Earth Surface Processes and Landforms, 36(8):1090–1104, 2011. (Cité en page 147.)

[169] M. Li, K. Xu, M. Watanabe, and Z. Chen. Long-term variations in dissolved silicate, nitrogen, and phosphorus flux from the Yangtze River into the East China Sea and impacts on estuarine ecosystem. Estuarine, Coastal and Shelf Science, 71(1):3–12, 2007. (Cité en page 63.)

[170] W. Lick and J. McNeil. Effects of sediment bulk properties on erosion rates. Science of the total environment, 266(1):41–48, 2001. (Cité en page 97.)

[171] I. G. Littlewood, C. D. Watts, and J. M. Custance. Systematic application of United Kingdom river flow and quality databases for estimating annual river mass loads (1975–1994). Science of the Total Environment, 210:21–40, 1998. (Cité en page 63.)

[172] M. López-Vicente, A. Navas, L. Gaspar, and J. Machín. Advanced modelling of runoff and soil redistribution for agricultural systems: The SERT model. Agricultural Water Management, 125:1–12, 2013. (Cité en page 153.)

[173] M. López-Vicente, J. Poesen, A. Navas, and L. Gaspar. Predicting runoff and sediment connectivity and soil erosion by water for different land use scenarios in the Spanish Pre-Pyrenees. CATENA, 102:62–73, 2013. (Cité en page 144.)

[174] W. Ludwig and J.-L. Probst. River sediment discharge to the oceans; present-day controls and global budgets. American Journal of Science, 298(4):265–295, 1998. (Cité en pages 3, 29, 30, 38, 39 et 53.)

[175] X.X. Luo, S.L. Yang, and J. Zhang. The impact of the Three Gorges Dam on the downstream distribution and texture of sediments along the middle and lower Yangtze River (Changjiang) and its estuary, and subsequent sediment dispersal in the East China Sea. Geomorphology, 2012. (Cité en page 147.)

[176] L. Lymburner. Mapping riparian vegetation functions using remote sensing and terrain analysis. PhD thesis, University of Melbourne, Department of Civil and Environmental Engineering, 2006. (Cité en page 103.)

[177] J. R. Malavoi and P. Adam. Les interventions humaines et leurs impacts hydromorphologiques sur les cours d'eau. Ingénieries, (50):35–48, 2007. (Cité en page 111.)

[178] V. Mano, J. Nemery, P. Belleudy, and A. Poirel. Assessment of suspended sediment transport in four alpine watersheds (France): influence of the climatic regime. Hydrological Processes, 23(5):777–792, 2009. (Cité en pages 30 et 38.)

[179] V. Mardhel, P. Frantar, J. Uhan, and M. Andjelov. Index of development and persistence of the river networks (IDPR) as a component of regional groundwater vulnerability assessment in Slovenia. In Proceedings on the International Conference on Groundwater vulnerability assessment and mapping, Ustron, Poland, pages 15–18, 2004. (Cité en pages 86 et 157.)

[180] V. Mardhel and A. Gravier. Carte de vulnérabilité simplifiée des eaux souterraines du bassin Loire Bretagne. Technical Report BRGM/RP-54553-FR, BRGM, 2006. (Cité en pages 53 et 157.)

[181] E. J. P. Marshall and A. C. Moonen. Field margins in northern Europe: their functions and interactions with agriculture. Agriculture, Ecosystems & Environment, 89(1):5–21, 2002. (Cité en page 172.)

[182] L. A. McKergow, I. P. Prosser, A. O. Hughes, and J. Brodie. Sources of sediment to the Great Barrier Reef World Heritage Area. Marine Pollution Bulletin, 51(1-4):200–211, 2005. (Cité en page 120.)

[183] M. Mekonnen, S. D. Keesstra, L. Stroosnijder, J. E. M. Baartman, and J. Maroulis. Soil conservation through sediment trapping: A review. Land Degradation & Development, 2014. (Cité en pages 152 et 169.)

[184] P. Merot. The influence of hedgerow systems on the hydrology of agricultural catchments in a temperate climate. Agronomie, 19(8):655–669, 1999. (Cité en pages 172 et 174.)

[185] K. Meßenzehl, T. Hoffmann, and R. Dikau. Sediment connectivity in the high-alpine valley of Val Müschauns, Swiss National Park – linking geomorphic field mapping with geomorphometric modelling. Geomorphology, 221:215–229, 2014. (Cité en pages 131 et 153.)

[186] M. Meybeck. Composition chimique des ruisseaux non pollués de France. Sci. Geol. Bull, 39(1):3–77, 1986. (Cité en pages 58 et 80.)

[187] M. Meybeck. Global occurrence of major elements in rivers. Treatise on Geochemistry, 5:207–223, 2003. (Cité en page 58.)

[188] M. Meybeck, A. J. Horowitz, and C. Grosbois. The geochemistry of Seine River Basin particulate matter: distribution of an integrated metal pollution index. Science of the total environment, 328(1):219–236, 2004. (Cité en page 58.)

[189] M. Meybeck, L. Laroche, H. H. Dürr, and J. P. M. Syvitski. Global variability of daily total suspended solids and their fluxes in rivers. Global and Planetary Change, 39(1-2):65–93, 2003. (Cité en pages 29, 35, 38, 45, 46, 71 et 137.)

[190] M. Meybeck and F. Moatar. Daily variability of river concentrations and fluxes: indicators based on the segmentation of the rating curve. Hydrological Processes, 26(8):1188–1207, 2012. (Cité en pages 58, 64 et 71.)

[191] M. Meybeck and A. Ragu. Presenting the GEMS-GLORI, a compendium of world river discharge to the oceans. In Freshwater Contamination (Proceedings of Rabat Symposium S4, Aprii-May 1997) IAHS Publ. no. 243,. PANGAEA, 1997. (Cité en page 59.)

[192] J. D. Milliman and R. H. Meade. World-wide delivery of river sediment to the oceans. The Journal of Geology, pages 1–21, 1983. (Cité en pages 3, 28, 56 et 59.)

[193] J. D. Milliman and J. P. M. Syvitski. Geomorphic/tectonic control of sediment discharge to the ocean: the importance of small mountainous rivers. The Journal of Geology, pages 525–544, 1992. (Cité en pages 3, 28 et 56.)

[194] J. P. G. Minella, D. E. Walling, and G. H. Merten. Establishing a sediment budget for a small agricultural catchment in southern Brazil, to support the development of effective sediment management strategies. Journal of Hydrology, 2014. (Cité en page 140.)

[195] F. Moatar, F. Birgand, M. Meybeck, C. Faucheux, and S. Raymond. Incertitudes sur les métriques de qualité des cours d'eau (médianes et quantiles de concentrations, flux, cas des nutriments) évaluées a partir de suivis discrets. La houille blanche, (3):68–76, 2009. (Cité en pages 61, 62, 63, 64 et 71.)

[196] F. Moatar and M. Meybeck. Riverine fluxes of pollutants: Towards predictions of uncertainties by flux duration indicators. Comptes Rendus Geoscience, 339(6):367–382, 2007. (Cité en pages 60 et 63.)

[197] F. Moatar, M. Meybeck, S. Raymond, F. Birgand, and F. Curie. River flux uncertainties predicted by hydrological variability and riverine material behaviour. Hydrological Processes, 27:3535–3546, 2012. (Cité en pages 63 et 64.)

[198] F. Moatar, G. Person, M. Meybeck, A. Coynel, H. Etcheber, and P. Crouzet. The influence of contrasting suspended particulate matter transport regimes on the bias and precision of flux estimates. Science of The Total Environment, 370(2-3):515–531, 2006. (Cité en pages 35 et 64.)

[199] P. Monbet. Dissolved and particulate fluxes of copper through the Morlaix river estuary (Brittany, France): mass balance in a small estuary with strong agricultural catchment. Marine pollution bulletin, 48(1):78–86, 2004. (Cité en pages 59 et 63.)

[200] J.-S. Moquet. Caractérisation des flux d'altération des contextes orogéniques en milieu tropical - Cas des bassins andins et d'avant pays de l'Amazone. PhD thesis, Université de Toulouse, Toulouse, 2011. (Cité en page 62.)

[201] R. P. C. Morgan. Soil erosion and conservation. John Wiley & Sons, 2005. (Cité en pages 84 et 86.)

[202] J. Mortatti and J.-L. Probst. Silicate rock weathering and atmospheric/soil CO2 uptake in the Amazon basin estimated from river water geochemistry: seasonal and spatial variations. Chemical Geology, 197(1):177–196, 2003. (Cité en page 67.)

[203] E. N. Mueller, J. Wainwright, and A. J. Parsons. Impact of connectivity on the modeling of overland flow within semiarid shrubland environments. Water Resources Research, 43(9), 2007. (Cité en page 131.)

[204] F. Nakamura, T. Sudo, S. Kameyama, and M. Jitsu. Influences of channelization on discharge of suspended sediment and wetland vegetation in Kushiro Marsh, northern Japan. Geomorphology, 18(3):279–289, 1997. (Cité en page 111.)

[205] O. Navratil, M. Esteves, C. Legout, N. Gratiot, J. Nemery, S. Willmore, and T. Grangeon. Global uncertainty analysis of suspended sediment monitoring using turbidimeter in a small mountainous river catchment. Journal of Hydrology, 398(3-4):246–259, 2011. (Cité en page 30.)

[206] O. Navratil, C. Legout, D. Gateuille, M. Esteves, and F. Liebault. Assessment of intermediate fine sediment storage in a braided river reach (southern French Prealps). Hydrological Processes, 2010. (Cité en page 45.)

[207] M. A. Nearing, L. Deer-Ascough, J. M. Laflen, and others. Sensitivity analysis of the WEPP hillslope profile erosion model. Transactions of the ASAE, 33(3):839–849, 1990. (Cité en page 106.)

[208] P. Négrel, C.J. Allègre, B. Dupré, and E. Lewin. Erosion sources determined by inversion of major and trace element ratios and strontium isotopic ratios in river water: The Congo Basin case. Earth and Planetary Science Letters, 120(1):59–76, 1993. (Cité en page 80.)

[209] P. Négrel and C. Grosbois. Changes in chemical and 87sr/86sr signature distribution patterns of suspended matter and bed sediments in the upper Loire river basin (France). Chemical geology, 156(1):231–249, 1999. (Cité en page 38.)

[210] P. Négrel, S. Roy, E. Petelet-Giraud, R. Millot, and A. Brenot. Long-term fluxes of dissolved and suspended matter in the Ebro River Basin (Spain). Journal of Hydrology, 342(3):249–260, 2007. (Cité en pages 58, 60 et 63.)

[211] E. J. Nelson and D. B. Booth. Sediment sources in an urbanizing, mixed land-use watershed. Journal of Hydrology, 264(1):51–68, 2002. (Cité en page 120.)

[212] Nordregio. Mountain Areas in Europe: Analysis of Mountain Areas in the European Union and in the Applicant Countries. pages 105 – 146. Luxembourg, 2004. (Cité en page 88.)

[213] A. Novara, L. Gristina, S.S. Saladino, A. Santoro, and A. Cerdà. Soil erosion assessment on tillage and alternative soil managements in a Sicilian vineyard. Soil and Tillage Research, 117:140–147, 2011. (Cité en page 165.)

[214] C. J. Ocampo, M. Sivapalan, and C. Oldham. Hydrological connectivity of upland-riparian zones in agricultural catchments: Implications for runoff

generation and nitrate transport. Journal of Hydrology, 331(3-4):643–658, 2006. (Cité en page 144.)

[215] C. Oeurng, S. Sauvage, and J.-M. Sánchez-Pérez. Dynamics of suspended sediment transport and yield in a large agricultural catchment, southwest France. Earth Surface Processes and Landforms, 35(11):1289–1301, 2010. (Cité en pages 30 et 38.)

[216] J.F. Ouvry, J.B. Richet, O. Bricard, M. Lhérriteau, M. Bouzid, and M. Saunier. Fascines et haies pour réduire les effets du ruissellement érosif. Technical report, Association Régionale pour l'Etude et l'Amélioration des Sols, 2012. (Cité en pages 173 et 190.)

[217] P. Owens. Conceptual Models and Budgets for Sediment Management at the River Basin Scale. Journal of Soils and Sediments, 5(4):201–212, 2005. (Cité en pages 3, 28 et 96.)

[218] S. Pelacani, M. Märker, and G. Rodolfi. Simulation of soil erosion and deposition in a changing land use: A modelling approach to implement the support practice factor. Geomorphology, 99(1):329–340, 2008. (Cité en pages 140 et 179.)

[219] M. J. Penven, T. Muxart, C. Cosandey, and A. Andrieu. Contribution du drainage agricole enterré à l'érosion des sols en région tempérée (Brie). Bulletin Réseau Erosion, 20:128–144, 2000. (Cité en page 90.)

[220] E. Petelet-Giraud and P. Négrel. Dissolved Fluxes of the Ebro River Basin (Spain): Impact of Main Lithologies and Role of Tributaries. In The Ebro River Basin, Handbook Environmental Chemistry, 2010, 13., pages 97–120. Springer-Verlag, Berlin Heidelberg, 2011. (Cité en pages 62 et 66.)

[221] J. M. Phillips, B. W. Webb, D. E. Walling, and G. J. L. Leeks. Estimating the suspended sediment loads of rivers in the LOIS study area using infrequent samples. Hydrological processes, 13(7):1035–1050, 1999. (Cité en pages 30 et 62.)

[222] C. Picouet. Geochemistry of a large river: Upper Niger river and inland delta (Mali). PhD thesis, Universite Montpellier II, 1999. (Cité en pages xxi, 60, 62 et 74.)

[223] C. Picouet, B. Dupré, D. Orange, and M. Valladon. Major and trace element geochemistry in the upper Niger river (Mali): physical and chemical weathering rates and CO2 consumption. Chemical Geology, 185(1):93–124, 2002. (Cité en page 64.)

[224] H. Piégay, D. E. Walling, N. Landon, Q. He, F. Liébault, and R. Petiot. Contemporary changes in sediment yield in an alpine mountain basin due to afforestation (the upper Drôme in France). CATENA, 55(2):183–212, 2004. (Cité en page 30.)

[225] R. E. Poeppl, M. Keiler, K. Von Elverfeldt, I. Zweimueller, and T. Glade. The influence of riparian vegetation cover on diffuse lateral sediment connectivity and biogeomorphic processes in a medium-sized agricultural catchment, Austria. Geografiska Annaler: Series A, Physical Geography, 94(4):511–529, 2012. (Cité en page 144.)

[226] J. Poesen, J. Nachtergaele, G. Verstraeten, and C. Valentin. Gully erosion and environmental change: importance and research needs. Catena, 50(2):91–133, 2003. (Cité en pages 86 et 172.)

[227] P. Pointereau, M. L. Paracchini, J.-M. Terres, F. Jiguet, Y. Bas, and K. Biala. Identification of High Nature Value farmland in France through statistical information and farm practice surveys. JRC Scientific and Technical Reports. EUR, 22786:76, 2007. (Cité en pages xiv, xix, 11, 21, 174, 223 et 224.)

[228] C. Poisvert. Etude du transfert des particules au sein du bassin Loire-Bretagne par modélisation semi-distribuée, amélioration de la prise en compte des processus sources : érosion de berge et mouvement de masse. Technical report, BRGM, 2013. (Cité en pages xvi, 87 et 89.)

[229] L. E. Polvi, E. Wohl, and D. M. Merritt. Modeling the functional influence of vegetation type on streambank cohesion. Earth Surface Processes and Landforms, 2014. (Cité en page 97.)

[230] V. Polyakov, A. Fares, and M. H. Ryder. Precision riparian buffers for the control of nonpoint source pollutant loading into surface water: A review. Environmental Reviews, 13(3):129–144, 2005. (Cité en page 173.)

[231] D. Pont, J.-P. Simonnet, and A.V. Walter. Medium-term Changes in Suspended Sediment Delivery to the Ocean: Consequences of Catchment Heterogeneity and River Management (Rhône River, France). Estuarine, Coastal and Shelf Science, 54(1):1–18, 2002. (Cité en page 30.)

[232] J.-L. Probst. Dissolved and suspended matter transported by the Girou River (France): mechanical and chemical erosion rates in a calcareous molasse basin. Hydrological Sciences Journal, 31(1):61–79, 1986. (Cité en page 76.)

[233] I. Prosser, P. Rustomji, B. Young, C. Moran, and A. Hughes. Constructing river basin sediment budgets for the National Land and Water Resources Audit. Technical Report 15/01, CSIRO Land and Water Canberra, 2001. (Cité en pages 97, 104 et 198.)

[234] R. Quilbé, A. N Rousseau, M. Duchemin, A. Poulin, G. Gangbazo, and J.-P. Villeneuve. Selecting a calculation method to estimate sediment and nutrient loads in streams: application to the Beaurivage River (Québec, Canada). Journal of Hydrology, 326(1):295–310, 2006. (Cité en page 64.)

[235] J. Raux, Y. Copard, B. Laignel, M. Fournier, and N. Masseï. Classification of worldwide drainage basins through the multivariate analysis of variables controlling their hydrosedimentary response. Global and Planetary Change, 76(3-4):117–127, 2011. (Cité en pages 53 et 54.)

[236] S. Raymond. Incertitudes des flux transportés par les rivières (Matière en suspension, nutriments, sels dissous) - Vers un système expert d'optimisation des méthodes de calcul. PhD thesis, Université François Rabelais-Tours, Tours, 2011. (Cité en pages 62 et 63.)

[237] S. M. Reaney, L. J. Bracken, and M. J. Kirkby. Use of the Connectivity of Runoff Model (CRUM) to investigate the influence of storm characteristics on

runoff generation and connectivity in semi-arid areas. Hydrological Processes, 21(7):894–906, 2007. (Cité en page 131.)

[238] Leslie M Reid and Thomas Dunne. Sediment production from forest road surfaces. Water Resources Research, 20(11):1753–1761, 1984. (Cité en page 145.)

[239] S. C. Reid, S. N. Lane, J. M. Berney, and J. Holden. The timing and magnitude of coarse sediment transport events within an upland, temperate gravel-bed river. Geomorphology, 83(1-2):152–182, 2007. (Cité en page 139.)

[240] S. C. Reid, S. N. Lane, D. R. Montgomery, and C. J. Brookes. Does hydrological connectivity improve modelling of coarse sediment delivery in upland environments? Geomorphology, 90(3-4):263–282, 2007. (Cité en pages 139 et 152.)

[241] K. G. Renard, G. R. Foster, G. A. Weesies, D. K. McCool, D. C. Yoder, and others. Predicting soil erosion by water: a guide to conservation planning with the revised universal soil loss equation (RUSLE). Agriculture Handbook (Washington), (703), 1997. (Cité en page 156.)

[242] F. Rey. Influence of vegetation distribution on sediment yield in forested marly gullies. Catena, 50(2):549–562, 2003. (Cité en page 144.)

[243] E. L. Rhoades, M. A. O'Neal, and J. E. Pizzuto. Quantifying bank erosion on the South River from 1937 to 2005, and its importance in assessing Hg contamination. Applied Geography, 29(1):125–134, 2009. (Cité en page 97.)

[244] R. A. Rittenburg, A. L. Squires, J. Boll, E. S. Brooks, Z. M. Easton, and T. S. Steenhuis. Agricultural BMP Effectiveness and Dominant Hydrological Flow Paths: Concepts and a Review. JAWRA Journal of the American Water Resources Association, 2015. (Cité en page 145.)

[245] M. Rode and U. Suhr. Uncertainties in selected river water quality data. Hydrology and Earth System Sciences Discussions, 11(2):863–874, 2007. (Cité en page 63.)

[246] J. Rodier, B. Legube, N. Merlet, and R. Brunet. L'analyse de l'eau. Dunod Paris, dunod paris edition, 2009. (Cité en pages 61 et 62.)

[247] S. Rodrigues, J.-G. Bréhéret, J.-J. Macaire, F. Moatar, D. Nistoran, and P. Jugé. Flow and sediment dynamics in the vegetated secondary channels of an anabranching river: The Loire River (France). Sedimentary Geology, 186(1-2):89–109, 2006. (Cité en pages 31, 104 et 144.)

[248] C. Ronfort, V. Souchère, P. Martin, C. Sebillotte, M.S. Castellazzi, A. Barbottin, J.M. Meynard, and Benoit Laignel. Methodology for land use change scenario assessment for runoff impacts: A case study in a north-western European Loess belt region (Pays de Caux, France). CATENA, 86(1):36–48, 2011. (Cité en pages 42 et 44.)

[249] S. Roy, J. Gaillardet, and C. J. Allegre. Geochemistry of dissolved and suspended loads of the Seine river, France: anthropogenic impact, carbonate and silicate weathering. Geochimica et cosmochimica acta, 63(9):1277–1292, 1999. (Cité en pages 30, 58, 59 et 61.)

[250] M.A. Russell, D.E. Walling, and R.A. Hodgkinson. Suspended sediment sources in two small lowland agricultural catchments in the UK. Journal of Hydrology, 252(1):1–24, 2001. (Cité en pages 90, 97 et 165.)

[251] I Rutherfurd. Some human impacts on Australian stream channel morphology. Wiley, Chichester, in brizga, s. and finlayson, b. river management: the australasian experience. edition, 2000. (Cité en pages 97 et 104.)

[252] J. D. Salas and H.-S. Shin. Uncertainty analysis of reservoir sedimentation. Journal of Hydraulic Engineering, 125(4):339–350, 1999. (Cité en page 29.)

[253] P.J. Sandercock and J.M. Hooke. Vegetation effects on sediment connectivity and processes in an ephemeral channel in SE Spain. Journal of Arid Environments, 75(3):239–254, 2011. (Cité en pages 135 et 144.)

[254] J. Schäfer, G. Blanc, Y. Lapaquellerie, N. Maillet, E. Maneux, and H. Etcheber. Ten-year observation of the Gironde tributary fluvial system: fluxes of suspended matter, particulate organic carbon and cadmium. Marine Chemistry, 79(3):229–242, 2002. (Cité en pages 30 et 59.)

[255] K. Semhi, P. Amiotte Suchet, N. Clauer, and J.-L. Probst. Impact of nitrogen fertilizers on the natural weathering-erosion processes and fluvial transport in the Garonne basin. Applied Geochemistry, 15(6):865–878, 2000. (Cité en page 59.)

[256] P. Serrat, W. Ludwig, B. Navarro, and J.L. Blazi. Variabilité spatio-temporelle des flux de matières en suspension d'un fleuve côtier méditerranéen: la Têt (France). Comptes Rendus de l'Académie des Sciences-Series IIA-Earth and Planetary Science, 333(7):389–397, 2001. (Cité en page 45.)

[257] F. D. Shields, R. E. Lizotte, S. S. Knight, C. M. Cooper, and D. Wilcox. The stream channel incision syndrome and water quality. Ecological Engineering, 36(1):78–90, 2010. (Cité en page 111.)

[258] A. Simon and A. J. C. Collison. Quantifying the mechanical and hydrologic effects of riparian vegetation on streambank stability. Earth Surface Processes and Landforms, 27(5):527–546, 2002. (Cité en page 97.)

[259] O. Singh, M. C. Sharma, A. Sarangi, and P. Singh. Spatial and temporal variability of sediment and dissolved loads from two alpine watersheds of the Lesser Himalayas. Catena, 76(1):27–35, 2008. (Cité en page 59.)

[260] G. Sipos, T. Kiss, and K. Fiala. Morphological alterations due to channelization along the lower Tisza and Maros Rivers (Hungary). Geografia Fiscica e Dinamica Quaternaria, 30(2):239–247, 2007. (Cité en page 111.)

[261] O. Slaymaker. Towards the identification of scaling relations in drainage basin sediment budgets. Geomorphology, 80(1-2):8–19, 2006. (Cité en page 3.)

[262] S. Sogon, M. J. Penven, P. Bonte, and T. Muxart. Estimation of sediment yield and soil loss using suspended sediment load and 137cs measurements on agricultural land, Brie Plateau, France. Man and river systems, pages 251–261, 1999. (Cité en pages 30, 146 et 197.)

[263] V. Souchere, D. King, J. Daroussin, F. Papy, and A. Capillon. Effects of tillage on runoff directions: consequences on runoff contributing area within agricultural catchments. Journal of hydrology, 206(3):256–267, 1998. (Cité en page 92.)

[264] N. Sougnez, B. van Wesemael, and V. Vanacker. Low erosion rates measured for steep, sparsely vegetated catchments in southeast Spain. CATENA, 84(1-2):1–11, 2011. (Cité en page 153.)

[265] C. Stoate, N.D Boatman, R.J Borralho, C.Rio Carvalho, G.R.de Snoo, and P Eden. Ecological impacts of arable intensification in Europe. Journal of Environmental Management, 63(4):337–365, 2001. (Cité en page 172.)

[266] M. I. Stutter, S. J. Langan, and R. J. Cooper. Spatial and temporal dynamics of stream water particulate and dissolved N, P and C forms along a catchment transect, NE Scotland. Journal of Hydrology, 350(3):187–202, 2008. (Cité en pages 63 et 67.)

[267] N. Surian and M. Rinaldi. Morphological response to river engineering and management in alluvial channels in Italy. Geomorphology, 50(4):307–326, 2003. (Cité en pages 96 et 111.)

[268] I. Takken, L. Beuselinck, J. Nachtergaele, G. Govers, J. Poesen, and G. Degraer. Spatial evaluation of a physically-based distributed erosion model (LISEM). Catena, 37(3):431–447, 1999. (Cité en page 3.)

[269] I. Takken, G. Govers, V. Jetten, J. Nachtergaele, A. Steegen, and J. Poesen. Effects of tillage on runoff and erosion patterns. Soil and Tillage Research, 61(1):55–60, 2001. (Cité en pages 92 et 144.)

[270] P. D. Taylor, L. Fahrig, K. Henein, and G. Merriam. Connectivity is a vital element of landscape structure. Oikos, pages 571–573, 1993. (Cité en page 131.)

[271] C. Teisson, M. Ockenden, P. Le Hir, C. Kranenburg, and L. Hamm. Cohesive sediment transport processes. Coastal Engineering, 21(1):129–162, 1993. (Cité en page 139.)

[272] D. Tetzlaff, J. Buttle, S. K. Carey, K. McGuire, H. Laudon, and C. Soulsby. Tracer-based assessment of flow paths, storage and runoff generation in northern catchments: a review. Hydrological Processes, 2014. (Cité en page 136.)

[273] D. Tetzlaff, J. Seibert, K. J. McGuire, H. Laudon, D. A. Burns, S. M. Dunn, and C. Soulsby. How does landscape structure influence catchment transit time across different geomorphic provinces? Hydrological Processes, 23(6):945–953, 2009. (Cité en page 140.)

[274] D. P. Thoma, S. C. Gupta, M. E. Bauer, and C. E. Kirchoff. Airborne laser scanning for riverbank erosion assessment. Remote Sensing of Environment, 95(4):493–501, 2005. (Cité en page 97.)

[275] C.J. Thompson, I. Takken, and J. Croke. Hydrological and sedimentological connectivity of unsealed roads. IAHS-AISH publication, pages 524–531, 2008. (Cité en page 145.)

[276] C. R. Thorne. Processes and mechanisms of river bank erosion. R.D. Hey, J.C. Bathurst, C.R. Thorne (Eds.), Gravel-Bed Rivers, Wiley, Chichester, pages 227 – 259, 1982. (Cité en page 97.)

[277] S. W. Trimble. Contribution of stream channel erosion to sediment yield from an urbanizing watershed. Science, 278(5342):1442–1444, 1997. (Cité en page 119.)

[278] S. W. Trimble and A. C. Mendel. The cow as a geomorphic agent—a critical review. Geomorphology, 13(1):233–253, 1995. (Cité en page 92.)

[279] H.J. Tromp-van Meerveld and J.J. McDonnell. Threshold relations in subsurface stormflow: 2. The fill and spill hypothesis. Water Resources Research, 42(2), 2006. (Cité en page 144.)

[280] L. Turnbull, J. Wainwright, and R. E. Brazier. A conceptual framework for understanding semi-arid land degradation: ecohydrological interactions across multiple-space and time scales. Ecohydrology, 1(1):23–34, 2008. (Cité en pages xvii, 136 et 137.)

[281] L. Valette, A. Chandesris, N. Mengin, J. R. Malavoi, Y. Souchon, and J.-G. Wasson. SYRAH CE: Principes et méthodes de la sectorisation hydromorphologique. Technical report, Cemagref, 2008. (Cité en page 100.)

[282] L. Valette and A. Cunillera. Cahiers techniques SYRAH_ce. Technical report, 2010. (Cité en page 104.)

[283] E. H. van der Zanden, P. H. Verburg, and C. A. Mücher. Modelling the spatial distribution of linear landscape elements in Europe. Ecological Indicators, 27:125–136, 2013. (Cité en pages xix, 174, 223 et 224.)

[284] H. J. van Meerveld, E.J. Baird, and W. C. Floyd. Controls on sediment production from an unpaved resource road in a Pacific maritime watershed. Water Resources Research, 2014. (Cité en page 145.)

[285] K. Van Oost, G. Govers, and P. Desmet. Evaluating the effects of changes in landscape structure on soil erosion by water and tillage. Landscape ecology, 15(6):577–589, 2000. (Cité en pages 145, 165 et 190.)

[286] K. Van Oost, W. Van Muysen, G. Govers, J. Deckers, and T. A. Quine. From water to tillage erosion dominated landform evolution. Geomorphology, 72(1):193–203, 2005. (Cité en page 92.)

[287] K. Van Oost, W. Van Muysen, G. Govers, G. Heckrath, T. A. Quine, and J. Poesen. Simulation of the redistribution of soil by tillage on complex topographies. European journal of soil science, 54(1):63–76, 2003. (Cité en page 92.)

[288] V. Vanacker, A. Molina, G. Govers, J. Poesen, G. Dercon, and S. Deckers. River channel response to short-term human-induced change in landscape connectivity in Andean ecosystems. Geomorphology, 72(1-4):340–353, 2005. (Cité en page 111.)

[289] M. Vanmaercke, J. Poesen, G. Verstraeten, J. de Vente, and F. Ocakoglu. Sediment yield in Europe: Spatial patterns and scale dependency. Geomorphology, 130(3-4):142–161, 2011. (Cité en pages 28, 29, 30, 38, 39 et 40.)

[290] A. Veihe, N. H. Jensen, I. G. Schiøtz, and S. L. Nielsen. Magnitude and processes of bank erosion at a small stream in Denmark. Hydrological Processes, 25(10):1597–1613, 2011. (Cité en page 97.)

[291] V. Viel, D. Delahaye, and R. Reulier. Evaluation of slopes delivery to catchment sediment budget for a low-energy water system: a case study from the Lingèvres

catchment (Normandy, western France). Geografiska Annaler: Series A, Physical Geography, (497-511), 2014. (Cité en pages 172 et 173.)

[292] J. Viers, B. Dupré, and J. Gaillardet. Chemical composition of suspended sediments in World Rivers: New insights from a new database. Science of The Total Environment, 407(2):853–868, 2009. (Cité en pages 58, 60 et 68.)

[293] O. Vigiak, L. Borselli, L.T.H. Newham, J. McInnes, and A.M. Roberts. Comparison of conceptual landscape metrics to define hillslope-scale sediment delivery ratio. Geomorphology, 138(1):74–88, 2012. (Cité en page 153.)

[294] J. Vogt, P. Soille, A. de Jager, E. Rimaviciuté, W. Mehl, S. Foisneau, K. Bodis, J. Dusart, M.L. Paracchini, P. Haastrup, and C. Bamps. A pan-European river and catchment database. European Commission, EUR 22920 EN—Joint Research Centre—Institute for Environment and Sustainability. Luxembourg: Office for Official Publications of the European Communities. 2007. (Cité en page 166.)

[295] A. Vongvixay, C. Grimaldi, C. Gascuel-Odoux, P. Laguionie, M. Faucheux, N. Gilliet, and M. Mayet. Analysis of suspended sediment concentration and discharge relations to identify particle origins in small agricultural watersheds. In Sediment Dynamics for a Changing Future, Proceedings of the ICCE symposium held at Warsaw University of Life Sciences–SGGW, Poland, pages 14–18, 2010. (Cité en page 36.)

[296] J. Wainwright, L. Turnbull, T. G. Ibrahim, I. Lexartza-Artza, S. F. Thornton, and R. E. Brazier. Linking environmental régimes, space and time: Interpretations of structural and functional connectivity. Geomorphology, 126(3-4):387–404, 2011. (Cité en pages 135 et 136.)

[297] M. Walker and I. Rutherfurd. An approach to predicting rates of bend migration in meandering alluvial streams. In Proceedings of the Second Australian Stream Management Conference, Adelaide, Australia, volume 2, pages 659–665, 1999. (Cité en page 97.)

[298] D. E. Walling. The sediment delivery problem. Journal of Hydrology, 65(1):209–237, 1983. (Cité en pages 3, 53, 140 et 152.)

[299] D. E. Walling. Linking land use, erosion and sediment yields in river basins. Hydrobiologia, 410:223–240, 1999. (Cité en pages 93 et 96.)

[300] D. E. Walling, M. A. Russell, R. A. Hodgkinson, and Y. Zhang. Establishing sediment budgets for two small lowland agricultural catchments in the UK. Catena, 47(4):323–353, 2002. (Cité en page 3.)

[301] D. E. Walling and B. W. Webb. Erosion and sediment yield: a global overview. IAHS Publications-Series of Proceedings and Reports-Intern Assoc Hydrological Sciences, 236:3–20, 1996. (Cité en pages 29 et 30.)

[302] D.E. Walling. Tracing suspended sediment sources in catchments and river systems. Science of The Total Environment, 344(1-3):159–184, 2005. (Cité en page 197.)

[303] D.E. Walling and A.L. Collins. The catchment sediment budget as a management tool. Environmental Science & Policy, 11(2):136–143, 2008. (Cité en pages 28, 152, 189 et 195.)

[304] D.E. Walling and B. W. Webb. The reliability of suspended sediment load data. In Erosion and Sediment Transport Measurement Symposium: proceedings of the Florence symposium, 22-26 June 1981, pages 177 – 194. International Association of Hydrological Sciences, 1981. (Cité en page 35.)

[305] D.E. Walling and B.W. Webb. Estimating the discharge of contaminants to coastal waters by rivers: some cautionary comments. Marine Pollution Bulletin, 16(12):488–492, 1985. (Cité en page 63.)

[306] C. Walter, P. Merot, B. Layer, and G. Dutin. The effect of hedgerows on soil organic carbon storage in hillslopes. Soil Use and Management, 19(3):201–207, 2003. (Cité en page 172.)

[307] J.-G. Wasson, A. Chandesris, H. Pella, and L. Blanc. Les hydro-écorégions de France métropolitaine. Approche régionale de la typologie des eaux courantes et éléments pour la définition des peuplements de réféence d'invertébrés. Technical report, Cemagref, 2002. (Cité en page 98.)

[308] R.J. Wasson, L. Furlonger, D. Parry, T. Pietsch, E. Valentine, and D. Williams. Sediment sources and channel dynamics, Daly River, Northern Australia. Geomorphology, 114(3):161–174, 2010. (Cité en page 111.)

[309] B. W. Webb, J. M. Phillips, D. E. Walling, I. G. Littlewood, C. D. Watts, and G. J. L. Leeks. Load estimation methodologies for British rivers and their relevance to the LOIS RACS (R) programme. Science of the total environment, 194:379–389, 1997. (Cité en page 29.)

[310] B. C. Wemple, J. A. Jones, and G. E. Grant. Channel network extension by logging roads in two basins, Western Cascades, Oregon1. Water Resources Bulletin, 32(6):1195 – 1207, 1996. (Cité en pages 138 et 145.)

[311] L.-S. Wen, K.-T. Jiann, and K.-K. Liu. Seasonal variation and flux of dissolved nutrients in the Danshuei Estuary, Taiwan: A hypoxic subtropical mountain river. Estuarine, coastal and shelf science, 78(4):694–704, 2008. (Cité en page 63.)

[312] A. W. Western, G. Bloschl, and R. B. Grayson. How well do indicator variograms capture the spatial connectivity of soil moisture? Hydrological processes, 12(12):1851–1868, 1998. (Cité en pages 132 et 139.)

[313] A.W. Western, G. Blöschl, and R.B. Grayson. Toward capturing hydrologically significant connectivity in spatial patterns. Water Resources Research, 37(1):83–97, 2001. (Cité en pages 138, 141 et 152.)

[314] G. V. Wilkerson. Improved Bankfull Discharge Prediction Using 2-Year Recurrence-Period Discharge. JAWRA Journal of the American Water Resources Association, 44(1):243–257, 2008. (Cité en page 104.)

[315] S. N. Wilkinson, C. Dougall, A. E. Kinsey-Henderson, R. D. Searle, R. J. Ellis, and R. Bartley. Development of a time-stepping sediment budget model for assessing land use impacts in large river basins. Science of The Total Environment, 2013. (Cité en page 3.)

[316] G. P. Williams. Bank-full discharge of rivers. Water resources research, 14(6):1141–1154, 1978. (Cité en page 102.)

[317] G. P. Williams. Sediment concentration versus water discharge during single hydrologic events in rivers. Journal of Hydrology, 111(1):89–106, 1989. (Cité en page 29.)

[318] W. H. Wischmeier, D. D. Smith, and others. Predicting rainfall erosion losses-A guide to conservation planning. Predicting rainfall erosion losses-A guide to conservation planning, 1978. (Cité en pages 3, 156, 174, 175 et 177.)

[319] F. Worrall, T. P. Burt, N. J. K. Howden, and M. J. Whelan. Fluvial flux of nitrogen from Great Britain 1974–2005 in the context of the terrestrial nitrogen budget of Great Britain. Global biogeochemical cycles, 23(3), 2009. (Cité en page 63.)

[320] F. Worrall, H. Davies, T. Burt, N. J. K. Howden, M. J. Whelan, A. Bhogal, and A. Lilly. The flux of dissolved nitrogen from the UK—Evaluating the role of soils and land use. Science of the Total Environment, 434:90–100, 2012. (Cité en page 63.)

[321] S. Yoshikawa, H. Yamamoto, Y. Hanano, and A. Ishihara. Hilly-Land Soil Loss Equation (HSLE) for Evaluation of Soil Erosion Caused by the Abandonment of Agricultural Practices. Japan Agricultural Research Quarterly, 38:21–30, 2004. (Cité en page 175.)

[322] Y. Yuan, R. L. Bingner, and M. A. Locke. A Review of effectiveness of vegetative buffers on sediment trapping in agricultural areas. Ecohydrology, 2(3):321–336, 2009. (Cité en page 173.)

[323] G. N. Zaimes, R. C. Schultz, and T. M. Isenhart. Streambank Soil and Phosphorus Losses Under Different Riparian Land-Uses in Iowa. JAWRA Journal of the American Water Resources Association, 44(4):935–947, 2008. (Cité en page 97.)

GéHCO - EA 6293
GéoHydrosystèmes COntinentaux
Université de Tours
Faculté des Sciences et Techniques
Parc de Grandmont, 37200 Tours
geosciences.univ-tours.fr

Géosciences pour une Terre durable
brgm

agence de l'eau Loire-Bretagne

Aurore GAY
Transfert de particules des versants aux masses d'eau sur le bassin Loire-Bretagne

Résumé

L'érosion et la redistribution des particules détachées représentent un enjeu environnemental, sociétal et économique majeur. Afin de mettre en place des mesures de protection, il est nécessaire d'identifier et quantifier les sources et puits de sédiments ainsi que leur dynamique spatiale et temporelle. L'objectif de cette thèse est donc de dresser le bilan sédimentaire d'un large bassin versant (Loire Bretagne, 155 000 km^2) aux paysages contrastés.

Sur les versants, les particules détachées issues des différentes sources (érosion diffuse, concentrée, mouvements de masse) représentent un apport de 1.5 * 10^7 $t.an^{-1}$ (contribution respective au stock : 82.4%, 12.9%, 4.7%). La prise en compte de la distribution spatiale des processus mis en jeu dans le transfert particulaire et des caractéristiques du site d'étude (ruissellement par saturation en zone de plaine et présence de haies) dans un indice qualitatif permet d'évaluer la connectivité des versants. L'érosion de berge contribue également au stock sédimentaire à hauteur de 6.9 * 10^5 $t.an^{-1}$.

Au final, seuls 5% des particules détachées, toutes sources confondues, sont transportées jusqu'à l'exutoire du bassin versant et témoignent du fort taux de dépôt au sein du bassin. En parallèle, une valorisation de la base de données des éléments dissous permet de montrer l'importance des flux sédimentaires exportés sous forme dissoute ($\sim$ 90% des exports totaux). La représentation de l'ensemble de ces résultats à différentes résolutions spatiales permet de développer une approche qualitative du transfert particulaire et dŠidentifier les zones à risque.

Mots clés : Bilan sédimentaire, Erosion de berges, Connectivité, Loire, Eléments dissous.

Abstract

Erosion and particles redistribution represent major environmental, societal and economic issues. To adopt protection measures, it is essential to identify and quantify sources and sinks of sediment and their spatial and temporal dynamic. The aim of this work is thus to establish a sediment budget for a large river basin (Loire and Brittany river basin 155,000 km^2) with contrasted landscapes.

On hillslopes, detached particles from the miscellaneous form of erosion (sheet and rill erosion, gullies and mass movements) represent a supply of 1.5 * 10^7 $t.yr^{-1}$ (contribution to the stock of 82.4%, 12.9%, and 4.7% respectively). The consideration of the spatial distribution of processes involved in sediment transport and the characteristics of the study site (soil saturation and presence of hedgerows) in a qualitative landscape-based index allows us to assess the hillslope connectivity. Bank erosion also participates in the sediment budget with 6.9 * 10^5 $t.yr^{-1}$ of material provided to the river network.

In the end, only 5% of detached particles, from all sources of sediment, reach the basin outlet indicating a substantial deposition on the way from source to outlet. In parallel, the use of the database of dissolved elements allows us to highlight the importance of the dissolved sediment fluxes (90% of the total exports of the Loire river). The presentation of all results at different spatial scales permits to provide a qualitative approach of sediment source-to-sink transfers and to identify hotspots of erosion and transfers.

Keywords: Sediment budget, Bank erosion, Connectivity, Loire river basin, Dissolved sediment yields.